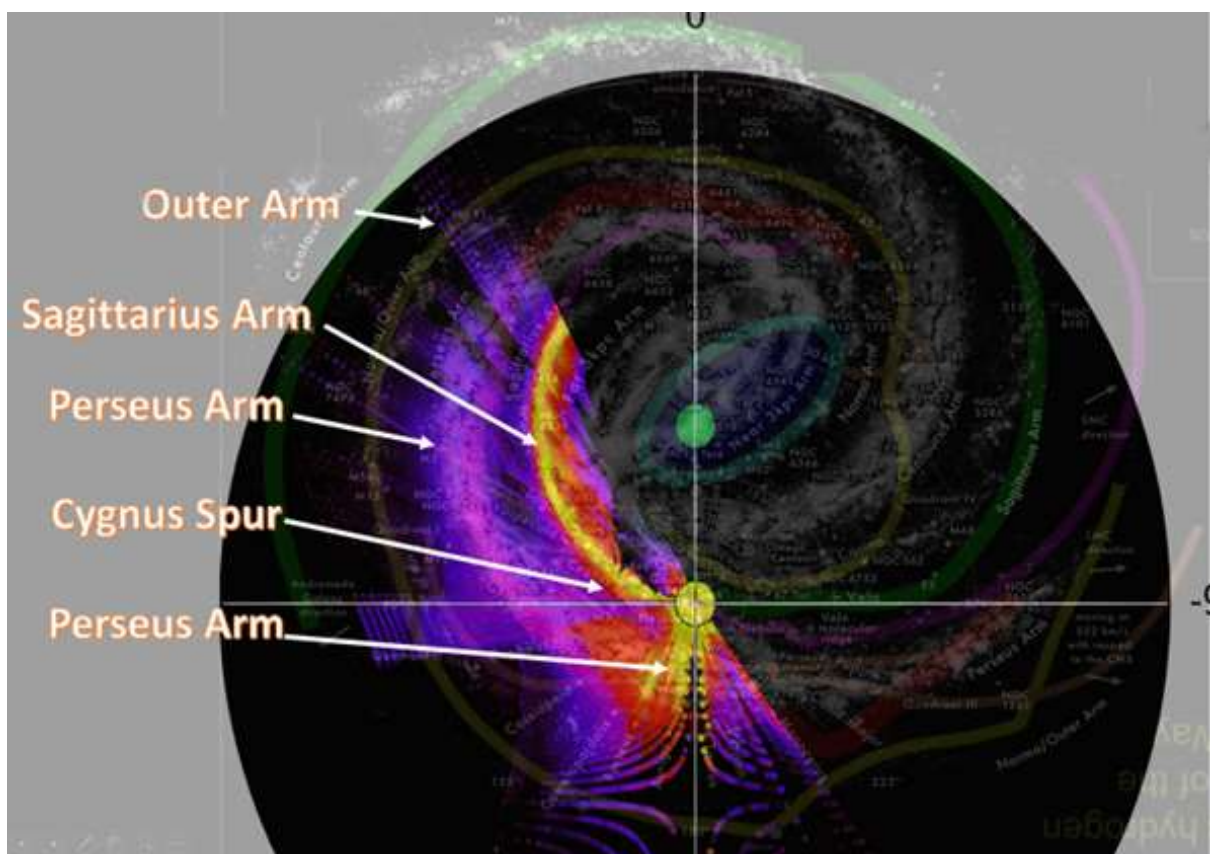


RADIO ASTRONOMY

Journal of the Society of Amateur Radio Astronomers
January – February 2025



Mapping the Milky Way in 3 Spatial Dimensions



Dr. Richard A. Russel
SARA President and Editor

Bogdan Vacaliuc
Contributing Editor

Radio Astronomy is published bimonthly as the official journal of the Society of Amateur Radio Astronomers. Duplication of uncopyrighted material for educational purposes is permitted but credit shall be given to SARA and to the specific author. Copyrighted materials may not be copied without written permission from the copyright owner.

Radio Astronomy is available for download only by SARA members from the SARA web site and may not be posted anywhere else.

It is the mission of the Society of Amateur Radio Astronomers (SARA) to: Facilitate the flow of information pertinent to the field of Radio Astronomy among our members; Promote members to mentor newcomers to our hobby and share the excitement of radio astronomy with other interested persons and organizations; Promote individual and multi station observing programs; Encourage programs that enhance the technical abilities of our members to monitor cosmic radio signals, as well as to share and analyze such signals; Encourage educational programs within SARA and educational outreach initiatives. Founded in 1981, the Society of Amateur Radio Astronomers, Inc. is a membership supported, non-profit [501(c) (3)], educational and scientific corporation.

Copyright © 2025 by the Society of Amateur Radio Astronomers, Inc. All rights reserved.

Cover Photo:
D. Andrew Thornett

Contents

President's Page	2
Editor's Notes	3
SARA NOTES	4
VINTAGE SARA - Charles Osborne.....	8
Announcing Radio JOVE 2.0.....	16
John Cook's VLF Report.....	21
BAA RA Section programme 2024	44
Featured Articles	46
Calculating ULF Waves Spectra from SAM-III Magnetometer Data -Whitham D. Reeve.....	46
ULF Wave Observations at the End of 2024 - Whitham D. Reeve.....	52
Wave Observations at the Beginning of 2025 - Whitham D. Reeve.....	60
<i>W75N/DR21 star formation cluster and 6.7 GHz methanol line observations</i> - Dimitry Fedorov	63
A Simple Weather-Resistant Housing for the Nooelec SAWBird H1 Low Noise Amplifier and 1420.405MHz SAW Filter. - Andrew Thornett.....	71
3D-processing of three days data using latest ezCon250124b.py script in ezRA suite & using meshes/matrix data tables in Rinearn 3D. - Dr Andrew Thornett.....	74
Review of two WTMicrowave Chinese Hydrogen Cavity Filter covering hydrogen band and first light results of their performance at Lichfield Radio Observatory (LRO). - Dr Andrew Thornett.....	92
Mapping the Milky Way galactic arms in three spatial dimensions using data from Lichfield Radio Astronomy Ptarmigan Array 1420MHz Radio Telescope (LRO-H1) - Andrew Thornett	108
A note on integration times in ezCol data collection programme in ezRA software suite. - Dr Andrew Thornett	120
Dear World Magnetic Model users,.....	121
Observation Reports	122
Observation report: M31 and M33 at 21 cm - Eduard Mol.....	122
INTERNATIONAL EARTH ROTATION AND REFERENCE SYSTEMS SERVICE (IERS)	131
Journal Archives and Other Promotions	132
What is Radio Astronomy?	133
Administrative	134
Officers, directors, and additional SARA contacts	134
Resources	135
Great Projects to Get Started in Radio Astronomy	135
Radio Astronomy Online Resources	137
Radio Astronomy Puzzle	141

SARA GOALS



We had a fantastic year in 2024 so here is a set of goals we can aim at in 2025.

- 1) Increase the membership to 500 active members
- 2) Increase the YouTube subscriptions from 2500 to 3000. Note that each subscriber is a potential new member!
- 3) Get more members involved in H1 antenna builds.
 - a. Milky Way measurements
 - b. Extra – galactic measurements
- 4) Increase the number of maser antenna builds and observing.
- 5) Increase the Radio-JOVE collaboration – note we have a joint Radio-JOVE Eastern Conference this year.
- 6) Increase the active 20 meter telescope usage.
- 7) Start an Amateur Radio Observatory collaboration:
 - a. Provide journal space for amateur radio observatories
 - b. Allow the SARA Logo to be used by approved observatories
 - c. Get input from observatories during the RTOP, Drake' and Drake's Lounge – Australia ZOOM meetings.

A lot more can be accomplished this year. Provide me feedback with your ideas.

Thanks!
Rich

Editor's Notes

We are always looking for basic radio astronomy articles, radio astronomy tutorials, theoretical articles, application and construction articles, news pertinent to radio astronomy, profiles and interviews with amateur and professional radio astronomers, book reviews, puzzles (including word challenges, riddles, and crossword puzzles), anecdotes, expository on "bad astronomy," articles on radio astronomy observations, suggestions for reprint of articles from past journals and other publications, and announcements of radio astronomy star parties, meetings, and outreach activities.

Subscribe to the SARA YouTube Channel

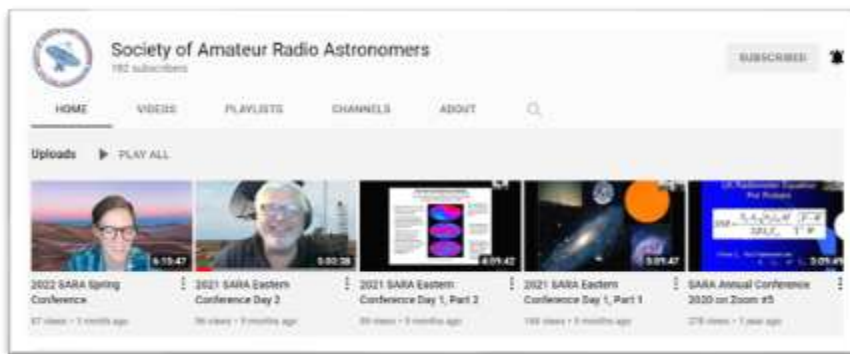
SARA has a YouTube channel at: <https://www.youtube.com/@radio-astronomy>

Don't forget to LIKE



the videos! It helps with the YouTube distribution algorithm.

We are also looking to add content to the site. Anyone who wants to help produce a series of 5 - minute videos relating to radio astronomy technology or observations please contact me. (drrichrussel@netscape.net)



Observation Reports

We are now accepting 1-2 page observation reports. These reports should include the astronomical object's RA/DEC plus UTC of the observation. Also include the telescope configuration, process used to observe the object and results. Picture of the setup and plots of the observation are a plus to the report.

If you would like to write an article for Radio Astronomy, please follow **the newly updated Author's Guide** on the SARA web site:

http://www.radio-astronomy.org/publicat/RA-JSARA_Author's_Guide.pdf.

Let us know if you have questions; we are glad to assist authors with their articles and papers and will not hesitate to work with you. You may contact your editors any time via email here: edit@radio-astronomy.org.

The editor(s) will acknowledge that they have received your submission within two days. If they do not reply, assume they did not receive it and please try again.

Please consider submitting your radio astronomy observations for publication: any object, any wavelength. Strip charts, spectrograms, magnetograms, meteor scatter records, space radar records, photographs; examples of radio frequency interference (RFI) are also welcome.

Guidelines for submitting observations may be found here: http://www.radio-astronomy.org/publicat/RA-JSARA_Observation_Submission_Guide.pdf

SARA NOTES

2025 SARA Western Conference Socorro, New Mexico, USA

The 2025 SARA Western Conference will be held at the Pete V. Domenici Science Operations Center in Socorro, NM and the Very Large Array near Magdalena, New Mexico on March 14 to 16, 2025.

The town of Socorro is the home of NRAO operations in New Mexico (NM). Located on the campus of the New Mexico Institute of Mining and Technology (New Mexico Tech), the Pete V. Domenici Science Operations Center houses scientific, engineering, technical, computer and support staff for both the Expanded Very Large Array (EVLA) and the Very Long Baseline Array (VLBA). The Science Operations Center also houses the control center and correlator for VLBA observations and hosts personnel working on the Atacama Large Millimeter/submillimeter Array (ALMA) project.

We will have a tour of the Very Large Array (VLA) site west of Socorro. We will also tour the Long Wavelength Array (LWA) (<http://lwa.unm.edu>) which is next to the VLA. In addition to presentations by SARA members, we plan to have presentations by speakers from the National Radio Astronomy Observatory Array Operations Center (NRAO AOC) in Socorro. Additional details will be published online and in the SARA journal as we get closer to the conference date. Register now to avoid the rush and to guarantee a seat at the conference.

VLA site tour: The Very Large Array consists of 27 parabolic dish reflector antennas in a Y-shaped configuration on the Plains of San Agustin approximately fifty miles west of Socorro: <http://www.vla.nrao.edu/> . Each antenna is 25 m in diameter.

LWA site tour: The Long Wavelength Array (256 bent dipole antennas) LWA-1 is located next to the VLA

There are three LWAs in New Mexico, two in the vicinity of the VLA and one north of Socorro in the Sevilleta National Wildlife Refuge. Each array consists of 256 crossed-dipole antennas and each antenna is about 1.5 m high.

Hotel

(575) 838-0556 Best Western (Socorro, NM).
SARA Western Conference (group name)

The "drop date" for all unused rooms is 2 weeks prior to arrival date

At this time, we only have 10 rooms reserved.

Ken Redcap
Western Conference Coordinator

Society of Amateur Radio Astronomers (SARA)

2025 SARA & Radio Jove Eastern Conference
June 7 (Sat) – June 11 (Wed) 2025
Green Bank Observatory (GBO) West Virginia (WV)



Block your calendars and start thinking about your travels for this summer. We have teamed up with the Radio Jove group and are holding a joint conference this summer!

- 2025 SARA and Radio Jove Eastern Conference
- June 7 (Sat) – June 11 (Wed) 2025
- Green Bank Observatory (GBO) West Virginia (WV)

Conference committee members include:

Rich Russel	Tom Jacobs	Ciprian Sufitchi	Kammie Russel
Don Latham	Dennis Farr	Jay Wilson	Ken Redcap
Tom Hagen	Dave Lacko	Gary Memory	Chuck Higgins

Abstracts are now being accepted, please submit your abstract to vicepresident@radio-astronomy.org

March 28, 2025 is the projected deadline for abstract submissions, reach out to us if you have any questions.

We will be following a similar format as years past with two additions. We have teamed up with Radio Jove and added more hands-on learning segments where attendees will assemble and operate the telescopes that SARA offers. For example:

- Saturday (6/7): Guided tours of public exhibits, Dave Lacko and Jay Wilson discussion on “What is Radio Astronomy Anyhow?”, hands on workshop assembling Scope in a Box and eZRA software
- Sunday (6/8): hands on workshop for 40’ telescope and 20-meter telescopes, with attendees able to plan and make observations
- Monday – Tuesday: SARA and Radio Jove technical discussions
- Evenings: Drake lounge discussions, flea market, and observations using Scope in a Box, Radio Jove, Super SID, 40’, 20m telescopes
- Wednesday (6/11): technical tours of GBO

Any comments and/or suggestions please reach out to the committee chair Marcus Fisher (vicepresident@radio-astronomy.org)

NEW The BYTE

A new section is being added to the bimonthly SARA journal focused on system software applicable for amateur radio astronomy (RA).

<p>Society of Amateur Radio Astronomers (SARA)</p> <p>2025 SARA Eastern Conference</p>	
---	--

Block off your calendars and start thinking about your travels for next summer! We have teamed up with the Radio Jove group and are holding a combined conference next year!

- 2025 SARA Eastern Conference and Radio Jove
- June 7 (Sat) – June 11 (Wed) 2025
- Green Bank Observatory (GBO) West Virginia (WV)

Planning is underway and more information will be coming as it develops. Any comments and/or suggestions please reach out to the committee chair Marcus Fisher (vicepresident@radio-astronomy.org)

2025 EU Conference on Amateur Radio Astronomy (EUCARA25)

We are pleased to announce the date of the *2025 EU Conference on Amateur Radio Astronomy* (EUCARA25) - Friday September 5th - Sunday 7th.

This will be held at the Visitor Center on the Harwell Campus. Further details will be published soon on our website – www.eucara.org .

We are honored that **Professor Jocelyn Bell Burnell** will be our keynote speaker.

When registration is open, we will let you know via the forums.

SARA Student & Teacher Grant Program

All, SARA has a grant program that is, sad to say, very underutilized. We will provide kits or money to students and teachers, including college students to help them with a radio telescope project. SARA can supply any of the following kits:

- [1] SuperSID
- [2] Scope in a Box
- [3] IBT (Itty Bitty Telescope)
- [4] Radio Jove kit
- [5] Inspire
- [6] Sky Scan

We can also provide up to five hundred dollars (\$500.00 USD) for an approved radio telescope project.

We have on occasion provided more money based on the merits of the project and the SARA Grant Committee approval.

More information on the grant program can be found at the URL below.

[SARA Student and Teacher Project Grants | Society of Amateur Radio Astronomers \(radio-astronomy.org\)](https://radio-astronomy.org)

All that is required is the SARA grant request form be filled out and sent in. If it needs more work for approval, we will work with the students to help ensure their success.

Please pass the word that SARA will fund any legitimate radio telescope project anywhere in the world.

If you have a question, contact me at crowleytj@hotmail.com .

Tom Crowley - SARA Grant Program Administrator

Drake's Lounge Australia

This new zoom forum is geared to the Melbourne, Australia time zone (UTC+10) in order to improve coordination with our Australia, New Zealand, and Japanese members. The meetings are scheduled for the 4th Friday of every month, 9 AM Melbourne time. A zoom announcement will be sent out to all SARA members before the meeting.

Radio Telescope Observation Party (RTOP)

RTOP is designed to demonstrate how to take observations using various radio telescopes. It will also cover how to record and analyze data.

RTOP is every month on the 1st Sunday at 2 pm Eastern time (1800 UTC). ZOOM email notifications will be sent to all members.

Drake's Lounge

Join the SARA community as we discuss the latest astronomy and radio astronomy news. The lounge also provides a forum to share and get advice on your radio astronomy projects from very experienced amateur radio astronomers.

Drake's Lounge is every month on the 3rd Sunday at 2 pm Eastern time (1800 UTC). ZOOM email notifications will be sent to all members.

VINTAGE SARA

CHARLES OSBORNE, SARA HISTORIAN

The Historic NRAO Little Big Horn

The Calibration Horn, also called the Little Big Horn, is not generally noticed by anyone on normal visits to Green Bank Observatory for the SARA Conference. And each year it becomes a lot harder to access as the forest retakes the land once cleared for it.



The 13 foot x 17.5 foot aperture end of the 120-foot long Calibration Horn Antenna, otherwise known as the “Little Big Horn,” at Green Bank. It was built in 1959 to observe the sky’s strongest non-solar radio source, Casseopeia A, and measure its total power output at a frequency of 1.4 GHz (L-band, 20cm wavelength). It was also used to map Cas A’s spectrum and take absolute temperature measurements of the background sky. [circa 1967 NRAO/AUI/NSF text/image]



SARA Conference field trip to the Little Big Horn circa 1995. Jeff Lichtman and Hal Braschwitz (sk) leading the group down the hill. Mike Gingell (sk) bringing up the rear.



Jim Carroll N4CAE connects the waveguide to coax transition to the horn to attach his receiver.

The metal below the transition is a trough which drains out below the building to get rid of water and trash collected by the horn during storms. One always has to remember to remove the transition. If not the amount of water and crud the horn could collect would be massive.



SARA member Kerry Smith WB3CAL climbed up into the throat of the horn to be a “noise source” or T-HOT during that 1995 Jim Carroll experiment. Below is a twenty year later 2015 view of how grown up the area has become. [NRAO/AUI/NSF image]





2025 Google Earth View of the Little Big Horn. It may be an optical illusion, but the horn doesn't look aligned with the building anymore. That may indicate some of the wooden supports may have given way. The steps going up the hill beside the horn and other lighter wooden parts of the structure were removed for safety reasons even before our 1995 field trip.

Bruce Randall NT4RT tried to find the horn on a recent conference trip and was unable to find the way, as it was too grown up to recognize. He'd been there possibly around 2018 and described it as quite snaky looking around the building. The AC power meter was still active or at least in place on the building then. To find it on Google Earth or the site maps look for the 20meter dish and then look about a quarter mile northeast. But the normal way to get there is via a road near some of the offsite GBO housing on Hannah Run Road going to the GBO employee recreation area/pool/target shooting range.

<https://www.everythingrf.com/rf-calculators/pyramidal-horn-antenna-gain-calculator>

$$G = \frac{4 \cdot \pi \cdot A}{\lambda^2} \cdot e_A$$

$$\text{Gain (dB)} = 10 \text{ Log (G)}$$

$A = W \times H = 13' \times 17.5' = 156'' \times 210'' \times 2.54''/\text{cm} = 211,354 \text{ cm}^2$

e_A = aperture efficiency or Effective Aperture estimated at 70%

Gain = $6022.578 \cdot e_A = 5215.8$ at 70% efficiency

$G(\text{dbi}) = 10 \text{Log} 5215.8 = 36.2 \text{ dBi}$

Estimated half power beam width = 3°

Estimated quarter dB beam width = 0.86°

Since a waveguide horn can be thought of as a matching device between a 50 ohm coax and 377 ohm free space impedance the length of the horn mostly improves efficiency and sidelobe suppression. Otherwise, the gain as the equations above shows is primarily defined by the size of the aperture.

Therefore, a quick approximation of the gain is equivalent to a dish sized similar to the horn mouth. A 13 to 17ft diameter dish being equivalent to the Little Big Horn. Though the dish sidelobes would likely be much worse.

In the initial picture from the 1960s notice there is a horn going thru the roof of the receiver building pointing at zenith. This appears to be a 1420 MHz "Standard Gain Horn" which is usually 15 dBi gain. I'm assuming that horn was used for a cold sky reference measurement.

Sometimes the Little Big Horn is talked about as a potential SARA group project to go down, clean it up, and connect a SAWBirdH1 LNA and SDR plus laptop for a recreation of Jim Carroll's experiment of thirty years ago. But from the looks of things, it's well past its prime and that would be a risky proposition today... especially if the transition was not removed by someone after use in the intervening thirty years. Not to mention bees, snakes, and rotten floorboards. I could be wrong. Heed the Danger signs. But I'm allergic to wasps so it has added risk aversion for me.



SuperSID
*Collaboration of Society
of Amateur Radio
Astronomers and
Stanford Solar Center*



- Stanford provides data hosting, database programming, and maintains the SuperSID website
- Society of Amateur Radio Astronomers (SARA) sells the SuperSID monitors for 48 USD to amateur radio astronomers and the funds are then used to support free distribution to students all over the world (image below as of Fall 2017)
- Jonathan Pettingale at SARA is responsible for building and shipping the SuperSID monitor kits: SuperSID@radio-astronomy.org
- SuperSID kits may be ordered through the SARA SuperSID webpage: <http://radio-astronomy.org/node/210>
- Questions about the SuperSID project may be directed to Steve Berl at Stanford: steveberl@gmail.com
- Jaap Akkerhuis at Stanford is responsible for the SuperSID software and SARA has provided financial support for his efforts
- SuperSID website hosted by Stanford: <http://solar-center.stanford.edu/SID/sidmonitor/>
- SuperSID database: <http://sid.stanford.edu/database-browser/>
- The data is searchable by time, station, date, and multiple plots may be placed on the same graph for comparison.



**SID Monitor
Distribution**
1078 instruments
82 countries
7 continents

Algeria - 2	Denmark - 3	Mexico - 21	Slovenia - 2
Antarctica - 1	Egypt - 3	Mongolia - 10	South Africa - 8
Australia - 7	Ethiopia - 14	Mozambique - 2	Spain - 1
Austria - 3	France - 6	Namibia - 1	St. Lucia - 1
Azerbaijan - 2	Gabon - 1	Netherlands - 5	Sweden - 3
Bangladesh - 1	Germany - 30	New Zealand - 7	Switzerland - 4
Bhutan - 1	Greece - 7	Nigeria - 37	Taiwan - 4
Bolivia - 1	Guyana - 1	Pakistan - 4	Thailand - 3
Bosnia-Herzegovina - 2	Hungary - 1	Peru - 10	Tunisia - 6
Brazil - 11	India - 33	Philippines - 1	Turkey - 2
British Virgin Islands - 1	Indonesia - 2	Poland - 2	Uganda - 3
Bulgaria - 2	Iran - 4	Portugal - 3	UK - 32
Burkina Faso - 1	Iraq - 1	Rep. of Congo - 3	Uruguay - 6
Canada - 33	Ireland - 9	Romania - 4	US Virgin Islands - 2
Chile - 1	Italy - 42	Russia - 3	USA - 491
China - 18	Kenya - 23	Rwanda - 1	Uzbekistan - 2
Colombia - 6	Korea (South) - 2	S. Africa - 4	Venezuela - 2
Costa Rica - 7	Laos - 11	Seychelles - 1	Vietnam - 1
Cyprus - 1	Libya - 1	Serbia - 1	Zambia - 2
Czech Republic - 1	Malaysia - 10	Singapore - 3	
D. Rep. of Congo - 4	Malta - 1	Slovak Repub. - 2	

For official use only Monitor assigned: _____ Site name: _____ Country: _____
--

SuperSID Space Weather Monitor Request Form

<i>Your information here</i>	
Name of site/school (if an institution):	
Choose a site name: (3-6 characters) No Spaces	
Primary contact person:	
Email:	
Phone(s):	
Primary Address:	Name School or Business Street Street City Country State/Province Postal Code
Shipping address, if different:	Name School or Business Street Street City Country State/Province Postal Code
Shipping phone number:	
Latitude & longitude of site:	Latitude: _____ Longitude: _____

I understand that neither Stanford nor the Society of Amateur Radio Astronomers is responsible for accidents or injuries related to monitor use. I will assure that a surge protector and other lightning protection devices are installed if necessary.

Signature: _____ **Date:** _____

I will need:

<i>What</i>	<i>Cost</i>	<i>How many?</i>
SuperSID distribution USB Power	\$48 (assembled)	
USB Sound card 96 kHz sample rate (or provide this yourself)	\$40 (optional)	
Antenna wire (120 meters) (or you can provide this yourself)	\$23 (optional) with connectors attached and tested	
RG 58 Coax Cable (9 meters) (or provide this yourself)	\$14 (optional) with connectors attached and tested	
Shipping	US \$12 Canada & Mexico \$40 all other \$60	
	TOTAL	\$

_____ I have included a \$ _____ check (payable to SARA)

_____ I will make payment thru www.paypal.com to treas@radio-astronomy.org

or

_____ If you are a Minority-serving institution, in a Developing or economically deprived nation, and/or you are using the monitor with students for educational purposes, you may qualify for obtaining a monitor at reduced or no cost. Check here if you wish to apply for this designation. Then tell us how you want to use the SuperSID monitor. Include type of site, number of students involved, whether public or private school, grade levels, etc. and describe your program.

The goal of the SuperSID project is to provide as many students with systems as possible. If you are able to pay for a system, even if you qualify for a free one, please do so and help support our goal.

For more details on the Space Weather Monitor project, see: <http://sid.stanford.edu>

To set up a SuperSID monitor you will need:

¹ Access to power and an antenna location that is relatively free of electric interference (could be indoors or out)

² A **PC**** with the following minimal specifications:

a. A sound card that can record (sample) up to 96 kHz, or a USB port to connect such a sound card (for North and South America)

i. All other countries can use AC97 sound card with 48 kHz record (sample) rate.
Most computers made after 1997 will have AC97.

b. Windows 2000 or more recent operating system

c. 1 GHz Processor with 128 mb RAM

d. Ethernet connection & internet browser (desirable, but not required)

e. Standard keyboard, mouse, monitor, etc.

³ An inexpensive antenna that you build yourself. You'll need about 120 meters (400 feet) of **insulated** wire. Solid wire is easier to wind than stranded. Magnet wire will work but be more fragile. You can use anything from #18 to #26 size wire. The antenna frame can be made of wood, PVC pipe, or similar materials. We'll provide instructions. You can purchase the wire from us or obtain your own.

⁴ RG58 coax cable with a BNC connector at one end to run from the antenna to the SuperSID receiver. 9 meters is recommended, but the length will depend on where you place the antenna. You can purchase the coax from us or obtain your own.

⁵ Surge protector and other protection against a lightning strike

Return this form to: SuperSID@radio-astronomy.org

or mail to:

SARA Treasurer

c/o Thomas Jacobs

P. O. Box 4245

Wilmington, NC 28406.

Announcing Radio JOVE 2.0

The Radio JOVE Team



Radio JOVE students and amateur scientists from around the world observe and analyze natural radio emissions of Jupiter, the Sun, and our galaxy using their own easy to construct radio telescopes.

Our Project announces Radio JOVE 2.0, where participants assemble a 16-24 MHz radio spectrograph to observe solar, Jupiter, Galactic, and Earth-based natural radio emissions and share their observations with fellow participants.

In the Beginning

Radio JOVE started as a NASA sponsored educational outreach project in 1999. We developed a radio telescope kit suitable for receiving signals from Jupiter, the Sun, the Galaxy, and Earth-based radio emissions. The original kit comprised a radio receiver (RJ1.1) and a dual dipole antenna for 20.1 MHz. An important goal was to teach electronic principles including how to build, solder, and assemble the radio receiver and antenna.

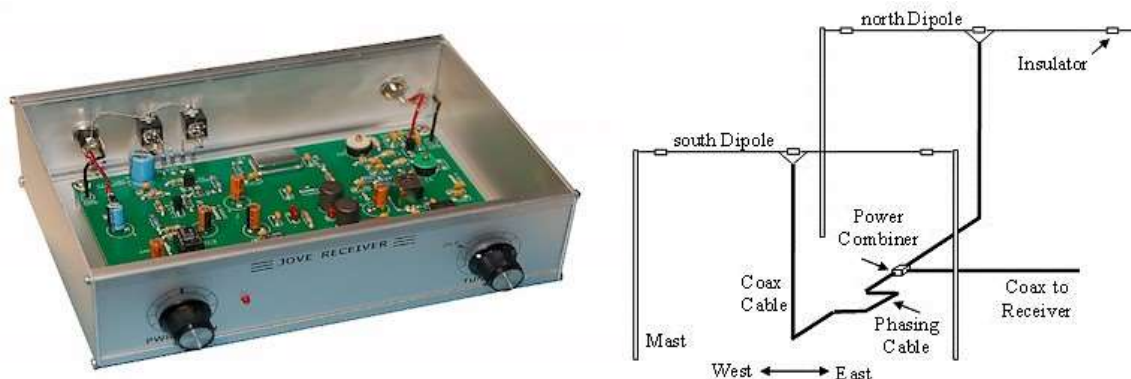


Figure 1. A Radio JOVE RJ1.1 receiver and a schematic of the dual-dipole antenna.

In addition to the hardware, three software packages were developed. These were Radio Jupiter Pro (Jupiter emission prediction program), Radio-SkyPipe (strip chart program) and Radio Sky Spectrograph (control and display of radio spectrograph data).

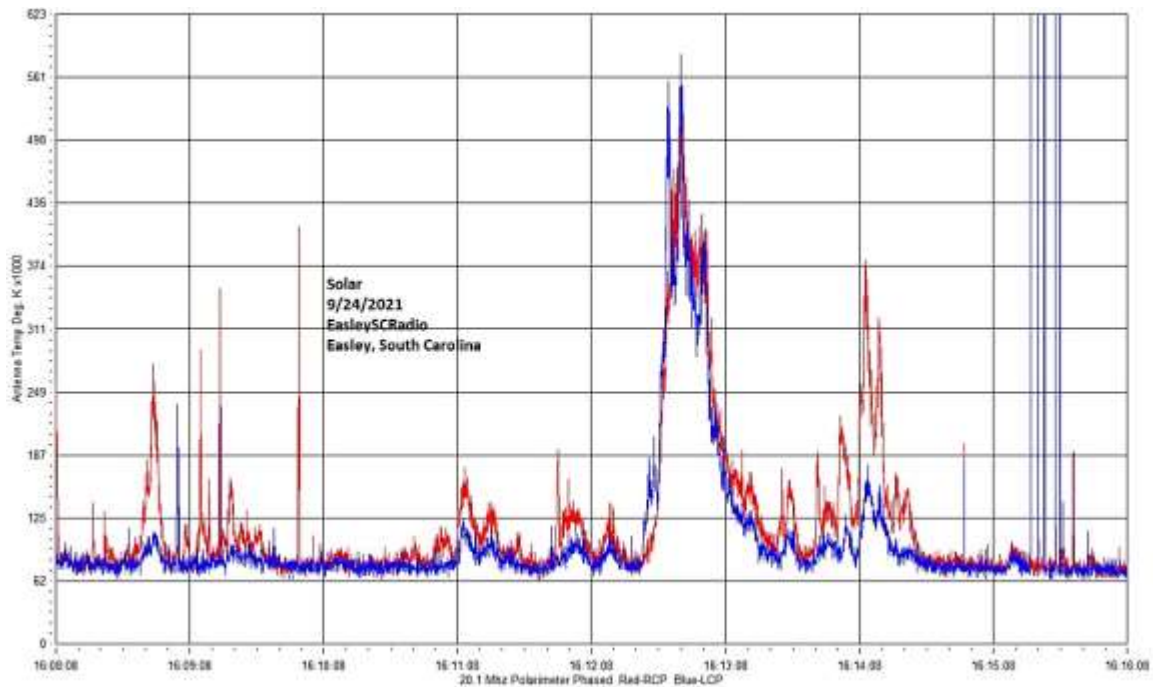


Figure 2. A SkyPipe strip chart showing multiple solar bursts using a JOVE receiver. John Cox, SC.

The Growth of Radio JOVE

As of Autumn 2021, over 2,500 kits have been sold at cost to schools and individuals around the world. Thousands of data submissions from observers have been made to the Radio JOVE data archive.

The Radio JOVE web site has always provided a wealth of information describing observation methods and various educational materials intended to teach radio astronomy techniques and scientific methods. Biannual newsletters are produced, and several telephone help sessions are held each year.

A sub-group of experienced observers known as the Spectrograph Users Group (SUG) evolved from the core JOVE group. These observers developed data collection and analysis techniques using more advanced equipment and techniques. SUG members have contributed to articles published in peer-reviewed scientific journals. This group remains active under the Radio JOVE listserv at <https://groups.io/g/radio-jove/>.

Moving Forward with New Technology

In the past, Radio JOVE provided the hands-on experience of building a radio kit. We have many RJ1.1 receivers in operation successfully contributing scientifically valuable data. It has, however, become increasingly difficult to obtain parts for the RJ1.1 receiver kits and we therefore decided to replace the RJ1.1 receiver with a new SDR-based design for the receiver portion of our radio telescope kits. While we continue to support the hardware and software for the original RJ1.1 receivers, the only kits now available for purchase from Radio JOVE contain this newly designed system.

In recent years, new technologies have made software defined radios (SDRs) ever more affordable. These radios can operate on a single frequency like the original JOVE receiver but can also generate spectrograms which depict radio activity as a function of both time and frequency. Such displays offer new insights into our studies of the Sun, Jupiter, the Galaxy, and both natural and artificial Earth-based radio emissions.

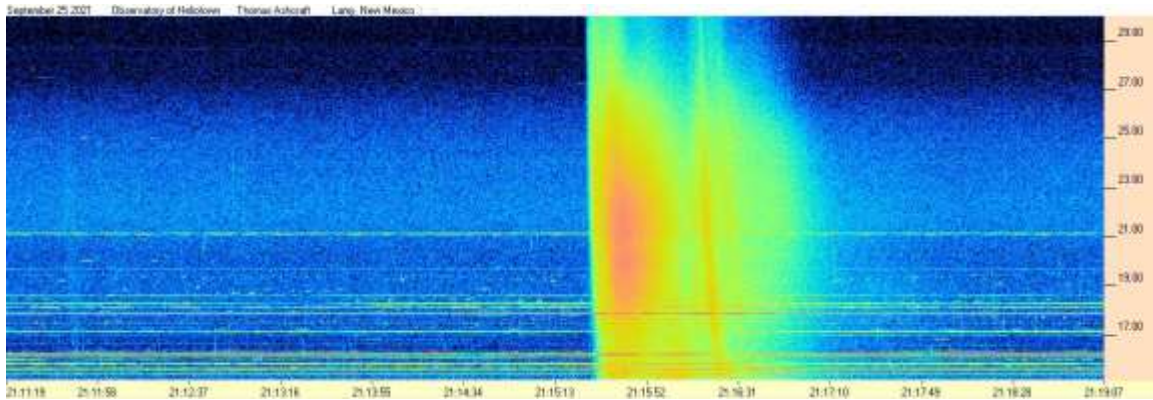


Figure 3. Radio spectrogram showing multiple solar bursts received by Tom Ashcraft in New Mexico. Horizontal scale is time, and the vertical scale is frequency. Amplitude is displayed using different colors corresponding to the strength of signals.

Radio JOVE continues to sell radio telescope packages including an antenna, receiver, and software; however, the receiver is now a commercially built SDR.



Figure 4. The JOVE team has had considerable success with the SDRPlay RSP1A unit and will provide support for using this instrument for our radio astronomy program. Not all SDR types can be supported, but it is our intent to provide support for some other SDRs as they become available during this period of rapid SDR development.

It continues to be our goal to introduce new observers to the scientific method and help them experience the thrill of receiving cosmic radio signals. Through a series of educational training modules and observing and analysis projects we aim to guide new observers to levels where they can contribute to Citizen Science projects.

We continue to support our large user base that uses JOVE RJ1.1 receivers – both in terms of technical support for the receivers but also with new and exciting observing projects for both RJ1.1 and SDR users.

We welcome both new and experienced observers to the JOVE 2.0 program as we share the excitement of receiving, studying, and understanding radio signals from our corner of the galaxy.

Please see the Radio JOVE web site at <https://radiojove.gsfc.nasa.gov> for more information.



RADIO JOVE 2.0 RADIO TELESCOPE KIT ORDER FORM

Order Online using PayPal™

* * * Please allow 2 to 3 weeks for delivery. * * *

IMPORTANT: Before you order the Jove receiver kit and/or the antenna kit, we suggest that you read the on-line manuals. You will need to provide additional materials and tools to complete the antenna. The cost of additional materials for the antenna support structure (masts, etc.) may be in the range of US\$75 to US\$100. Also note that the optimal antenna height can be up to 20ft, depending upon your latitude.

<p>Item # RJK2u – Complete 2.0 Kit: Receiver + Unbuilt Antenna Kit + Software</p> <p>This kit includes an SDRplay RSP1A, USB Cable, SMA/BNC cable, F-adapter, unbuilt Antenna Kit (RJA), printed assembly manuals, and Radio-Sky Spectrograph (RSS) software.</p> <p>Note: Kit does not include antenna support structure.</p> <p>Price: \$215 + Shipping (See reverse for shipping)</p>	<p>Item # RJK2p – Complete 2.0 Kit: Receiver + Professionally Built Antenna Kit + Software</p> <p>This kit includes an SDRplay RSP1A, USB Cable, SMA/BNC cable, F-adapter, Professionally Built Antenna Kit (RJA2), printed assembly manuals, and Radio-Sky Spectrograph (RSS) software.</p> <p>Note: Kit does not include antenna support structure.</p> <p>Price: \$384 + Shipping (See reverse for shipping)</p>
<p>Item # RJA – Unbuilt Antenna Kit</p> <p>The RJA Radio JOVE Antenna Kit includes a printed construction manual, stranded copper easy-to-solder antenna wire, ceramic insulators, RG-59 easy-to-solder coax cable, screw-on F connectors, and a power combiner.</p> <p>Note: Kit does not include antenna support structure. Assembly requires a soldering gun and other tools.</p> <p>Price: \$90 + Shipping (See reverse for shipping)</p>	<p>Item # RJA2 – Professionally Built Antenna Kit</p> <p>The RJA2 Radio JOVE Antenna Kit includes a printed installation manual, two professionally assembled dipole antennas constructed of #14 Copperweld wire with Budwig center insulators and center support rope attachment points, high quality RG-6 coax with pre-installed commercial grade connectors, and a power combiner.</p> <p>Note: Kit does not include antenna support structure.</p> <p>Price: \$249 + Shipping (See reverse for shipping)</p>
<p>Item # LTJ2 – Listening to Jupiter, 2nd Ed. by R. S. Flagg</p> <p>PDF download of Richard Flagg's book "Listening to Jupiter, 2nd Ed., 2005". The file is downloaded from a secure website.</p> <p>Price: \$10 + \$0 shipping (PDF file download)</p>	<p>Item # RJR2 – Radio JOVE 2.0 Receiver-Only Kit</p> <p>This kit includes one SDRplay RSP1A SDR receiver, USB Cable, SMA/BNC cable, and F-adapter, printed assembly manuals, and Radio-Sky Spectrograph (RSS) software.</p> <p>Price: \$135 + Shipping (See reverse for shipping)</p>

RADIO JOVE 2.0 RADIO TELESCOPE KIT ORDER FORM (continued)

Order Online at https://radiojove.net/kit/order_form.html

OR

Complete this form and mail with payment

Payment may be made by Credit Card via PayPal™, U.S. Check, U.S. Money Order, International Money Order in U.S. funds drawn on a U.S. bank, or Western Union Money Transfer made payable to **The Radio JOVE Project**. No bank-to-bank wire transfers are accepted. Purchase Orders are accepted from U.S. Institutions.

Send to: The Radio JOVE Project
 1301 East Main St
 MTSU Box 412
 Murfreesboro, TN 37132, USA
 email: chiggins@mtsu.edu
 FEIN: 20-5239863

Item	Description	Quantity	Item Price	Shipping (see below)	Subtotal
RJK2u	Complete Radio JOVE 2.0 Kit Receiver + unbuilt Antenna		\$215		
RJK2p	Complete Radio JOVE 2.0 Kit Receiver + Professionally Built Antenna		\$384		
RJA2	Professionally Built Antenna-Only Kit		\$249		
RJA	Unbuilt Antenna-Only Kit		\$90		
RJR2	Receiver-Only Kit		\$135		
LTJ2	Listening to Jupiter, 2 nd Ed., by R.S. Flagg (PDF download)		\$10	\$0	
Total:					

Shipping Fees for Radio JOVE: We ship all packages using USPS Priority Mail flat rate boxes.
 U.S.A.: \$17.00
 Canada: \$57.00
 All Other International Shipping: \$85.00

Ship to: (Please print clearly)

Name: _____
 Address: _____
 City, State, Postal Code: _____
 Province, Country: _____
 Email: _____

Visit the Radio JOVE web site and fill out the team application form at https://radiojove.net/sign_up_form.php even if you are just an interested individual so that you can receive important information about kit updates, online services, and activities within the project as they occur!



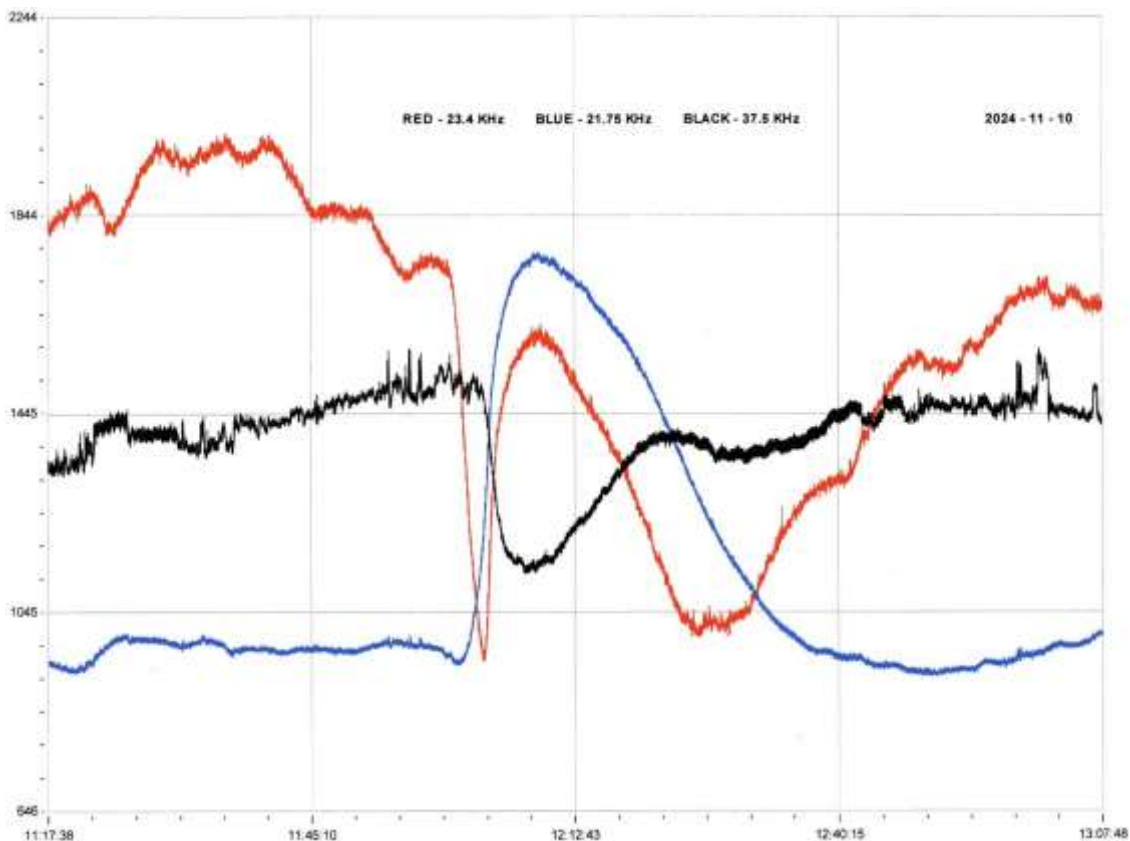
Please send questions, reports, and observations to John Cook: jacook@jacook.plus.com
BAA Radio Astronomy Section, Director: Paul Hearn

RADIO SKY NEWS

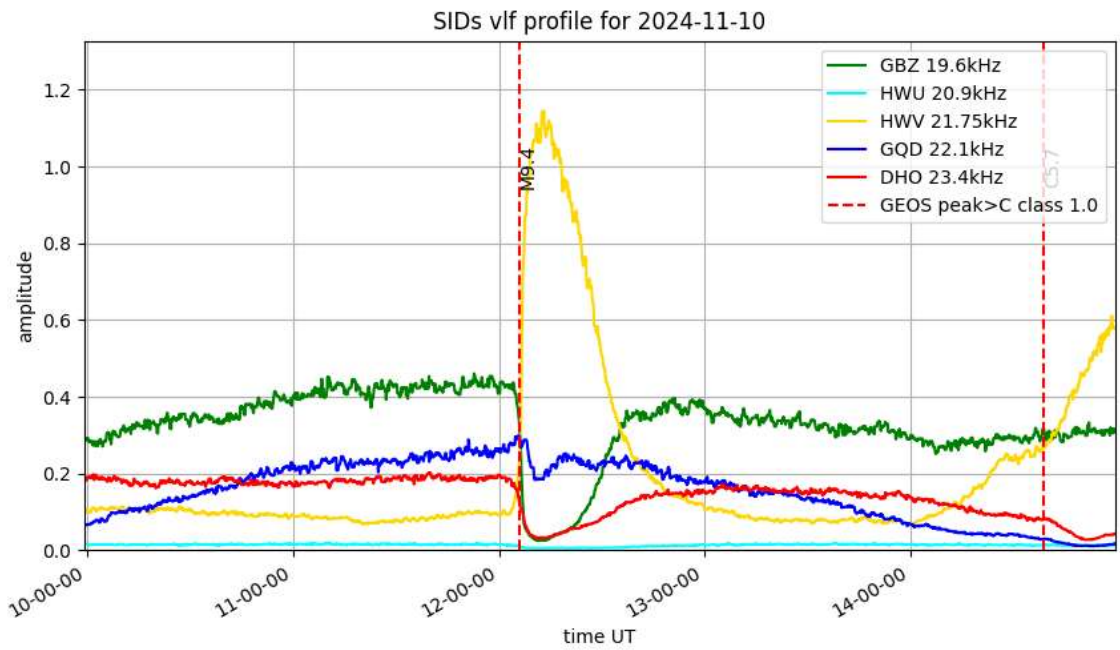
2024 NOVEMBER

VLF SID OBSERVATIONS

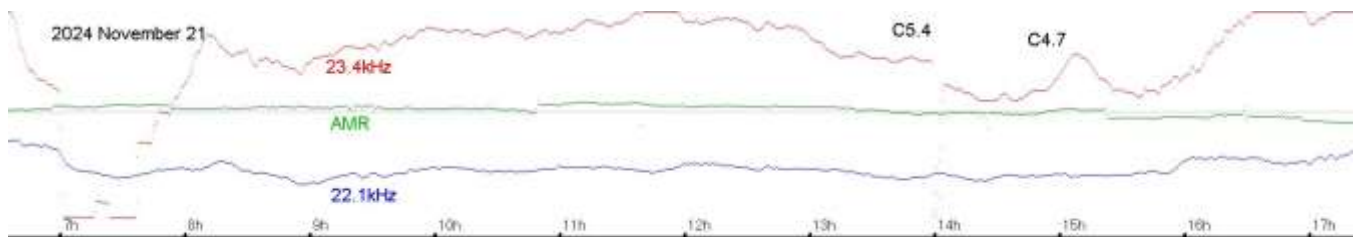
Solar flare activity has been slowly decreasing over the last three months, a total of 83 classified flares being recorded as SIDs in November. In October there were 91. The strength of the flares has however increased slightly, with 51% C-class and 48% M-class. In October it was 66% C-class and 33% M-class. We did only record a single X-flare, compared with three in October. Some of our signals have been very disturbed due to the low solar altitude, so this has perhaps biased our detection ability to the stronger events. There are also plenty of flares that have overlapped to produce double peaked SIDs on some signals, and single SIDs on other signals.



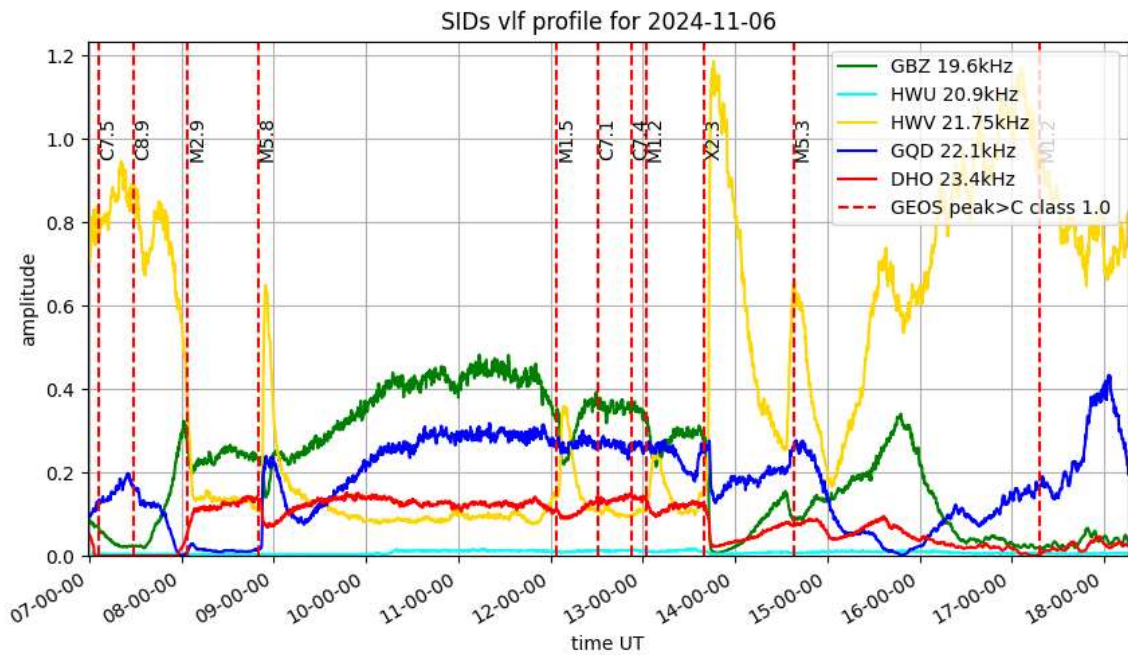
This recording by Colin Clements shows the M9.4 flare peaking just after midday on the 10th. Just shy of X-category, these three signals very clearly show the different SID shapes. 21.75kHz (blue) has a rising signal, while 37.5kHz (black) is inverted. 23.4kHz (red) has a ‘spike and wave’ shape, its true peak clearly aligned with the other two shapes.



This recording by Mark Prescott includes some more signals, a very strong response recorded at 21.75kHz. The other signals have all produced a fall in signal strength.

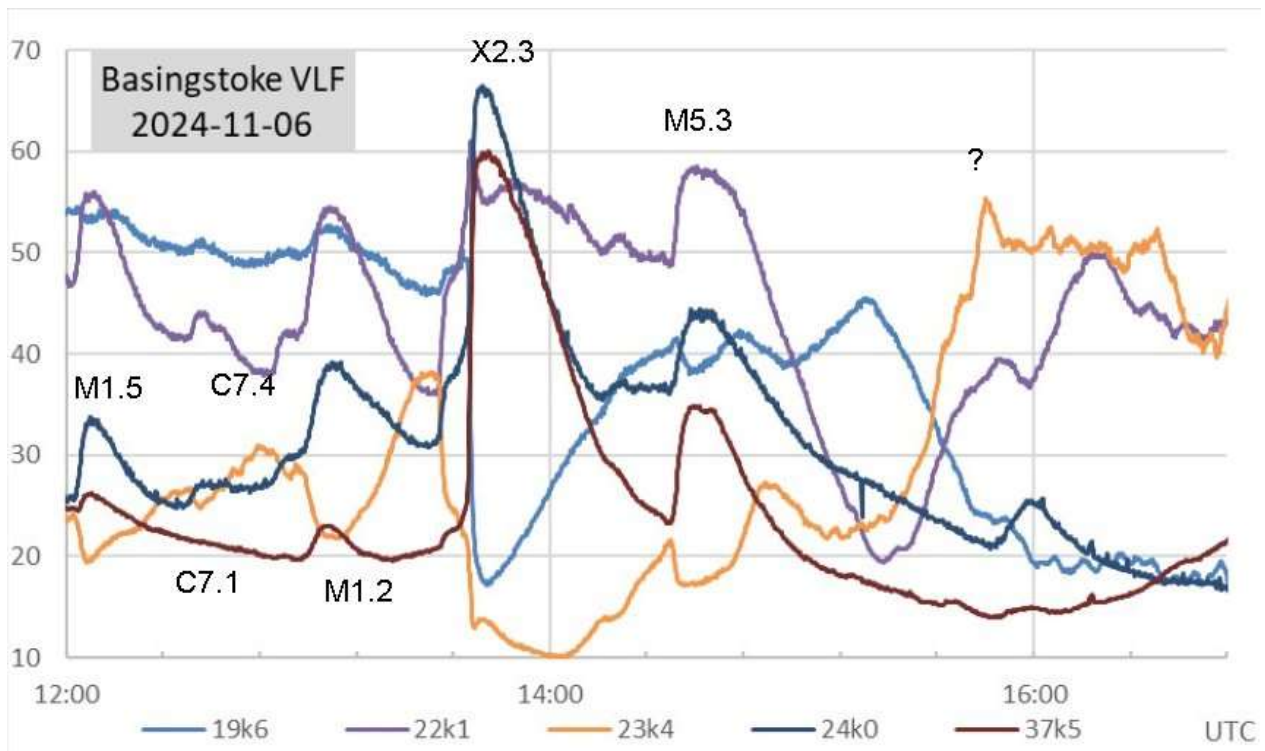


Not all days were as clear as the 10th. My recording shows the 21st, with a very noisy 23.4kHz. The two C-class flares have been completely hidden by the general ionospheric instability. I have marked their rough positions. It also shows the very early sunset, starting around 15:30UT.

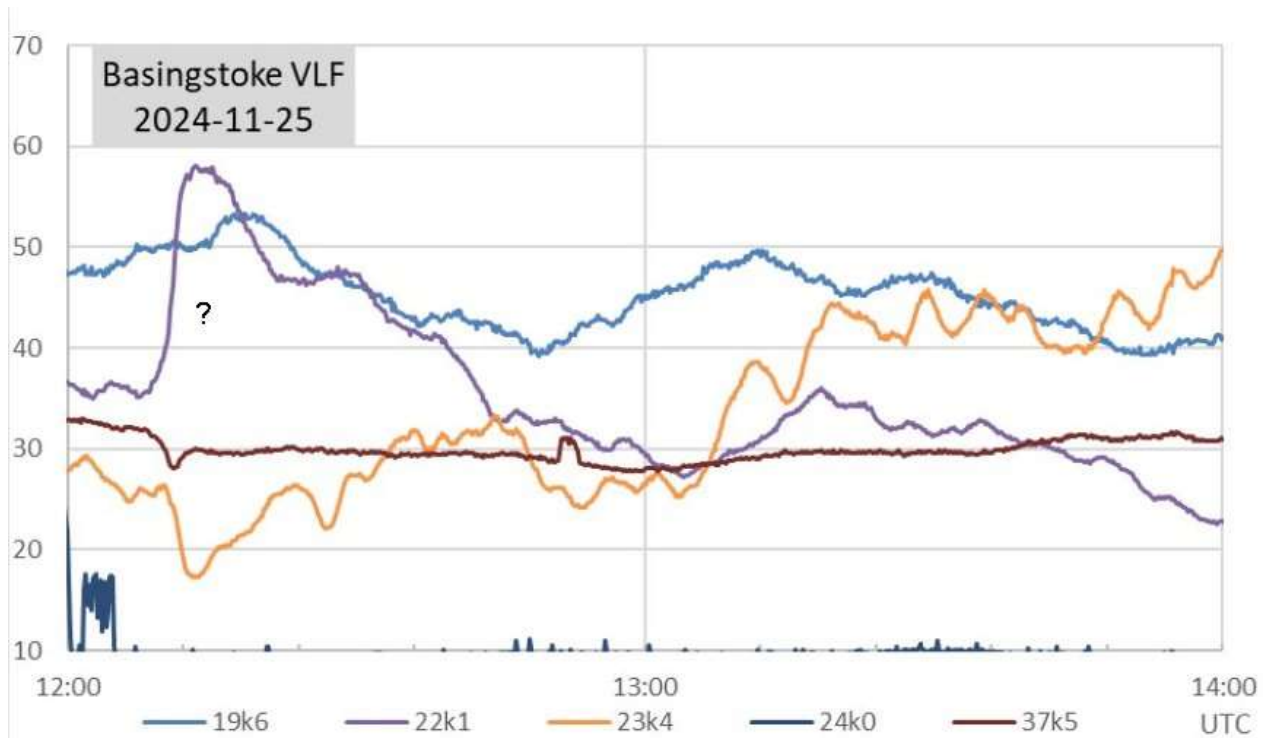


The 6th was the busiest day in November, including the X2.3, shown in Mark Prescott's recording.

The strongest of the flares are clearly recorded as SIDs, but the strong C7.1 and C7.4 flares are well hidden.

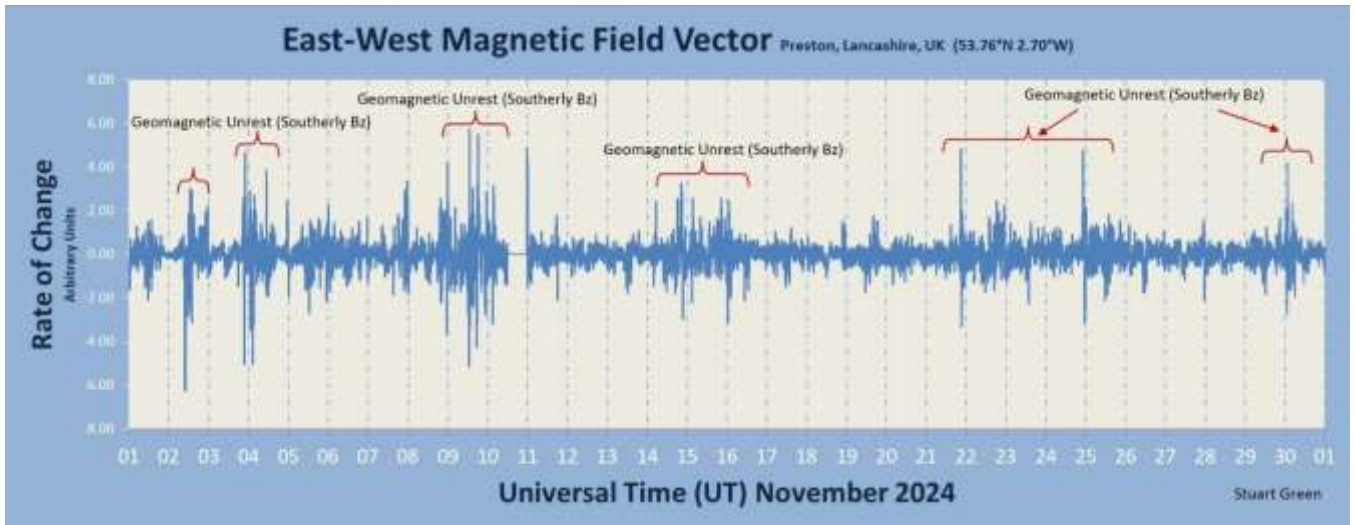


Paul Hyde’s recording shows just the afternoon period but again shows a very weak response to the C7.1 and C7.4 flares. The X2.3 flare is interesting as all of the signals appear to have a double-peaked SID; an effect not seen in other recordings. The ‘spike and wave’ SID at 23.4kHz has a very strange shape, tricky to analyse without guidance from the other signals. This was the only X-flare in the GOES satellite data for November, so we were lucky that it was so well timed.

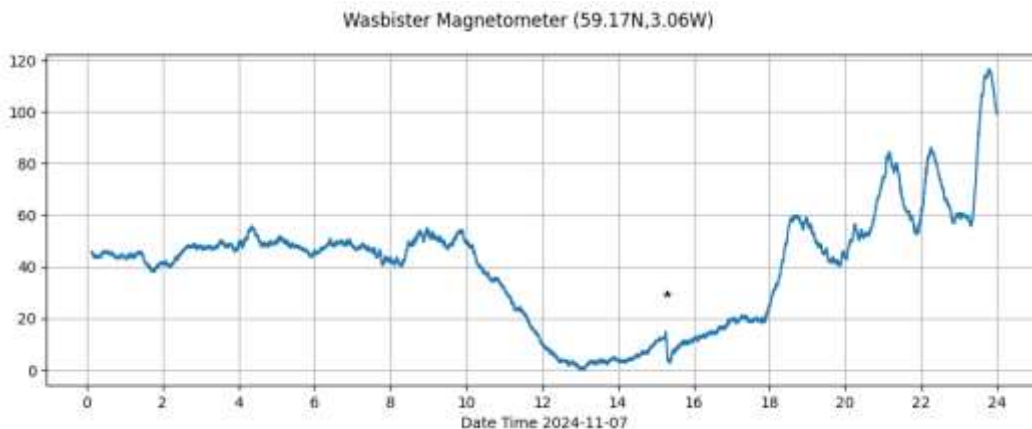


Activity decreased towards the end of the month, Paul Hyde’s recording from the 25th showing just a single unclassified SID during the afternoon. This event was recorded by nine observers, and so is not local interference. There was an M9.4 flare early in the morning followed by a C5.4 flare at 10:48UT, but they were not widely recorded.

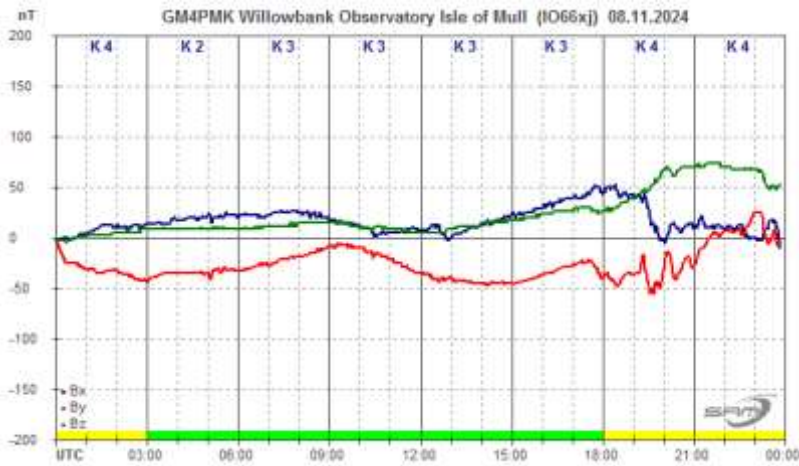
MAGNETIC OBSERVATIONS



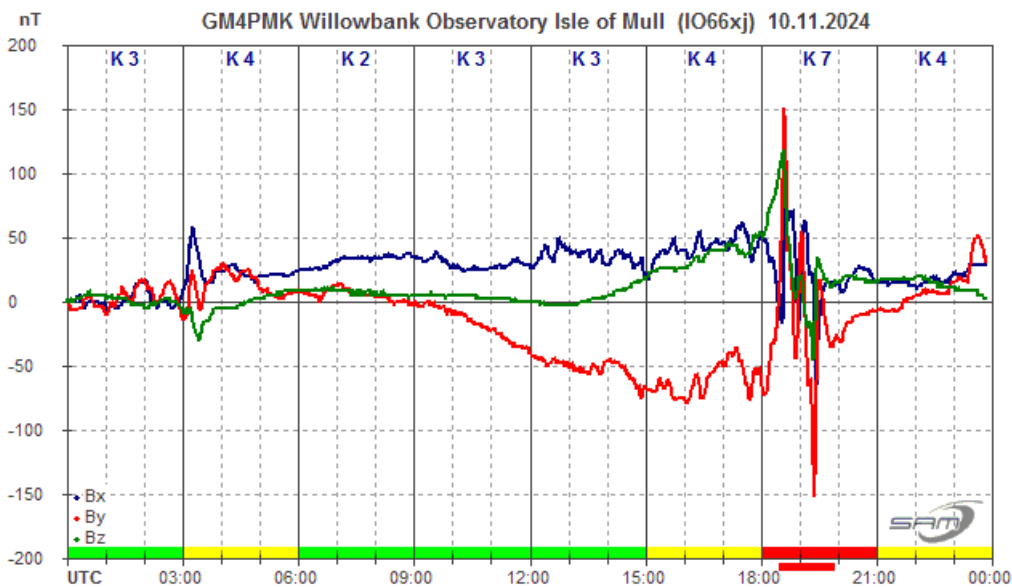
Stuart Green's summary of the month's activity shows some disturbance through most of the period. The Bartels chart also shows long periods of disturbance. Most of the activity was fairly mild and appears to be from the solar wind rather than CMEs. We did record one potential CME impact, shown in Callum Potter's chart from the 7th:



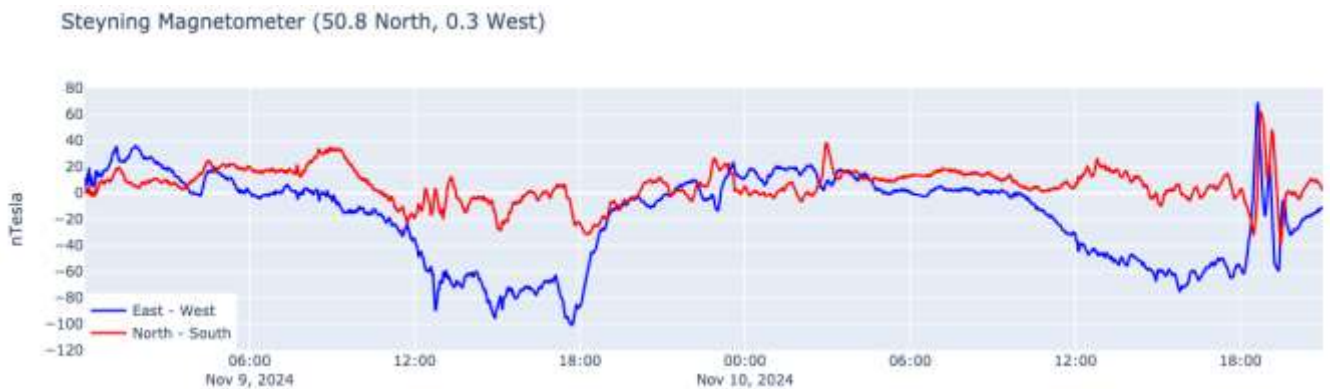
The impact is at about 15:15 UT, marked '*.' The STCE bulletin suggests that a CME from the 4th was the cause. There were lots of strong flares early in the month, some with CMEs directed away from Earth, so the exact source is not known. The resulting activity was very mild, shown in Roger Blackwell's recording from the 8th:



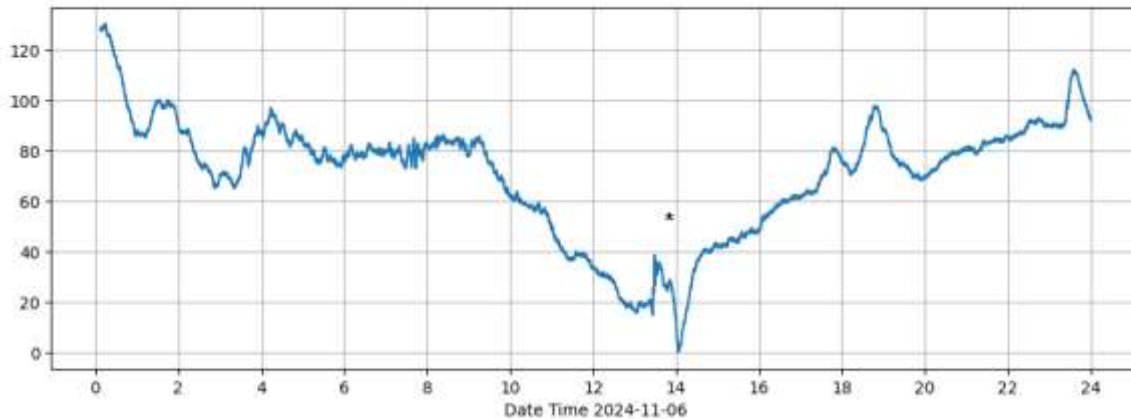
The most active period was the evening of the 10th. This appears to be due to a turbulent solar wind, possibly assisted by small CME effects.



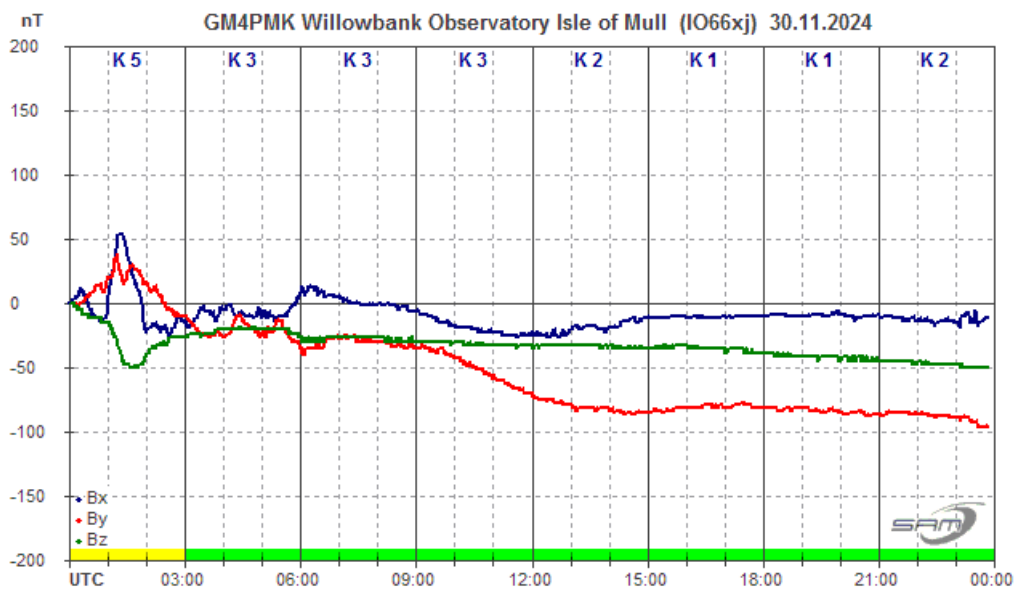
Roger Blackwell's chart shows the short active period from 18UT to 20UT, with a smaller disturbance earlier in the morning. Nick Quinn's recording also includes some activity on the previous day.



Wasbister Magnetometer (59.17N,3.06W)

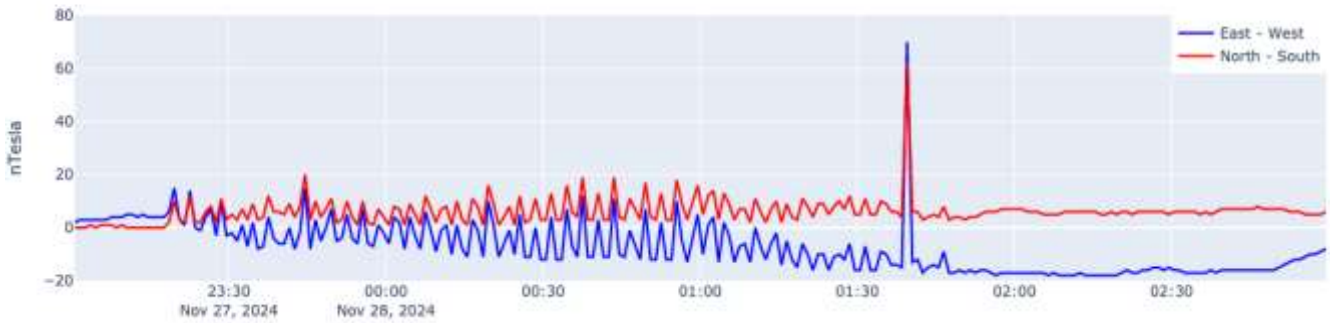


The X2.3 flare at 13:43 on the 6th has produced a Solar Flare Effect (SFE), where the sudden increase in ionisation of the D-region causes a strong electrical current to flow, thus rapidly altering the local magnetic field. Callum Potter has recorded this, marked ‘*’ on his chart.



Magnetic disturbance remained very mild for the rest of the month, Roger Blackwell’s recording from the 30th showing some weak effects from the solar wind.

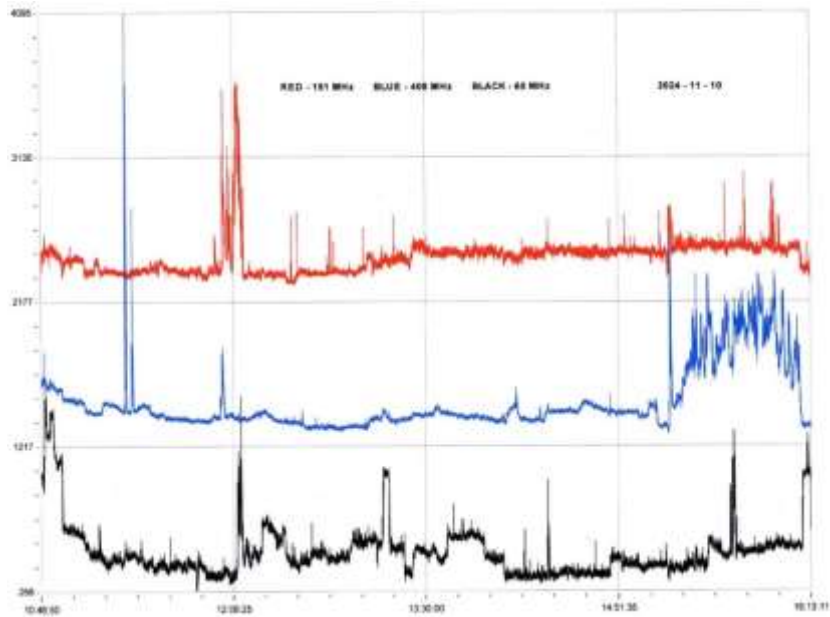
Steyping Magnetometer (50.8 North, 0.3 West)



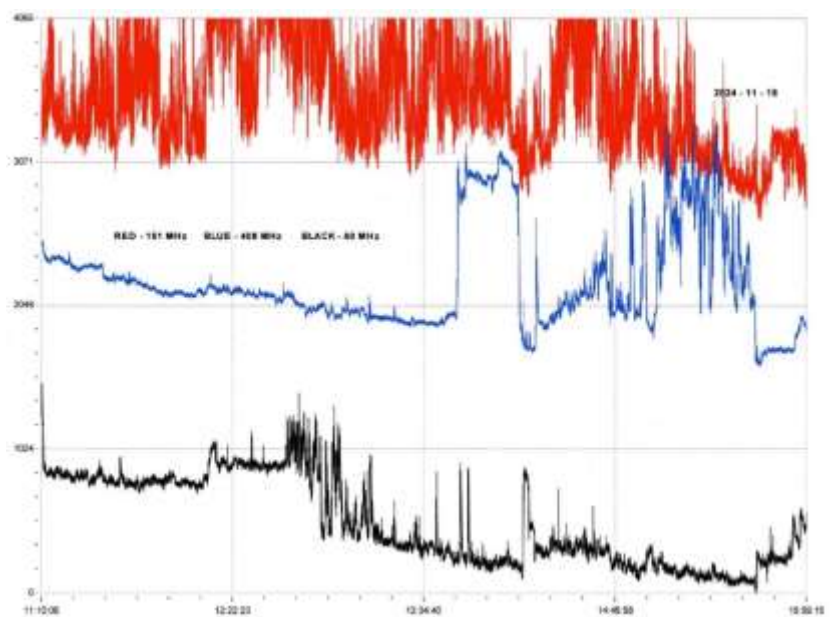
This recording from the 27th – 28th by Nick Quinn is rather a mystery. At first it looks very much like the example of PC2 waves shown in the October report, except that these waves have a period of about 3 minutes compared to 8 seconds for the PC2 waves. The sharp spike at the end of the cycle is also very different. None of our other observers have recorded anything similar, and so it must be some sort of local interference. The source however is unknown. A similar, but weaker, example was recorded on the 18th – 19th. Nick has eliminated household appliances as the cause by noting when they are used. All of the local interference that I have seen usually shows with sharp edges rather than a smooth cyclical pattern. I have seen the effects of local seismic disturbance of the sensor, but that would not be expected to last for over two hours. I have found references to minor seismic events in the north of England over this period, but nothing near the south coast. All suggestions welcome!

Magnetic observations received from Roger Blackwell, Callum Potter, Nick Quinn, and John Cook.

SOLAR EMISSIONS

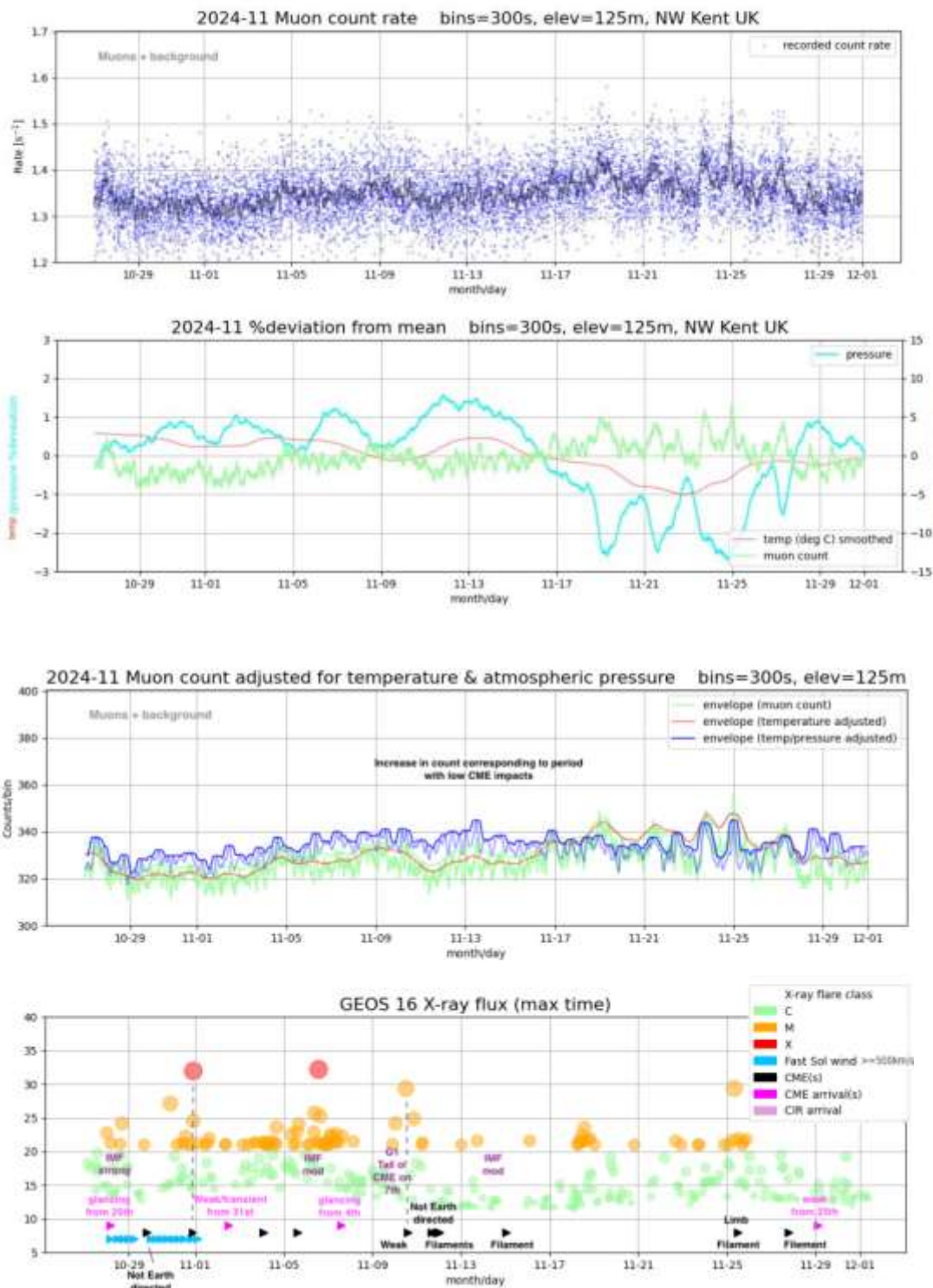


We recorded just a single SID on November 10th, from an M9.4 flare peaking at about 12:06–12:08UT. Colin Clements recorded a strong noise pulse on all three of his frequencies that match this flare very well. The 408MHz (blue) signal later in the day matches a smaller flare that we did not record as a SID.



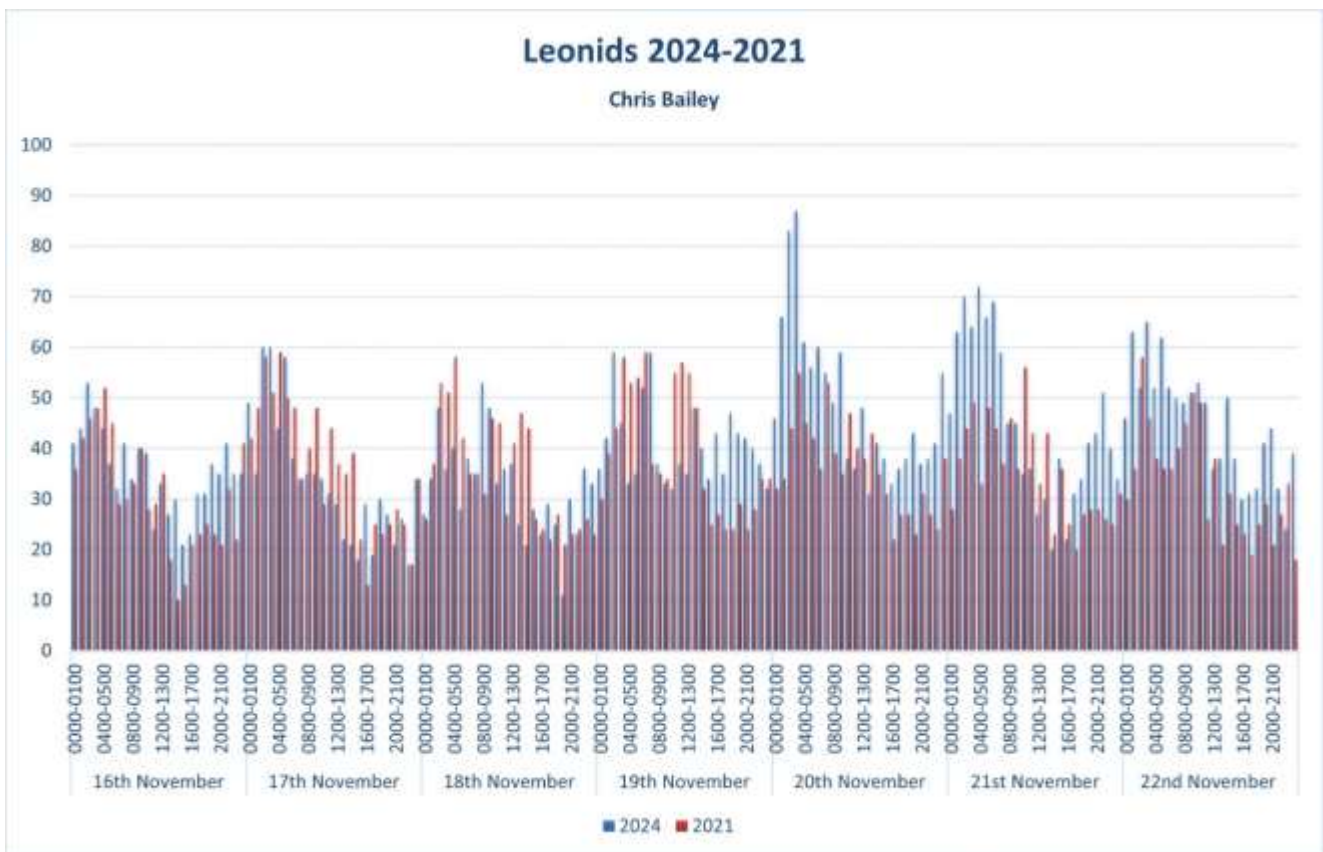
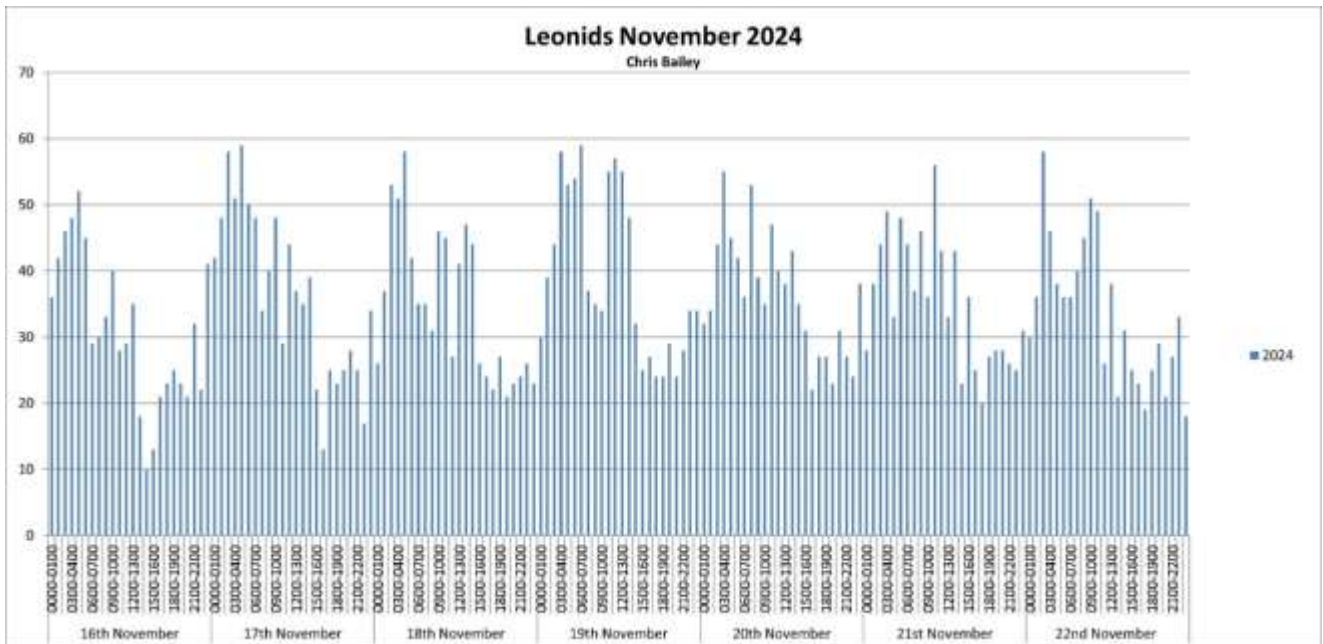
We recorded five M-class flares during the morning of the 18th, which may well have caused the 151MHz (red) noise in Colin’s recording. 60MHz (black) has a shorter burst of noise that could be from the M3.7 flare, while 408MHz shows more noise later in the afternoon. A C4.3 flare later in the afternoon may well be related, although precise relationships are not clear. A very confusing pattern of activity.

MUONS



The Muon charts recorded by Mark Prescott show the dramatic drop in atmospheric pressure at the end of November as much as they show the Muon count. The raw data in the top chart shows the rise in Muon count with the low pressure, although the cause of the peaks on the 23rd and 24th is not clear. Higher solar activity earlier in the month has pushed up the counts, reaching a maximum by the 13th.

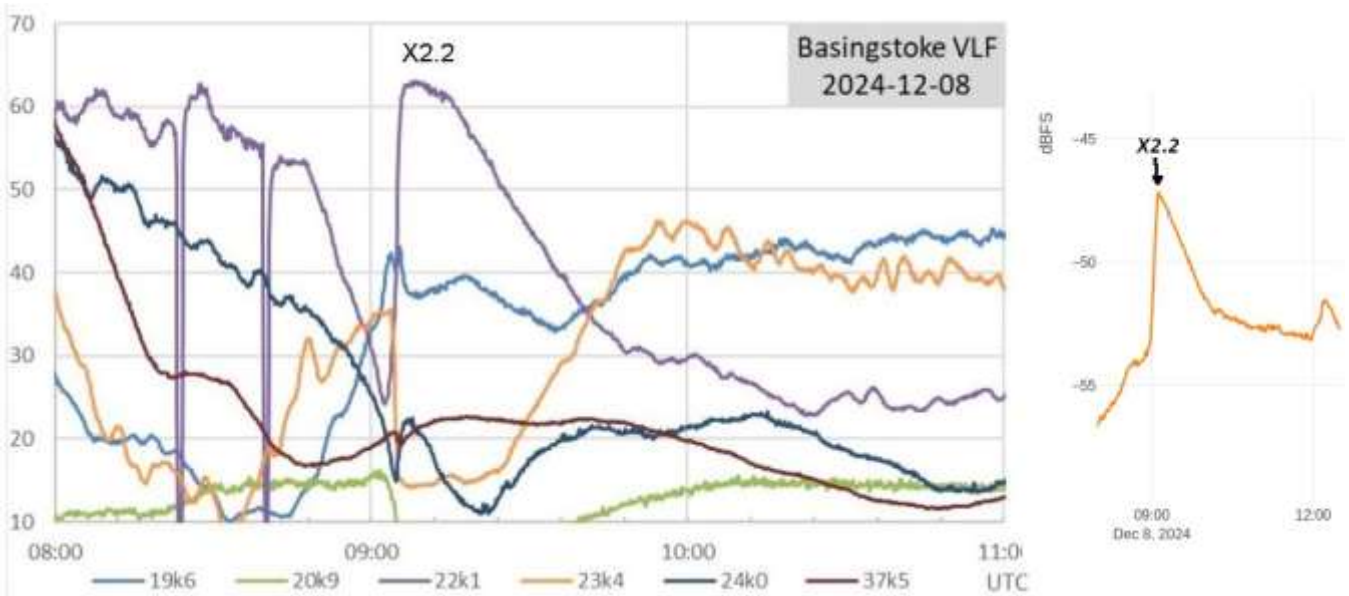
METEORS



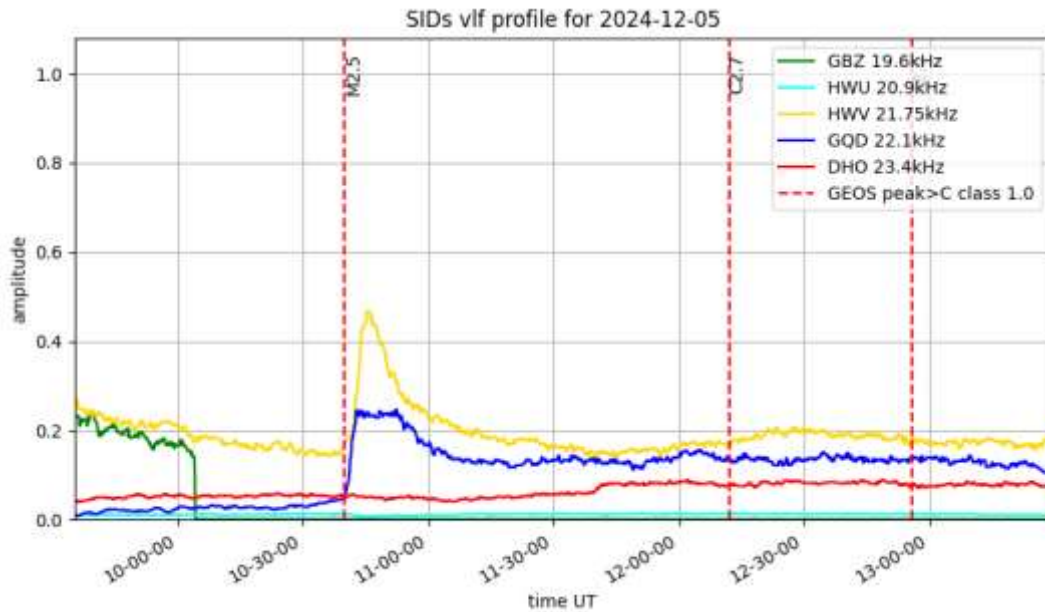
Chris Bailey recorded the annual Leonid meteor shower, comparing it with his data from 2021. Counts seem to be fairly consistent from the 16th to 22nd, with a small peak on the 20th. Each day shows a peak early in the morning, as expected, with lower counts during the afternoon.

VLF SID OBSERVATIONS

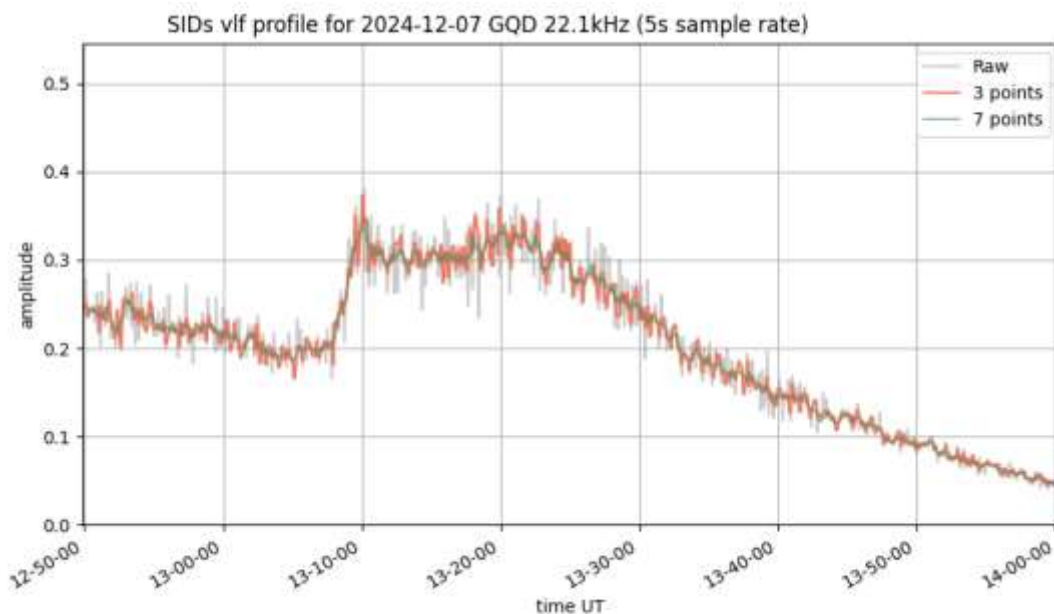
The number of SIDs recorded has been slowly decreasing since September, partly due to the shorter day lengths after the autumn equinox. The relative sunspot count, R, has also been slightly lower over this period. In December we recorded 33 M-class and 33 C-class flares, as well as a single X-flare. Signals have again been very noisy, hiding many C-class flares, and also making some SIDs from M-flares hard to see. 23.4kHz took its usual holiday break from December 23rd to the 31st.



The X2.2 flare on the 8th was widely recorded, despite being very early in the morning. The left chart is by Paul Hyde, showing a very strong response on the 37.5kHz signal from Iceland. The American 24kHz also shows a clear spike-and-wave SID at the end of the sunrise dip. The right-hand chart is from Thomas Mazzi in Italy. The flare was produced by AR13912, which also produced much of the flaring in the previous week. It was very close to the solar limb at the time, rotating out of view over the next few days.

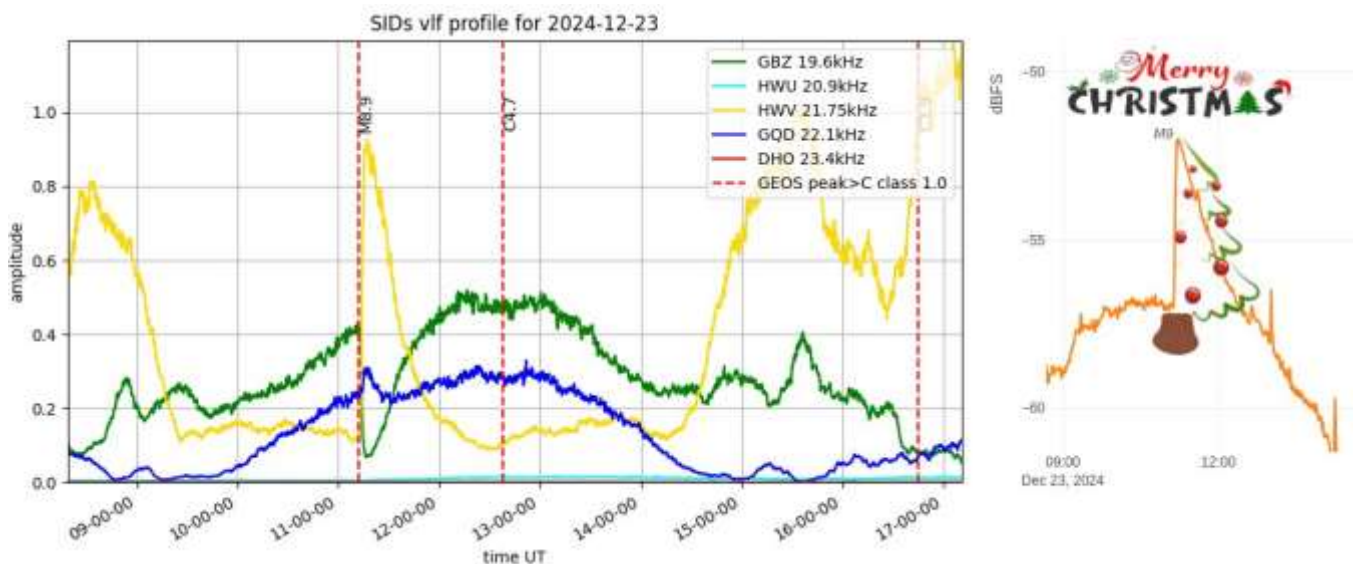
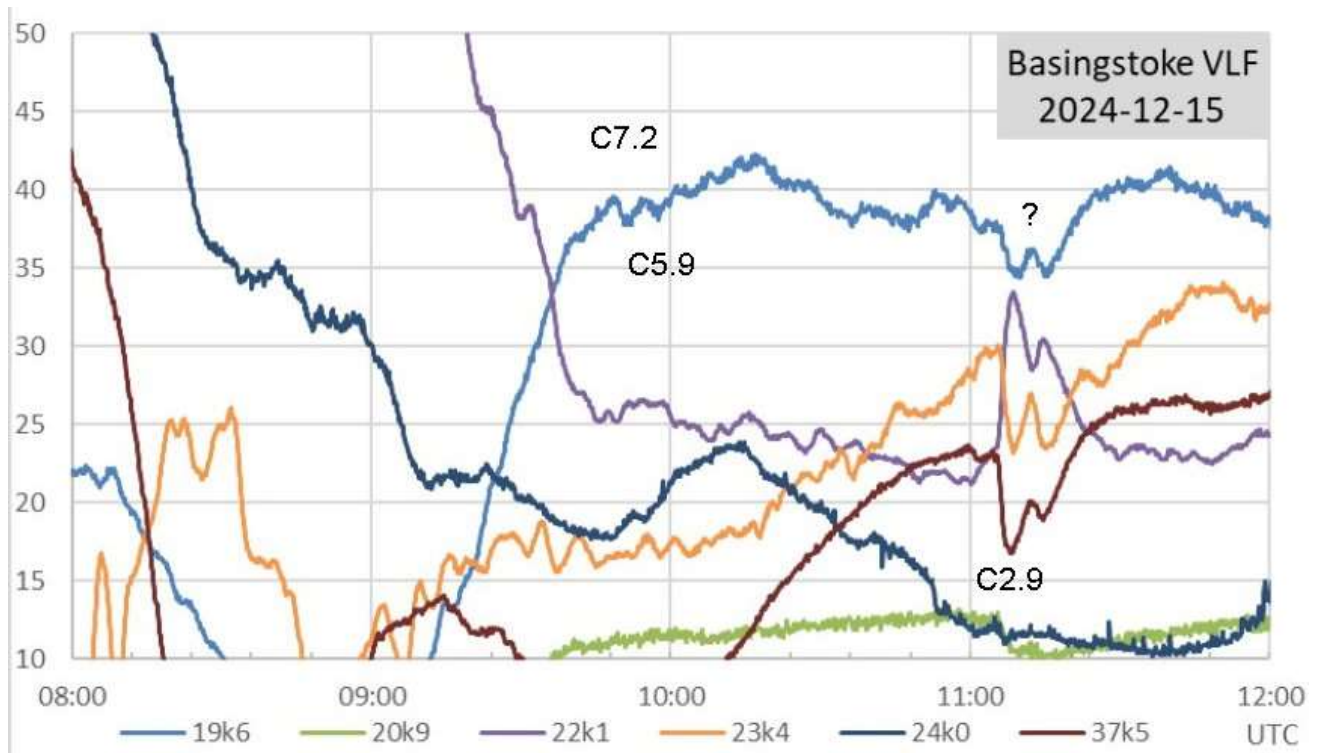


Mark Prescott noticed some very unusual looking SIDs at 22.1kHz, this one from the 5th apparently having a flat top. 21.75kHz shows a normal SID. This was from an M2.5 flare. 23.4kHz was active at the time but shows no response. A similar effect was seen from the M2.3 flare on the 7th. Mark has produced a more detailed recording of this SID, showing that it has a very shallow spike-and-wave shape. The SID on the 5th is right on the borderline, where the sky wave / ground wave interference pattern has matched the change in X-ray flux very closely during the flare's peak.



The strong M-flaring continued through to the 13th, followed by a short period of very low activity. On the 15th we recorded six small C-flares, some of which are shown in Paul Hyde's recording on the next page. The C7.2 and C5.9 flares have been lost in the early

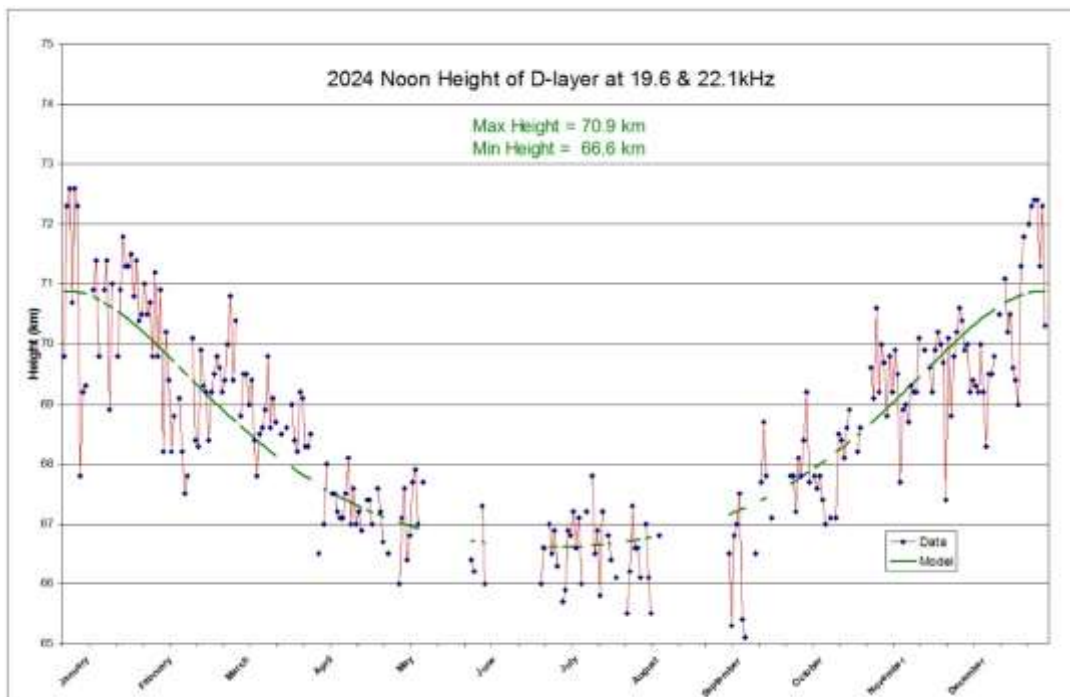
morning noise on most of the signals, with just a hint of SIDs at 19.6kHz. The later C2.9 flare has produced a very clear SID, despite being much weaker. It appears with two peaks on most of the signals, although 20.9kHz and 24kHz show little effect.

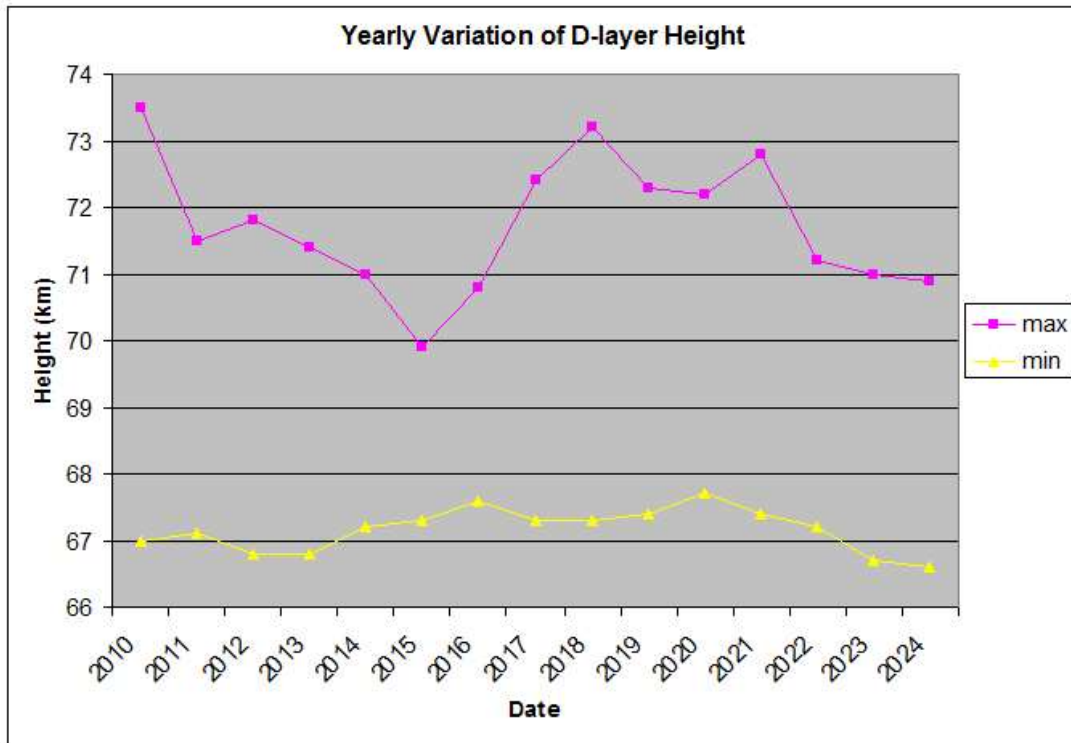


Flaring strength increased again after the 19th, with an M8.9 recorded on the 23rd. Mark Prescott's recording on the left shows clear SIDs on all of the active signals. The later C4.7 flare was not recorded. Thomas Mazzi has decorated his recording of the M8.9 SID to suit its seasonal appearance.

This strong activity continued to the end of the month, the satellite X-ray data including three more X-flares. These were during our night-time, so were not recorded. In 2024 we recorded a total of 2080 SIDs compared to 1294 in 2023.

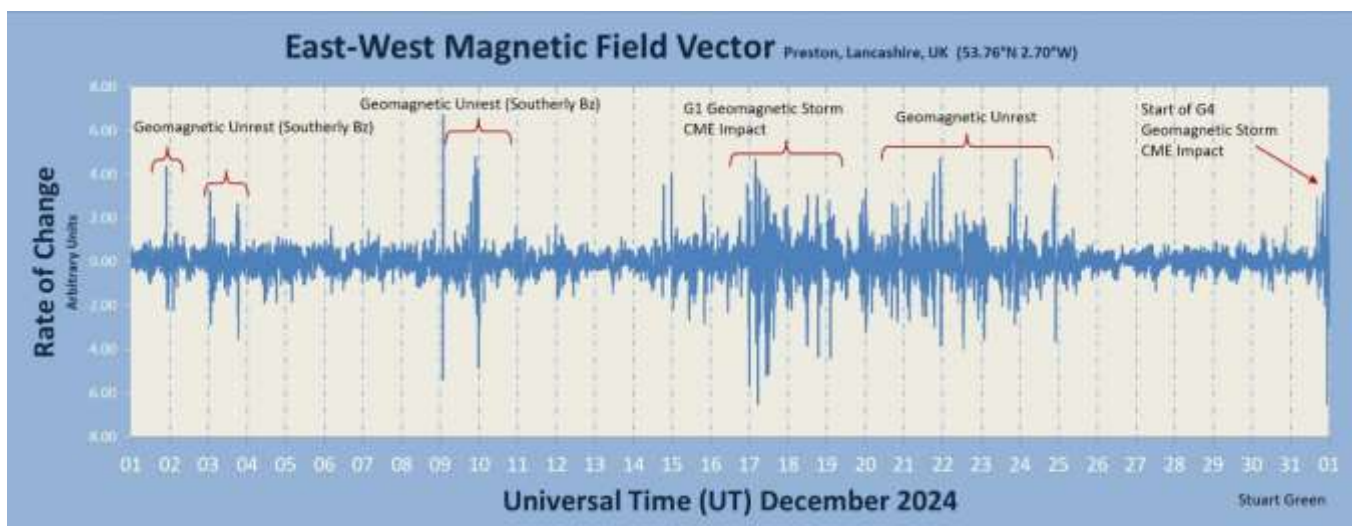
Mark Edwards has provided a chart of the D-region height during the year, analysed from his VLF recordings at 19.6 and 22.1kHz. There are some breaks during the summer when data was not available. The raw data (red trace) is quite variable during the winter months but is more stable than in 2023.





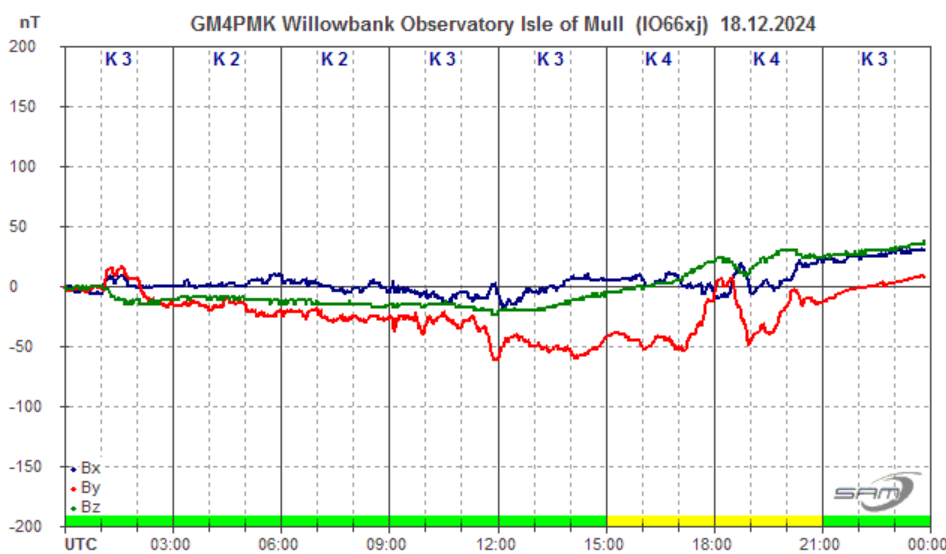
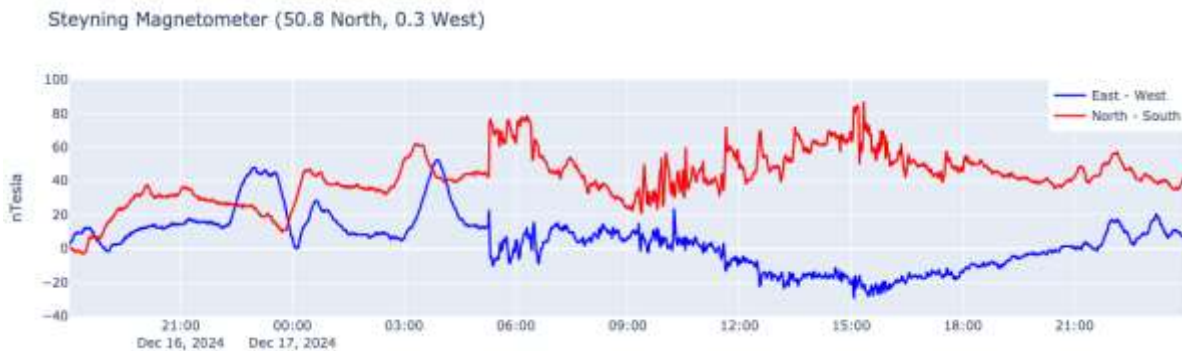
The lower chart shows how the heights have varied since 2010. 2012 to 2015 was the peak of cycle 24 and shows the lowest of the maximum heights. We are currently in the maximum period of cycle 25, again showing lower maximum heights due to the higher levels of X-ray flux. The minimum heights show much less variability.

MAGNETIC OBSERVATIONS

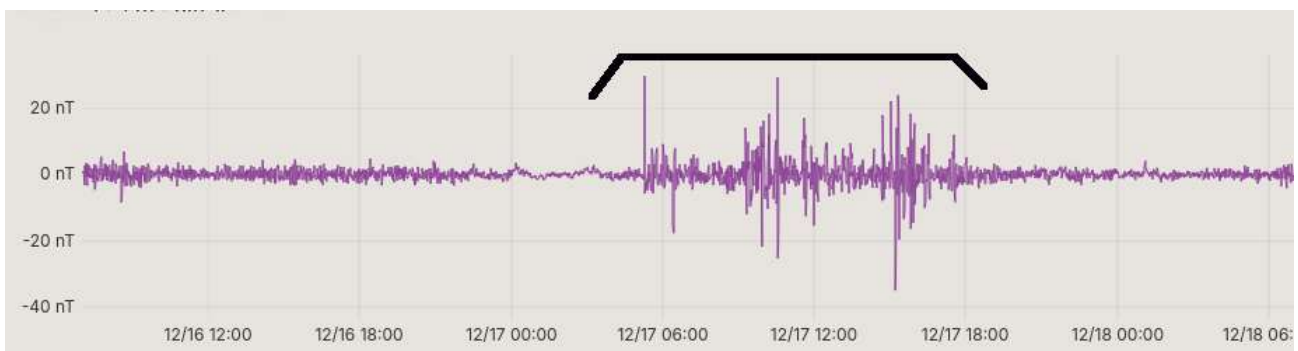


Stuart Green's summary of December's magnetic activity shows a long period of disturbance starting on the 15th, just as the solar flare activity was falling. On the 17th there

was a very strong CME impact recorded at 05:15UT with a magnitude of about 40–50nT. It is very clear on Nick Quinn’s recording:

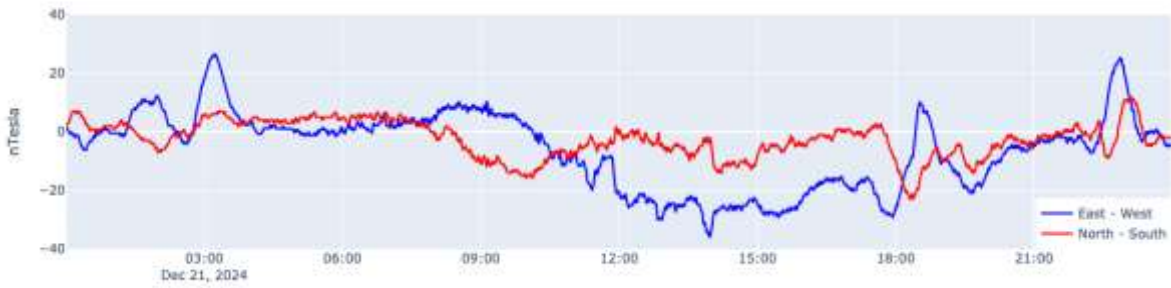


The disturbance faded out in the evening of the 17th, with just a mild disturbance on the 18th shown in Roger Blackwell’s recording.

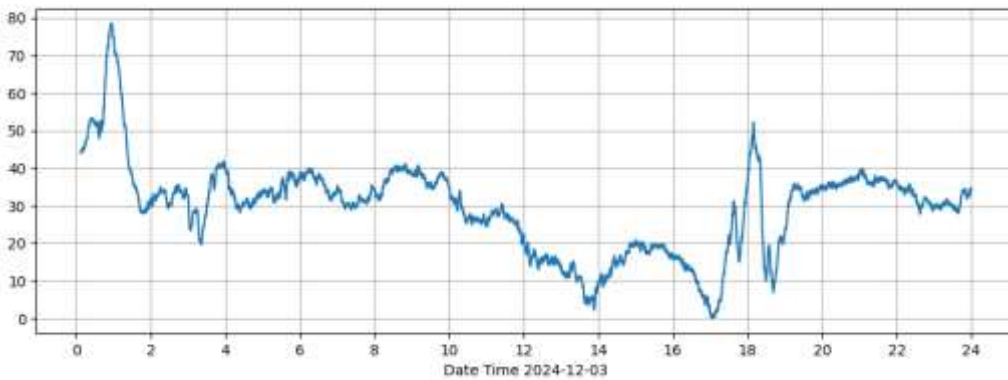


Thomas Mazzi also recorded the activity in Italy, again with a sharp impact around 05:30UT. Strong solar winds added to the disturbance, which then continued over several days. Nick Quinn’s recording shows activity on the 21st:

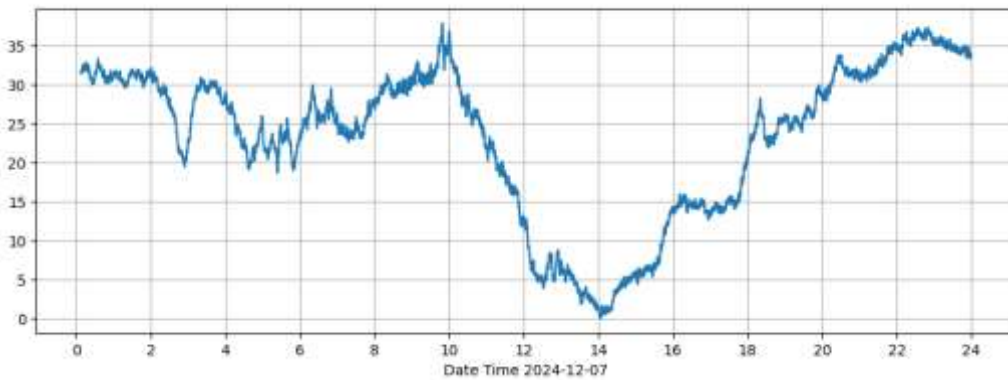
Steyning Magnetometer (50.8 North, 0.3 West)



Wasbister Magnetometer (59.17N,3.06W)



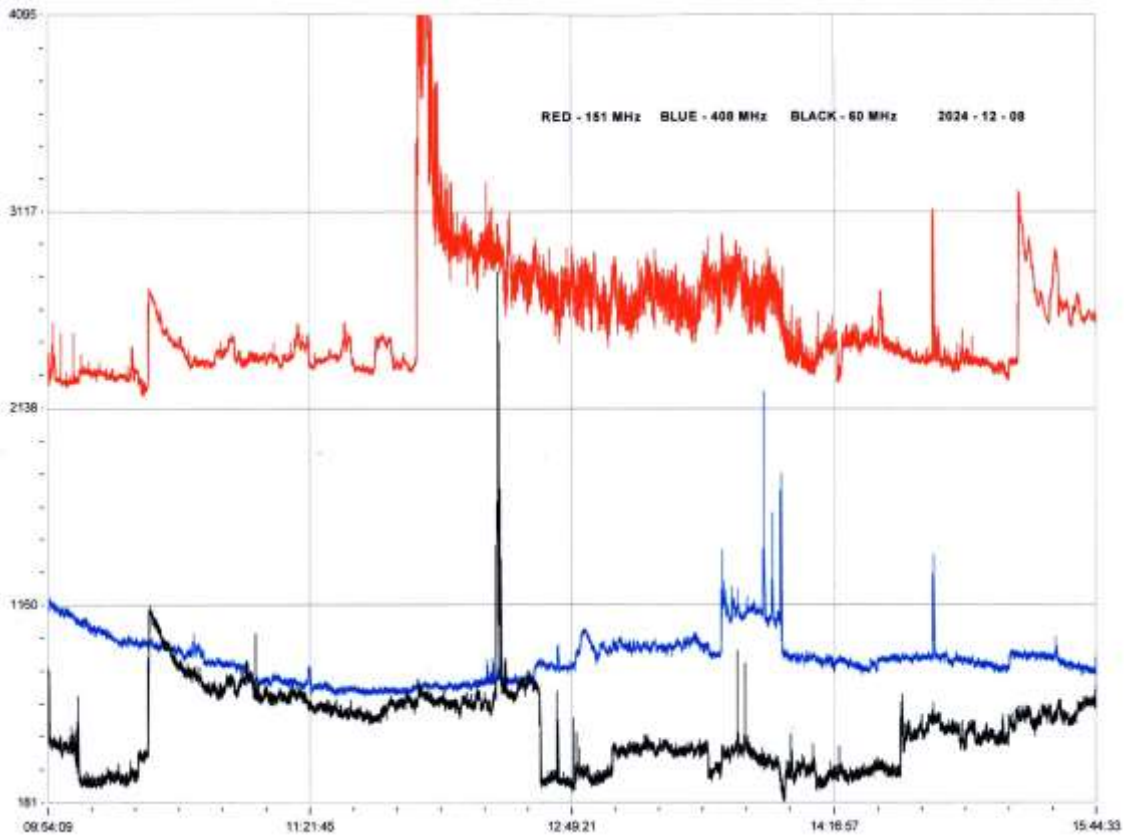
Wasbister Magnetometer (59.17N,3.06W)



Callum Potter's recordings show activity on the 3rd and 7th, again from solar wind effects.

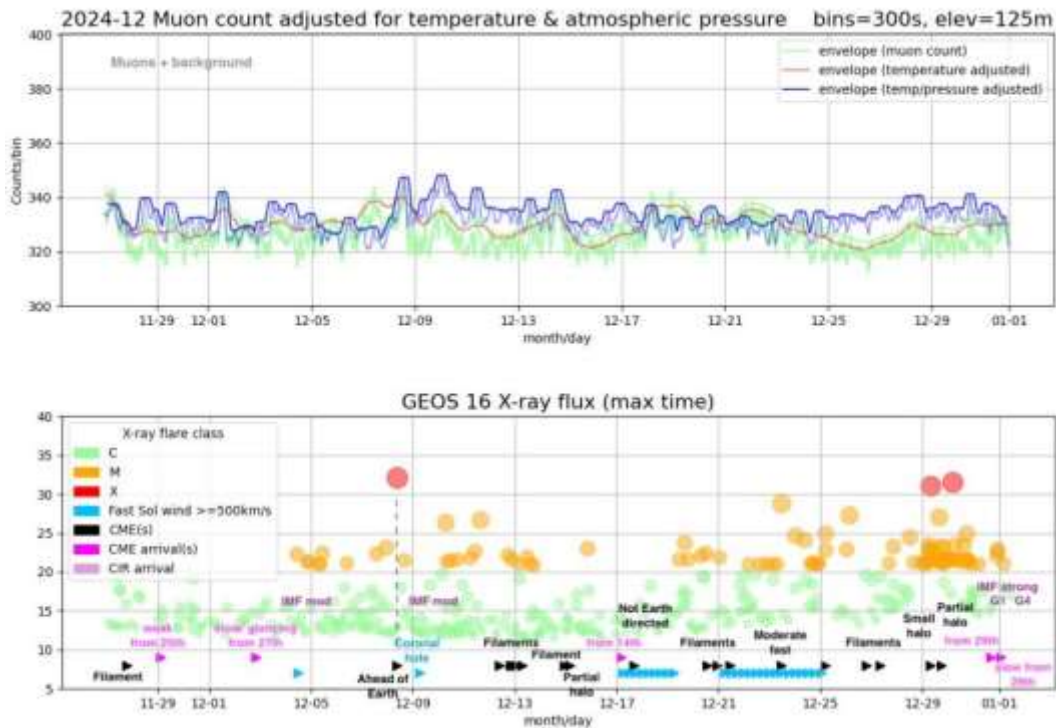
Magnetic observations received from Roger Blackwell, Stuart Green, Thomas Mazzi, Callum Potter, Nick Quinn, and John Cook.

SOLAR EMISSIONS

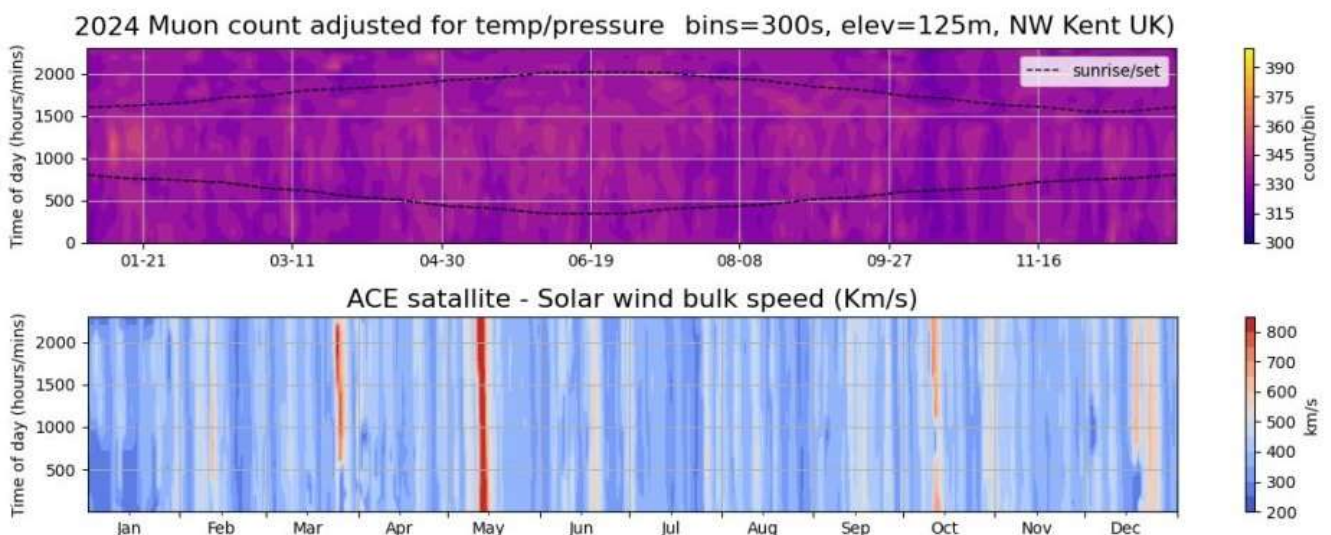


Colin Clements recorded this strong 151MHz noise burst starting at about 11:57UT. It sits between the X2.2 and C8.0 flares and so is rather a puzzle. It could be a delayed effect from the X flare, the lower frequency signal emitted as the flare's shock wave propagated through the varying density of the solar atmosphere.

MUONS



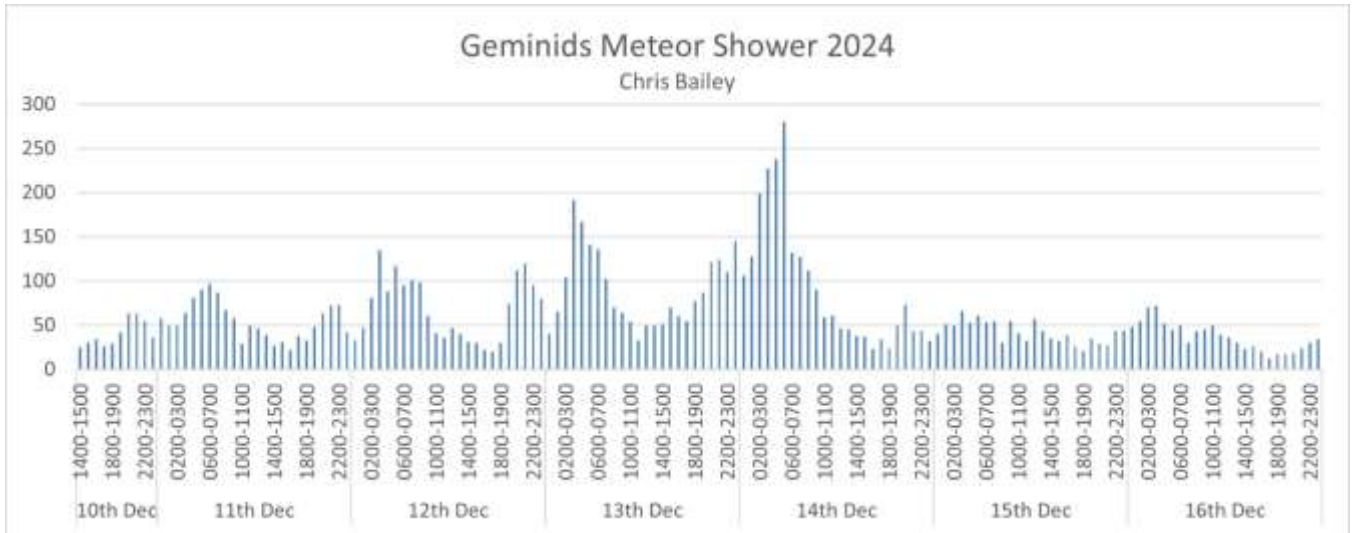
Mark Prescott's chart of Muon counts shows an increase from the 8th to the 15th, a period of lower solar wind speed. The strong CME impact that we recorded on the 17th is followed by a period of lower counts while the wind speed remained high. There was a small rise again in the last week, before a fall at the end of the month. Mark has also provided a chart of the activity through the year:



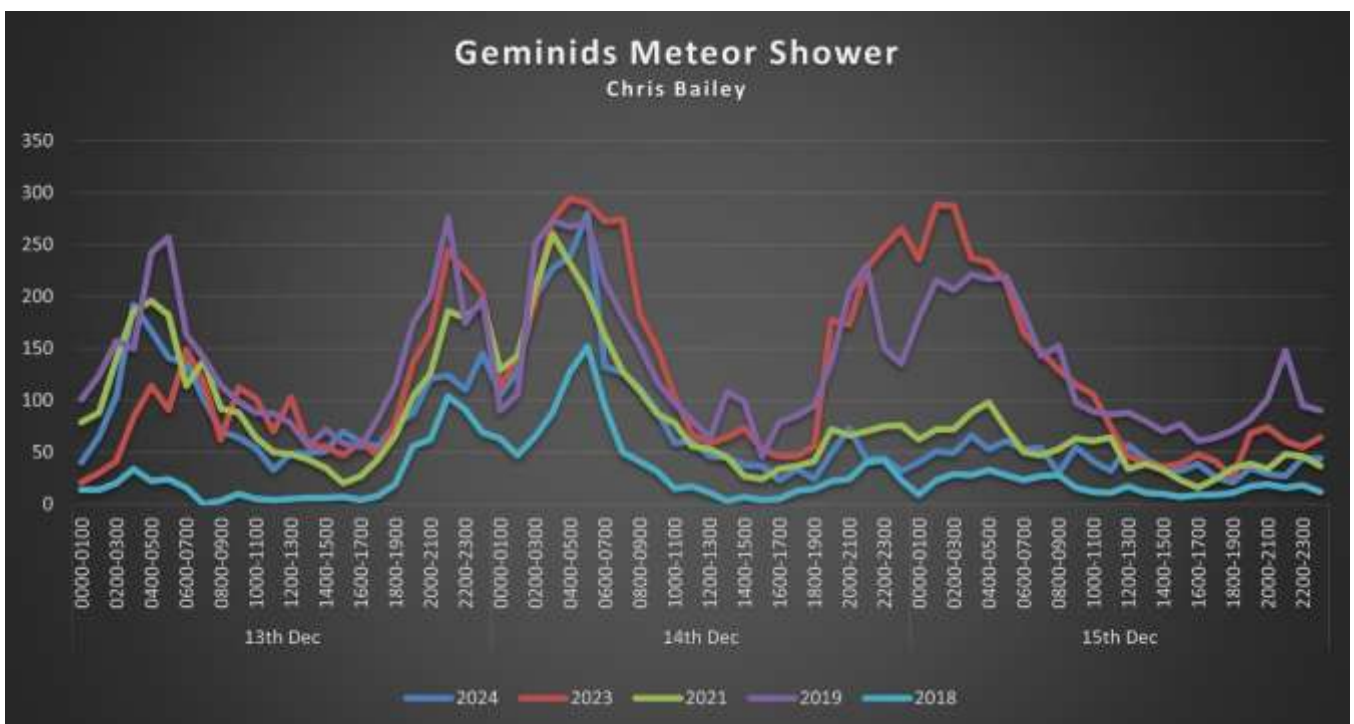
The very high wind speeds recorded in May are clear in the lower panel and are followed by lower muon counts shown in the upper panel. The May copy of Radio Sky News shows this in more detail. May and August gave our highest flare counts of the year, lower muon counts also seen in the upper chart in August. Some of the highest counts were in January, a time

when the sun had a very low altitude during the day and lower solar wind speeds were recorded.

GEMINIDS



Chris Bailey monitored the December Geminid meteor shower, his chart showing a general rise in meteor counts from the 10th, with a strong peak in the morning of the 14th. This matches well with the predictions in the BAA Handbook. The fall-off in counts was very fast after the peak.



This chart compares the Geminid activity over recent years. In each year overnight activity from the 13th to 14th shows a short drop around midnight. 2019 and 2023 also shows overnight activity from the 14th into the 15th with much less of a midnight dip. General activity levels were also much lower in 2018, with very low activity in the morning of the 13th.

Many of our observers will be aware of the EUCARA meetings for Amateur Radio Astronomy. This year it is being held at the Harwell campus of RAL space, near Oxford, on the 5th to 7th of September. The main speaker will be Professor Jocelyn Bell Burnell. The meeting is still being organised, to find further details and register an interest, go to eucara.org.

Thank you for all of your reports and observations in 2024, I look forward to seeing how solar activity changes in 2025, the 20th year of data in the activity chart.

BARTELS CHART

Kilohertz	KEY	DISTURBED	ACTIVE	SPE	B, C, M, S = FLARE MAGNITUDE										Specify rotation start (longitude)										
					B	C	M	S	B	C	M	S	B	C	M	S	B	C	M	S					
2575					2268	2022 June																			
2576					2269	2022 July																			
2577					2280	2022 August																			
2578					2281	2022 September																			
2579					2282	2022 October																			
2580					2283	2022 October																			
2581					2284	2022 November																			
2582					2285	2022 December																			
2583					2286	2022 January																			
2584					2287	2022 February																			
2585					2288	2022 March																			
2586					2289	2022 April																			
2587					2290	2022 May																			
2588					2291	2022 June																			
2589					2292	2022 July																			
2590					2293	2022 August																			
2591					2294	2022 September																			
2592					2295	2022 October																			
2593					2296	2022 October																			
2594					2297	2022 November																			
2595					2298	2022 December																			
2596					2299	2022 January																			
2597					2280	2024 February																			
2598					2281	2024 March																			
2599					2282	2024 April																			
2600					2283	2024 May																			
2601					2284	2024 June																			
2602					2285	2024 July																			
2603					2286	2024 August																			
2604					2287	2024 September																			
2605					2288	2024 October																			
2606					2289	2024 November																			
2607					2290	2024 December																			
2608					2291	2025 January																			
2609					2292	2025 February																			
2610					2293	2025 March																			



British Astronomical Association

Supporting amateur astronomers since 1890

Radio Astronomy Section



Director: Paul Hearn

The Radio Astronomy Section aspires to encourage and support the construction of radio telescopes by amateurs, their use for observing programmes, and the development of a deeper understanding of the science underlying what is being observed. Programmes can be aimed at any radio astronomical phenomenon, at any radio frequency. This encouragement will be through the operation of continuing group programmes, and through building communication and information exchange between individuals and groups pursuing their own projects. The main purpose of the Group is to act as a reservoir and clearing house for information on radio telescope design, construction and debugging, and how to use these instruments effectively. This will include the discussion of observing techniques and data analysis. Members should be able to exchange ideas, give advice and help each other. Establishing a pool of design information and software suitable for use in observing and data processing is a priority.

BAA Radio Astronomy Section Seminar programme.

March 7th. 19:30 (19:30 UTC)

Project HLine3D

Alex Pettit Winter Springs, Fla

A Beginners Guide to Hydrogen Emission Line Microwave Radio Astronomy

A student project described (<https://github.com/AP-HLine-3D/HLine3D>)

April 4th 19:30 BST (18:30 UTC)

Open forum Member presentations. Anything to share, observations, instruments, data - Please contact Paul if you want a slot

EU Conference on Amateur Radio Astronomy - EUCARA25

The conference for the amateur Radio Astronomer - Registration is now open.

Visit <https://eucara.org/> Note: on site hotel accommodation is limited, book early to avoid disappointment

[Join the RA conversation](#)
[Join the muon conversation](#)
[Join the UK Beacon conversation](#)
[Society of American Radio Astronomers](#)
[UK Radio Astronomy Association \(UKRAA\)](#)
[BAA RA YouTube channel](#)

Paul Hearn
BAA Radio Astronomy Section Director
UKRAA Trustee

||| British Astronomical Association ||
https://britastro.org/section_front/24

e paul@hearn.org.uk
a RG6 1BU UK
t +44 (0)7967 388 578

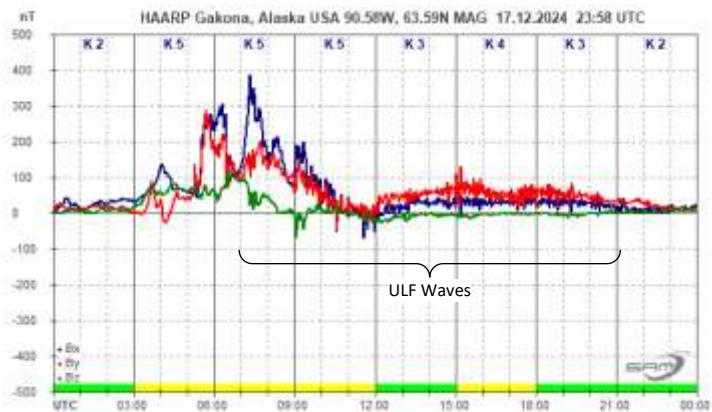
Calculating ULF Waves Spectra from SAM-III Magnetometer Data

Whitham D. Reeve

1. Introduction



The SAM-III magnetometer collects discrete time series data and displays it on a magnetogram similar to the one shown right. ULF Waves are seen as rapidly varying, low amplitude signals riding on the X-component (blue) and Y-component (red) traces. In this example, ULF Waves are visible from about 0700 to 2100.



The time domain data may be converted to the frequency domain by the *Discrete Fast Fourier Transform* (abbreviated FFT) for analysis of the

ULF Waves frequency components. Software applications are available that perform the FFT calculations including Matlab, Mathematica, Mathcad, Python and Excel. This document describes using the *FFT Analysis* tool in Excel. FFT Analysis is part of the *Analysis Toolpak* and is installed in Excel as an *Add-in*. The tool is poorly documented, so this article provides detailed procedures. Some procedural information in this document related to using this Add-in was adapted from online sources.

The FFT Analysis returns a table that contains the two-sided power spectrum (amplitude and frequency) corresponding to the SAM-III time-domain data (amplitude and time). The table has both positive and negative frequency components and a dc (zero frequency) term.

2. Considerations

Data Use: The *original* data produced by the SAM-III magnetometer should never be altered. The data should be copied to a new file or Sheet in Excel before it is analyzed or processed. The SAM-III data file formats are described in more detail in the *SAM-III Software Setup Guide*.

Windows internal processes: The Microsoft Windows operating system internal processes are known to occasionally corrupt the incoming serial bit stream from the SAM-III processor as it is being collected by the SAM_VIEW software. Data corruption is rare and occurs most often around a HH:00:00 time stamp but can occur at any random time. Corruption manifests as errored data on a single line that is easily repaired. The errored data represent a very small fraction of the total data acquired in a 24 hour period.

Data selection: Generally, data is selected for the time range of interest, in particular, the time range of the ULF Waves to be analyzed. The entire 24 hour file is not selected unless 24 hours of data are to be analyzed. This avoids scrolling through large amounts of unneeded data when setting up and plotting the FFT for ULF Waves that last only a few hours.

Number of datapoints: The number of datapoints N to be used in the Excel FFT Analysis tool and related calculations must be a power of 2 (for example, ..., 256, 512, 1024, ...). The higher the number of datapoints

for a given sample interval, the better the frequency resolution of the transform. However, larger datasets require longer calculation times, and Excel becomes bogged down by large datasets. Datasets as large as 4096 samples have been analyzed with the Excel FFT Analysis tool while developing these procedures. See next item.

Sample interval: The SAM-III sample interval (or sample period) may be set from 1 to 120 seconds (sample rates from 1 Hz to 8.3 mHz) in 1 second steps. Common settings are 1, 10 and 60 seconds, corresponding to sample rates of 1 Hz, 100 mHz and 16.7 mHz. If the SAM-III is set to a 10 second sample interval, each hour of data contains 360 samples. If the analysis period is, say, 4 hours, there will be 1440 data samples produced during that period. In this case, the number of datapoints to be used for analysis in the Excel FFT is limited to 1024, not 1440, because the FFT requires the number of datapoints to be a power of 2. For reference, in a 24 hour period, a 1 second sample interval results in 86 400 datapoints, a 10 second sample interval results in 8640 datapoints, and a 60 second sample interval results in 1440 datapoints.

Windowing: Windowing, or tapering, is often used when transforming data from the time to frequency domain. In practical datasets – datasets of limited size – windowing is used to reduce spectra leakage (or sidelobes), which is where the energy of a signal is spread across more than one frequency bin. Without windowing, the FFT spectrum output does not perfectly match the actual input signal. However, windowing introduces amplitude errors. These errors depend on the type of window and type of input signal (sine, pulse, noise). When windowing is applied, the data is multiplied by a window function. A common window function is the Hamming Window, which is approximated by the coefficients $h(k) = 0.54 - 0.46 \cos(2\pi k/N)$, where k is the data index and N is the total number of datapoints. In this case, the window has a cosine shape. A Rectangular Window (also called Uniform Window), in which the data is multiplied by 1, does not alter the data and is the same as not applying a window at all. Many other window functions exist, such as Blackman, Hann (also called Hanning), Flattop and Sine, and may be used depending on specific requirements or preference.

Aliasing: Aliasing is the folding of higher frequencies to lower frequencies during data processing, thus contaminating the output spectra. Aliasing is avoided by filtering the input signal so that it contains no frequency components higher than one-half the sample rate. For example, if the SAM-III is set to a 10 second sample interval (100 mHz sample rate), the ULF Wave frequency measurements must be limited to periods longer than 20 seconds (frequencies < 50 mHz), corresponding to Pc 3, Pc 4, Pc 5, Pi 1 and Pi 2 ULF Waves pulsations. The frequency response of the SAM-III fluxgate sensors is not known but it is believed to be below 500 mHz. If the sample interval is, say, 10 seconds, frequency components higher than 50 mHz may contaminate the FFT. It is possible to apply a lowpass filter to the SAM-III data during post processing but prior to applying the FFT. Lowpass filtering of the SAM-III data is not covered here.

Frequency resolution: Frequency bin (or FFT bin) spacing is equivalent to frequency resolution and is f_s/N , where f_s is sample rate and N is the number of datapoints. Equivalently, the resolution is $1/(N * ts)$, where ts is the sample interval. For example, if the dataset has 512 samples and a sample rate of 100 mHz, the resolution is (100 mHz/512 =) 0.2 mHz. In this example, frequency components separated by < 0.2 mHz cannot be resolved. For a given sample rate, the resolution cannot be improved without longer observation times (and more datapoints); however, ULF Waves do not necessarily occur for long time periods, thus limiting the frequency resolution in many practical situations.

Other FFT processing errors: In addition to the errors due to leakage (spectra) and windowing (amplitude), other errors creep into FFT processing including scalloping loss and processing loss. These affect the power amplitude of the transformed signal and are ignored in this document because the presence of the spectra is more important than its exact amplitude.

Plotting: The FFT analysis produces the power amplitude of each frequency component, including a dc component. The relative power amplitudes are sufficient for the purposes of analysis. The two FFT frequency components are identical, so only the positive component is usually plotted. The dc component represents low frequency components below the resolution of the analysis, typically lower than a fraction of a mHz, so it

does not need to be plotted. The amplitudes and frequencies are plotted on linear scales in this document. Either of these quantities may be plotted on a logarithmic scale but that is not covered here.

3. Procedures

The procedures described in this section consist of four basic steps: Prepare the SAM-III data files; Calculate the FFT of the data using the Excel FFT Analysis tool; Calculate the frequency scale associated with the transform; and Plot the results.

A. Prepare the SAM-III data files

- 1) The SAM_VIEW application software produces several files during normal operation. The filename to be used for the transform is the *yyyymmdd.txt*, where *yyyy* is the year, *mm* is the month and *dd* is the day of the file. This file contains comma and space delimited, columnar, time-stamped, raw data for each of the three magnetic components, X (north-south), Y (east-west) and Z (vertical).
- 2) Start Excel, navigate to the SAM-III data folder and then Open the desired .txt file (in the File Explorer window that opens, select Text Files in the dropdown to the right of the File name field to see the .txt files in the folder). Step 1 of 3 of the Text Import Wizard appears. Select the Delimited radio button. The .txt file does not have headers. Click Next.
- 3) Step 2 of 3 appears. Select Comma and Space and click Next.
- 4) Step 3 of 3 appears. The first data column is automatically selected. Select the *Date* radio button and the format *D/M/Y*. All other columns are *General format*. Click Finish.
- 5) Immediately after the file opens in Excel, Save As a .xls or .xlsx file. Do not skip this step because the original text file data may be accidentally overwritten. The data to be analyzed will be in Sheet1.
- 6) In the new Excel file, delete the columns containing only the text X, Y and Z. Each of these columns are simply indicators for the magnetic component data in the column to its right. The actual data columns are labeled in the next step.
- 7) Insert a row at the top of Sheet1 and label the associated columns, in order, Date, Time, X-data, Y-data and Z-data. At this point, there should be columns A (Date), B (Time), C (X-data), D (Y-data), and E (Z-data).
- 8) Scroll through the data and repair any corrupted lines and missing time-stamps. There are no ill-effects of replicating data or inserting a missing time-stamp on occasional, single lines of data.
- 9) Calculate the horizontal magnetic component, H, from the X- and Y-components. Label a new column F as *H*. Insert the formula = SQRT (C-cell² + D-cell²), where C-cell and D-cell are the data cells in the X-data and Y-data columns, respectively. Example: For the X-data in cell C2 and Y-data in cell D2, the formula in cell F2 is =SQRT(C2²+D2²). Copy the formula to all cells in the column corresponding to the data. For convenience, Format all cells in column F as Number with 0 Decimal Places.
- 10) Normalize the horizontal component data. Label a new column G as *H-Norm* for normalized data. Normalize the data by subtracting the first *H* value (cell F2) from itself and from all other *H*-data cells. If only part of the dataset is being used in the transform, normalize only from the beginning to the end of the time period to be used. Example: The data to be used starts at cell F2. The formula in cell G2 is =F2-F\$2 and in G3 is =F3-F\$2, and so on. Alternatively, the actual value of cell F2 may be subtracted, as in =F2-10360, = F3-10360, and so on, where the constant 10360 represents the actual value of the data in cell F2 used for normalizing.
- 11) Select and copy the *H-Norm* data in column G of Sheet1. Paste (as Values) the data into column B of new Sheet2. If more than one time period is to be analyzed, the data for each time period may be

placed in new Sheet3, Sheet4, and so on. This allows different time periods to be analyzed on different Sheets. Note that the time-stamps are not needed in the new Sheet2 so it is helpful to Rename the new Sheet2 tab to the time period being analyzed. Example: If the time period is 15:00 to 18:00, Rename Sheet2 to *H 1500-1800*, where H indicates Horizontal component data.

- 12) Label column A in the new Sheet2 as *Index k*. Enter the *index k* values starting with the value 0 as the first index value. Increment the index by 1 for each subsequent value. The index should count from 0 to $N - 1$. Example: Cell A2 contains 0 and cell A3 contains $=A2+1$, cell A4 contains $=A3+1$, and so on. If $N = 4096$ datapoints, then the last *index k* cell value is 4095.
- 13) The new Sheet2 should now have two occupied columns: Column A labeled *Index k* and column B labeled *H-Norm*.

B. Calculate the Fast Fourier Transform

- 1) Enter the window function formula into a new column C in new Sheet2, and label it *Win*. Generally, the function will include a reference to the *Index k* in column A and the total number of datapoints N to be used. Copy the function to the cells in column C. Example: For the Hamming Window and $N = 4096$ datapoints, in cell C2 enter $= 0.54-0.46*\cos(2*\pi()*A2/4096)$. If the Rectangular Window is used, enter the value 1 in the cells in column C.
- 2) Label a new column D as *H-Win*. Multiply the *H-Norm* cells in column B by the *Win* cells in column C. Example: in cell D2 enter $= B2*C2$. Copy the multiplication to all cells in column D corresponding to the data to be used. Column D now contains windowed data. If the Rectangular Window is used, the values in columns B and D are identical. For other window types, the data will vary with position in the column. For convenience, Format the cells in column D as Number with 3 or 4 Decimal Places.
- 3) Label four new columns E as *FFTk*, F as *xk (Hz)*, G as *xk (mHz)*, and H as $|FFTk|$.
- 4) Select the *Data Analysis...* option from the Tools menu or the Data ribbon. The *Data Analysis* window will open. If the *Data Analysis* option is not available, use online resources to learn how to install the *Analysis Toolpak Add-in* (it is free).
- 5) The *Data Analysis* window will show a list of *Analysis Tools*. Select *Fourier Analysis* and click OK. The *Fourier Analysis* window will open (right).
- 6) Click in the field to the right of *Input Range*: and select the cell in column D that is on the same row as the first datapoint used. Drag the selection in the input data column D to select the desired data. Be sure this data is the same as used in the previous steps and the number of datapoints is a power of 2.
- 7) Click on the *Output Range* radio button under the *Output Options*. Click in the field to the right of *Output Range*: and select the cell in column E that is on the same row as the first datapoint to be used. Drag the selection along column E the same length as the input data in column D.
- 8) Click OK to calculate the complex FFT coefficients and place them in column E. Excel provides a warning and will not do the calculation if the data range is not a power of 2. Note that Excel always displays 15 digits for both the real and imaginary parts of the FFT coefficients, and the number of displayed digits cannot be changed. If, after the analysis is run and the coefficients have been calculated, any changes are made to the data being transformed, the FFT Analysis tool does not automatically update the coefficients and the analysis must be run again.
- 9) Calculate the magnitude of the complex FFT coefficient. Select the cell in column H that is on the same row as the first datapoint used and enter the formula $=IMABS(FFTk-cell) * (2/N)$ where *FFTk-cell*



cell is the cell of the first generated FFT value in column E and *N* is the number of datapoints. Example: For cell H2 and *N* = 4096 datapoints, enter =IMABS(E2)*(2/4096). Copy this cell formula to all cells in column H corresponding to the data to be used. For convenience, Format the cells in column H as Number with 1 or 2 Decimal Places.

C. Calculate the Frequency Scale

- 1) Populate column F with the formula = $k\text{-cell} / (N * ts)$ where *k-cell* is the corresponding value for the *Index k* from column A, *N* is the number of datapoints, and *ts* is the sample interval in seconds. Example: For cell F2, *N* = 4096 datapoints and 10 second sample interval, enter =A2/(4096*10).
- 2) Populate the column G cells with the formula = $(xk\text{-cell}) * 1000$, where *xk-cell* is the corresponding value in column F. Example: In cell G2 enter =F2*1000. Columns F and G now contain frequencies in Hz and mHz, respectively. Either may be used as the frequency scale in the next step, but mHz is more convenient for ULF Waves.

Upon completion of Steps A, B and C, the first three rows of Sheet2 should look similar to below, but the values will depend on *N* and the sample interval.

	A	B	C	D	E	F	G	H
1	Index K	H-Norm	Win	H-Win	FFTk	xk (Hz)	xk (mHz)	FFTk
2	0	0	= 0.54-0.46*COS(2*PI()*A2/4096)	=B2*C2	1154....	=A2/(4096*10)	=F2*1000	=IMABS(E2)*(2/4096)
3	1	3	= 0.54-0.46*COS(2*PI()*A3/4096)	=B3*C2	2140....+138...i	=A3/(4096*10)	=F3*1000	=IMABS(E3)*(2/4096)

Columns:

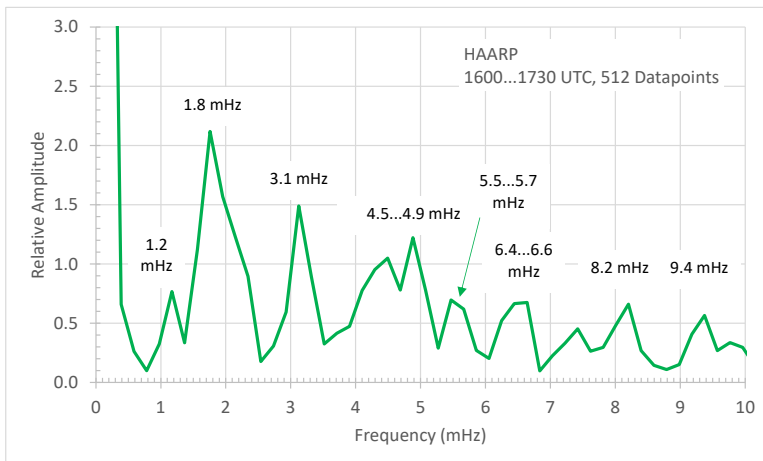
- A Index k = 0 ... N-1 in increments of 1, where N is the number of datapoints (4096 in this example);
- B Normalized H-component data from Sheet1, a total of N rows not including header row
- C Window function, the example shows the Hamming Window
- D Windowed data from Window function in column C applied to the H-Norm data in column B
- E Resulting FFT data, real + imaginary of the form $r + i$
- F Frequency scale in Hz based on the index, sample period (10 s) and N (4096)
- G Frequency scale in column F converted to mHz (to be plotted on horizontal scale)
- H Magnitude (absolute value) of the FFT data in column E with *N* = 4096 (to be plotted on vertical scale)

D. Plot the Spectra Relative Magnitudes with Respect to Frequency

- 1) The plot X-axis uses the *xk* values in mHz from column G and the Y-axis uses the $|FFTk|$ relative magnitude values (no units) from column H. Both axes are plotted on a linear scale.
- 2) The FFT is two-sided and both sides are identical, so only one side needs to be plotted. Select the upper one-half of the data in columns G and H and then Insert Chart Type *X-Y (Scatter)* with *Straight Lines*. When selecting the first-half of the FFT data, note that the first data cell contains only a real number (dc or zero frequency coefficient) and the cell immediately after one-half of the FFT data ends contains another real number (folding frequency coefficient); all cells in between contain real + imaginary numbers. The folding frequency is one-half the sample rate, or $fs/2$. The dc and folding frequency components need not be plotted. Example: The FFT contains *N* = 4096 datapoints and the corresponding index values range from 0 to 4095. Select the FFT ($|FFTk|$) and frequency [*xk (mHz)*] data corresponding to index values from 0 to 2047. This range includes the dc component but not the folding frequency component. If the dc component is not to be plotted, select the FFT and frequency data corresponding to index values of 1 to 2047.
- 3) In general, the frequency axis will have values from 0 to $fs/2$. Example: If the sample rate of the SAM-III data is 100 mHz (10 second sample interval), the frequency axis of the resulting chart will have values from 0 to 50 mHz. Similarly, if the sample rate is 1 Hz, the frequency axis will have values from 0 to 500 mHz.
- 4) Format and label the axes, traces and chart area as desired. Generally, the range of values displayed by both the x- and y-axis will require reduction to effectively zoom into the frequencies of interest,

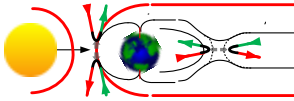
typically frequencies < 10 mHz. Suggested chart details: Aspect ratio: 1.67, Size: 3"x 5" (or 4" x 6.667"), Axis font: 9 or 10 point Calibri, Axis title and chart title font: 10 or 11 point Calibri, Plot line width: 2.0 pt, Arrow callouts width: 1.0 pt.

The annotated plot below shows an example of the results from Steps A, B, C and D above using 512 datapoints. This plot corresponds to the time period 1600 to 1730 on the magnetogram at the beginning of this document. Both the vertical and horizontal scales have been truncated from the full FFT Analysis to better show the individual spectrum components from 0 to 10 mHz.



ULF Wave Observations at the End of 2024

Whitham D. Reeve



Ultralow Frequency Waves (*ULF Waves*) are periodic electromagnetic waves in Earth's magnetosphere that can be observed by ground magnetometers; they are seen as low amplitude, rapidly varying traces on a 24 hour magnetogram. ULF waves have frequencies of a few mHz to a few Hz, corresponding to periods from several minutes to fractions of a second. This article describes ULF Waves observed on 17 December 2024 with the SAM-III magnetometers at Anchorage Radio Observatory and HAARP Radio Observatory in Alaska (figure 1). A comprehensive description of ULF Waves and observations in Alaska in 2023 is given in [Reeve23].



Figure 1 ~ Map of Southcentral Alaska showing the locations of Anchorage Radio Observatory (left marker) and HAARP Radio Observatory (right). The great circle distance between the two, shown by the black line, is 286 km. HAARP is 2° farther north in magnetic latitude than Anchorage and 4° east in longitude.

Geomagnetic coordinates:

Anchorage: 61.72° N : 94.41° W (2022)

HAARP: 63.62° N : 90.42° W (2024)

Note: Geomagnetic coordinates change over time because of the wandering nature of Earth's internal dipole field.

Image source: <http://www.movable-type.co.uk/scripts/latlong.html>

Near-Earth Magnetic Conditions: The shock wave associated with multiple coronal mass ejections (CME) from 13 and 14 December was observed at 0445 on 17 December by the ACE spacecraft. At that time the component of the interplanetary magnetic field (IMF) aligned with Earth's dipole axis (B_z) reached a maximum of -20 nT (southward). Soon after, the total field (B_t) increased from about 8 nT to 30 nT and the solar wind speed increased from about 400 to 650 km s^{-1} (<https://www.swpc.noaa.gov/products/ace-real-time-solar-wind>). The disturbed magnetic conditions on 17 December expanded the auroral oval southward so that both Anchorage and HAARP observatories were directly under it (figure 2).

Local Magnetic Conditions: Magnetograms show the local magnetic field flux density vectors over a 24-hour period. The Anchorage and HAARP magnetograms show the magnetic field components in the geographic coordinate system with the B_x -component oriented true north-south, B_y -component oriented true east-west and B_z -component oriented vertical. ULF Waves are generally seen only in the B_x - and B_y -components and are quite clear in the latter two-thirds of the 17 December magnetograms (figure 3).

Close examination of the magnetograms show a Sudden Impulse from the CMEs of approximately 40 nT amplitude at 0519 followed immediately by magnetic storm conditions. Under these conditions, the impulse event more correctly is called a *Storm Sudden Commencement (SSC)*.

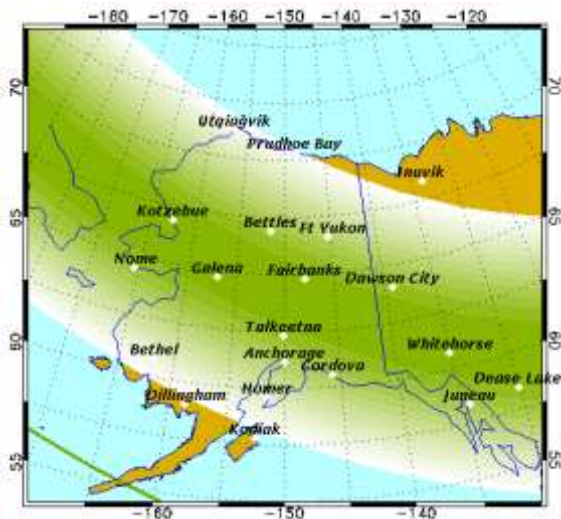


Figure 2 ~ Forecasted Auroral Oval for 17 December. Anchorage is at lower-middle of the map, HAARP is not marked. The green gradient indicates the probability of viewing the aurora.

The Auroral Oval maps the footprints of open magnetic field lines that allow energetic particles in the solar wind to enter the magnetosphere where they can enable the production of ULF Waves.

Image source: <https://www.gi.alaska.edu/monitors/aurora-forecast>

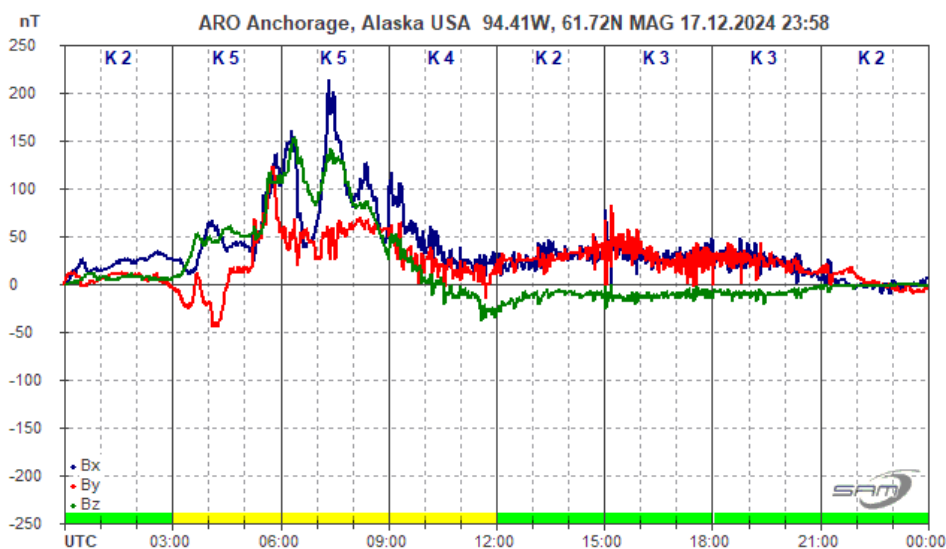


Figure 3.a ~ Magnetogram for Anchorage for 17 December. The ULF Waves, seen as low amplitude “noisy” traces appear to start about the same time as the disturbance (K5) at about 0720 UTC and continue to at least 2100. Local solar midnight is 1000 UTC, so these times correspond to local solar times in the pre-midnight-to-dawn sector. Note that the ULF Waves are indicated only in the Bx (blue trace) and By (red trace) components of the magnetic field.

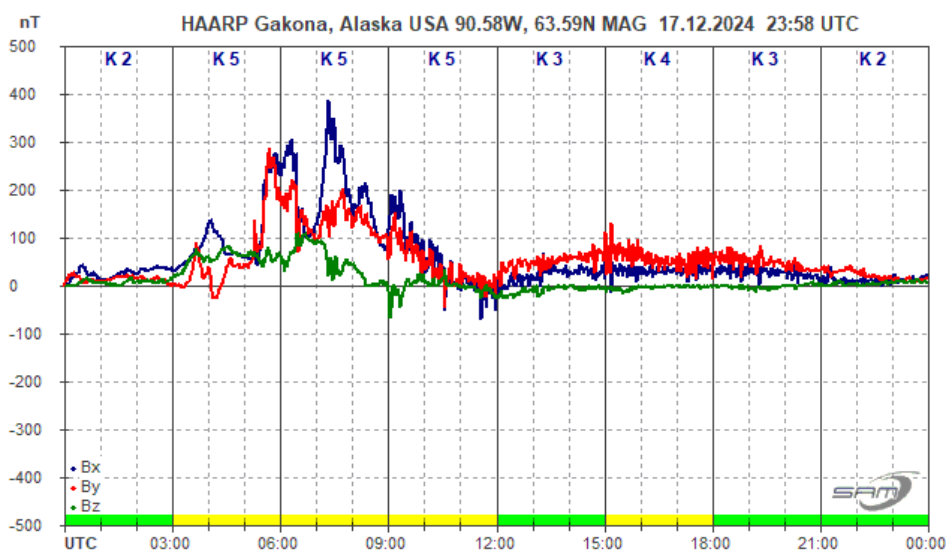


Figure 3.b ~ Magnetogram for HAARP for 17 December. Only minor differences are seen throughout the day compared to Anchorage. Some differences are due to the position of the auroral electrojets and some could be distortion of the magnetic field by local geology. Although the K-Index values for each 3-hour synoptic period also show some differences throughout the day they do track very closely over longer time periods.

ULF Waves: The brief descriptions in this section are adapted from {Reeve23}. ULF Waves are divided into two basic types, *continuous* and *irregular*, based on how they appear in ground magnetometer records such as a magnetogram. The continuous pulsations are quasi-sinusoidal lasting more than several cycles (sometimes several hours) whereas the irregular pulsations are relatively short-lived (less than a few cycles). The generally accepted frequency ranges and corresponding periods are listed in table 1.

Table 1 ~ ULF Wave Classifications

Type	Name	Frequency (mHz)	Period (s)
Continuous Pulsations	Pc 1	200 – 5000	0.2 – 5
	Pc 2	100 – 200	5 – 10
	Pc 3	22.2 – 100	10 – 45
	Pc 4	6.7 – 22.2	45 – 150
	Pc 5	1.7 – 6.7	150 – 600
Irregular Pulsations	Pi 1	25 – 1000	1 – 40
	Pi 2	6.7 – 25	40 – 150

Pc 5 waves with specific frequencies consistently appear in detailed spectral analyses and are called *magic frequencies*: 0.7, 1.3, 1.9, 2.6 – 2.7, 3.2 – 3.4, and 4.8 mHz (see {Reeve23}). The frequencies are observed to vary a little depending on the study. Statistical studies show these frequencies, or frequencies close to them, occur in the solar wind upstream of the magnetosphere as well as in the dayside magnetosphere. The wavelengths of Pc 3, Pc 4 and Pc 5 waves are comparable to the size of the magnetosphere.

Data Analysis: The plots in this section are based on the local magnetic field horizontal component H, which is the vector sum of Bx and By. H is calculated during post processing of the data from each observatory. Time domain plots of H for the full 3-hour period from 1500 to 1800 are followed by plots of the Fast Fourier Transforms (FFT) of that data (figure 4). The FFT converts the serial time domain data to the frequency domain and allows identification of specific frequencies in the ULF Wave spectra. The spectra plots for the full 3-hour time period extend to 50 mHz with annotations of the higher amplitude components.

Subsequent time domain and frequency domain plots (figures 5, 6 and 7) show shorter overlapping time periods 1500 to 1630, 1600 to 1730 and 1700 to 1800. The time periods were arbitrarily chosen and have no other significance. The frequency range shown for these shorter time periods is reduced to 10 mHz because, as seen in the plots for the full 3 hour period, spectra above 10 mHz are very weak by comparison.

All FFTs were calculated using the Hamming window to reduce spectral leakage. The FFT calculations were performed in Microsoft Excel 2019 using raw magnetometer data that has been normalized to the start of each time period. No effort was made correct or compensate for any amplitude errors resulting from the windowing or transform. The time domain plots show the actual, uncorrected recorded magnetic flux density and have not been normalized.

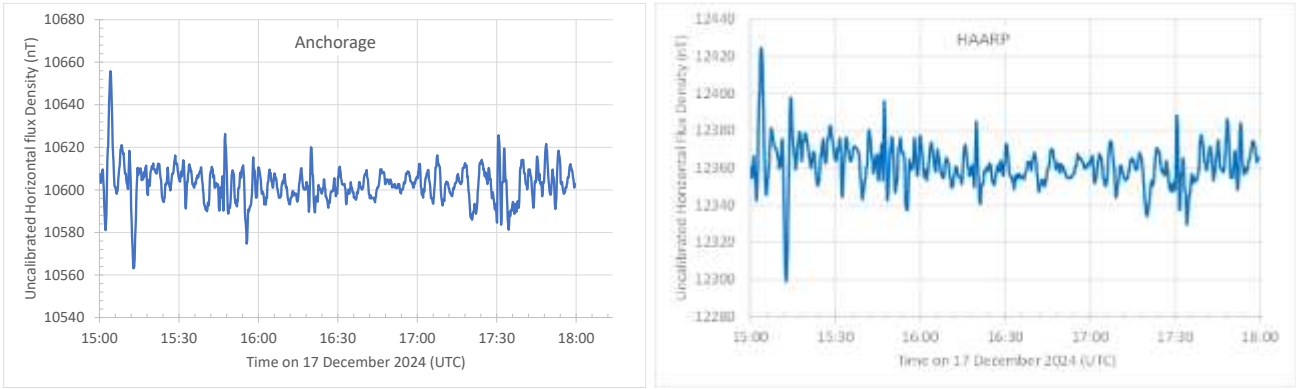


Figure 4.a ~ Time domain plots for Anchorage (left) and HAARP (right): Abridged magnetogram showing the time period from 1500 to 1800 UTC. Several periodicities are visible and possibly an irregular (single cycle) pulsation near the beginning. The vertical scales are uncalibrated. For comparison, the calculated H-component intensity using the World Magnetic Model WWM-2020 for 17 December was 15 156 and 13 977 nT for Anchorage and HAARP, respectively.

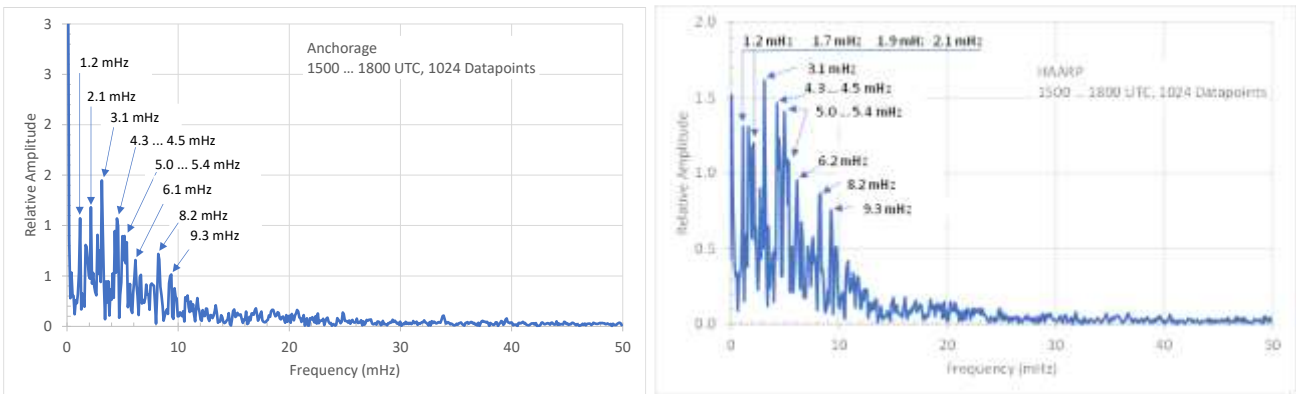


Figure 4.b ~ Frequency domain plots of data from figure 4.a calculated using the FFT; frequency resolution is 0.1 mHz. The full 50 mHz frequency range is shown although any spectra above about 10 mHz is very weak. Pc 4 (6.7 to 22.2 mHz) and Pc 5 (1.7 to 6.7 mHz) pulsations are labeled. The 4.3 to 4.5 and 5.0 to 5.4 mHz frequencies overlap, possibly indicating drift during the 3 hour period.

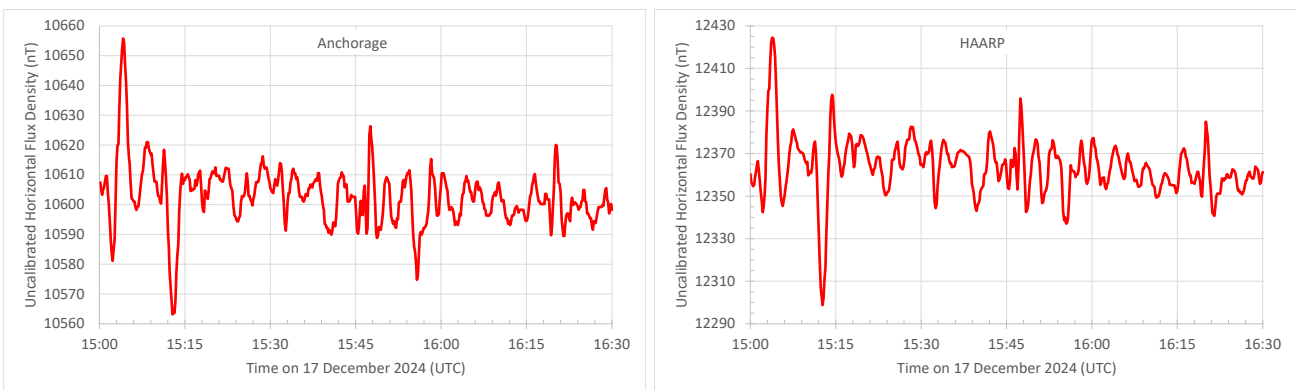


Figure 5.a ~ Time domain plots for Anchorage (left) and HAARP (right): Abridged magnetogram showing the 1.5 hour time period from 1500 to 1630 UTC. The irregular pulsation near the beginning is more apparent than in the plots for the full 3-hour period. The vertical scales are uncalibrated.

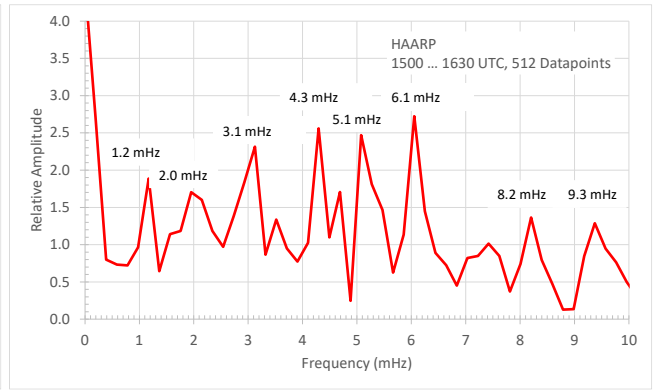
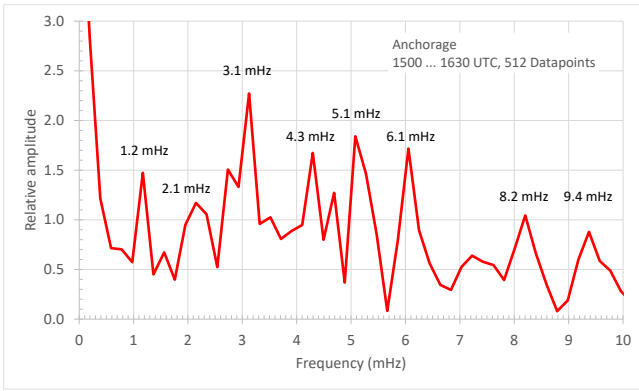


Figure 5.b ~ Frequency domain plots of data from figure 5.a. The plotted frequency range has been reduced to 10 mHz; frequency resolution is 0.2 mHz. Pc 4 (6.7 to 22.2 mHz) and Pc 5 (1.7 to 6.7 mHz) pulsations are visible and the two observatories show remarkable correlation.

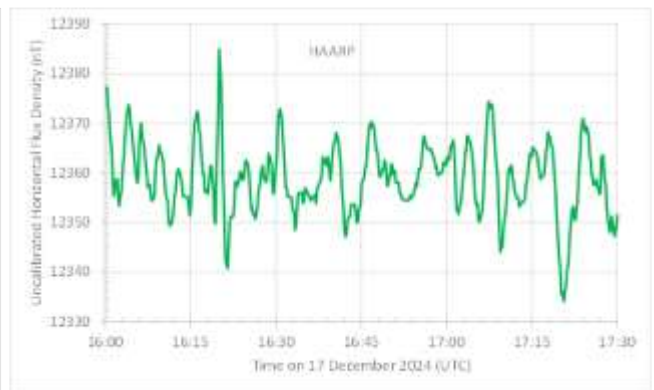
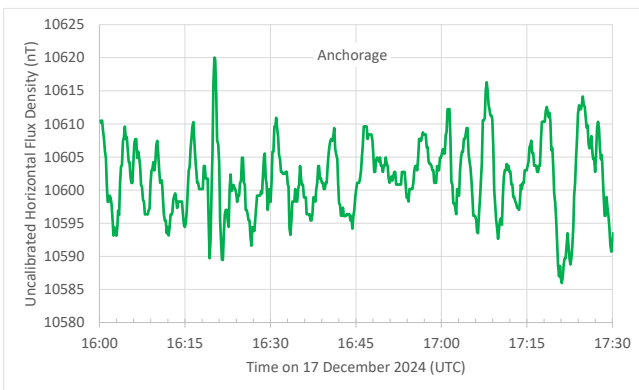


Figure 6.a ~ Time domain plots for Anchorage (left) and HAARP (right): Abridged magnetogram showing the 1.5 hour time period from 1600 to 1730 UTC. A possible Pi is visible at about 1620.

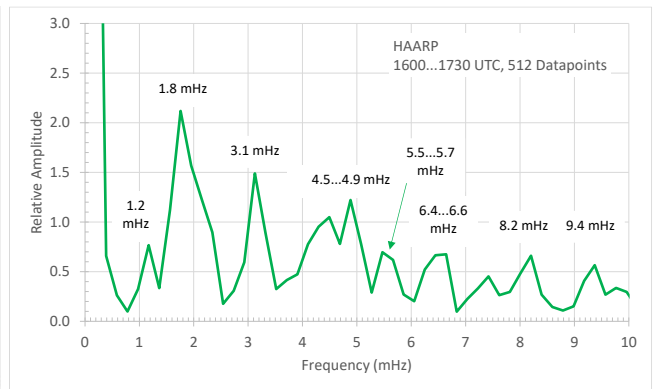
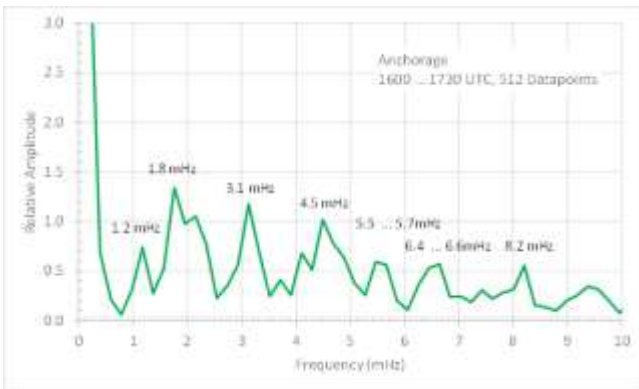


Figure 6.b ~ Frequency domain plots of data from figure 6.a. As above, the frequency range has been reduced to 10 mHz and frequency resolution is 0.2 mHz.

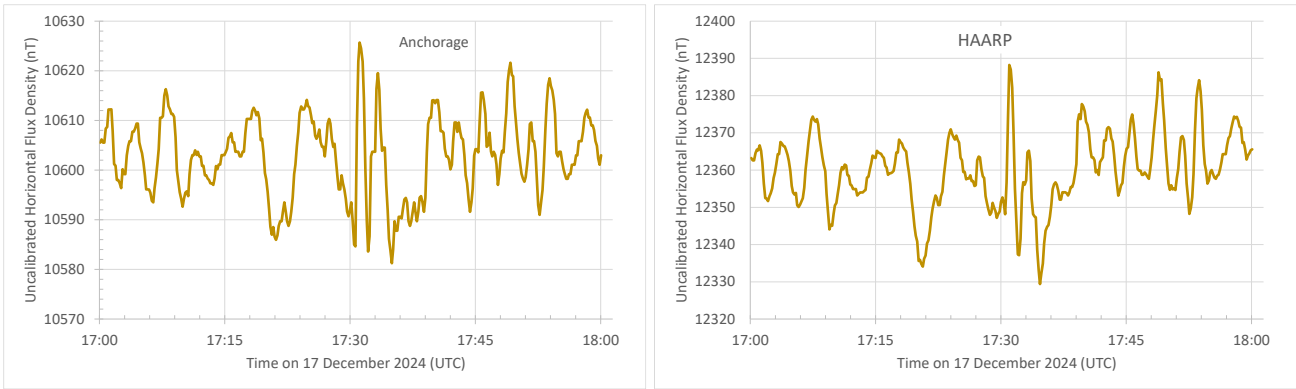


Figure 7.a ~ Time domain plots for Anchorage (left) and HAARP (right): Abridged magnetogram showing the 1 hour time period from 1700 to 1800 UTC. A possible Pi is visible about 1735. The resemblance between the two observatories is very high.

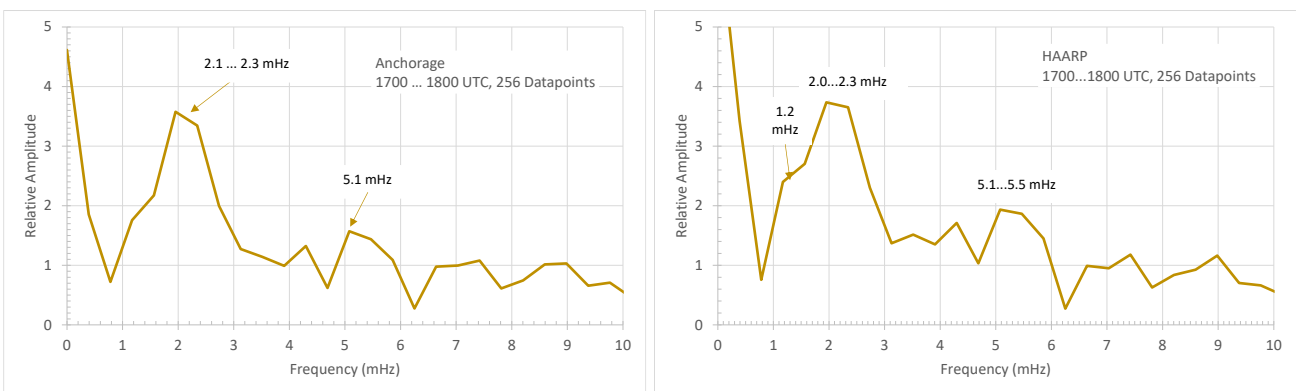


Figure 7.b ~ Frequency domain plots of data from figure 7.a for the time period from 1700 to 1800 UTC; frequency resolution is 0.39 mHz. During this time period, the peaks are not sharp due to the lower frequency resolution, and there are not nearly as many peaks visible compared to earlier time periods. As with the time domain plot, the resemblance is very high between the two observatories.

Discussion: The time domain (magnetograms) and frequency domain (FFT) plots are remarkably the same for the two observatories, not only for the entire 3-hour time period but also the individual 1.5- and 1-hour segments. This is not particularly surprising given the close proximity of the two observatories (286 km), but it serves to increase confidence in the observations and calculations.

ULF Waves are often observed in the Anchorage and HAARP magnetograms throughout the year, but they do not always persist for the long period observed on 17 December. In terms of a solar time scale, the ULF Waves seen in the magnetograms occurred in the midnight through dawn to the noon time sectors (figure 8). These ULF Waves started coincidentally with the magnetic disturbance caused by multiple CMEs and likely are related to them.

The inverted magnetic bays seen in the above Anchorage and HAARP full-day magnetograms between 0700 and 1000 occurred soon after the CMEs arrived. The impact caused the auroral oval to expand and the auroral electrojets to flow directly overhead of both Anchorage and HAARP. The inverted bays indicate an enhancement of the local magnetic fields, although the enhancements amounted to only 1% of the ambient Bx-component (north-south) at Anchorage and 3% at HAARP.

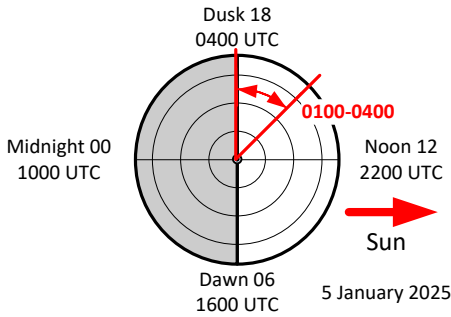


Figure 8 ~ Solar time scale for Anchorage with corresponding times in UTC. UTC times at HAARP are 20 minutes earlier. The ULF Waves on 17 December occurred in the midnight-to-dawn and dawn-to-midnight sectors. The waves discussed in this article were detected around local solar dawn and may have been caused by shear between the relatively higher speed CME plasma and Earth's magnetosheath.

The so-called *magic frequencies* (see {Reeve23}) are clearly visible in the FFT plots for both observatories and they are almost identical (table 2). Other frequencies are visible at both observatories. Most, but not all, frequencies fall into the Pc 5 range (1.7...6.7 mHz). The observations of higher frequencies in the Pc 4 range (6.7...22.2 mHz) may be limited by the sample rate setting of the two SAM-III magnetometers (10 seconds). Some spectral peaks seen in the FFT plots are relatively broad and may indicate frequency drift, spectral leakage or simply the result of relatively low frequency resolution.

Table 2 ~ Frequencies observed for Continuous Pulsations (Pc) taken from FFT plots for all time periods

Observatory	Frequencies, Pc 5: 1.7 ~ 6.7 mHz	Frequencies, Pc 4: 6.7 ~ 22.2 mHz
Anchorage	1.2, 1.8, 2.1...2.3, 3.1, 4.3...4.5, 5.0...5.4, 5.7, 6.1, 6.4...6.6	8.2, 9.3...9.4
HAARP	1.2, 1.7, 1.9, 2.0...2.3, 3.1, 4.3...4.5, 4.5...4.9, 5.0...5.4, 5.5...5.7, 6.1...6.2, 6.4...6.6	8.2, 9.3...9.4

Instrumentation: The SAM-III Magnetometer installations at Anchorage and HAARP are nearly identical (figure 9). The differences are listed in table 3. Both stations use the SAM_VIEW software to display and log the three magnetic components. Real-time magnetograms are available at: https://reeve.com/SAM/SAM_simple.html (Anchorage) and https://reeve.com/SAM/SAM-HAARP/SAM-HAARP_simple.html (HAARP).

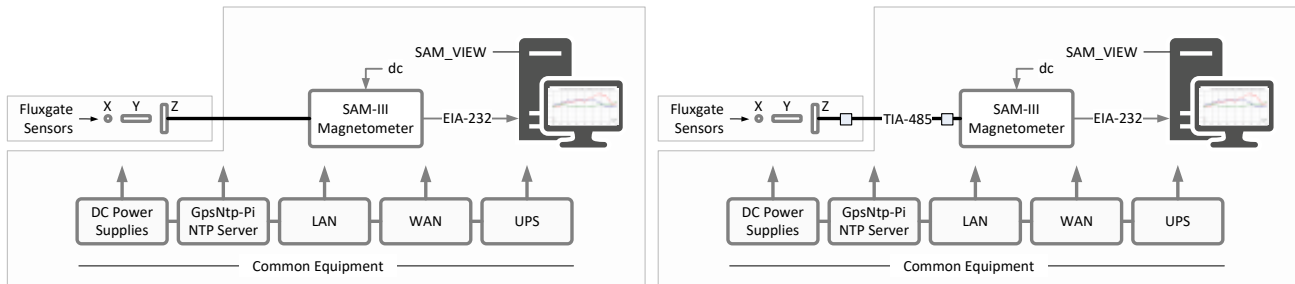


Figure 9 ~ SAM-III Magnetometer block diagrams for Anchorage (left) and HAARP (right). The two are operationally identical and differ only in a few technical details (see table).

Table 3 ~ Differences between magnetometer stations

Observatory	Anchorage	HAARP	Remarks
Sensor type	FGM-3	FG-3+	Performance nearly identical
Sensor voltage	12 Vdc	5 Vdc	Anchorage has 5 V voltage regulators at the sensors whereas HAARP has them on the controller
Sensor transmission	Cable only	TIA-485 + Cable	HAARP uses CAT5E cable and TIA-485 transmission interfaces

References:

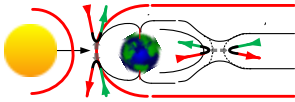
{[Reeve23](#)} Reeve, W., Observations of ULF Waves at Anchorage, Alaska, 2023:
https://reeve.com/Documents/Articles%20Papers/Reeve_ULFWaveObsrv.pdf

Readers may refer to articles about ULF Waves and other geomagnetic phenomena observed and recorded by the SAM-III magnetometers in Alaska:

https://reeve.com/RadioScience/Radio%20Astronomy%20Publications/Articles_Papers.htm#Observations

ULF Wave Observations at the Beginning of 2025

Whitham D. Reeve



Introduction: Ultralow Frequency Waves (*ULF Waves*) are regularly observed by the SAM-III magnetometers in Alaska. The present article discusses ULF Wave observations soon after the beginning of the new year 2025 at Anchorage and the HAARP facility near Gakona, Alaska. Another article in this journal issue discusses ULF Waves observed in mid-December 2024 and provides additional background information and references. The observations in January were during a different time of day than those in December, possibly indicating a different source or cause.

Observations: The magnetograms for the UTC morning on 5 January 2025 show rapidly varying traces indicative of ULF Waves (figure 1). ULF Waves usually are observed in the horizontal component of Earth's magnetic field and are seen here in its constituents Bx (north-south) and By (east-west). These ULF Waves reached peak-to-peak amplitudes higher than 40 nT. The local ambient magnetic fields at the two observatories are about 350 times stronger, indicating why ULF Waves historically were called *micropulsations*.

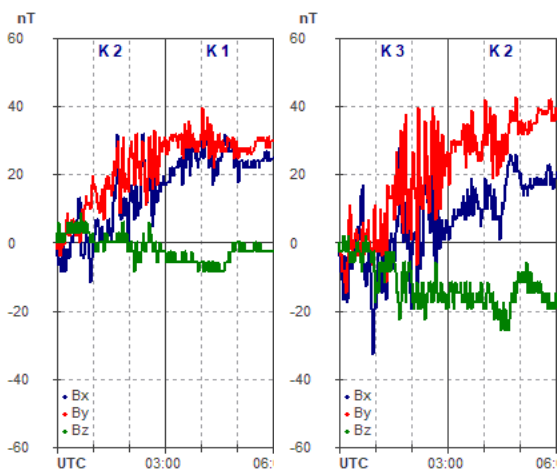


Figure 1 ~ Cropped magnetograms for Anchorage (left) and HAARP (right) showing the time period 0000 to 0600 UTC on 5 January 2025. ULF Waves are quite strong between about 0100 and 0500, especially in the east-west component. The vector sum of Bx (north-south, blue trace) and By (east-west, red trace) defines the horizontal, or H, component. The quasi-K-Index values along the top of the plot are based on local settings for each magnetic component and the two locations track each other over the long term but not necessarily during every 3-hour synoptic period. The variations in Bz (vertical, green trace) at HAARP are thought to be due to stray ground currents from the local underground power distribution system.

Analysis: A portion of the raw data produced by the two magnetometers is plotted to show the 3-hour time period from 0100 to 0400 (figure 2). The time domain plots show the actual, uncorrected magnetic flux density. The discrete time-series data are transformed to the frequency domain to extract individual wave frequencies. The FFT is calculated using the Hamming window to reduce spectral leakage. The SAM-III magnetometers at Anchorage and HAARP are setup to sample the local magnetic field at 10 second intervals; thus, the 3-hour time period consists of 1080 datapoints.

The Fast Fourier Transform (FFT) analysis tool in Microsoft Excel is used here to convert the time series data to the frequency domain. It requires that the number of datapoints be a power of 2 so, of the 1080 datapoints available, 1024 were used. With a sample rate $f_s = 100$ mHz (10 second sample interval) and $N = 1024$ datapoints, the frequency resolution is $f_s/N = 0.1$ mHz. The resulting FFT has a relatively large dc component, which is truncated in the plots. The vertical axes of the FFT plots are labeled *Relative Amplitude* because no effort was made correct or compensate for any amplitude errors resulting from the windowing function or transform.

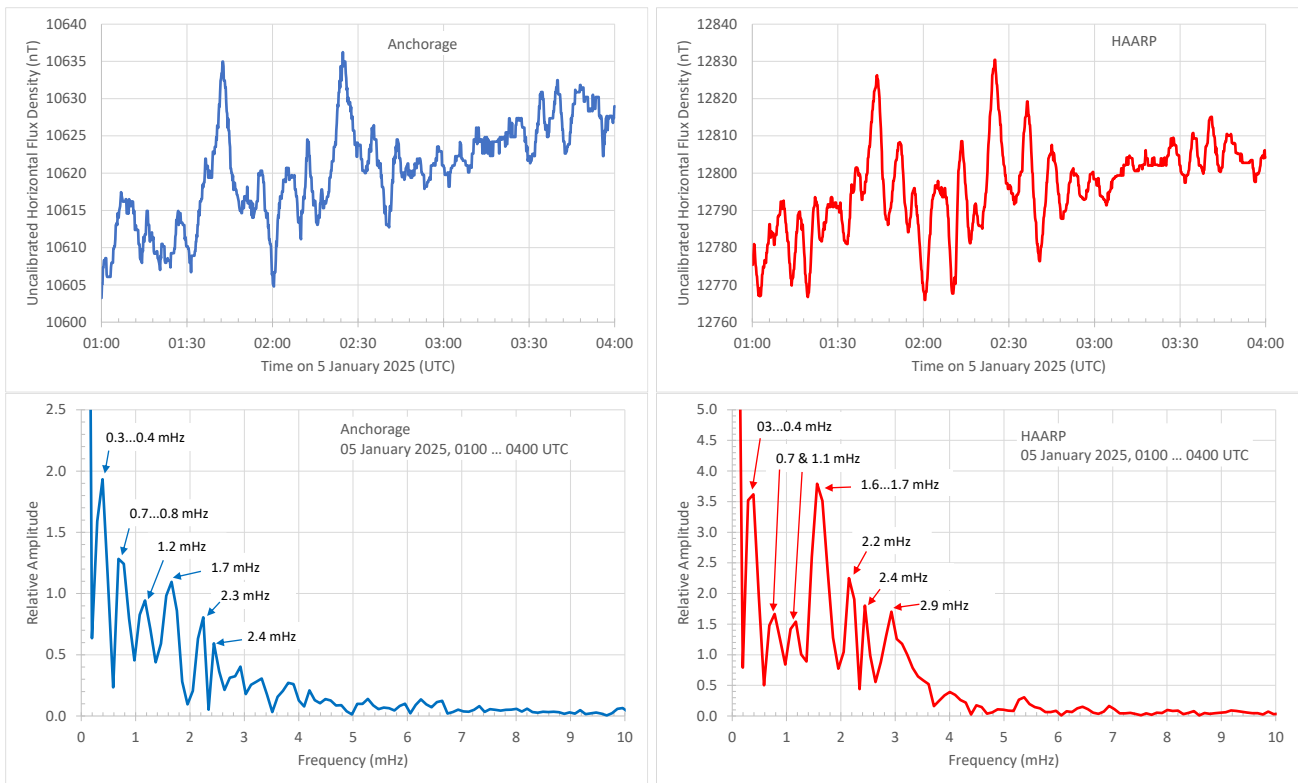


Figure 2 ~ Anchorage (left) and HAARP (right) data for 5 January 2025. The upper plots show the time domain data between 0100 and 0400 UTC, and the lower plots show the frequency domain transforms of the serial-time data. Note the basic commonality between the two locations in both the time and frequency domains. The vertical scales in the time domain plots are raw, uncorrected data. The vertical scales in the frequency domain plots are relative amplitudes determined from the Fast Fourier Transforms of the magnetic flux density variations measured from the beginning of the time period. The frequency resolution of the transform is 0.1 Hz. The frequencies of major spectral indications are annotated. Some are shown as ranges because of close-by peaks and may indicate frequency drift throughout the time period. Note the strong indications below 1 mHz, which may indicate periodic density structures in the solar wind.

Coincident events: According to Space Weather Prediction Center, a 10 MeV proton event was observed at geosynchronous orbit beginning at 2235 UTC on 4 January, only a few hours before the ULF Waves were observed at Anchorage and HAARP. The proton event was associated with a long-duration C7.6 flare.

A proton event consists of energetic particles (mostly hydrogen and helium nuclei) emitted by the Sun that travel at a significant fraction of light speed and arrive in Earth's vicinity within hours. The event peaked at 0055 on 5 January and ended at 0940; thus, it was time-coincident with the ULF Waves observations. Also, the near-Earth environment observed by the Advanced Composition Explorer (ACE) spacecraft experienced some variations in the interplanetary magnetic field (IMF) and solar wind speed and temperature (figure 3). These variations were primarily due to geoeffective coronal hole high-speed streams.

Discussion: The FFT spectra show significant spectra in the ranges 0.3 to 0.4 and 0.7 to 0.8 mHz (periods from about 20 to 55 minutes), below the generally classified frequencies of ULF Waves. Previous analyses of ULF Waves observed in Alaska by the SAM-III magnetometers indicate these lower frequencies are common. The source (or sources) of these spectra is not known but they could be instrumental effects (environmental effects are excluded because of the two completely different locations and temperature and humidity regimes) or related to periodic density structures (PDS) in the solar wind. Periodic density structures modulate the magnetosphere and can produce periodic magnetic signatures on the ground.

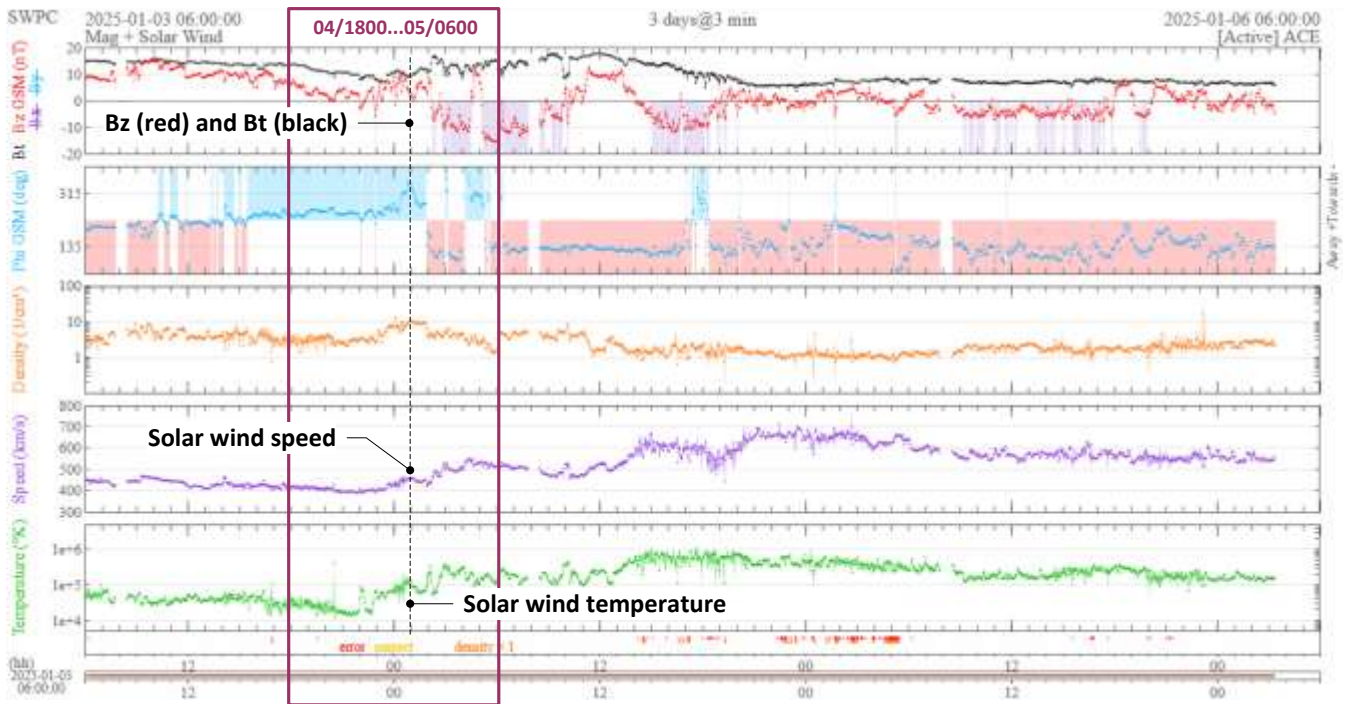


Figure 3 ~ ACE spacecraft data for the 3 days 4 through 6 January. The period from 1800 on 4 January to 0600 on 5 January is boxed to overlap the time period of the ULF Waves observations (0100 to 0400 on the 5th) and a dashed line and callouts are added to indicate 0100. The notable activity consists of southward deflection of Bz (ACE Bz is aligned with Earth's dipole field) around 0200 and modest increases in both the solar wind speed and temperature. Image source: <https://www.swpc.noaa.gov/products/real-time-solar-wind>

The ULF Waves were observed during the 0100 to 0400 UTC time period when Anchorage and HAARP were in the dusk sector (figure 4). This was in contrast to the waves in December that were observed during the midnight-to-dawn and dawn-to noon sectors. Although different mechanisms may be responsible for the December and January waves, both include the possibility of shear and turbulence between the interplanetary magnetic field (IMF) carried in the solar wind and Earth's magnetosheath as the wind blows around the magnetosphere's flanks. The ULF Waves could be the result of a combination of causes including PDS, the proton event as well as the large number of flares the day before the ULF Wave observations.

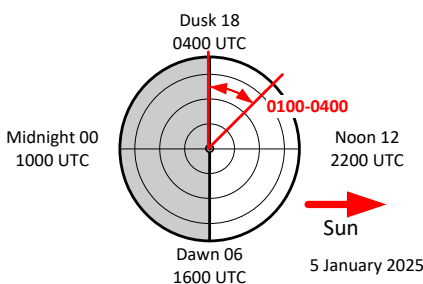
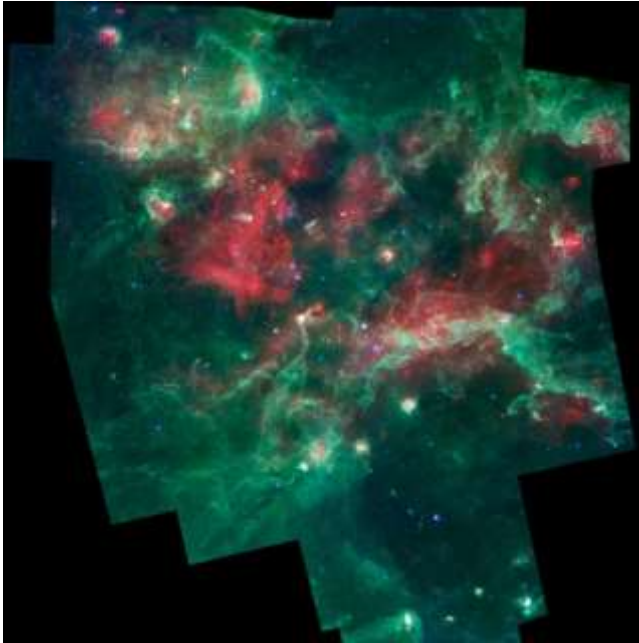


Figure 4 ~ Solar time scale for Anchorage with corresponding times in UTC. UTC times at HAARP are 20 minutes earlier. The ULF Waves on 5 January occurred in the dusk sector.

W75N/DR21 star formation cluster and 6.7 GHz methanol line observations

by Dimitry Fedorov UA3AVR

W75N/DR21 is a star formation cluster of two close regions W75N and DR21; they are a part of large Cygnus X complex, see colored infrared image of Cygnus X in Figure 1 [1]. This report is about observations of methanol



radiation 6.7 GHz from regions location in November 2024 - February 2025 with small single dish radio telescope 2.4 m. The methanol line 6.7 GHz appears due to the molecular transition $5_1 \rightarrow 6_0$, A⁺ molecule type, accurate frequency 6668.5192 MHz [2]. Observed radiation is of maser amplification nature. Methanol 6.7 GHz masers belongs to class II, i.e. molecular clouds are pumped to the inverse state by the infrared radiation in objects where they are reside, and can work as a molecular tracers in the regions. Star forming objects are characterized usually by high infrared luminosity. Coordinates for W75N G81.87+0.78, for DR21 G81.76+0.59 by the methanol radiation (iMet identifiers [3]). As one can see both regions are located close really.

Figure 1. Spitzer infrared image of Cygnus X [1], observations 2012. Colors are: blue – 3.6 μm, blue-green – 4.5 μm, green – 8 μm, red – 24 μm.

More info about W75N/DR21 and its methanol radiation

Here some info about regions W75N and DR21 is collected. Distance to regions is about 2 kpc, far-infrared (FIR) luminosity for W75N up to $8 \times 10^4 L_{\odot}$; DR21 is brighter with FIR luminosity $1.5 \times 10^5 L_{\odot}$ [4]. HII compact spots are detected in both regions [4], O and B spectral type stars are present [1].

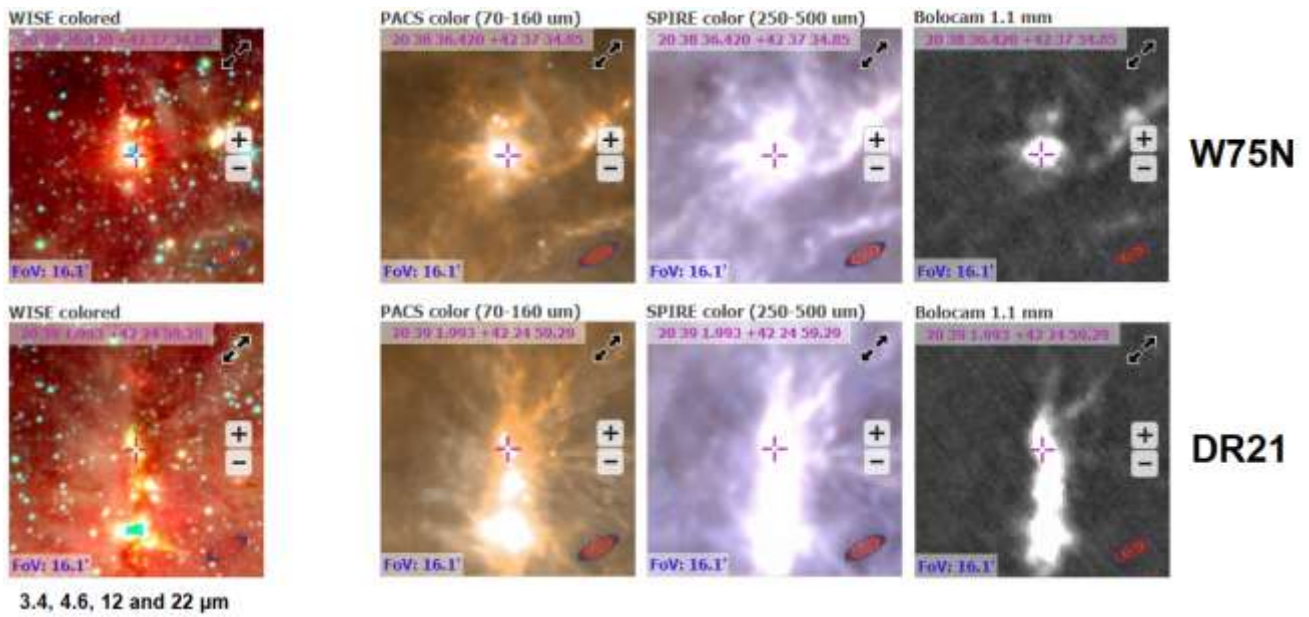
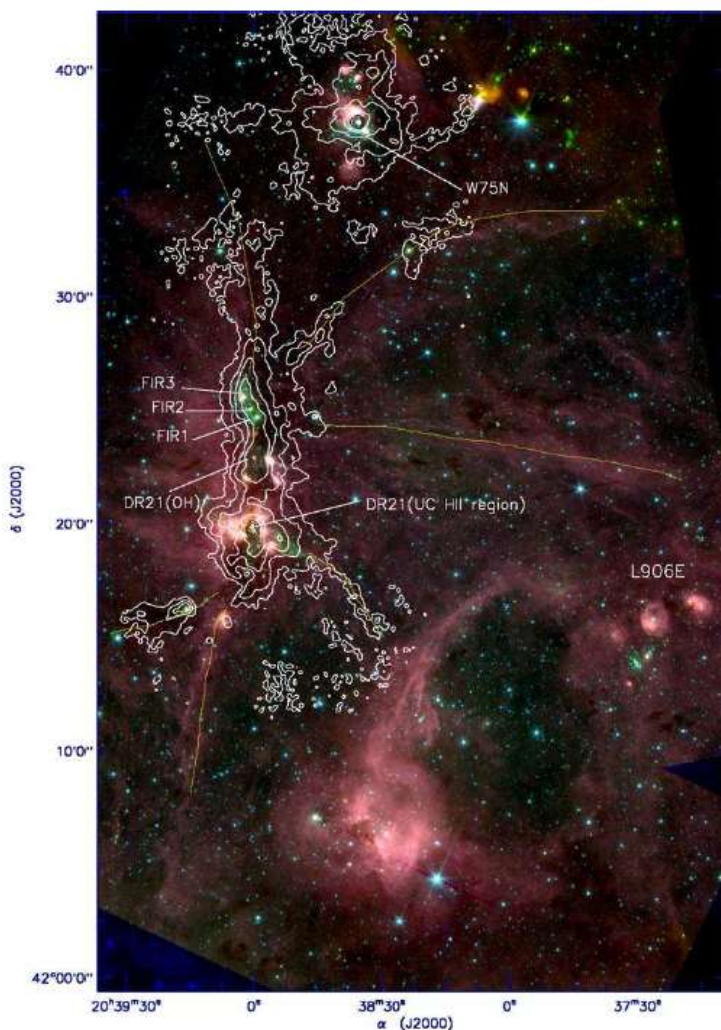


Figure 2. Infrared spots from W75N and DR21 regions by database [5] in different wavelength including far-infrared, sub-mm and mm-waves.



Infrared spots from the regions are shown in Figure 2 [5]. DR21 is elongated in infrareds; picture centers are pointing to methanol radiation in the upper part of the region. In literature, DR21 coordinates can point to the most luminous in near- and mid- infrared bottom part. More detailed infrared image with marked far-infrared (FIR) contours is shown in Figure 3. One can see the FIR spots (FIR1, FIR2 and FIR3) is concentrated in the top part of DR21.

The methanol luminosity of DR21 is lower than W75N despite its higher far-infrared luminosity. Moreover, maser spectral lines from W75N significantly stronger than from DR21 [3], see Figure 4. Both spectra are rich by different features (lines) and show moderate variability according the data. Ibaraki instruments (single dishes 32 m) can distinguish W75N and DR21 despite their proximity.

Figure 3. Detailed infrared map of W75N and DR21 [4]. Colors are Spitzer's blue – 3.6 mm, green – 4.8 mm, red – 8 mm, contours – 850 mm (SCUBA JCMT).

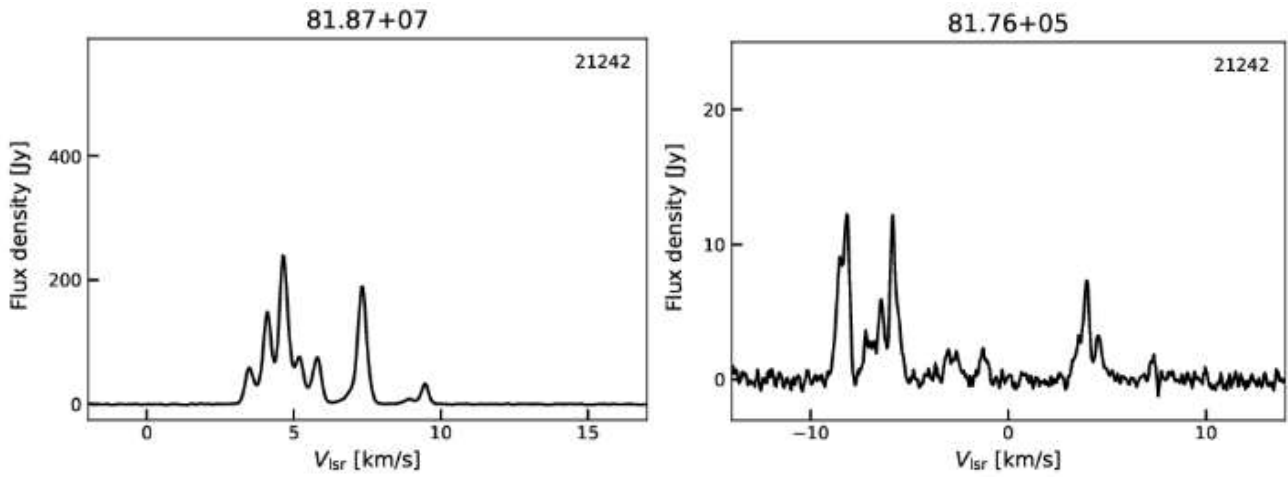


Figure 4. Typical methanol maser spectra for W75N (left) and DR21 (right), Ibaraki iMet database [3].

Next data about observed star formation cluster is a molecular map of W75N (see Figure 5) showing maser spots in the region [6]. Water H₂O maser spots in W75N were marked on the map also. Continuum radiation contours corresponds to proto-star objects, the radiation with wavelength about 1.3 cm can excite methanol molecules and pump the methanol masers too.

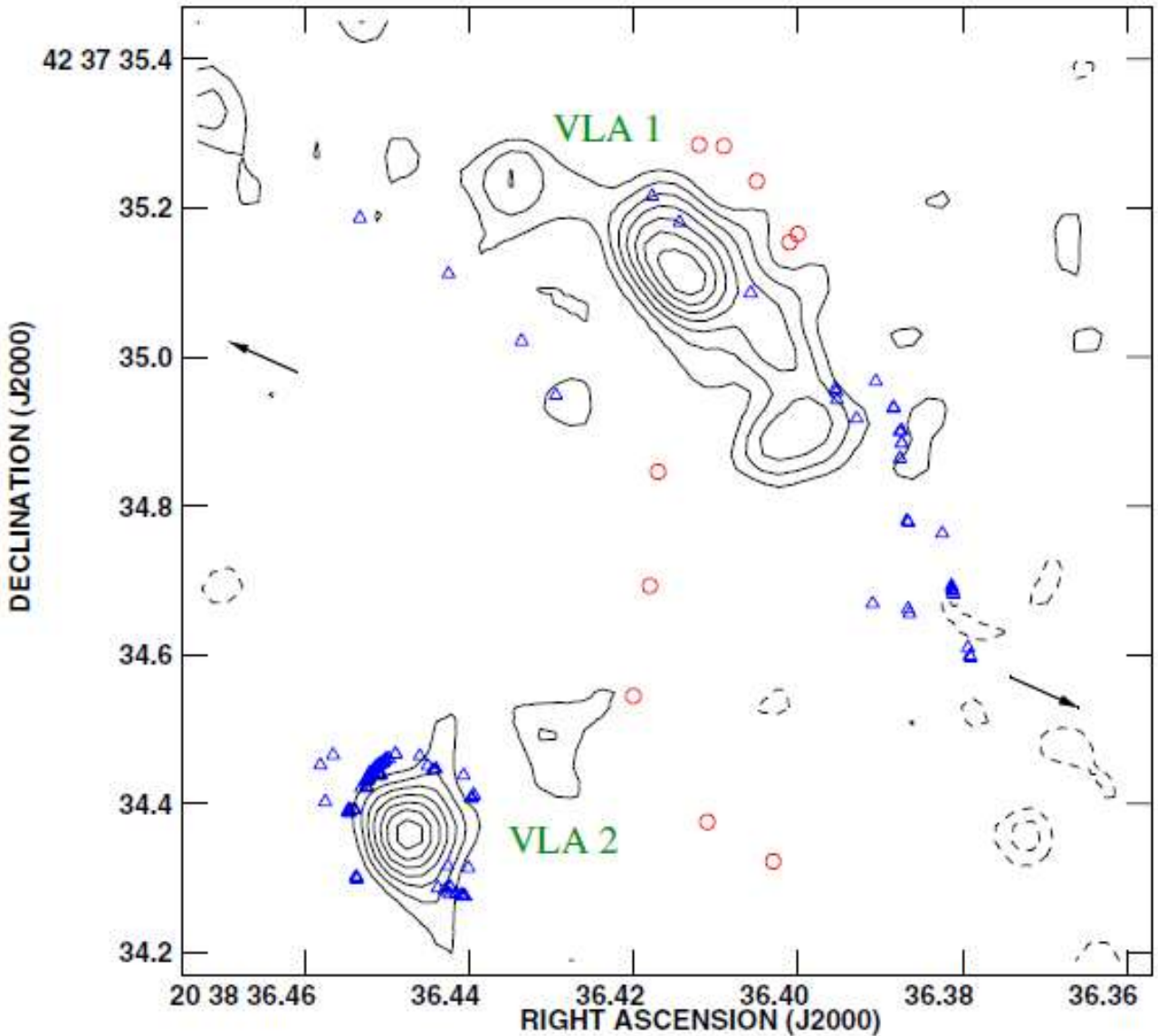


Figure 5. Molecular map of W75N [6]. Red – methanol masers, Blue – water masers, Green (VLA1 & VLA2) and contours – proto-stars continuum radiation 1.3 cm.

Instrumentation

Observations at 6.7 GHz were made using 2.4 m small single dish telescope, see Figure 6.

Dish size $D = 2.4$ m, Half Power Beam Width $\delta_{HPBW} = 1.3^\circ$. The beamwidth defines the telescope resolution. This dish cannot distinct W75N and DR21 regions and receives radiation from their area as a whole.

Telescope characteristics:

$\eta_A = 0.65$ – Aperture Efficiency obtained by solar measurements [7] and Learmonth solar observatory data [8] interpolated to 6.7 GHz. Antenna Half Power Beam width $\delta_{HPBW} = 1.3^\circ$ is comparable with the Sun angular size $\delta_{sun} = 0.53^\circ$; hence, the Beam filling factor $= 1 - 2^{-\left(\frac{\delta_{sun}}{\delta_{HPBW}}\right)^2}$ was included in calculations (ch. 8.2.3 in [9] and [10]), dish sensitivity (forward gain) $\Gamma = 0.001$ K/Jy;

$T_{sys} = 110$ K – from Y-factor Moon measurements [11], $T_{sys} = 120$ K, obtained from known receiver NF and estimated spillover;

$SEFD = T_{sys} / \Gamma = 112690 \text{ Jy}$ (with worst value $T_{sys} = 120 \text{ K}$);

Minimal detectable peak flux density $\approx 80 \text{ Jy}$ (RBW $\approx 5 \text{ kHz}$, 1 hour of integration). Methanol radiation from DR21 turns out under detection threshold. From W75N/DR21 cluster only maser tracers in W75N would be seen on the output spectra.

Linear polarization. Source automatic tracking during all the integration time (with F1EHN software).

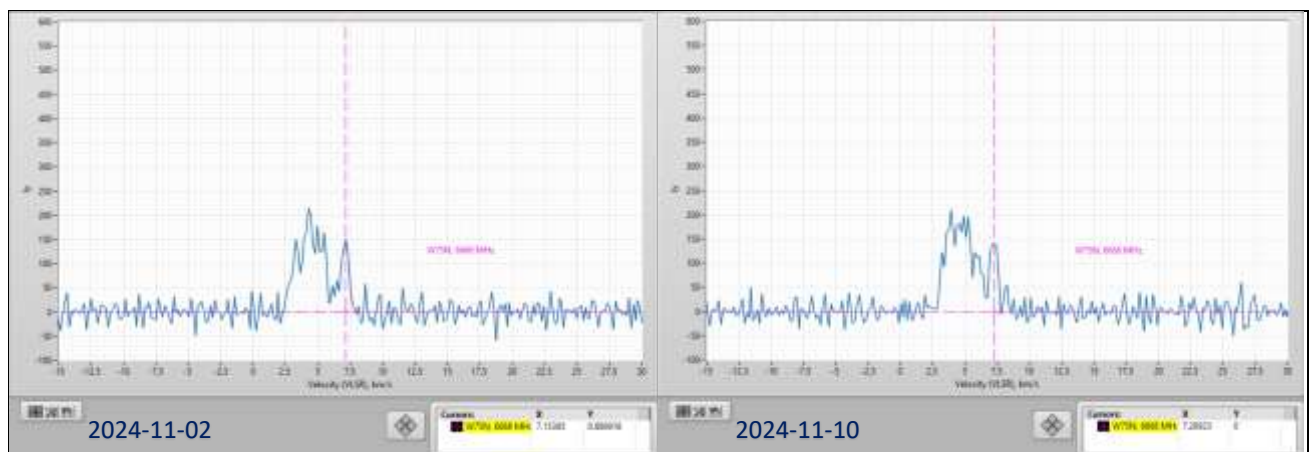
Outdoor downconverter: Terrasat 6.4-7.1 GHz RX module (LO 5.7 GHz) + LNA (NF=1.2 dB). Indoor IF receiver: USRP B200mini, receiver resolution – 5 kHz by noise bandwidth (about 0.2 km/s in velocity units), total receiver bandwidth – 1.5 MHz. The indoor IF receiver USRP B200mini is controlled using LabVIEW software with on-fly averaging of spectra (no intermediate data are stored), see more details about IF receiver and post-processing procedures in papers [12].

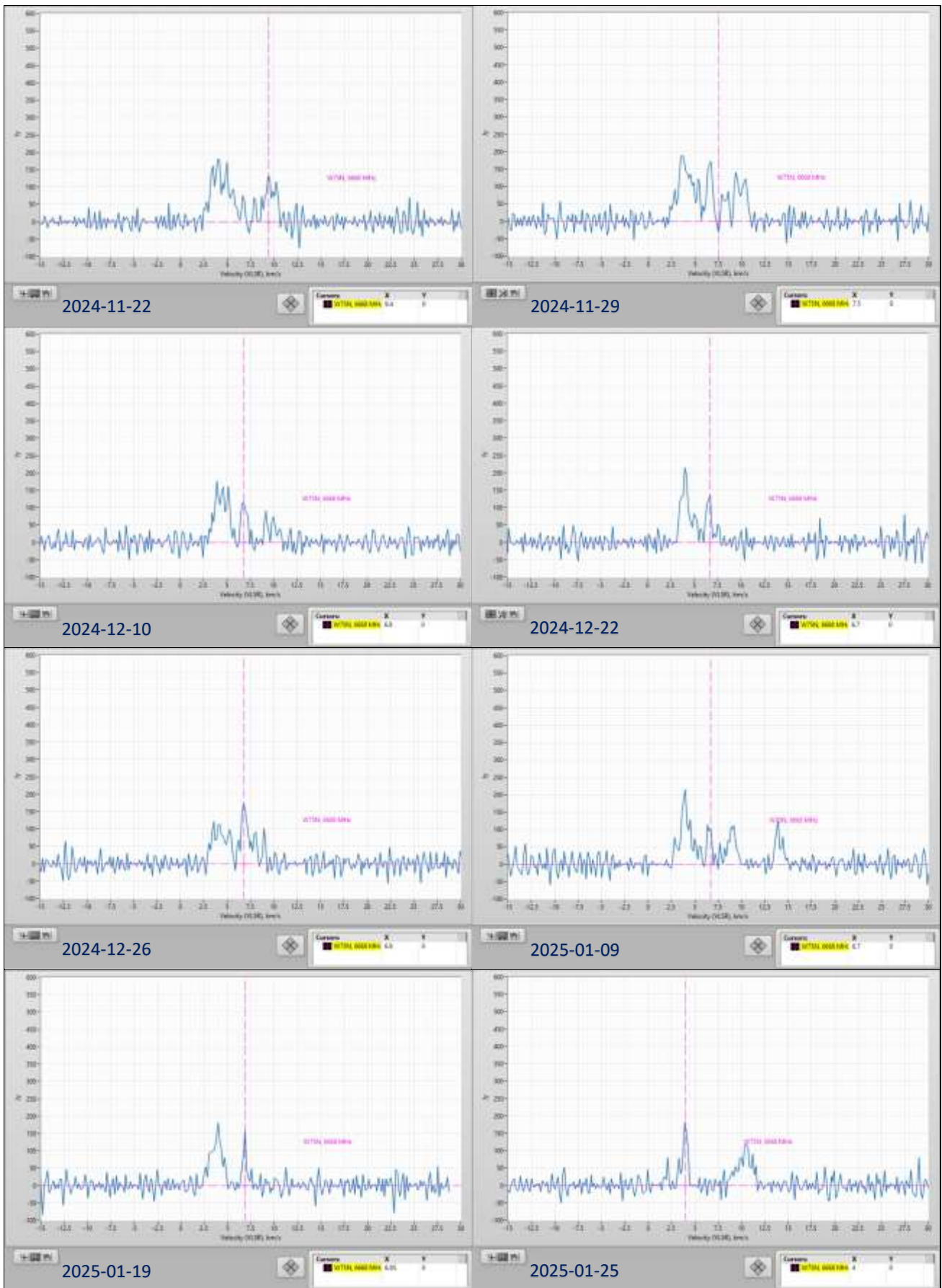


Figure 6. 2.4 m dish mounted on the roof of apartment building ([55°46'00.5"N 37°49'25.8"E](#)) with 6.7 GHz RX downconverter at the focus. The dish was designed by Sergei Zhutyayev RW3BP for mm-waves initially.

Results and discussion

Observed spectra from the regions location are shown at Figure 7. Integration time was 1 hour. As expected DR21 lines are under the detection threshold, and the telescope sees W75N spectra only. Other possible 6.7 GHz sources in Cygnus X are also expected under the threshold. Observed levels can be underestimated in comparison to Ibaraki iMet data (Figure 5 or [3]), presumably due to polarization effects.





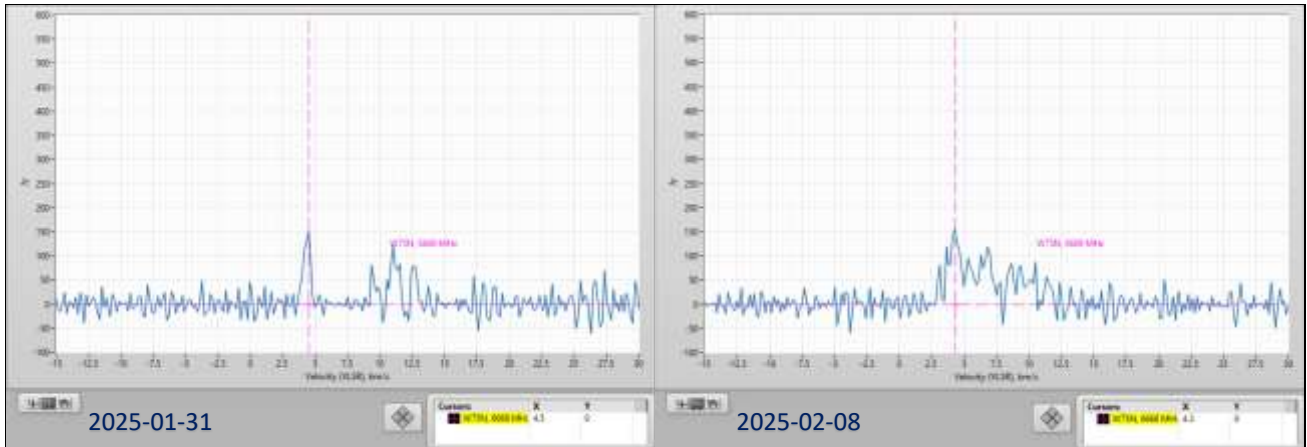


Figure 7. Observed W75N methanol spectra 6.7 GHz from November 2024 to February 2025, integrations 1 hour.

A noise reduction was applied in post-processing procedures except the velocity ranges where maser lines were expected. The noise floor under expected lines (and under other clearly seen bumps in raw spectrums) is interpolated by smooth lines; in other places it is fitted by splines with relative small numbers of points. Having such smoothed noise floor the background correction is applied next. I should remind the detection threshold is about 80 Jy, and the post-processing procedures work with signals on the noise level or somewhat higher. So, unexpected lines in 2024-11-29 plot (wide line about 8 km/s), 2024-12-10 plot (lines about 10 km/s), 2024-12-26 plot (narrow line 9 km/s), 2025-01-09 plot (lines 9 and 14 km/s), 2025-01-31 (lines about 10 km/s) can turn out a post-processing artifact. Rather wide lines 9 and 14 km/s on the 2025-01-09 plot are higher than 100 Jy and can be of RFI nature too.

Nevertheless, the spectra Figure 7 show variability and changes in the methanol masers in W75N. The quiet state of first half of November has evolved to disturbed one with disappearing the line about 7.5 km/s, and appearing lines about 10 km/s. Next, the line 7.5 km/s has restored with a little bit lower velocity about 7 km/s, and the lines about 10 km/s are fading. In addition, the line about 4.5 km/s has sharpened, become narrower. Spectra 2025-01-25, 2025-01-31 has lost the line about 7-7.5 km/s again. As it seems, lines about 10 km/s have appeared again too; at least, some irregularities in the noise floor were noted, and I did not remove them in the post-processing.

It would be noted also, there is a small possibility of seeing methanol flares in other parts of Cygnus X besides W75N.

Acknowledgments

A lot of thanks to Sergei Zhutyayev RW3BP for access to his 2.4 m dish, Figure 6, a lot of works with its tracking system, and valuable help in observations.

References

- [1] Spitzer infrared image of Cygnus X with short description in <https://www.spitzer.caltech.edu/image/ssc2012-02a1-stars-brewing-in-cygnus-x>.
- [2] H.S.P. Mueller et al, *Accurate rest frequencies of methanol maser and dark cloud lines*, [arXiv:astro-ph/0408094](https://arxiv.org/abs/astro-ph/0408094) (2004).
- [3] Ibaraki iMet database, W75N data <https://vlbi.sci.ibaraki.ac.jp/iMet/data/81.87+07/>, DR21 data <https://vlbi.sci.ibaraki.ac.jp/iMet/data/81.76+05/>.
- [4] M.S.N. Kumar et al, WFCAM, *Spitzer/IRAC and SCUBA observations of the massive star-forming region DR21/W75 – II. Stellar content and star formation*, MNRAS 374, 54–62 (2007).
- [5] Database of astrophysical masers maserDb.net, W75N <https://maserdb.net/object.pl?object=G81.871+0.781>, DR21 <https://maserdb.net/object.pl?object=G81.764+0.596>.

- [6] G. Surcis et al, *The structure of the magnetic field in the massive star-forming region W75N*, *Astronomy&Astrophysics* 527, A48 (2011).
- [7] Wolfgang Herrmann, *Refurbishing an SRT, Part 4: Characterization and Observation Examples*, *Radio Astronomy, Journal of the Society of Amateur Radio Astronomers*, September – October 2022, p. 42.
- [8] Learmonth solar observatory, radio flux, <https://www.sws.bom.gov.au/Solar/3/4>.
- [9] T.L. Wilson, K. Rohlfs, S. Hüttemeister, *Tools of Radio Astronomy*, 6th ed, Springer, 2013.
- [10] Joachim Köppen DF3GJ, *A Closer Look at Filling Factors*, *DUBUS* 4/2021, v 50, p 15.
- [11] D. Fedorov UA3AVR, *System temperature Tsys by measurements the Moon radiation*, *Radio Astronomy, Journal of the Society of Amateur Radio Astronomers*, January – February 2024, p. 62.
- [12] D. Fedorov UA3AVR, *Methanol maser lines 12 GHz observations*, *Radio Astronomy, Journal of the Society of Amateur Radio Astronomers*, September – October 2022, page 71; D.Fedorov UA3AVR, *Notes on building a maser receiver*, *Radio Astronomy, Journal of the Society of Amateur Radio Astronomers*, March – April 2024, p. 71; D.Fedorov UA3AVR, *Antenna unit for 6.7 GHz methanol maser telescope*, *Radio Astronomy, Journal of the Society of Amateur Radio Astronomers*, May – June 2024, p. 89.

About the author



Dimitry Fedorov was first licensed as radio amateur since 1982, as UA3AVR since 1983. In 1990 graduated as MS in electronics in Moscow Power Engineering University. Now works as research and development engineer in wireless industry, LTE/5G NR, RF and microwave modules development. Previous scientific experience in nuclear and particle physics, worked in Moscow State University, Institute of Nuclear Physics and Universität Tübingen, Institut für Theoretische Physik, see profile blog at <https://www.researchgate.net/profile/Dimitry-Fedorov-2>. Radio Astronomy hobby since 2012, mainly in applications for weak signals reception. You can contact the author at ua3avr@yandex.ru.

Errata

- To paper D. Fedorov UA3AVR, *Observations of methanol masers 6.7 GHz in W51 star forming nebula*, *Radio Astronomy, Journal of the Society of Amateur Radio Astronomers*, November – December 2024, page 70. In caption of Figure 1 correct reading has to be "observations 2020", not "observations 2012".
Formula for the Beam filling factor, page 73 have to be read $=1 - 2^{-\left(\frac{\delta_{sun}}{\delta_{HPBW}}\right)^2}$, i.e. with sign "-" in exponent.
- To paper D. Fedorov UA3AVR, *Observation of G09.621+0.196 methanol maser 6.7 GHz*, *Radio Astronomy, Journal of the Society of Amateur Radio Astronomers*, September – October 2024, page 60. Formula for the Beam filling factor, page 61 have to be read $=1 - 2^{-\left(\frac{\delta_{sun}}{\delta_{HPBW}}\right)^2}$, i.e. with sign "-" in exponent.

A Simple Weather-Resistant Housing for the Nooelec SAWBird H1 Low Noise Amplifier and 1420.405MHz SAW Filter.

Andrew Thornett, M6THO, Lichfield Radio Observatory, Lichfield, UK www.astronomy.me.uk

The need for a cost-effective water-resistant housing for low noise amplifiers on the hydrogen line radio telescopes at Lichfield Radio Observatory.

Lichfield Radio Observatory (LRO) is located at latitude 52.6815 north, longitude -1.8255 (1.8255 west) in Staffordshire, central England, UK, north of Birmingham. The observatory currently includes three radio telescopes designed for the hydrogen line (1420.405MHz). The aerial used on the LRO-H1 Radio Telescope is composed of a Ptarmigan Triffid ex-military 4x4 dipole array, measuring 86cm x 86cm in size, whereas LRO-H2 was constructed from a 1.5m (150cm) parabolic aluminium dish sold by its makers as a solar cooker. The aerial for LRO-H3 was constructed by Alex Pettit from SARA and uses a tuned Plate Yagi design.

All three systems use a Nooelec SAWBird H1 cascaded dual low noise amplifier and SAW filter to narrow the detected signal band down to 1420MHz +/- 30MHz. These low noise amplifiers and filters are not water-proof. They are best located immediately behind the aerial before the coaxial cable run down to the receiver and computer, which can then be placed quite some distance away, as the signal now has been amplified at the aerial.

Therefore, there is a need for a cheap, simple, and effective water-resistant housing that can be used for the Nooelec SAWBird H1 LNA on the hydrogen line radio telescopes at LRO. In this paper, I describe such a housing which has been implemented at Lichfield Radio Observatory.

Obtaining an appropriate housing.

I was able to purchase an appropriate housing from ebay.co.uk for only a few British pounds. The internal dimensions are 28mm x 83mm. External dimensions are 120mm x 35mm. There are two convenient screw holes for attaching the housing to either aerial or mount. The main box has a lip, over which the lid fits, supplying water-resistance.

Photos of housing:



Effectiveness of the housing.

The Nooelec SAWBird H1 LNA comes in two forms, one with a plastic cover around the PCB and the other without, the “bare-bones” version. The version with cover does not fit into this housing, so it is best used with the bare-bones version.

One advantage of using a housing of this nature is that alternative connectors can be screwed onto the housing, which are less liable to damage from bending pressure on the connection, and which are more water-resistant. In this case, it allows N-type chassis connectors to be used and then connectors internally to the SMA connector on the SAWBird LNA.

The size of the SMA connectors on the Nooelec SAWBird H1 Bare-Bones LNA is such that when screwed onto the SMA connector on inside of the N-type-SMA chassis connector on both sides, then the chassis plate projects slightly outside of the length of the housing. As a result, a shim is required between the plate on each side and the housing to compensate for this difference.

In addition, the SAWBird PCB contains a white LED which lights to indicate that the device is powered. This is important as the device is powered via a bias-tee and it is important to be able to confirm that this has been correctly set in software such as Easy Radio Astronomy or SDR Sharp. Without this confirmation, then it would be easy to accidentally not power the SAWBird H1 and hence not obtain either amplification or filtering of the signal picked up by the aerial.

To be able to observe this LED light, a small hole needs to be drilled into the side of the housing which can then be protected from ingress of water by gluing a small piece of clear plastic over the hole.

Photos showing housing and Nooelec SAWBird H1 and how this fits into housing:



Further information.

Further information about this project is available on the www.astronomy.me.uk website or by contacting me using the “contact us” page on that website.

3D-processing of three days data using latest ezCon250124b.py script in ezRA suite & using meshes/matrix data tables in Rinearn 3D.

Dr Andrew Thornett, M6THO, Lichfield Radio Observatory, Lichfield, UK www.astronomy.me.uk

Presenting hydrogen line data.

Amateur radio astronomers have successfully measured hydrogen intensity within the Milky Way using a range of equipment, both self-made and available off the shelf. This data has a major “Wow” factor when we show it to the public at large. However, they find it difficult to comprehend, and such issues extend even to members of the wider amateur astronomy community. The need to produce new methods of displaying data, to make it easier to interpret, extends to ourselves as amateur radio astronomers – particularly those of us with an engineering, physics or telecommunications background often find the results of our radio astronomy experiments unfathomable!

A new script in Easy Radio Astronomy Suite (ezRA).

Ted Cline’s free Easy Radio Astronomy Suite (ezRA, <https://github.com/tedcline/ezRA>) is a popular option for collecting a processing Milky Way hydrogen line data. Many of us have large data sets available which will benefit from a new method of presenting this data. Rinearn 3D is another free software package, which can be used to present the data in a more accessible picture form. However, Rinearn 3D is limited in the amount of data it can process due to the processing and RAM requirements for 3D interpretation of large data sets. Rinearn 3D can use two alternative types of data, both presented as CSV files. The usual method produces much larger data sets, but there is an alternative which stores the data within the CSV file as a matrix, leading to a file size up to ten times smaller than the first storage format. The use of this method allows much larger data sets to be processed by Rinearn 3D.

There is now a new script available for ezRA (ezCon250124b) which will process ezCol data sets (ezRA’s data collection programme) and create a matrix CSV file capable of being processed in Rinearn 3D.

Relief maps.

The ability to process such data sets in this way allows the production of relief graphs of the Milky Way, emphasising where higher levels of hydrogen-line signal can be detected. If the plot is completely flattened and contour lines added in Rinearn 3D, then a heat map is generated. Such maps are like those which are experienced in everyday life – from world maps showing the relief of mountain ranges to meteorological charts.

Lichfield Radio Observatory (LRO) data.

Latitude (52.6815 Longitude, -1.8255 Lichfield) is a cathedral city and civil parish in Staffordshire, England. One of eight civil parishes with city status in England, Lichfield is situated roughly 16 miles (26 km) north of Birmingham.

Lichfield Radio Observatory (LRO) is a small private observatory located within the town. There are three hydrogen line radio telescopes, LRO-H1 based on an ex-military 86cm x 86cm dipole array, LRO-H2, built around an 150cm parabolic solar cooker dish, and LRO-H3, the aerial of which was built by Alex Pettit of SARA, and is a multi-element Patch Yagi tuned to 1420MHz.

Results of processing data from LRO.

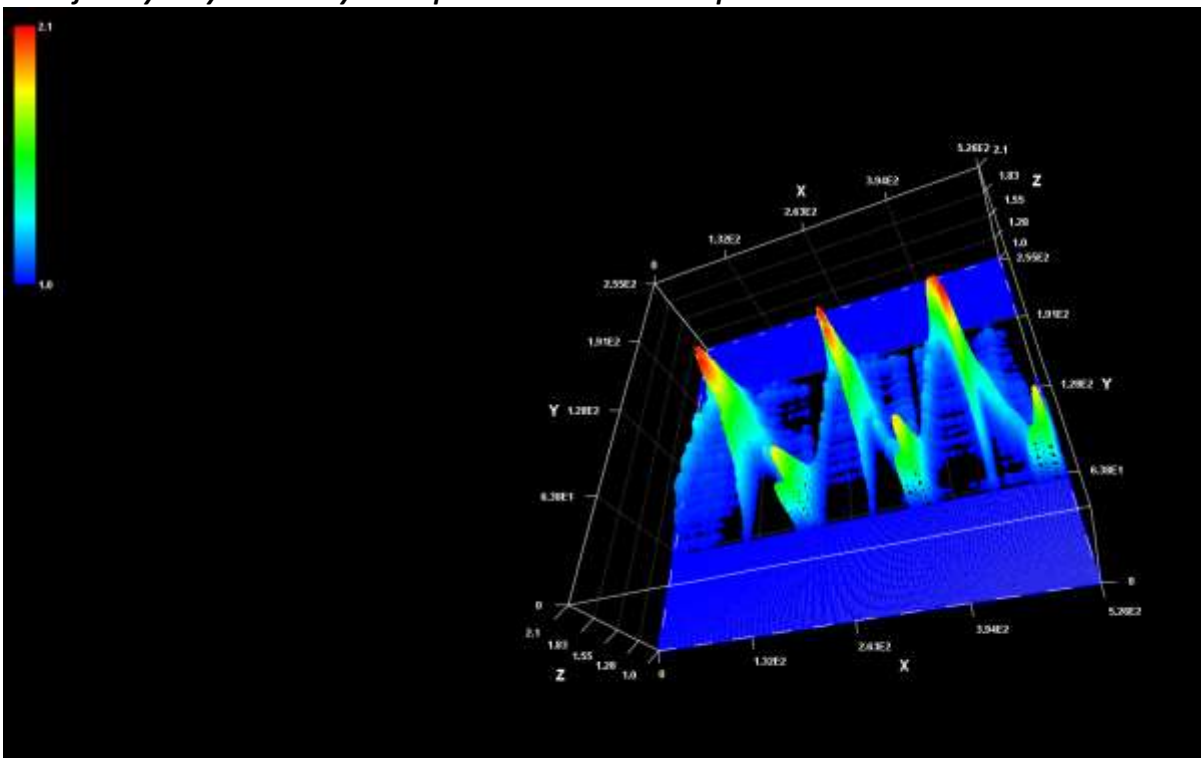
The plots below are produced from three days of data collected in January 2025 from the LRO-H1 (Ptarmigan) radio telescope.

Some of the plots show the full three days. These plots demonstrate a repeating pattern – each repeat representing one day. Other plots have concentrated on only part of the data set, and these do not include a repeating pattern.

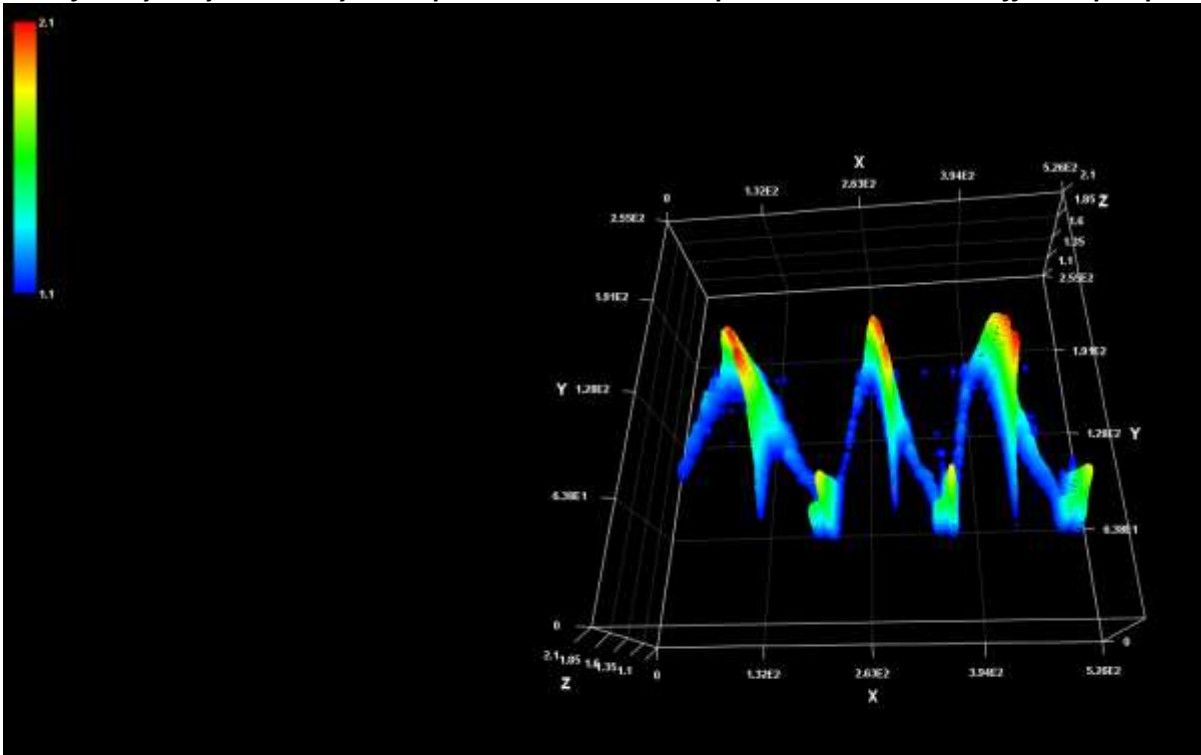
There are also plots, where the data has been flattened in time direction to emphasize relationship between frequency and intensity of signal detected.

For most of the plots, x axis = frequency, y axis = time, z axis = signal intensity; although there are some (3-day plots) where x and y are reversed.

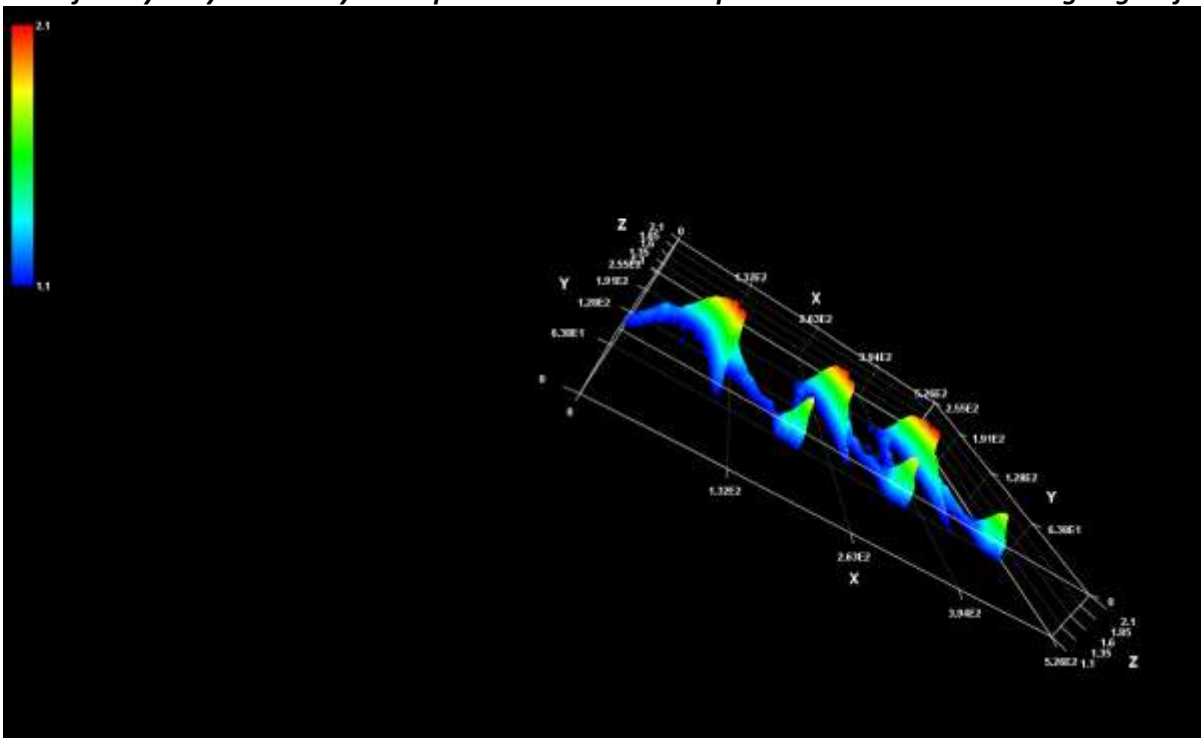
Plot of Milky Way over 3 days in 2 spatial dimensions with power on 3rd access:



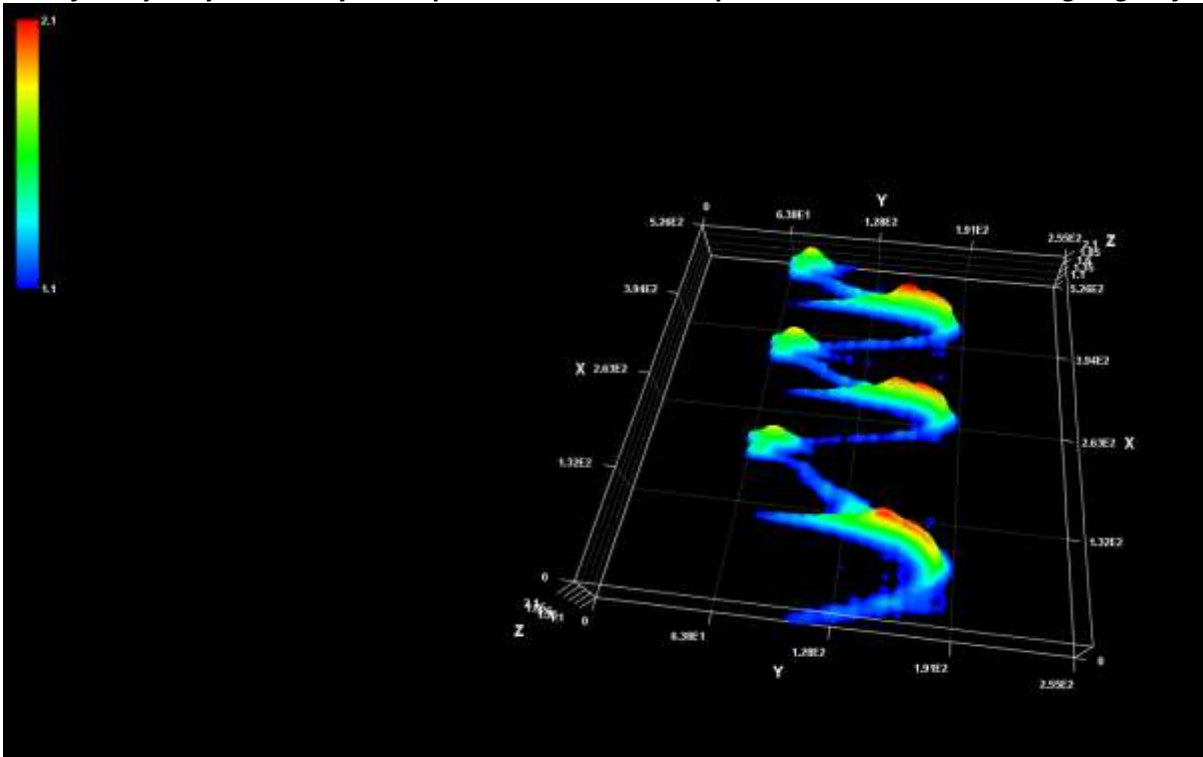
Plot of Milky Way over 3 days in 2 spatial dimensions with power on 3rd access – different perspective:



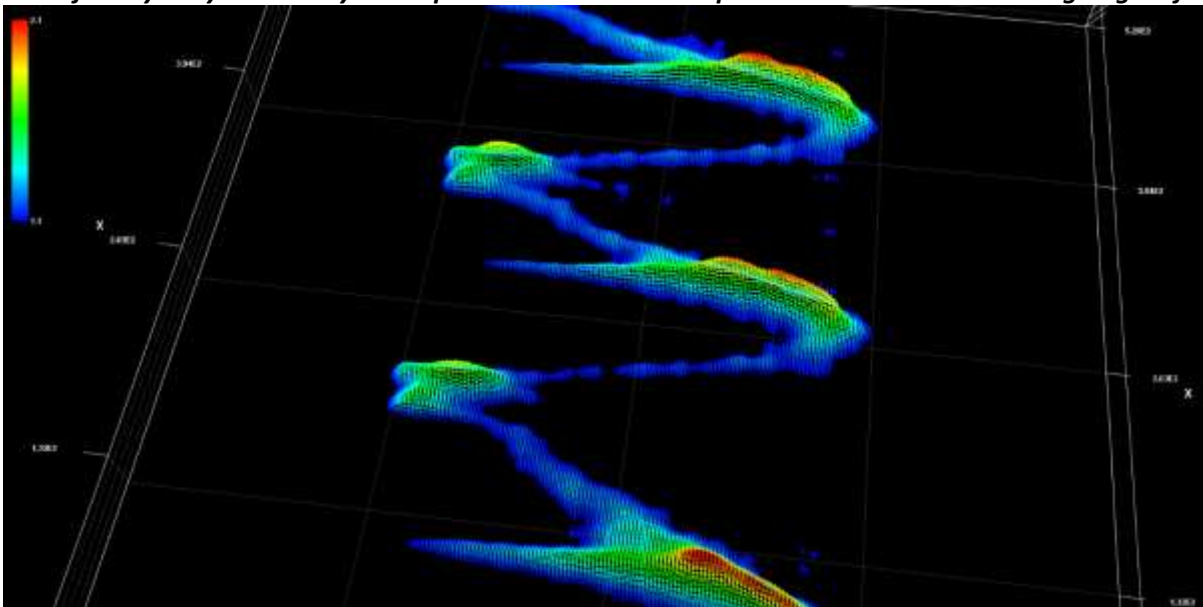
Plot of Milky Way over 3 days in 2 spatial dimensions with power on 3rd access – altering angle of view:



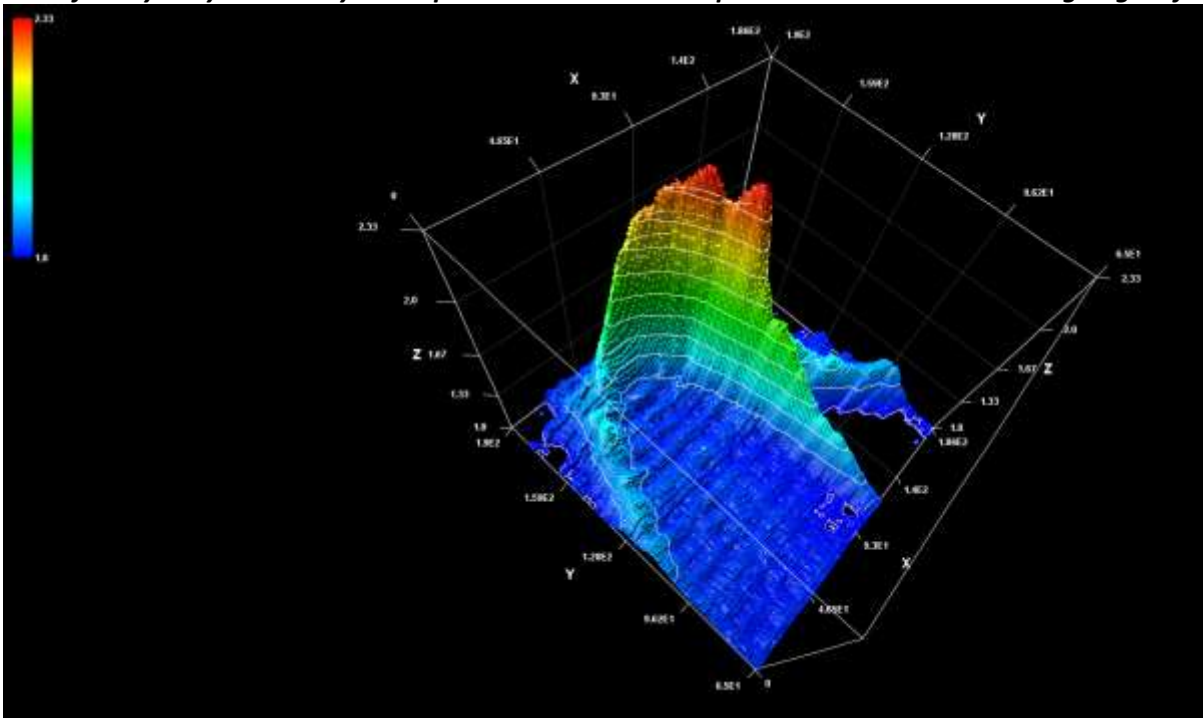
Plot of Milky Way over 3 days in 2 spatial dimensions with power on 3rd access – altering angle of view:



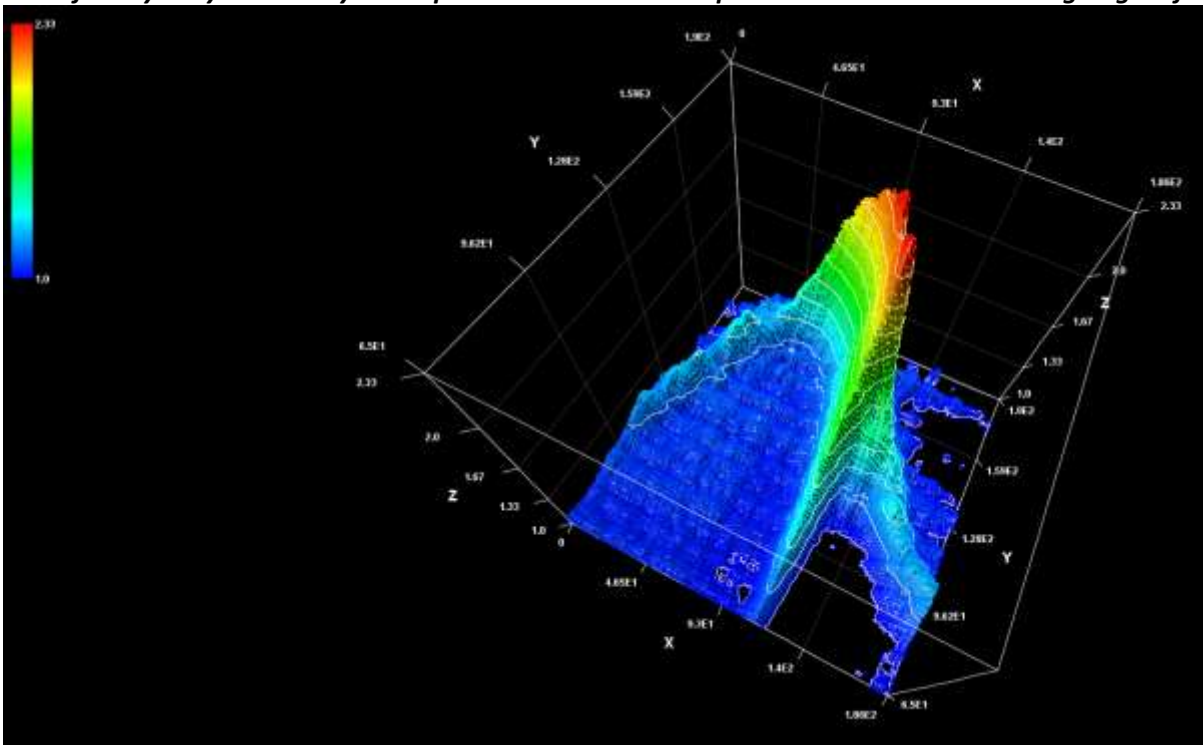
Plot of Milky Way over 3 days in 2 spatial dimensions with power on 3rd access – altering angle of view:



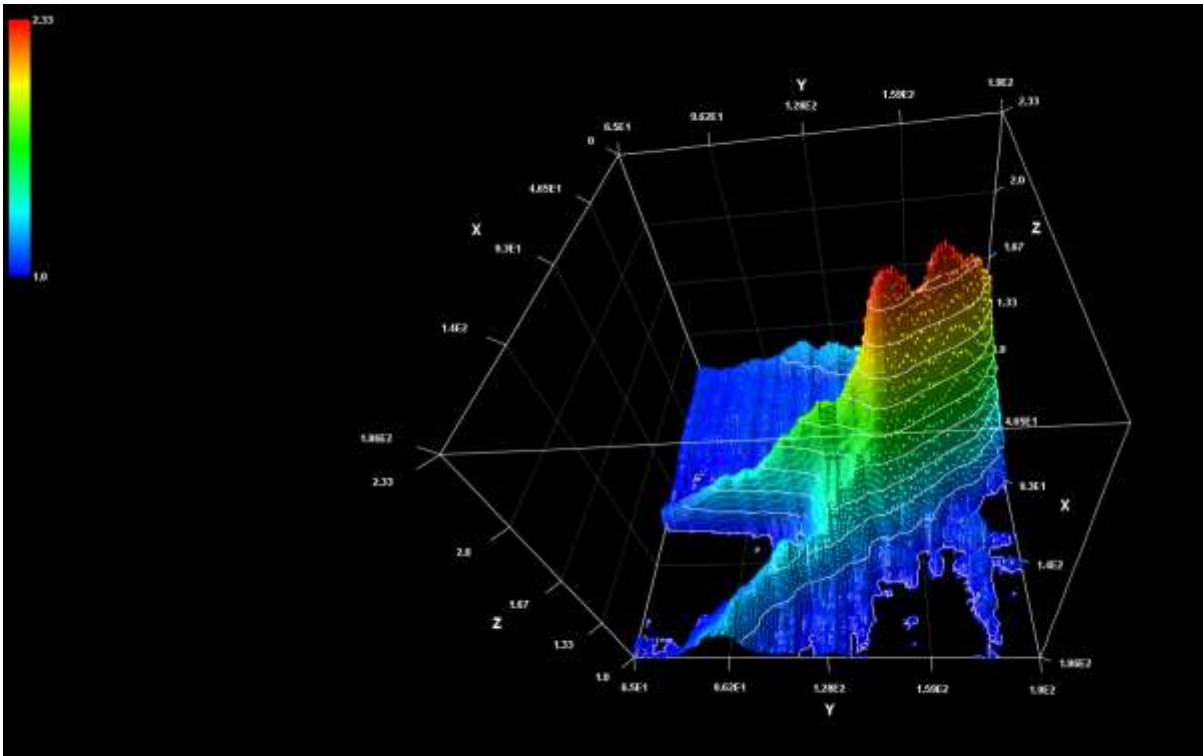
Plot of Milky Way over 3 days in 2 spatial dimensions with power on 3rd access – altering angle of view:



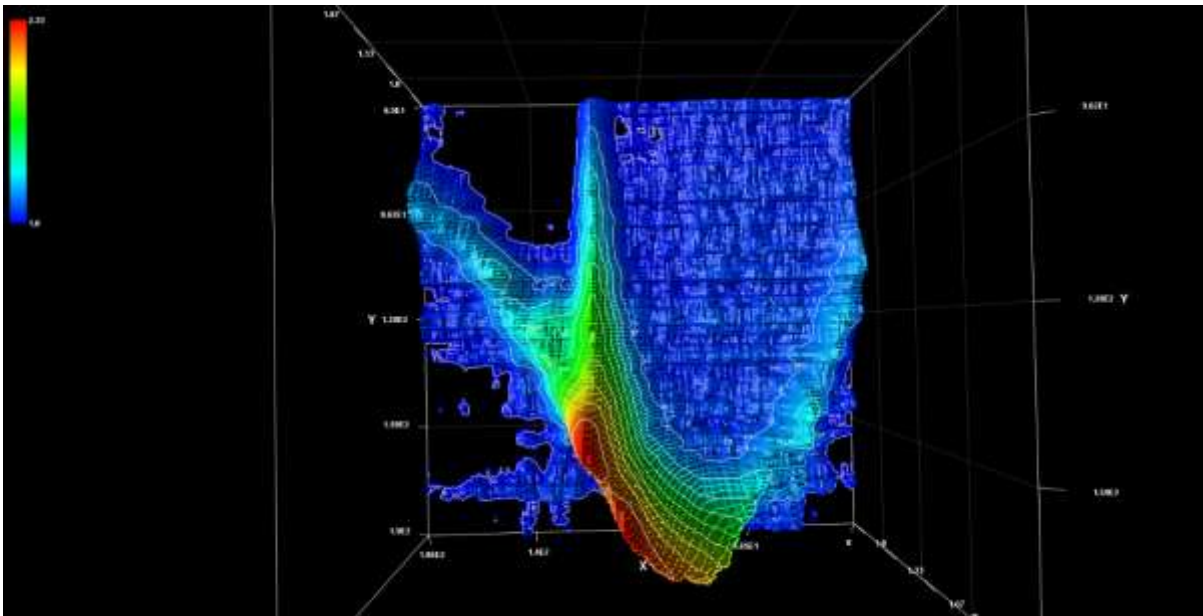
Plot of Milky Way over 3 days in 2 spatial dimensions with power on 3rd access – altering angle of view:



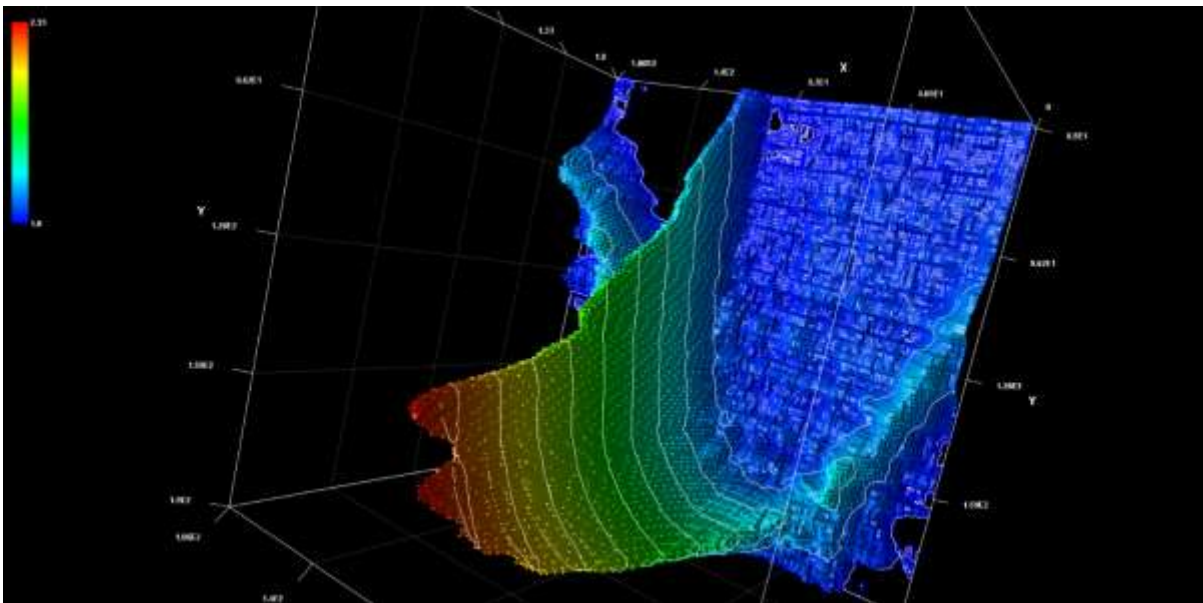
Plot of Milky Way over single days in 2 spatial dimensions with power on 3rd access – altering angle of view:



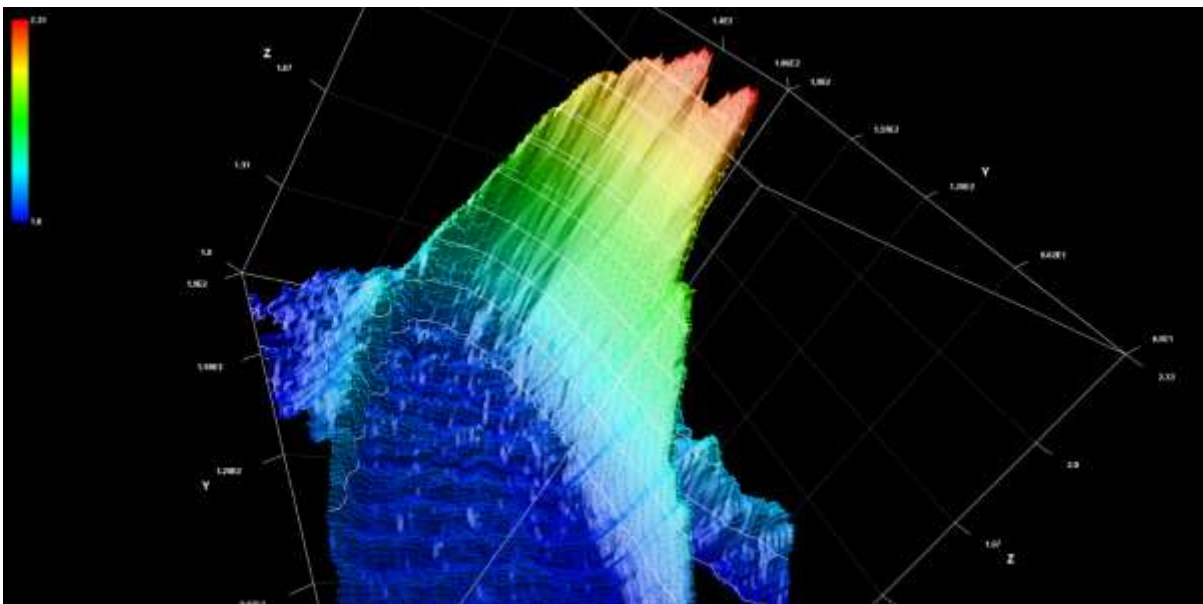
Plot of Milky Way over single days in 2 spatial dimensions with power on 3rd access – altering angle of view:



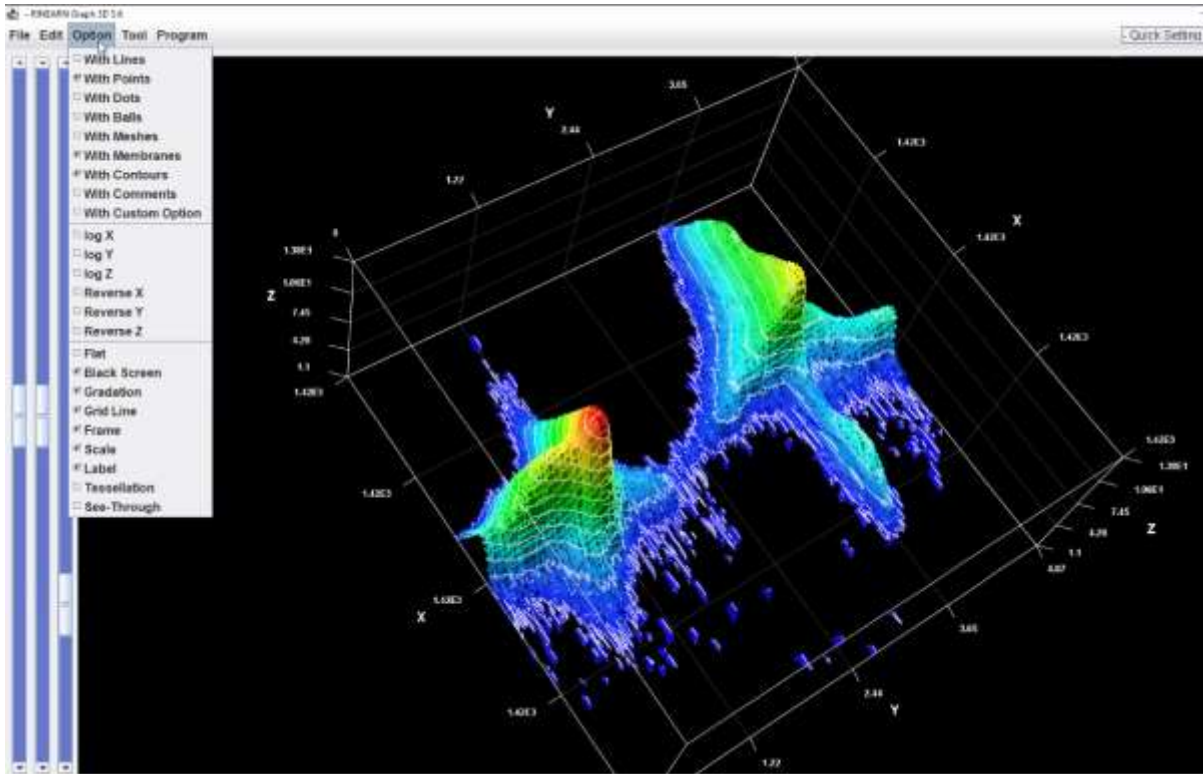
Plot of Milky Way over single days in 2 spatial dimensions with power on 3rd access – altering angle of view:



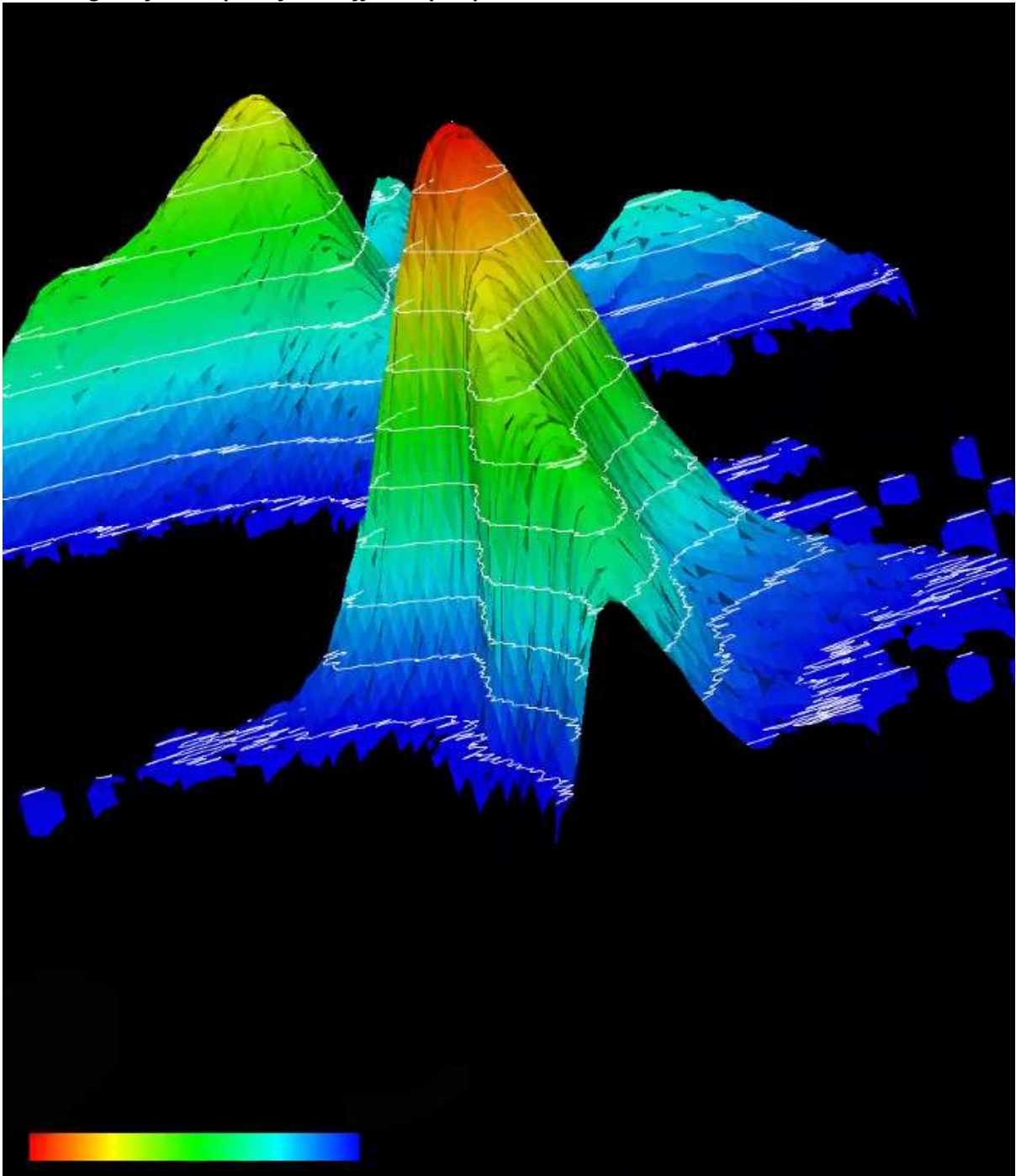
Plot of Milky Way over single days in 2 spatial dimensions with power on 3rd access – altering angle of view:

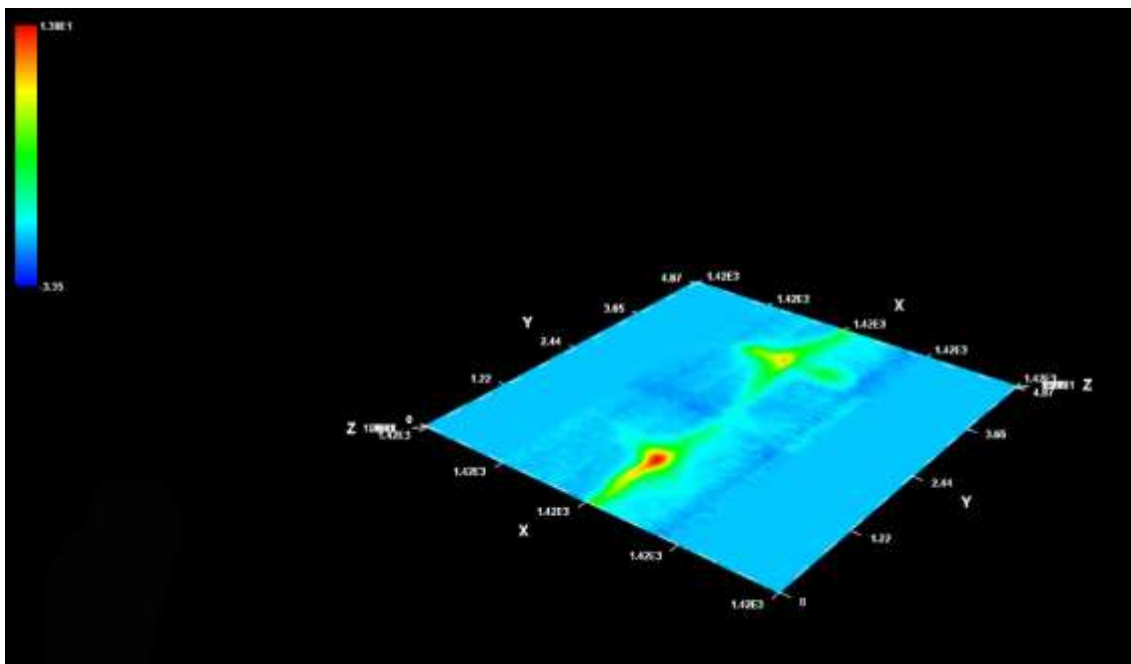
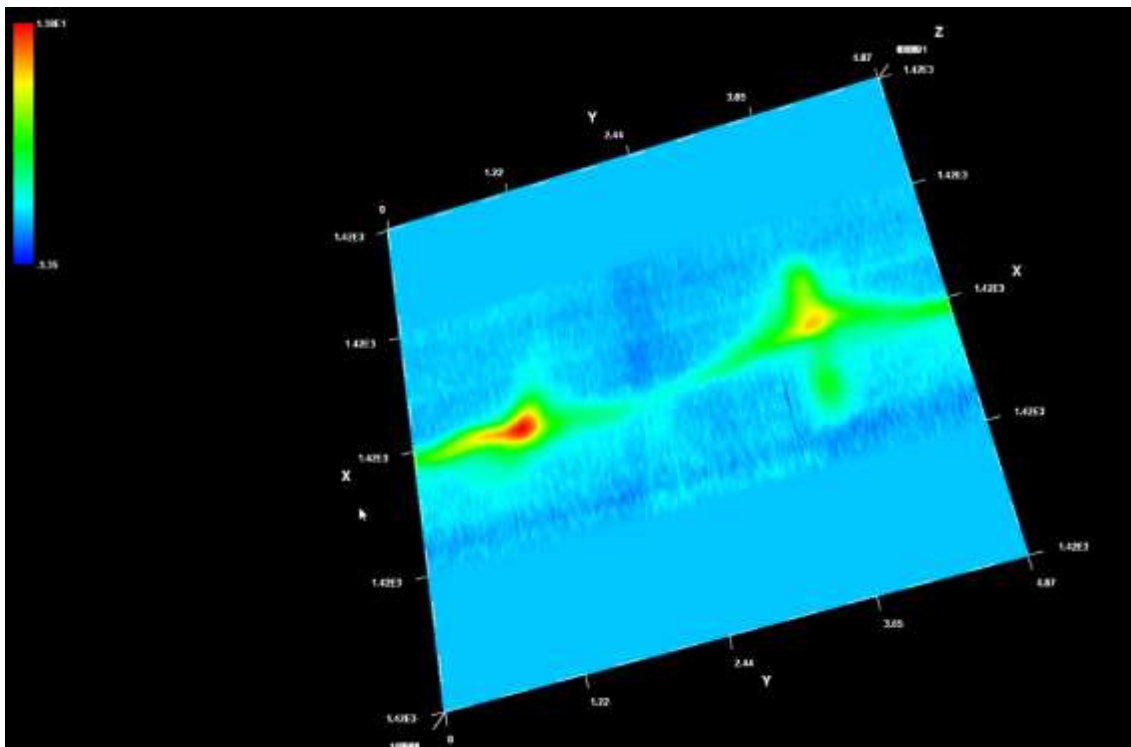


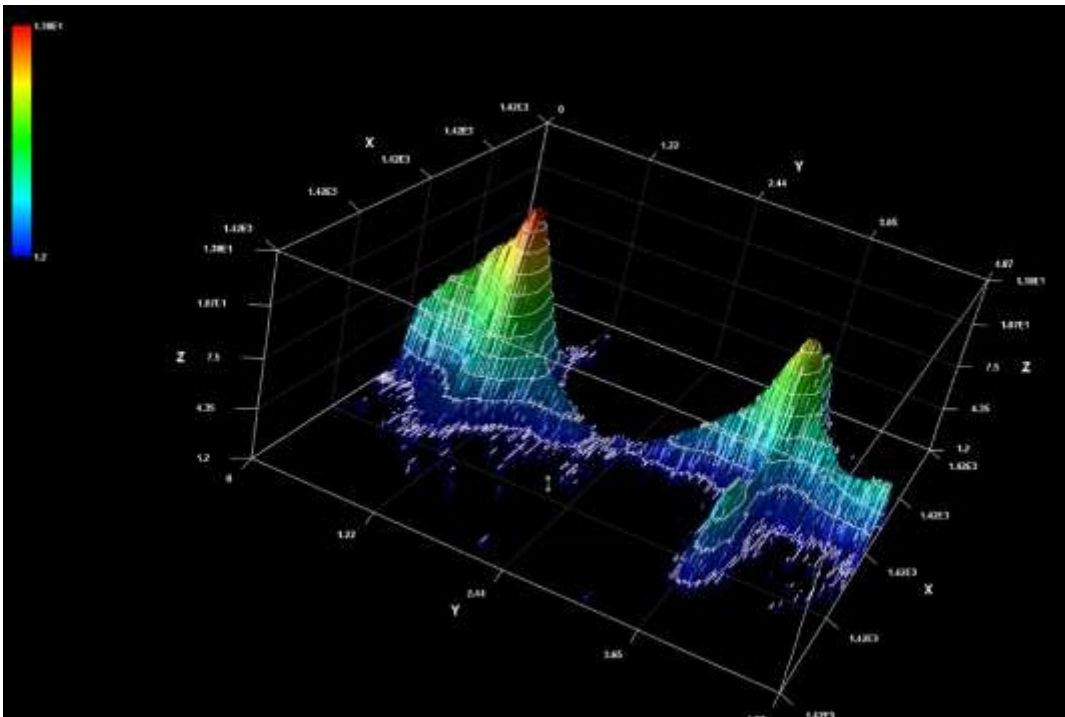
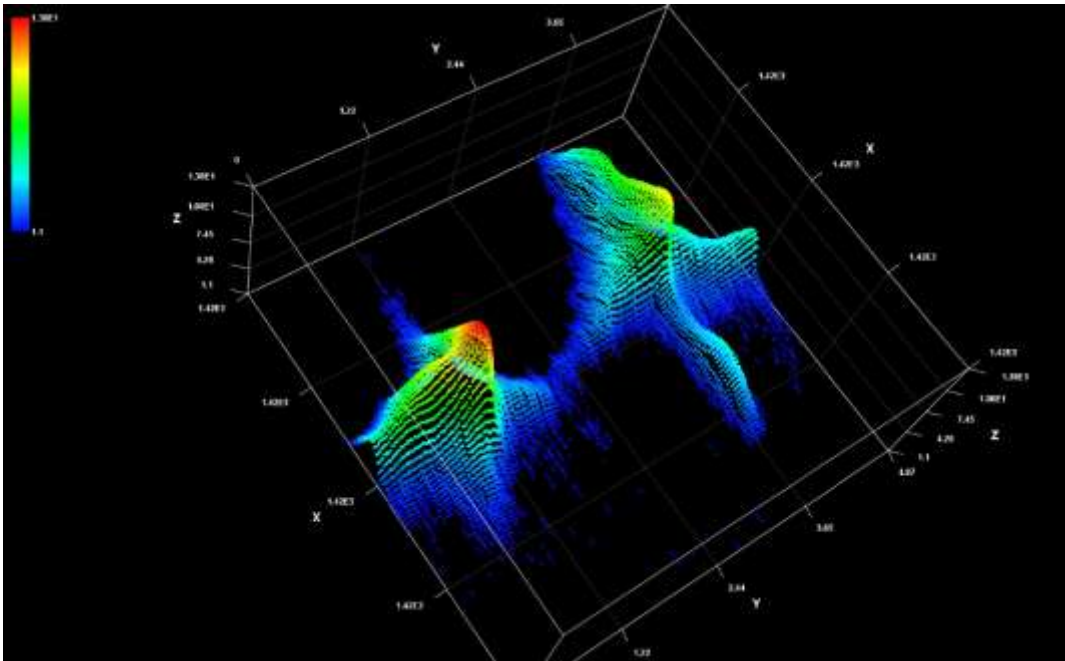
Plot of Milky Way over single days in 2 spatial dimensions with power on 3rd access – settings in Rinearn3D:

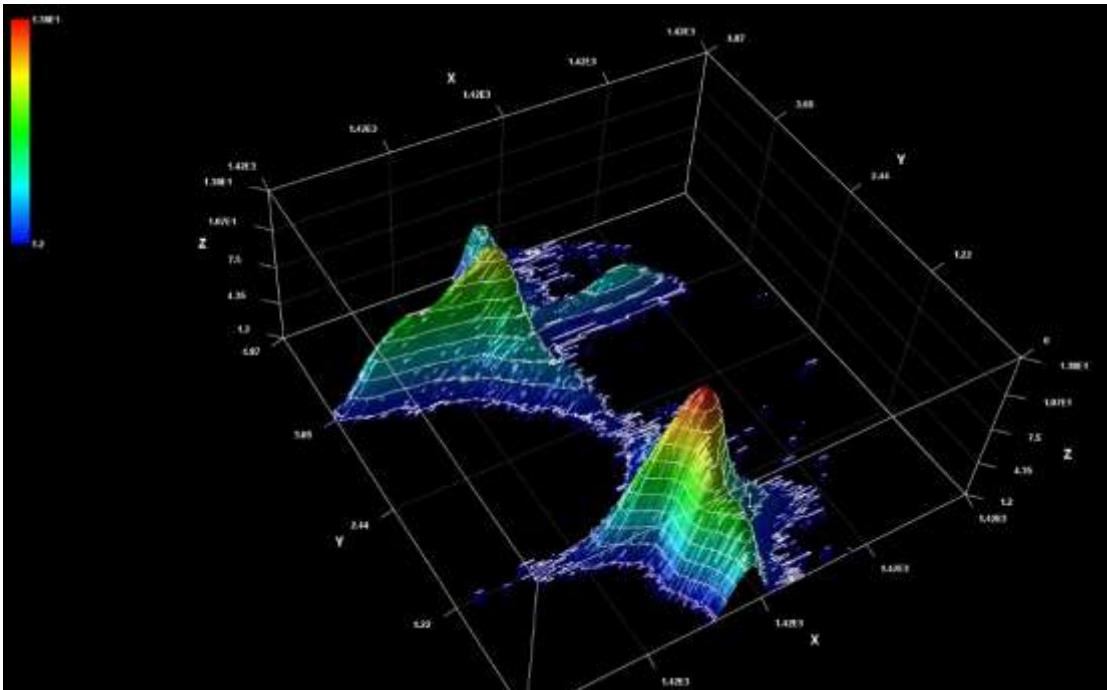
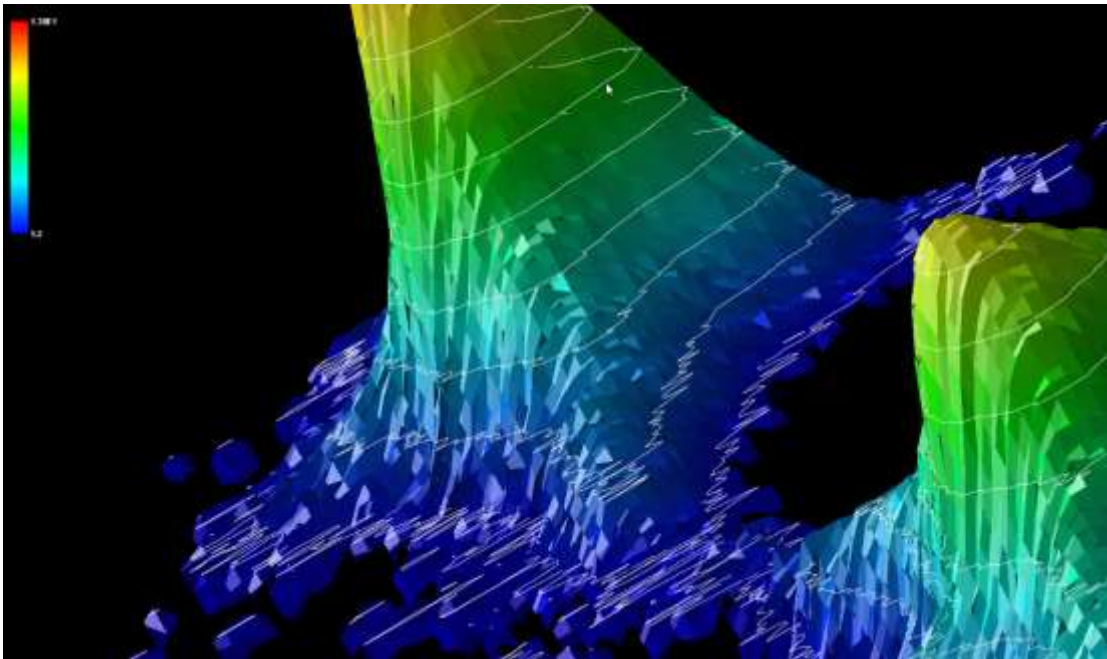


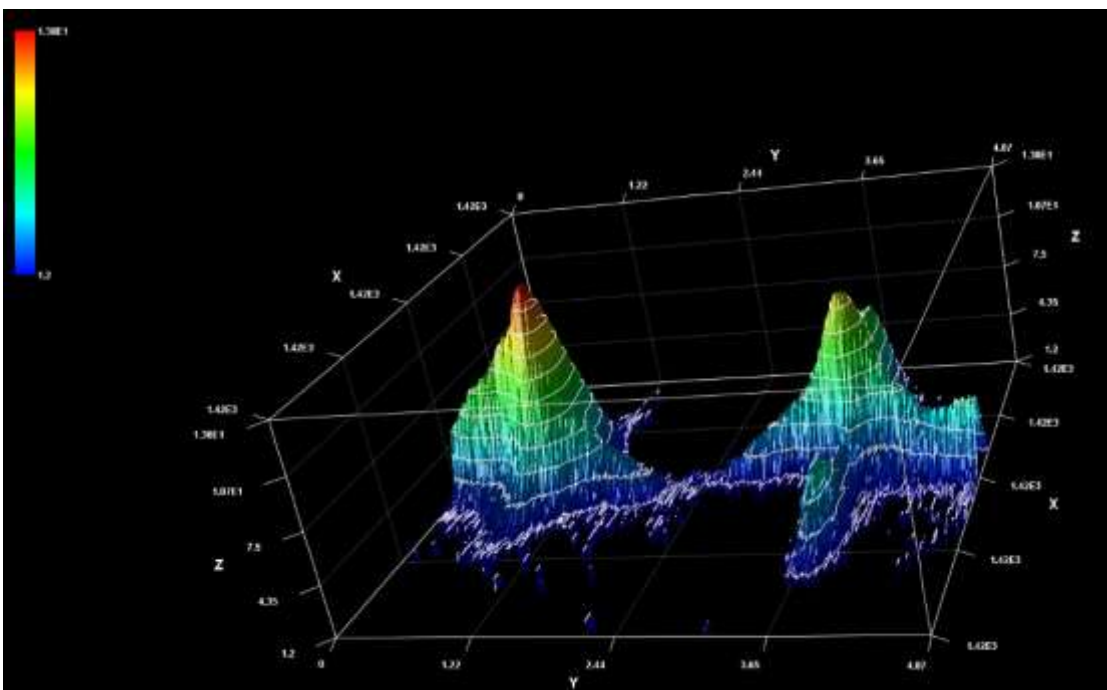
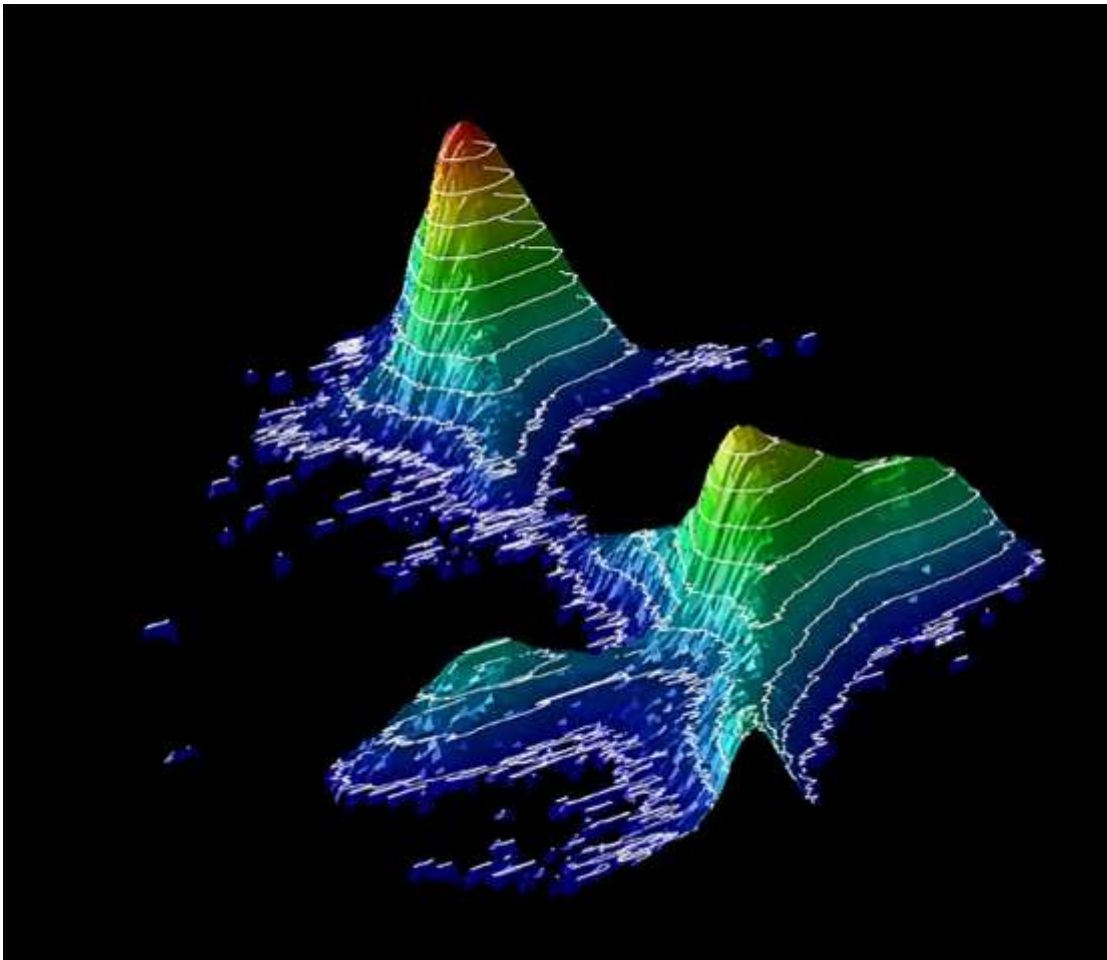
Following are further plots from different perspectives:

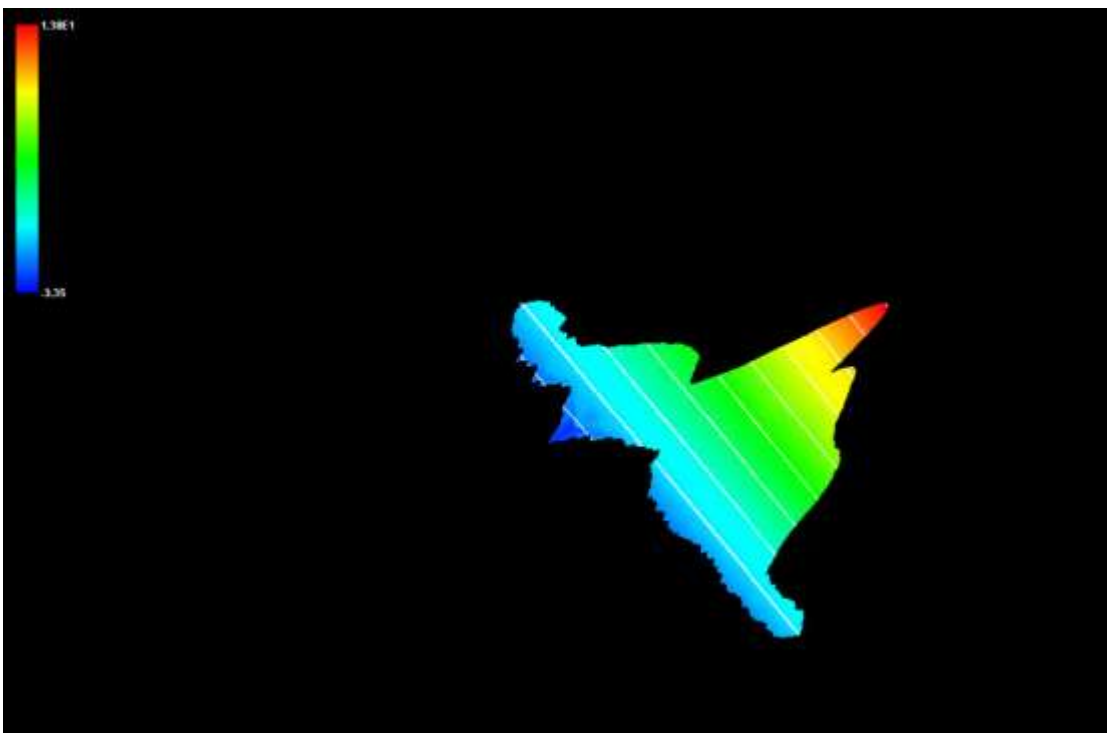
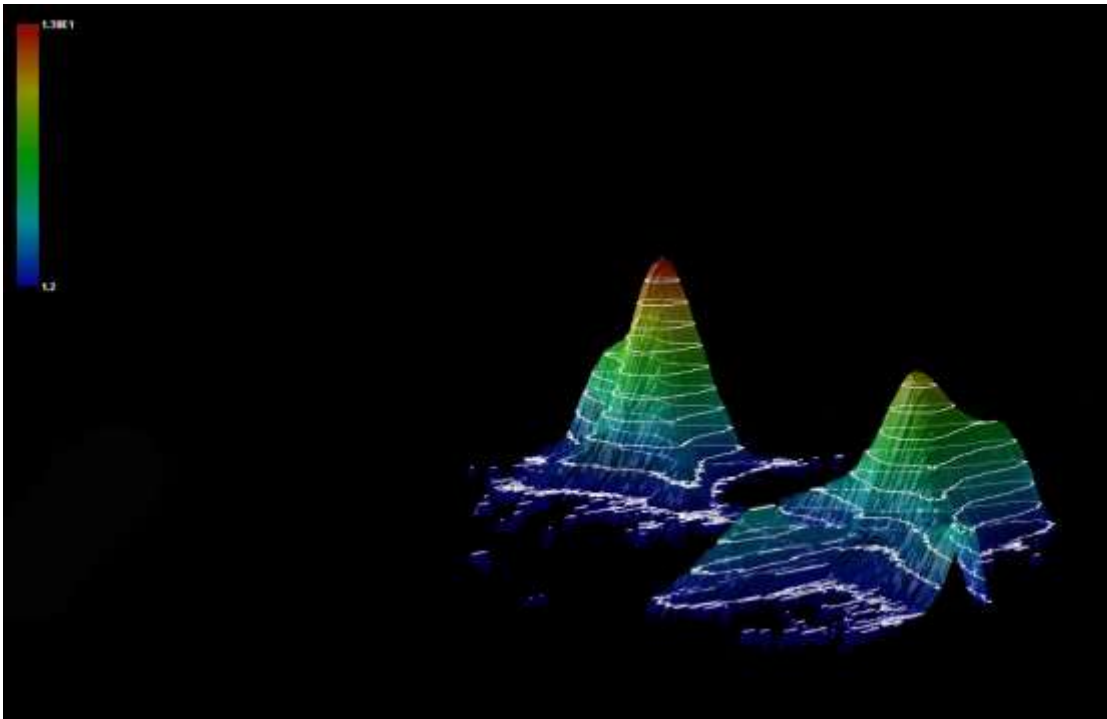


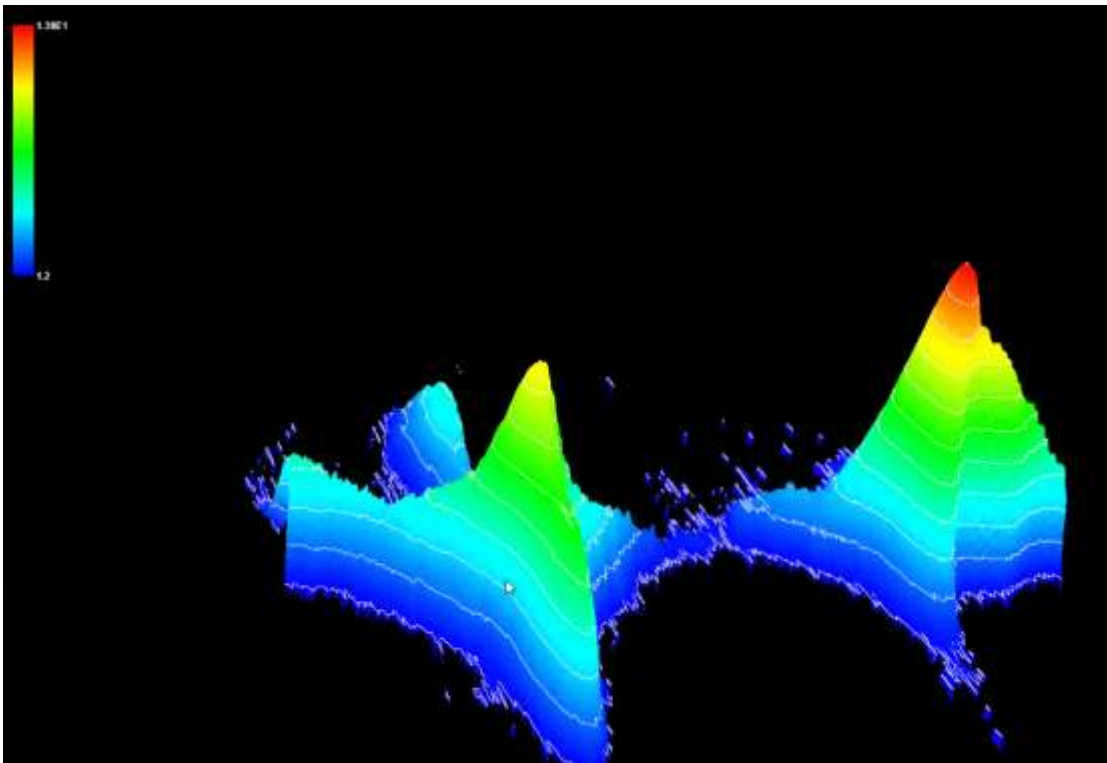
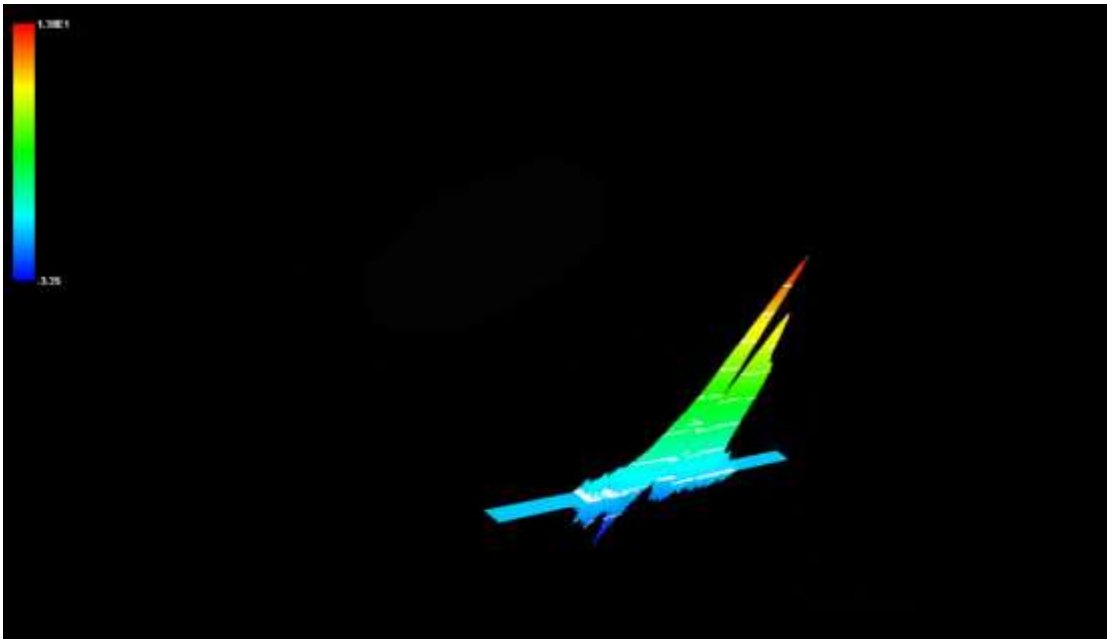


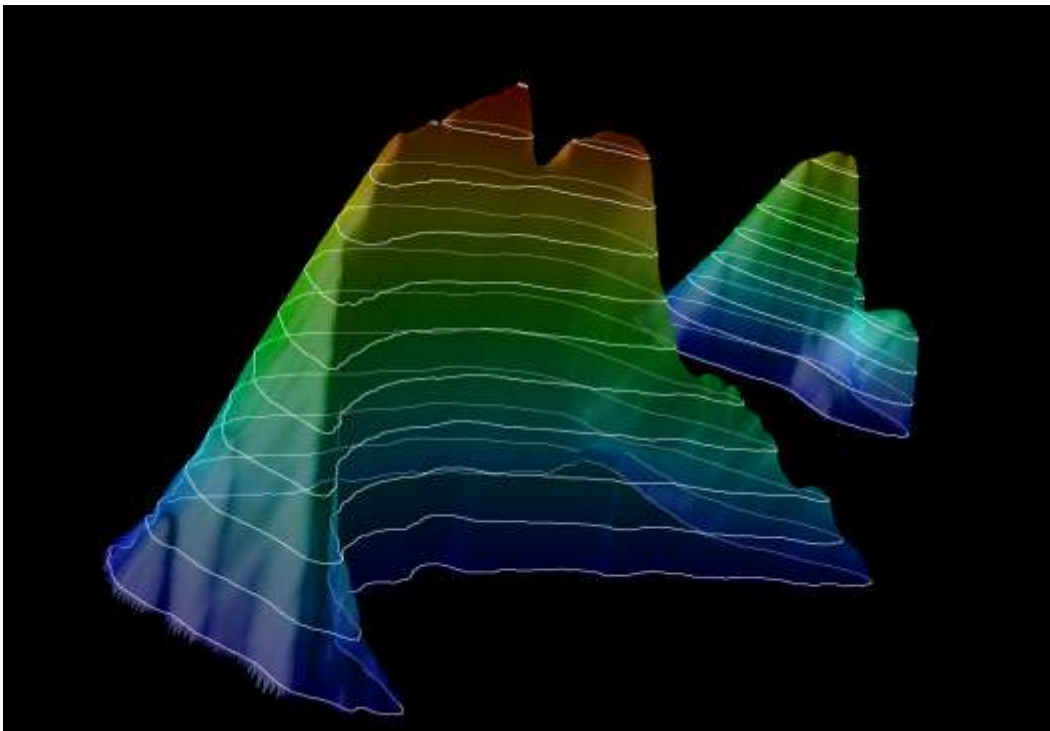
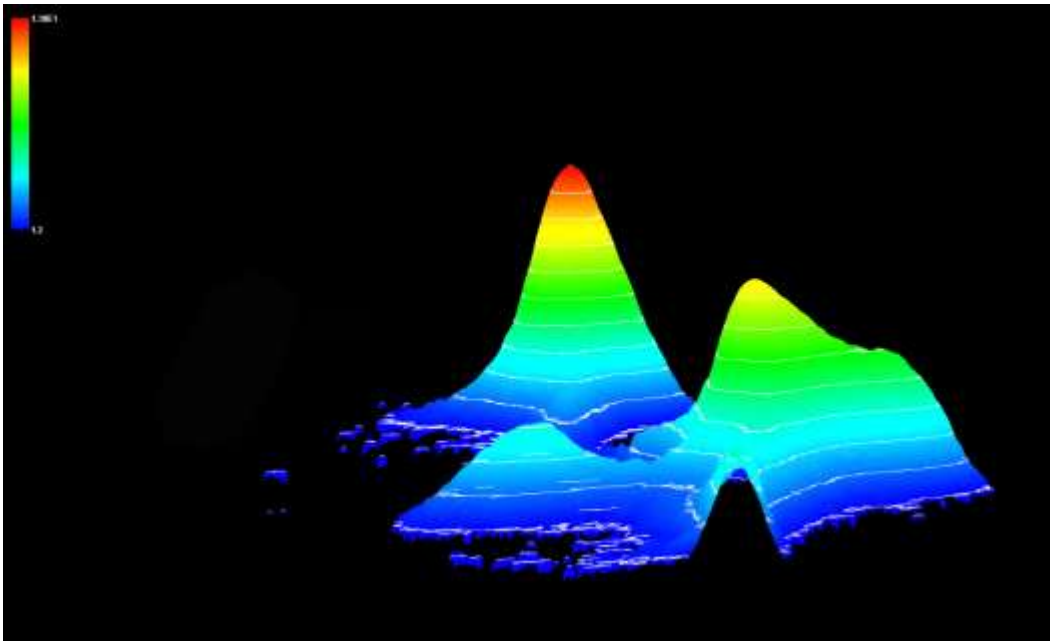


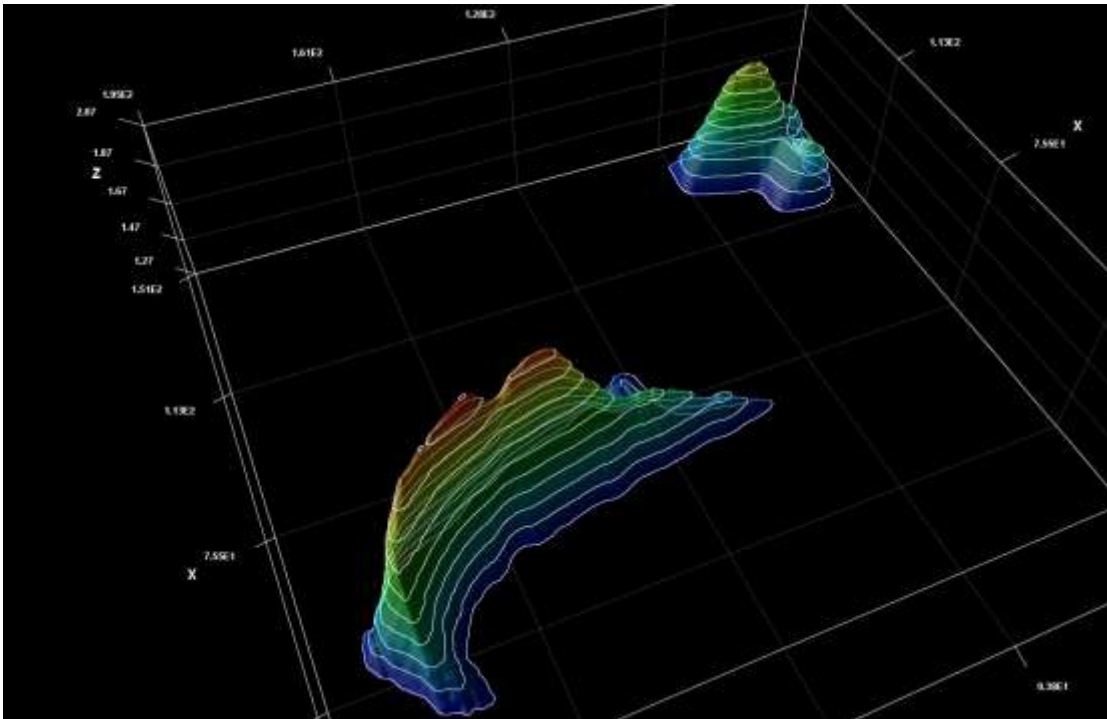












Further information.

Further information about this project is available on the www.astronomy.me.uk website or by contacting me using the “contact us” page on that website.

Many amateur radio astronomers use the Nooelec SAWBird H1 low noise amplifier (LNA) to achieve this filtering (<https://www.nooelec.com/store/sdr/sdr-addons/sawbird.html>), available for \$44.95 at the time of writing of this article on amazon.com (<https://www.amazon.com/Nooelec-SAWbird-H1-Applications-Frequency/dp/B07XPV9RX2>). The SAW filter in this device provides significant attenuation at +/- 30 MHz either side of 1420 MHz, and also provides a dual cascaded low noise amplifier within a small compact unit.

SAWBird H1 LNA Dongle (below):



Chinese Cavity Filters for the Hydrogen Line.

This current paper looks at a pair of alternative filters using a different design that provides an attenuation over a narrower frequency range, promising to improve signal to noise ratio and give clearer hydrogen signals and improved detail in the maps produced in systems using them.

Cavity Filters are a type of radio frequency (RF) filter used in communication systems to filter out noise and select signals at specific frequencies. They are typically composed of one or more hollow metal cavities containing conductor structures (www.temwell.com/en/pages/what-is-cavity-filter).

Cavity Filters operate using resonance. They contain a resonator with a tuning screw (to fine-tune the frequency) inside a conducting box. An RF or microwave resonator is a closed metallic structure (i.e., waveguides with both ends terminated in a short circuit). The resonator oscillates with higher amplitude at a specific set of frequencies, called resonant frequencies. When an RF signal passes through the cavity filter, a resonator acts as a band-pass filter and passes RF signals at specific resonant frequencies while blocking other nearby non-resonant frequencies. The resonant frequency of the cavity resonator depends on its dimension (length, width, height), mode number, dielectric constant (ϵ_r), and magnetic permeability (μ_r) of the material of construction. In a cavity filter, the resonator is fitted with a screw to tune the frequency range which allows to modify the physical length (inner space length) of the resonator as well as its capacitance to the ground, hence tuning the resonant frequency. Cavity filters are used in the MHz/GHz frequency range. They provide high Q-factor (i.e., high-selectivity/sharply attenuates the unwanted signals), low insertion loss, and robust temperature stability when compared to other forms of filters commonly used in amateur radio astronomy. These advantages make cavity filters ideal for use in microwave and millimetre-wave systems, particularly in professional systems, which need filters with high-Q factor, lower insertion loss, and temperature stability. Advantages of cavity filters: (1) High Q-factor (up to the order of 10^6), low insertion loss, and robust temperature stability. (2) Superior selectivity and good frequency stability. (3) Reduces the transmitter sideband noise and protects receivers against desensitization. (4) Better performance in microwave range

(including 1420MHz that we use for hydrogen detection) when compared to other common forms of filter (<https://www.everythingrf.com/community/what-are-cavity-filters>).

Traditionally, amateur radio astronomers have had to make their own cavity filters if they wished to use one, a labour-intensive exercise requiring some skill and a lot of fiddling and ideally additional expensive equipment to tune the filter accurately. Commercial versions have been very expensive, limiting their use to professional observatories. However, like most areas of technology, new ranges of these devices have become available from China at much more competitive prices, and these new models provide an opportunity to consider these filters for amateur applications.

I obtained a pair of samples of cavity filters covering the hydrogen band, but will slightly different specifications from WTMicrowave (www.wtmicrowave.com), based in China. The company is also prepared to produce custom-designed filters, should amateurs have a need for them. Prices for the two filters discussed in this article are around \$150 each plus carriage.

This article follows on from a previous article published in the November-December 2024 edition of the Journal of the Society of Amateur Radio Astronomy where I discussed the specifications of one of these two filters, the WT-A9940-Q08 cavity filter. which is designed to cover 1400-1427 MHz, and gives up to 69 dB attenuation either side of this. This gives a range of -20 MHz to +7 MHz from 1420 MHz, an improvement over the +/-30 MHz of the Nooelec SAWBird H1 LNA.

WTMicrowave WT-A9940-Q08 cavity filter 1400-1427 MHz.

The WT-A9940-Q08 cavity filter is designed to cover frequencies between 1400-1427 MHz. It provides up to 69 dB attenuation either side of this. This gives a range of -20 MHz to +7 MHz from 1420 MHz, an improvement over the +/-30 MHz of the Nooelec SAWBird H1 LNA.

WTMicrowave WT-A9940-Q08 cavity filter 1400-1427 MHz (below):

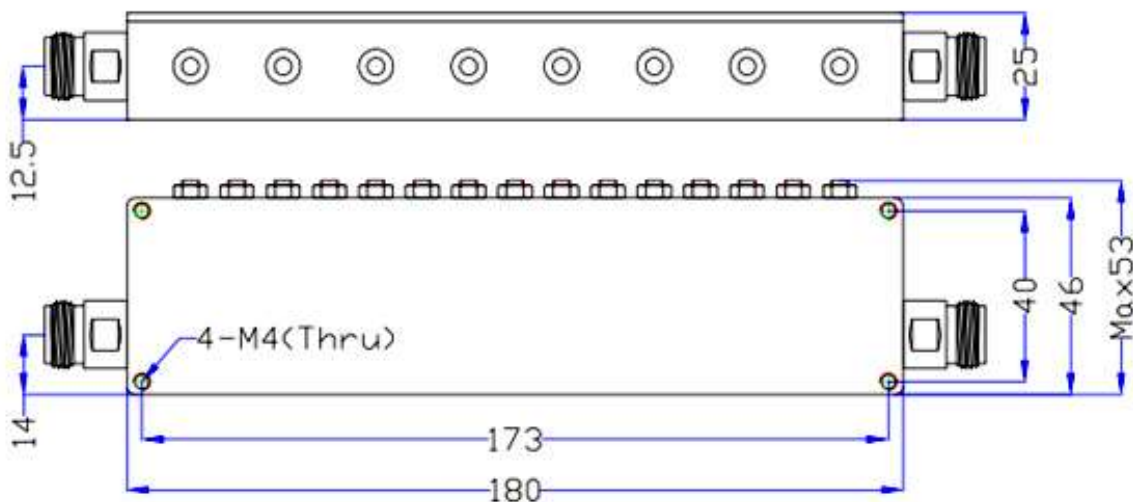


This cavity filter has N-type connectors at either end, so adapters are required to use with cables terminated with SMA connectors commonly used in amateur radio astronomy stations where software-defined radios are usually used, or the connector needs to be changed on the cable. Those users who control their systems with an amateur radio transceiver should be able to directly connect to the filter.

Specifications of the WT-A9940-Q08 cavity filter (below):

S/N	Item	Parameters
1	Center Frequency(F0)	1413.5MHz
2	Pass Band Frequency	1400 ~ 1427MHz **
3	Pass Band Insertion Loss	≤1.5dB
4	Pass Band Ripple	≤0.6dB
5	Pass Band Return Loss	≥23dB
6	Stop Band Rejection	≥50dB @ DC ~ 1375MHz ≥50dB @ 1452 ~ 3500MHz
7	Impedance	50 Ohms
8	Power Handling	200W Max.
9	Connectors	N-Female
10	Surface Finish	Painted Black
11	Temperature Range	-30°C ~ +70°C
12	Material	Housing: 6061 Aluminum alloy Resonant column: H59 Copper alloy Cover: LY12 Aluminum alloy Connectors: H59 Copper, Plated ternary alloy Tuning screw: H62 Copper alloy Other screw: Stainless Steel
13	Dimensions	180*46*25mm
14	Net weight	0.374 KG

Outline Drawing of the WT-A9940-Q08 Cavity Filter (below, dimensions units: mm, dimension tolerance +/- 0.5mm):

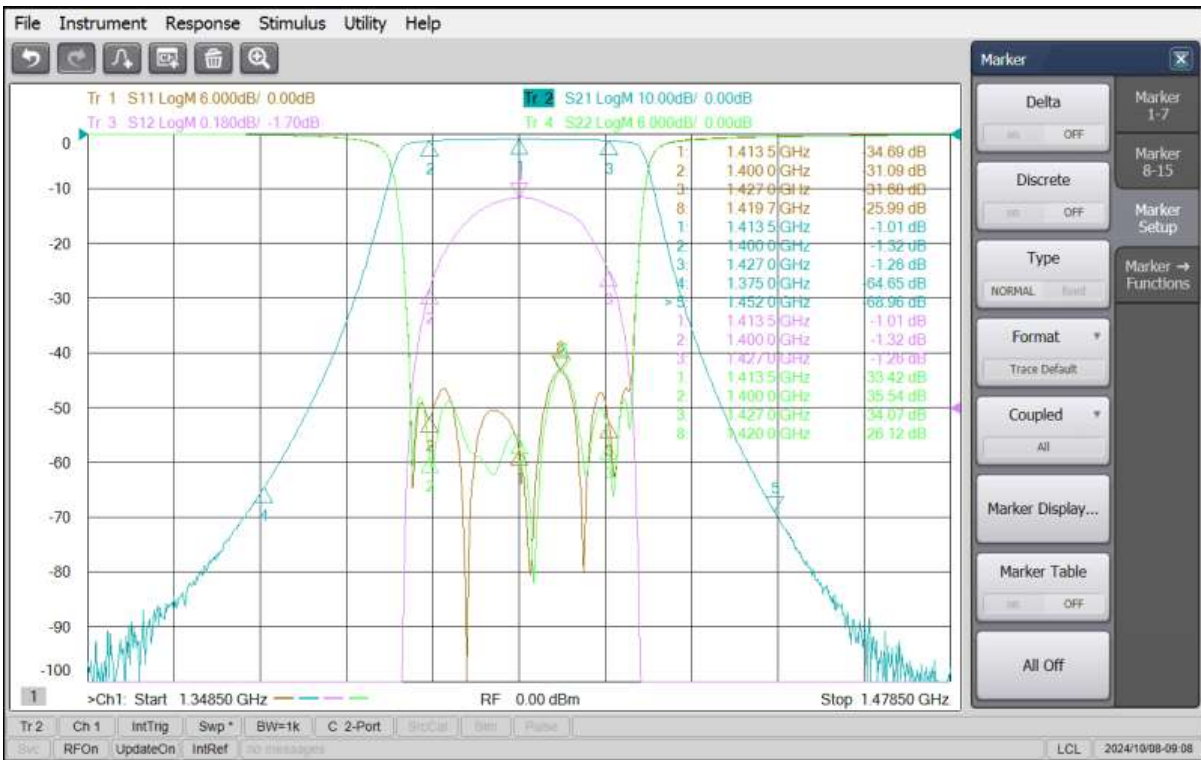


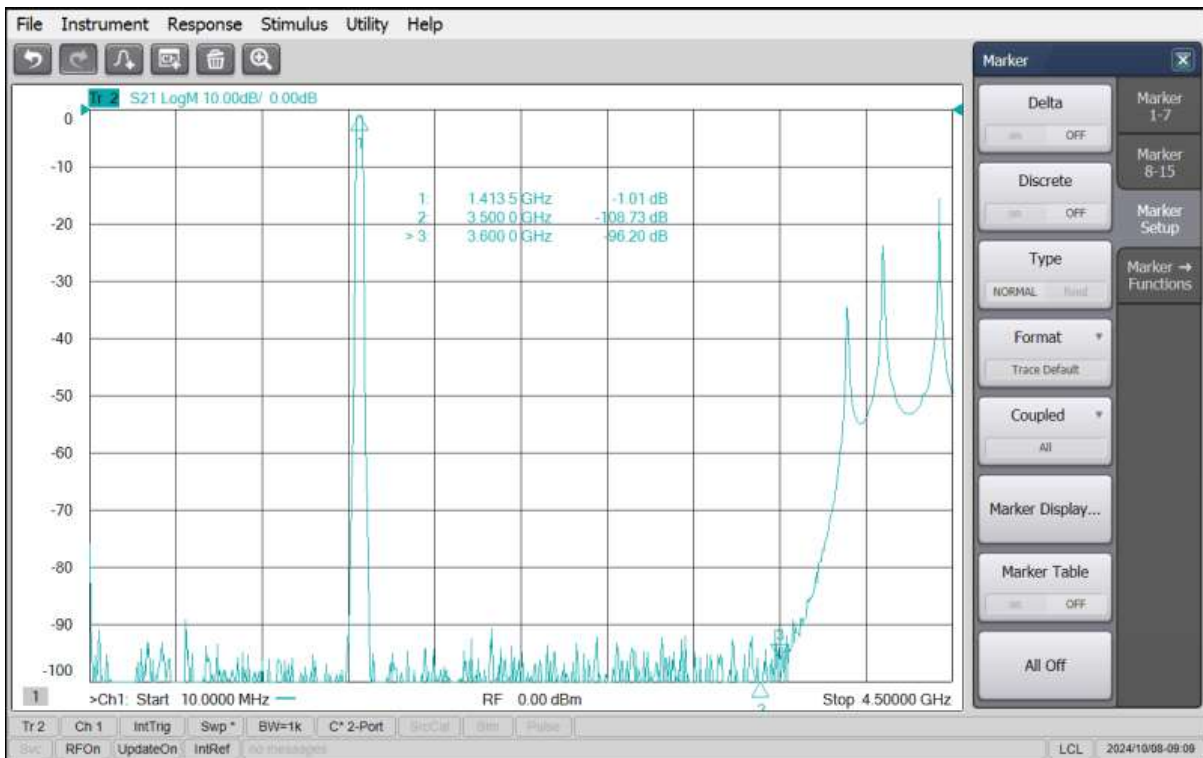
****The actual design bandwidth will be greater than the Pass Band Frequency, and there is no bandwidth limit.**

The plots below show test report and curves for an example of these filters that I have been sent by the company (below).

Product Inspection Records

Model	WT-A9940-Q08	Item	Cavity Band Pass Filter	Quantity	3pcs		
Test Data							
Appearance	Major Parameter				Other Parameter		
	Pass Band 1400 ~ 1427MHz F0=1413.5MHz			Stop Band		Connectors	Surface Finish
Reference value	Insertion Loss	Ripple	Return Loss	DC ~ 1375MHz	1452 ~ 3500MHz	N-Female	Painted Black
S/N	<1.5dB	<0.6dB	>23dB	>50dB	>50dB		
1	1.32	0.31	25.9	64	69	N-Female	Painted Black
2	1.29	0.27	27.2	63	69		
3	1.33	0.31	27.1	66	71		
Verdict:						Inspection way: Full inspection	Data recording mode: Full record
Test Equipment: NS227B		Date: 2024-10-08		Tester: Lijiong Yong		Check: Xiaotao Yang	





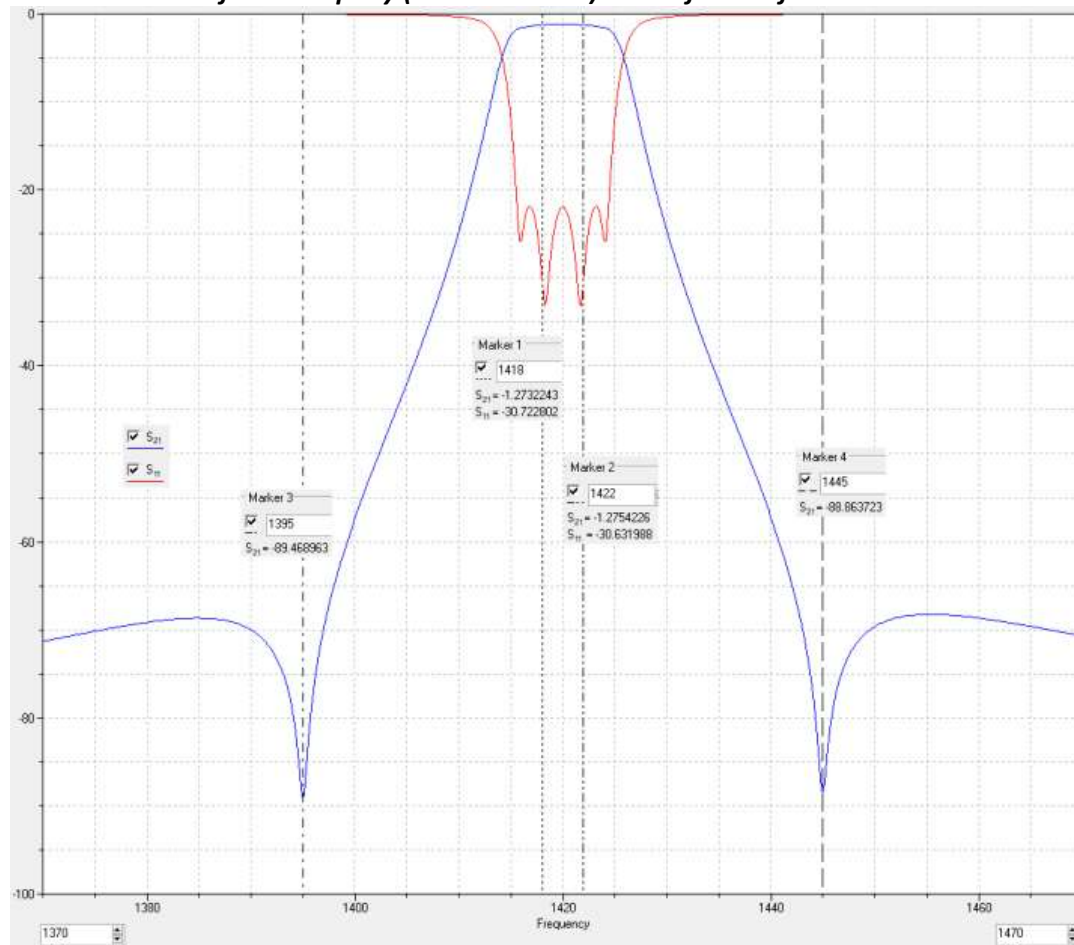
WTMicrowave Cavity Band Pass Filter WT-A11654-Q04 (1418-1422MHz).

The second filter is also from WTMicrowave, but has a narrower bandwidth of only 4MHz, centralised on 1420MHz. It presented an opportunity to provide better attenuation outside the hydrogen band, when high levels of radio frequency interference (RFI) are present, such as at Lichfield Radio Observatory (LRO), which is located in the centre of a moderately large town of 30,000+ inhabitants. Unlike the previous filter, this one has SMA connectors, so does not require adapters for most amateur radio astronomy systems. I received three of this type of filter.

WTMicrowave Cavity Band Pass Filter WT-A11654-Q04 (1418-1422MHz) (below):



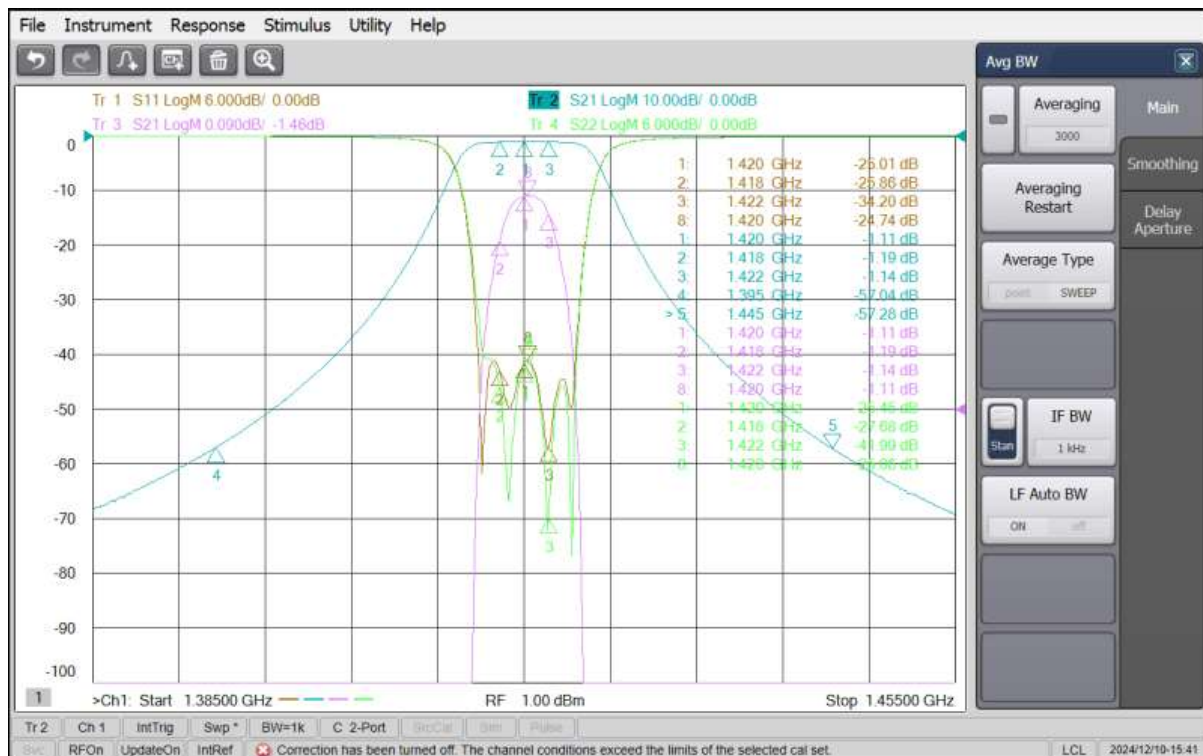
Simulation curve from company (WTMicrowave) below for this filter:

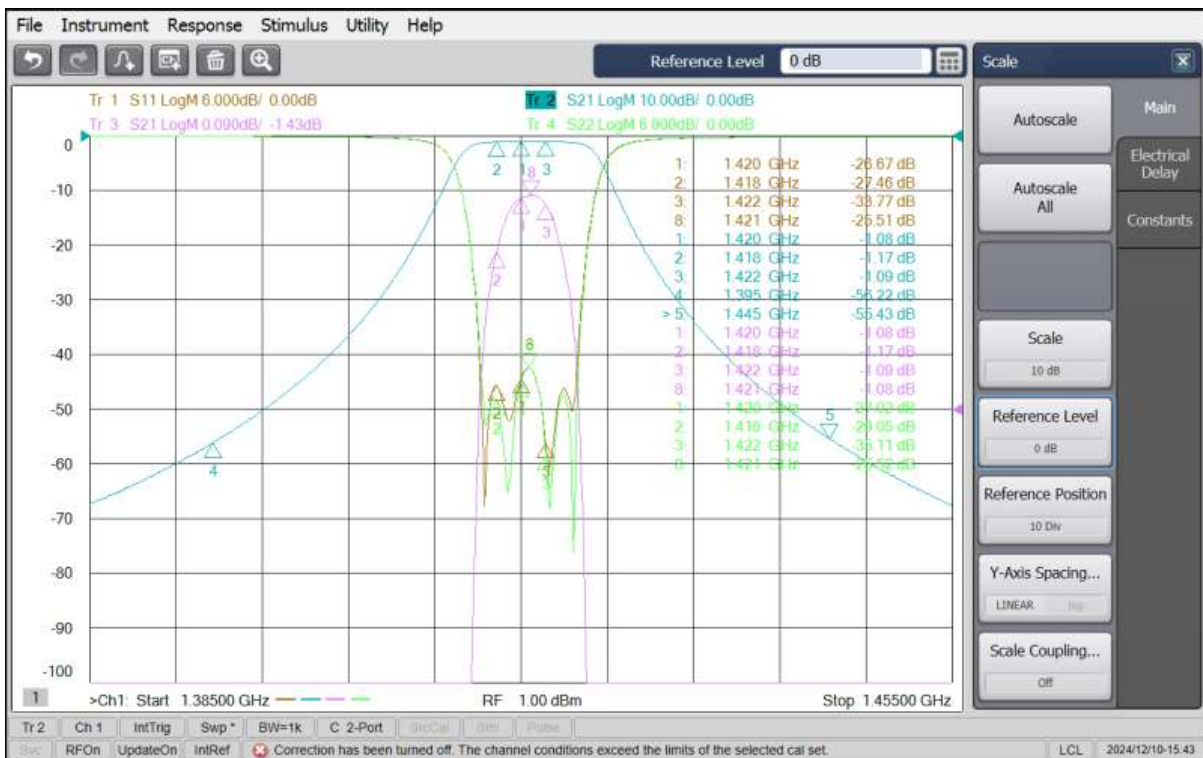
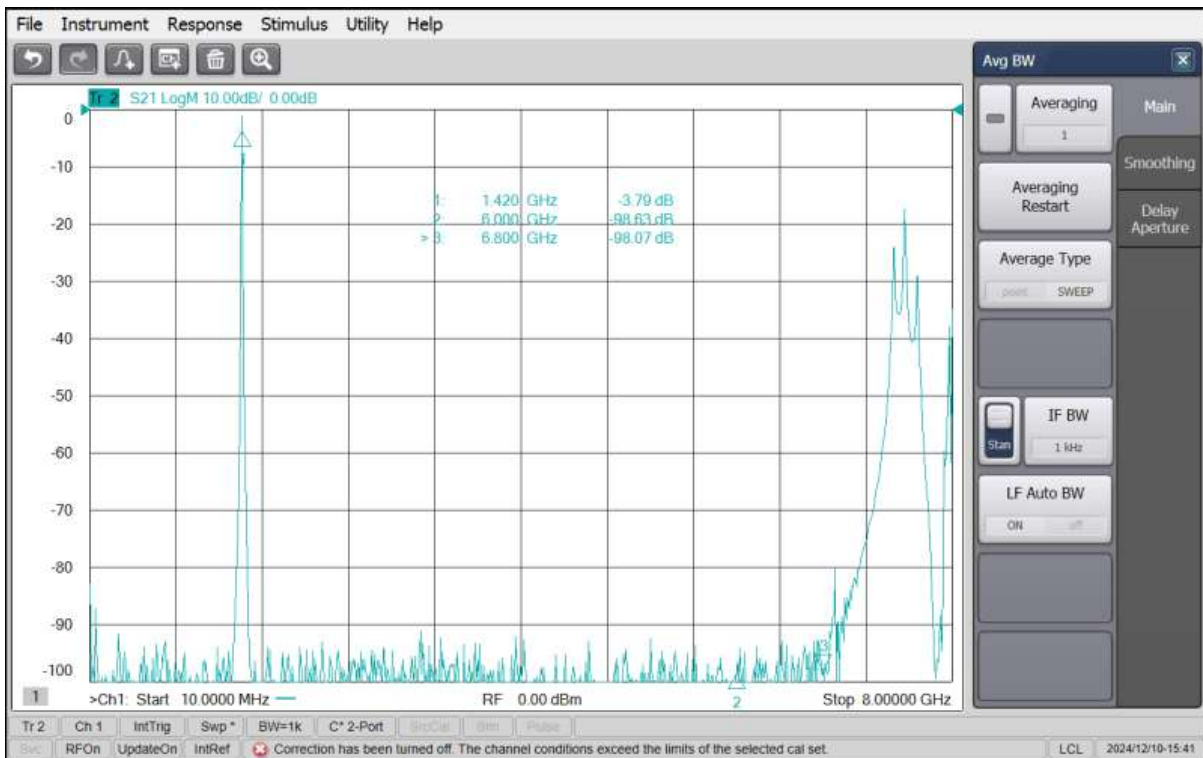


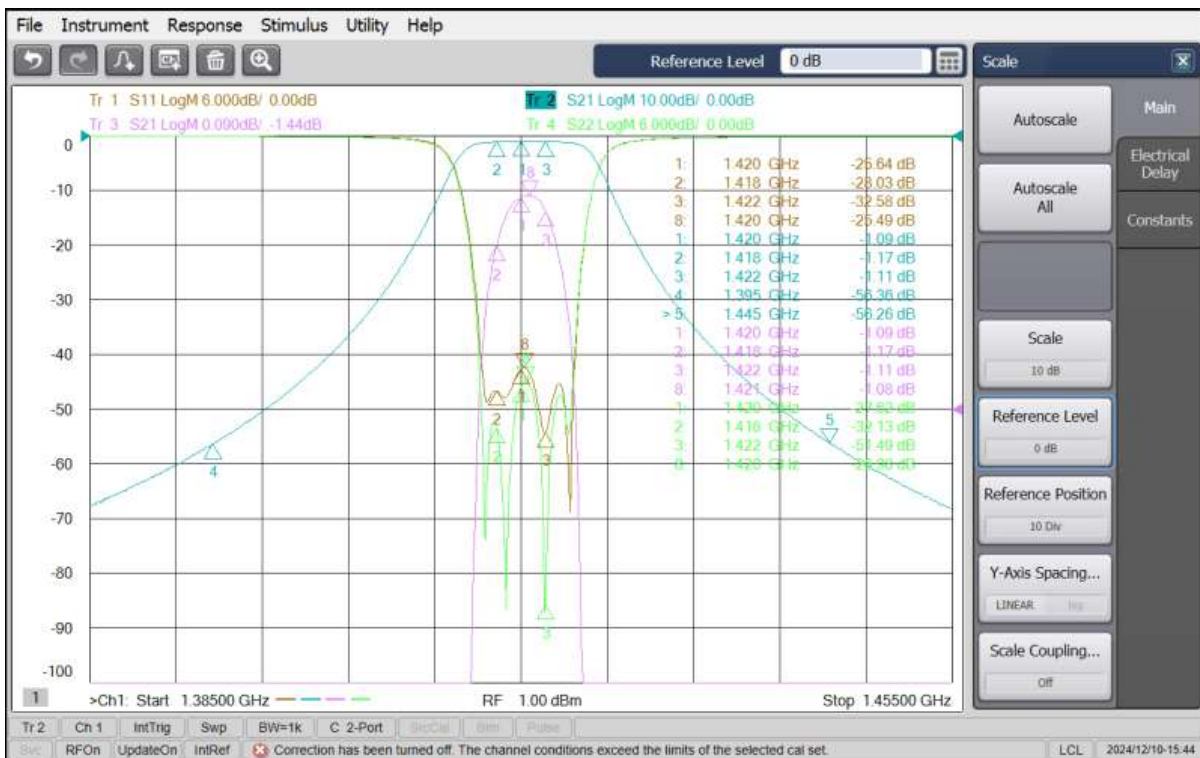
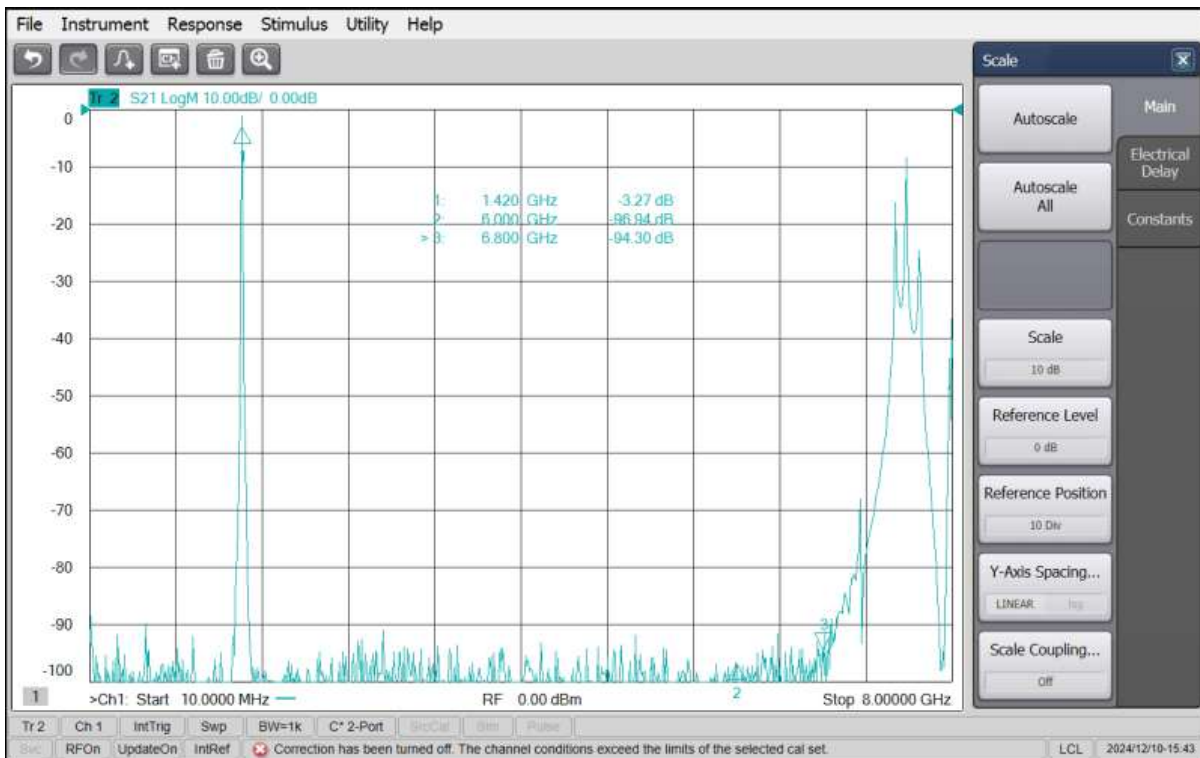
Actual test curves and test data for the three filters of this type I received:

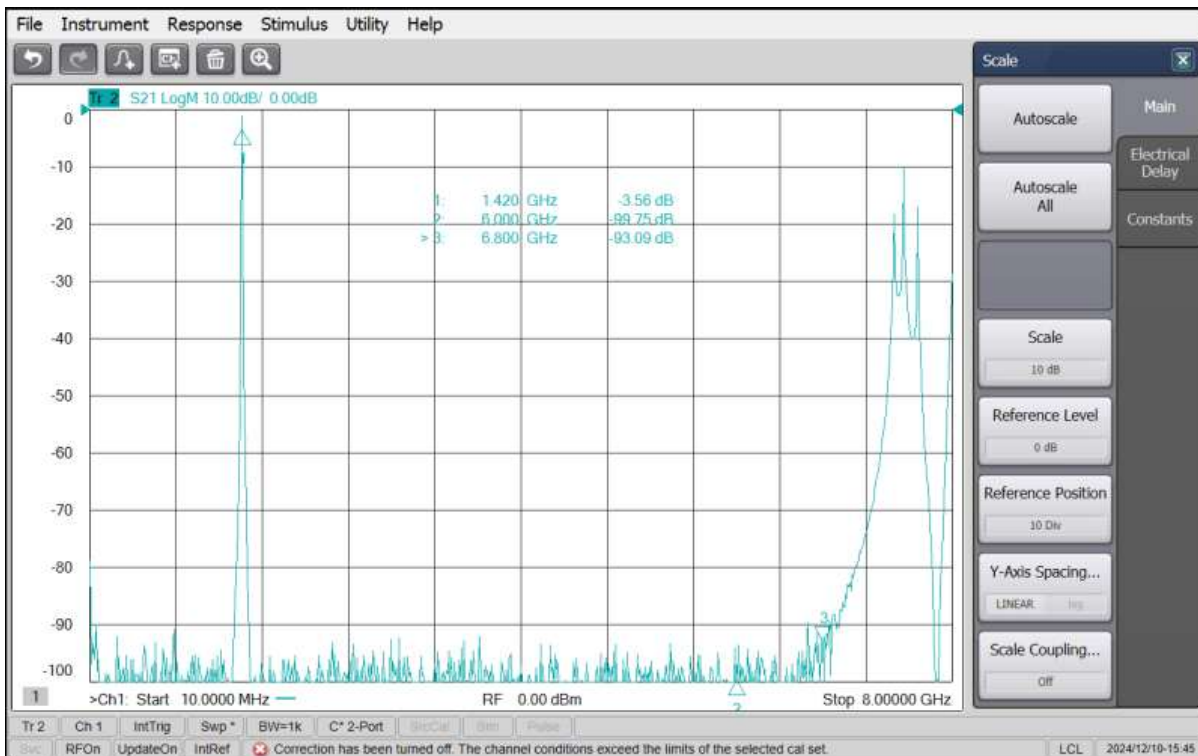
Product Inspection Records

Model	WT-A11654-Q04	Item	Cavity Band Pass Filter	Quantity	3pcs		
Test Data							
Appearance	Major Parameter				Other Parameter		
	Pass Band 1418 ~ 1422MHz F0=1420MHz			Stop Band		Connectors	Surface Finish
Reference value S/N	Insertion Loss	Ripple	Return Loss	DC ~ 1395MHz	1445 ~ 6000MHz	SMA-Female	Painted Black
	≤1.5dB	≤0.3dB	≥23dB	≥50dB	≥50dB		
1	1.19	0.08	24.7	57	57	SMA-Female	Painted Black
2	1.17	0.09	25.5	56	55		
3	1.17	0.09	25.5	56	56		
Verdict:		Inspection way: Full inspection			Data recording mode: Full record		
Test Equipment: N5227B		Date: 2024-12-10		Tester: Liqiong Yong		Check: Xiaotao Yang	









Comparison of results from processing LRO-H1(Ptarmigan Array Data) collected by ezCol.py (ezRA software suite) with three filter arrangements 1st to 12th January 2025.

I have installed the cavity filter in line before the SAWBird H1 on both of my hydrogen line radio telescopes (LRO-H1 and LRO-H2) at Lichfield Radio Observatory, UK (www.astronomy.me.uk), and compared results for three filter arrangements. Results are given below for LRO-H1, the Ptarmigan ex-military dipole array.

Filter arrangement 1:

Ptarmigan Dipole Array ==> WT Microwave 1418-1422 MHz Cavity Filter ==> Nooelec SAWBird LNA ==> RTL-SDR Blog V3 Software Defined Radio.

Filter arrangement 2:

Ptarmigan Dipole Array ==> Nooelec SAWBird LNA ==> RTL-SDR Blog V3 Software Defined Radio.

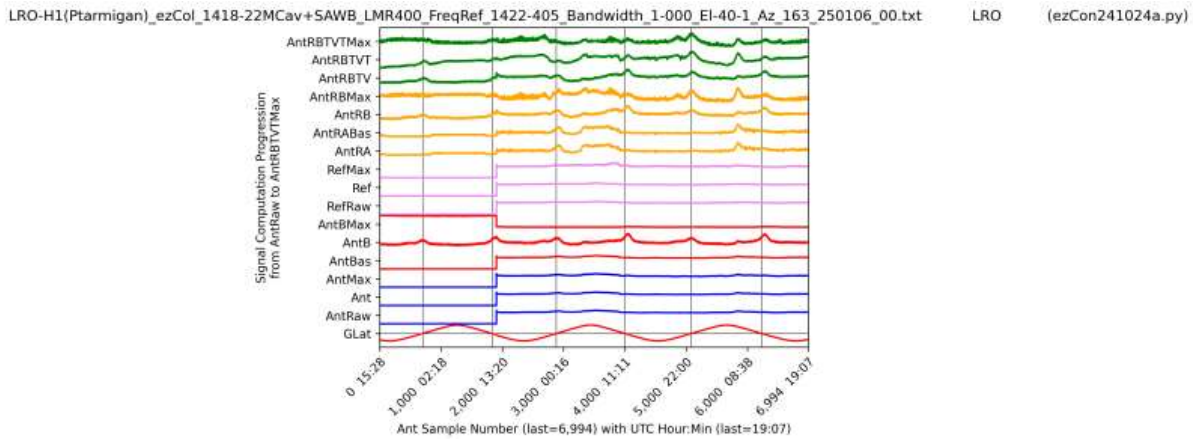
Filter arrangement 3:

Ptarmigan Dipole Array ==> WT Microwave 1400-1427 MHz Cavity Filter ==> Nooelec SAWBird LNA ==> RTL-SDR Blog V3 Software Defined Radio.

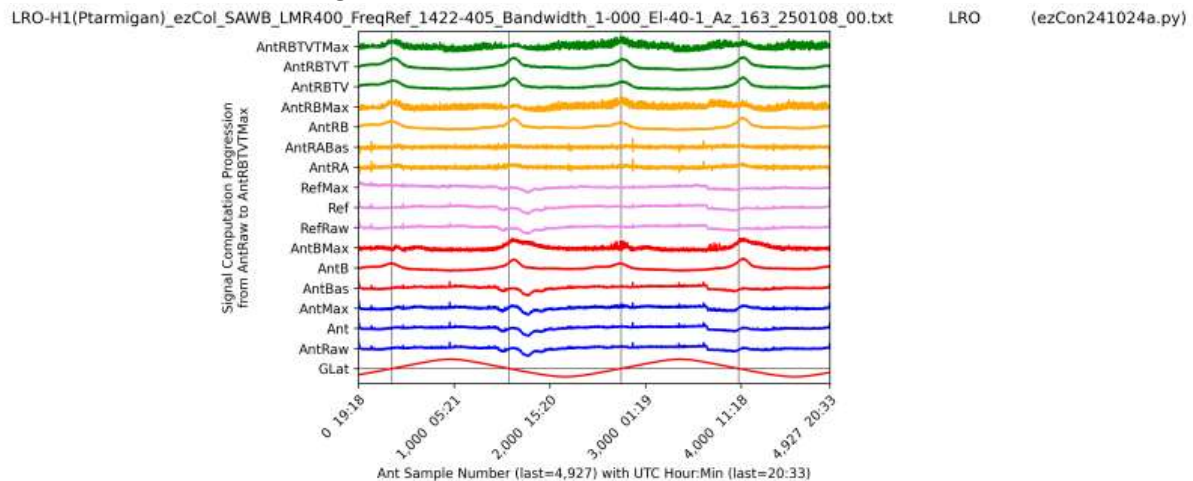
Results:

ezCon Plot 191:

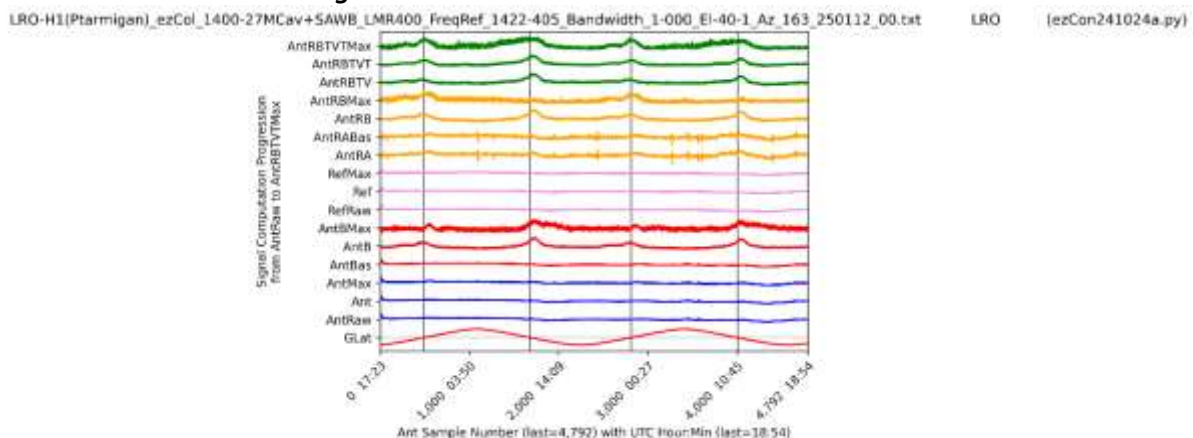
ezCon Plot 191 – Filter arrangement 1:



ezCon Plot 191 – Filter arrangement 2:



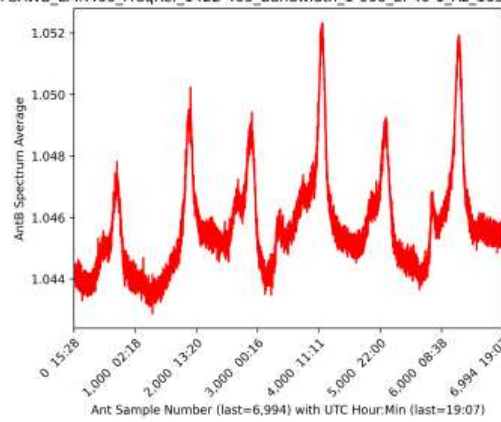
ezCon Plot 191 – Filter arrangement 3:



ezCon Plot ezCon114antBAvg:

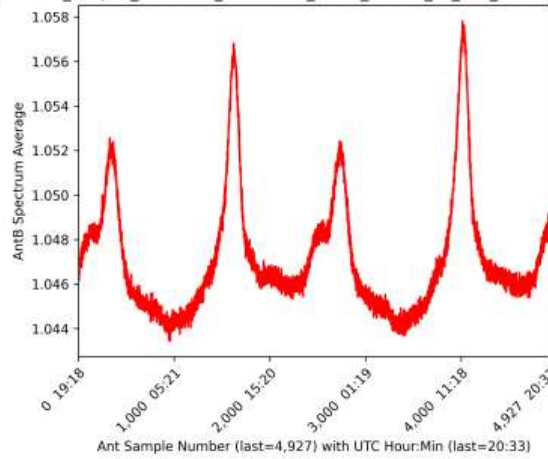
ezCon Plot ezCon114antBAvg – Filter arrangement 1:

LRO-H1(Ptarmigan)_ezCol_1418-22MCav+SAWB_LMR400_FreqRef_1422-405_Bandwidth_1-000_EI-40-1_Az_163_250106_00.txt LRO (ezCon241024a.py)



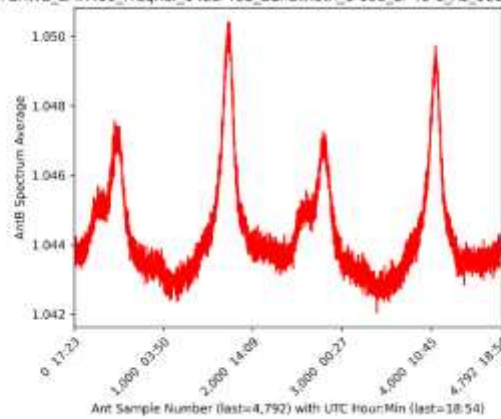
ezCon Plot ezCon114antBAvg – Filter arrangement 2:

LRO-H1(Ptarmigan)_ezCol_SAWB_LMR400_FreqRef_1422-405_Bandwidth_1-000_EI-40-1_Az_163_250108_00.txt LRO (ezCon241024a.py)



ezCon Plot ezCon114antBAvg – Filter arrangement 3:

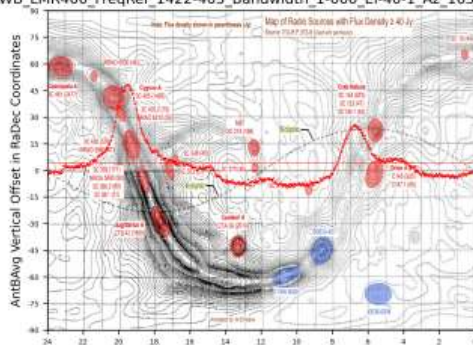
LRO-H1(Ptarmigan)_ezCol_1400-27MCav+SAWB_LMR400_FreqRef_1422-405_Bandwidth_1-000_EI-40-1_Az_163_250112_00.txt LRO (ezCon241024a.py)



ezCon Plot ezSky200RBVO_14AntBAvg:

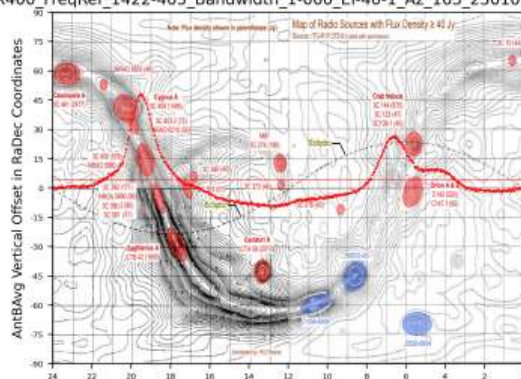
ezCon Plot ezSky200RBVO_14AntBAvg – Filter arrangement 1:

LRO-H1(Ptarmigan)_ezCol_1418-22MCav+SAWB_LMR400_FreqRef_1422-405_Bandwidth_1-000_EI-40-1_Az_163_250106_00.ezb LRO (ezSky241201a.py)



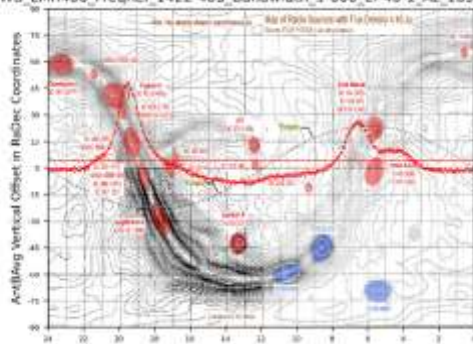
ezCon Plot ezSky200RBVO_14AntBAvg – Filter arrangement 2:

LRO-H1(Ptarmigan)_ezCol_SAWB_LMR400_FreqRef_1422-405_Bandwidth_1-000_EI-40-1_Az_163_250108_00.ezb LRO (ezSky241201a.py)



ezCon Plot ezSky200RBVO_14AntBAvg – Filter arrangement 3:

LRO-H1(Ptarmigan)_ezCol_1400-27MCav+SAWB_LMR400_FreqRef_1422-405_Bandwidth_1-000_EI-40-1_Az_163_250112_00.ezb LRO (ezSky241201a.py)



Conclusion.

The differences are subtle but the addition of a cavity filter in front of the Nooelec SAWBird H1 LNA does appear to have improved the signal, and the narrower band 1418-1422MHz cavity filter appears to more slightly effective than the wider band 1400-1427MHz filter.

These filters are considerably cheaper than alternatives manufactured in Europe or America, and the company is prepared to design filters to meet the specific needs of amateur radio astronomers. The units tested in this review were well-made, solid in construction, and performed well during testing. Delivery from China was within a quick timescale, and the units arrived well-packaged and protected.

Further information.

Further information about this project is available on the www.astronomy.me.uk website or by contacting me using the “contact us” page on that website.

Mapping the Milky Way galactic arms in three spatial dimensions using data from Lichfield Radio Astronomy Ptarmigan Array 1420MHz Radio Telescope (LRO-H1)

Andrew Thornett, M6THO, Lichfield Radio Observatory, Lichfield, UK www.astronomy.me.uk

The Lichfield LRO H1 Radio Telescope

Lichfield Radio Observatory (LRO) is located at latitude 52.6815 north, longitude -1.8255 (1.8255 west) in Staffordshire, central England, UK, roughly 16 mi (26 km) north of Birmingham. The LRO H1 Radio Telescope is composed of a Ptarmigan Triffid ex-military 4x4 dipole array, measuring 86cm x 86cm in size. Filtering is two-stage using a 1400-1427MHz cavity filter, followed by a Nooelec SAWBird H1 LNA/filter. The system uses an RTL-SDR Blog V3 Software Defined Radio and data for this paper was recorded using Easy Radio Astronomy Software Suite (ezRA; Ted Cline; <https://github.com/tedcline/ezRA>).

The telescope is mounted on a simple wooden mount that allows variation in elevation. It points at the same azimuth constantly – data is collected using 24-hour drift scans which allow individual azimuth points to be calculated by the software during the sidereal day.

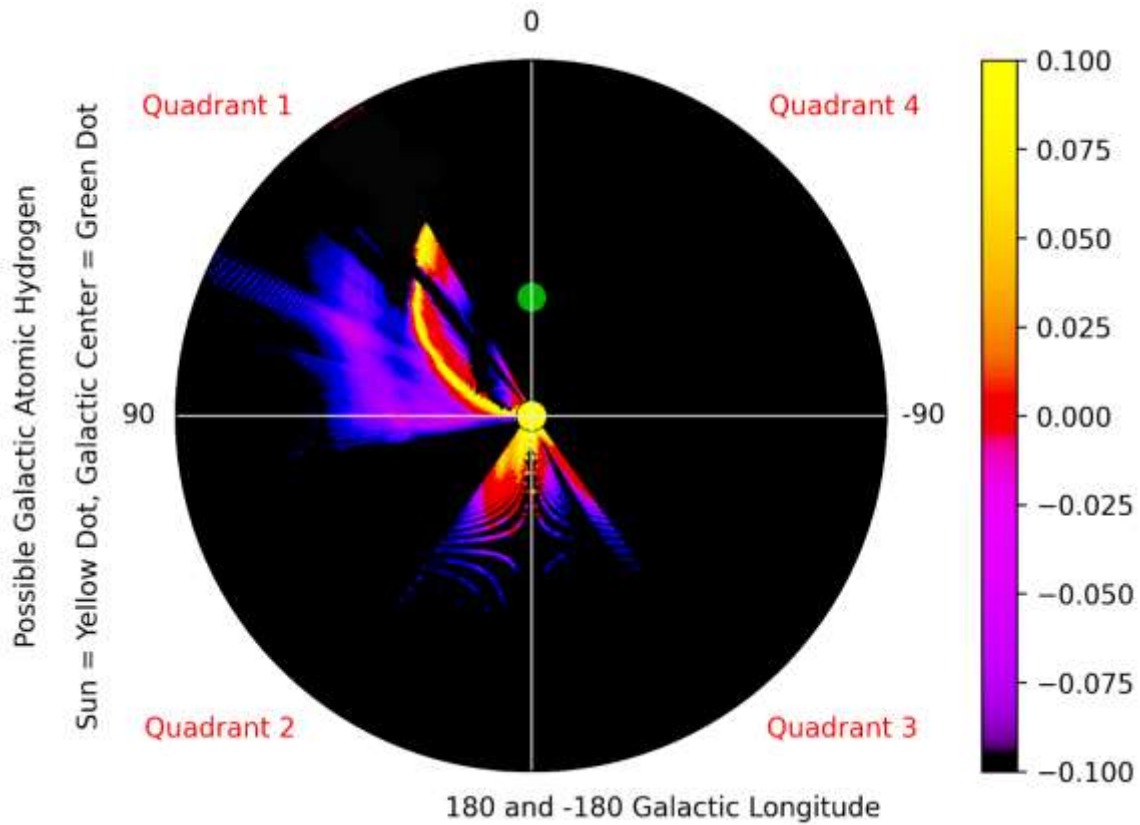
Ptarmigan Triffid Band 3 Ex-Military Dipole Array on simple wooden mount (below):



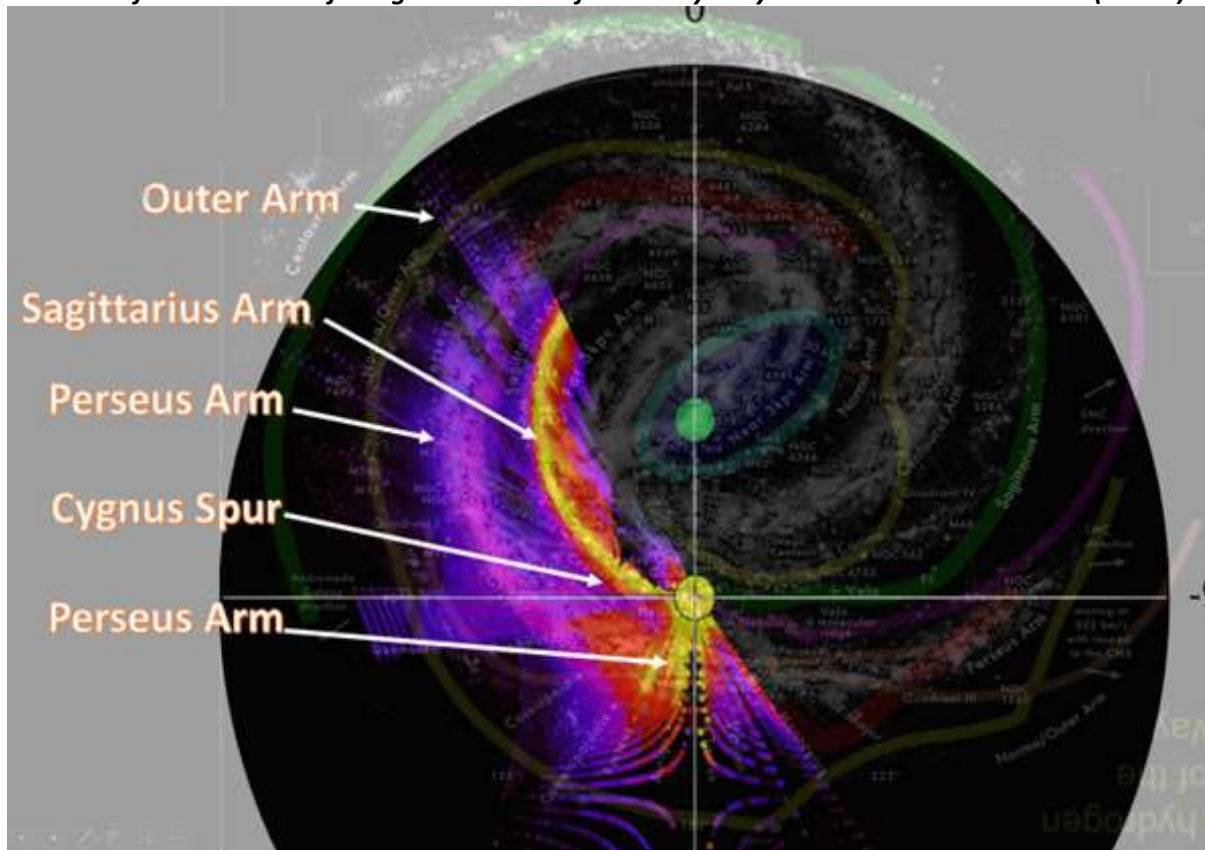
Data collected for this paper

Data was collected for this paper between 6th January 2024 and 16th November 2024. It is composed of 582,492 samples (approx. 2,500 hours of data). Most of the data is within Milky Way galactic longitudes 0-90 degrees. It demonstrates several galactic arm features.

2D map of Milky Way from LRO using data collected between 6th January 2024 and 16th November 2024:



Features of the structure of the galactic arms of the Milky Way demonstrated in the data (below):



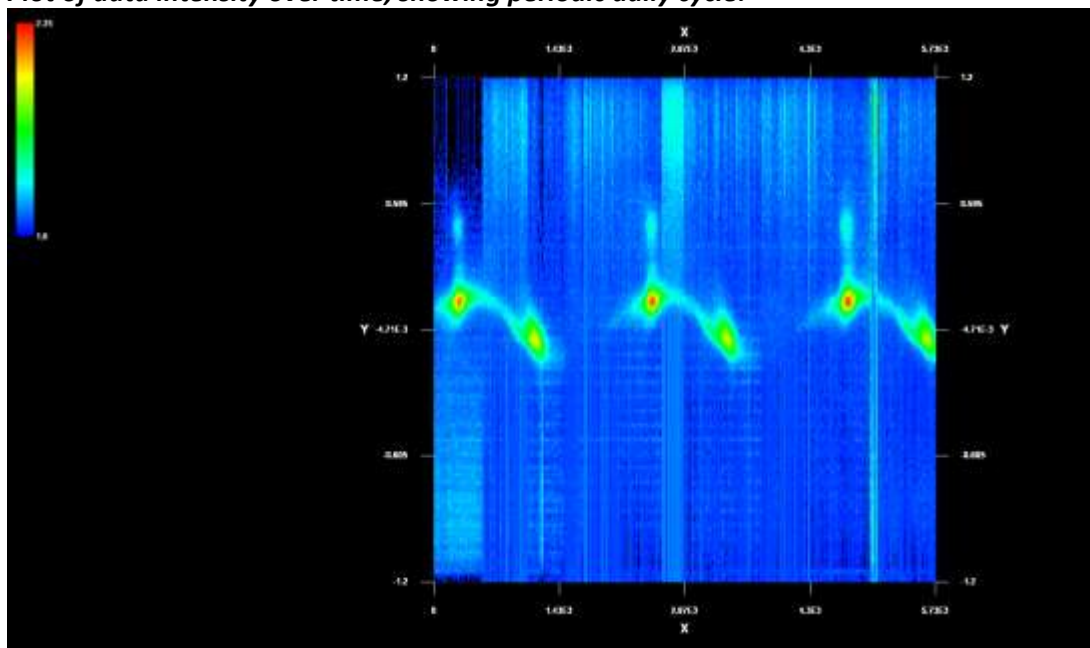
Mapping the Milky Way in 3 spatial dimensions:

Revisions to the Easy Radio Astronomy Suite (ezRA) have allowed the production of CSV files compatible with Rinearn3D software (<https://www.rinearn.com/en-us/graph3d/>). This software allows data to be plotted in three spatial dimensions, and, using a process developed by Ted Cline, the author of Easy Radio Astronomy, maps of the Milky Way arms can be produced using this software.

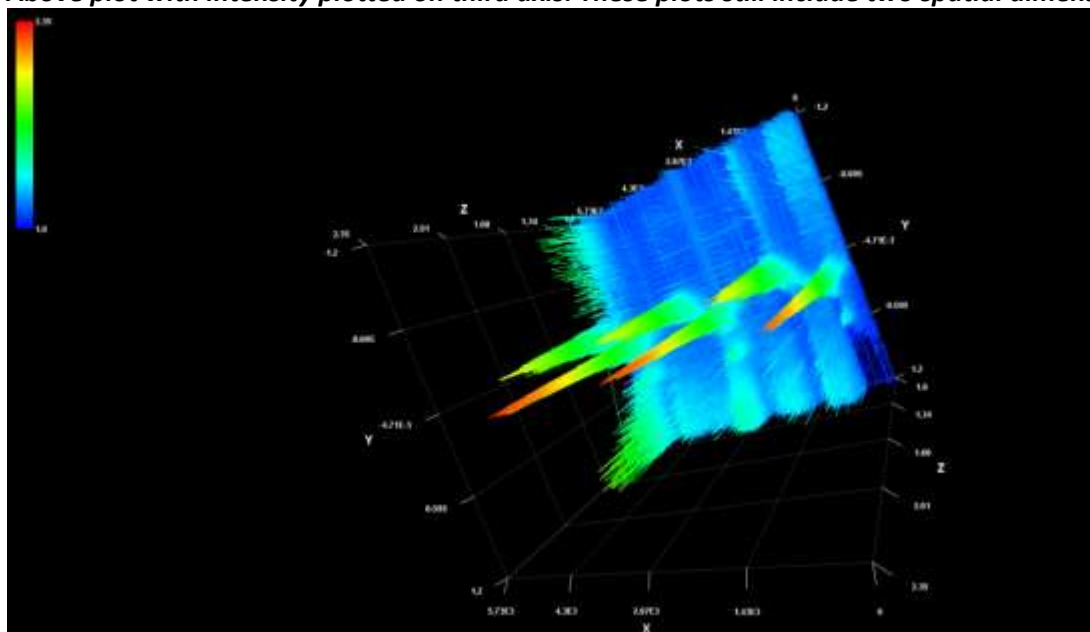
Results.

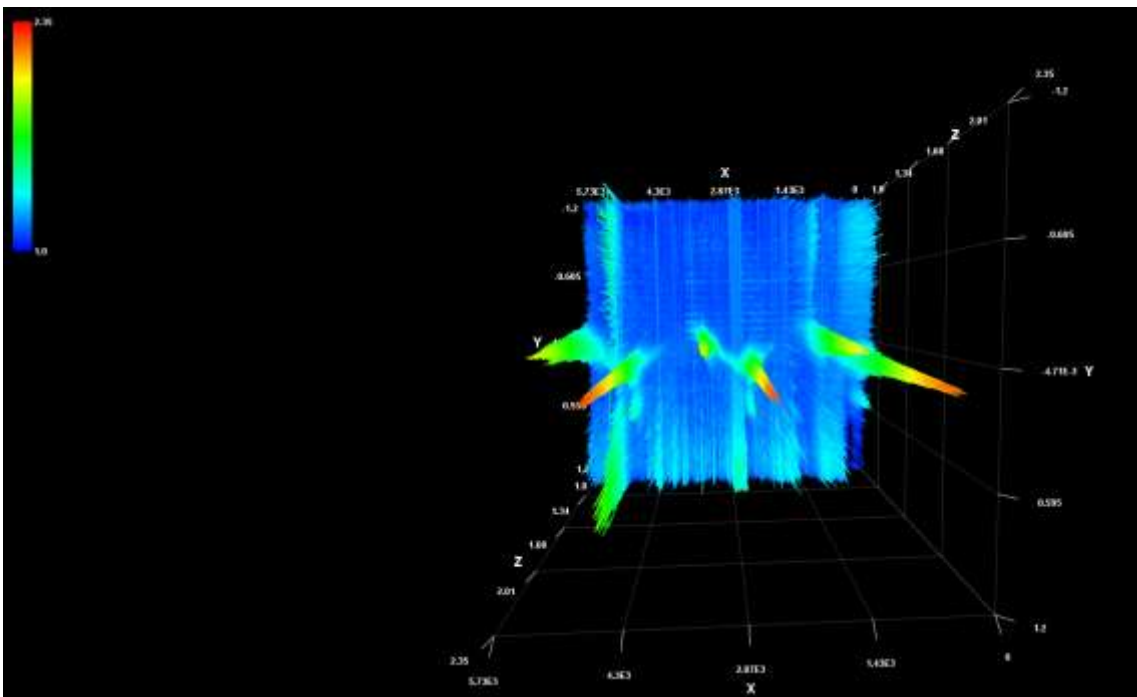
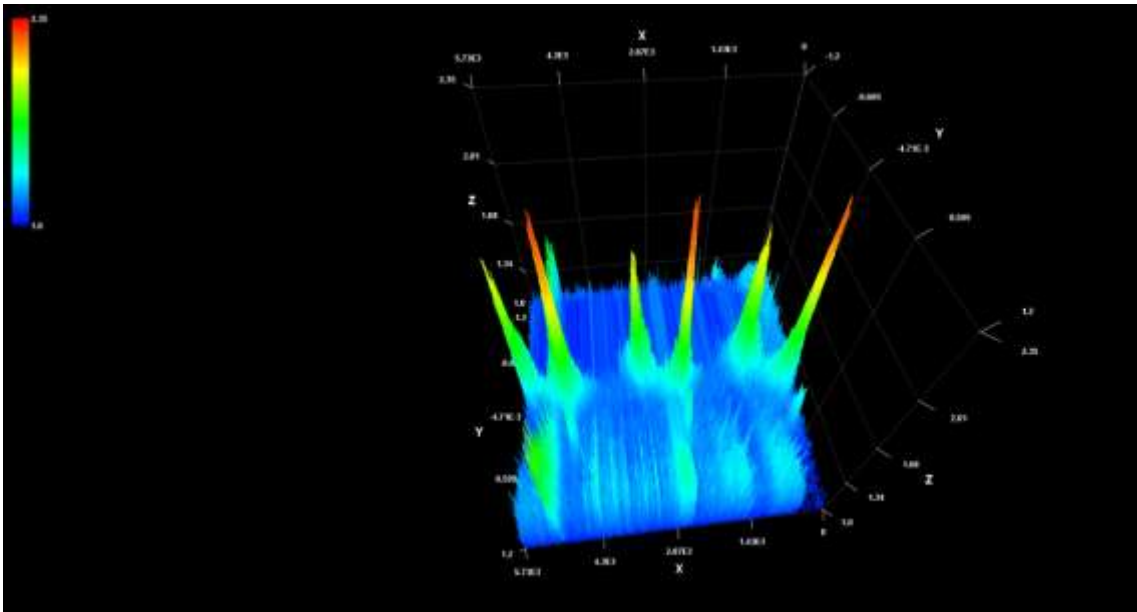
The following plots are produced using Rinearn3D, using data from LRO-H1.

Plot of data intensity over time, showing periodic daily cycle:



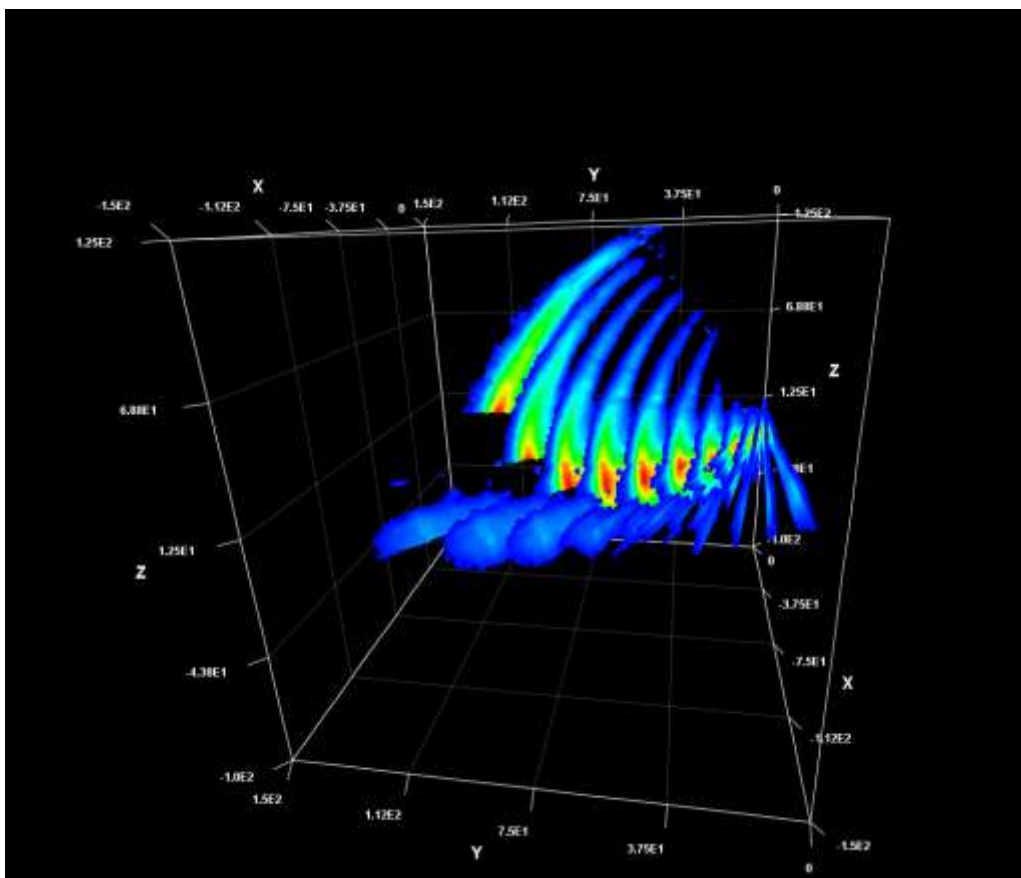
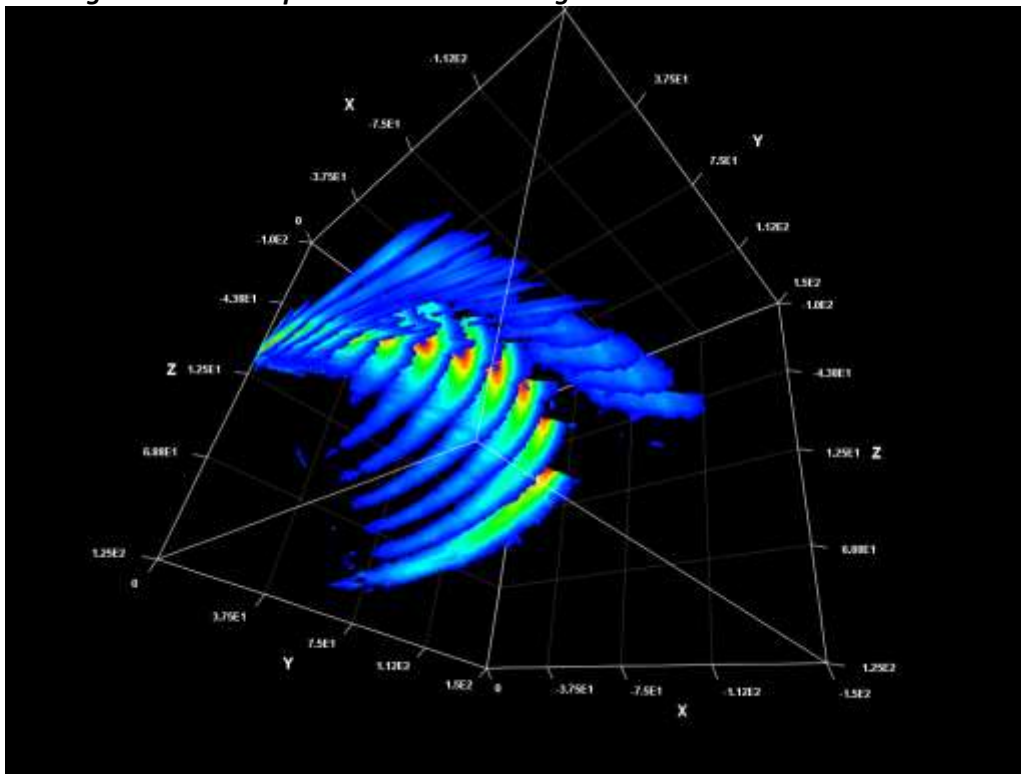
Above plot with intensity plotted on third axis. These plots still include two spatial dimensions:

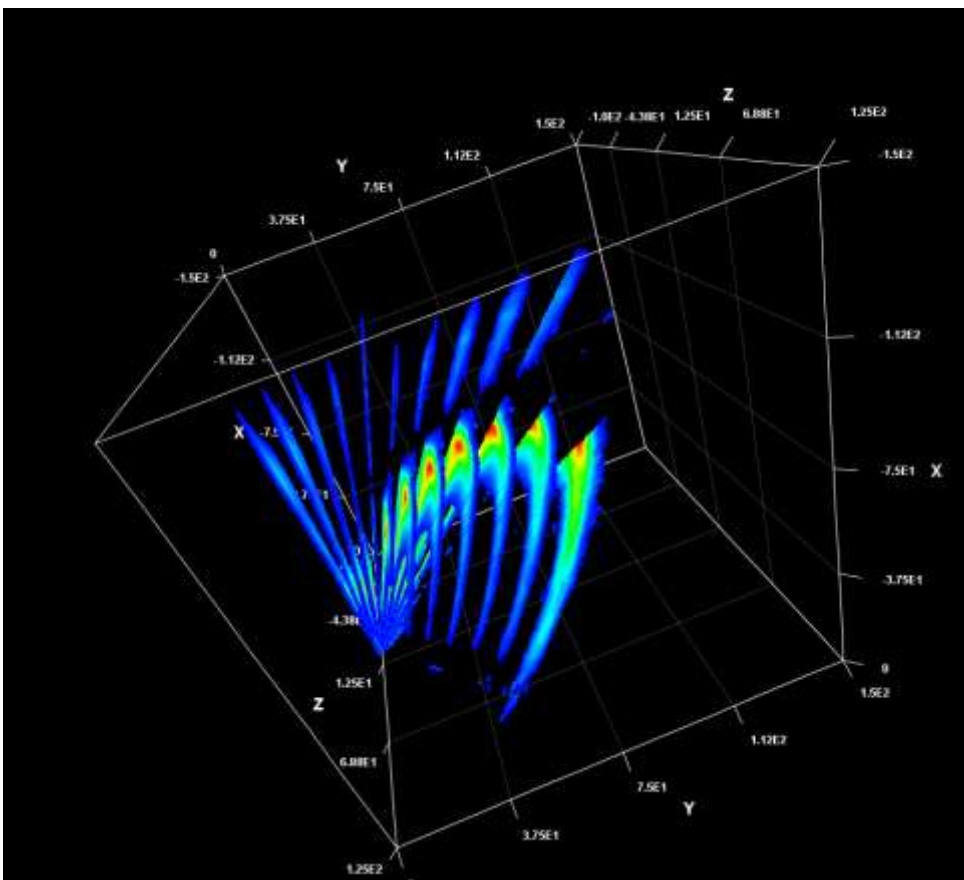
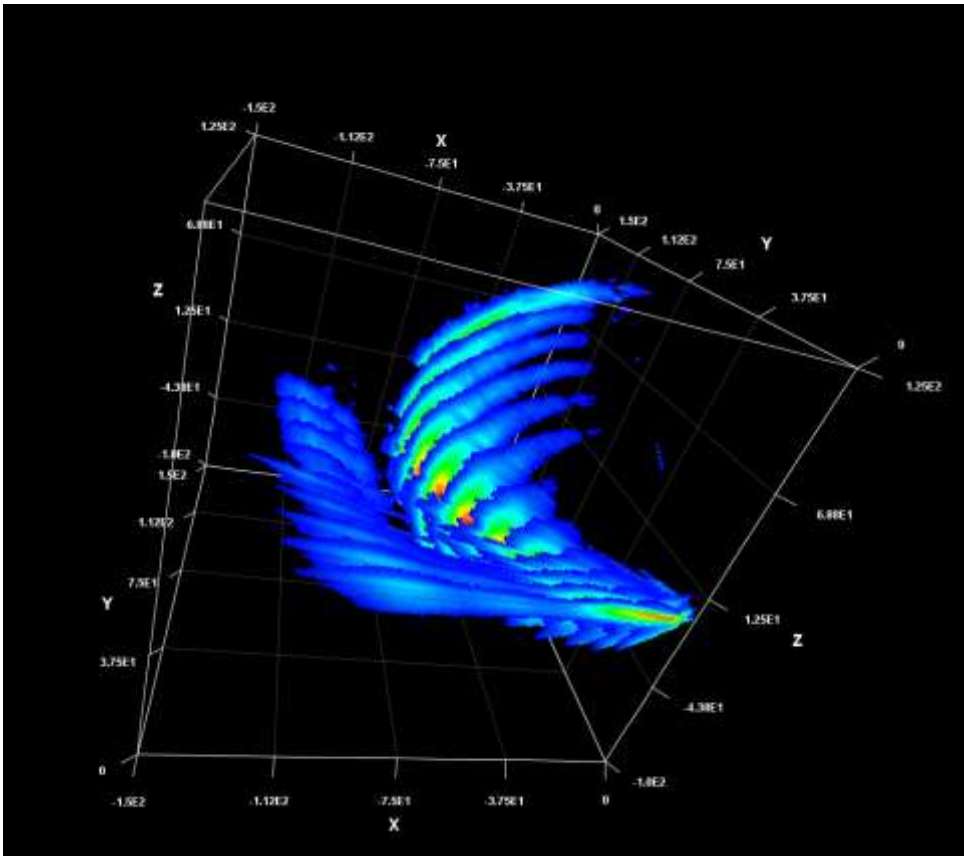


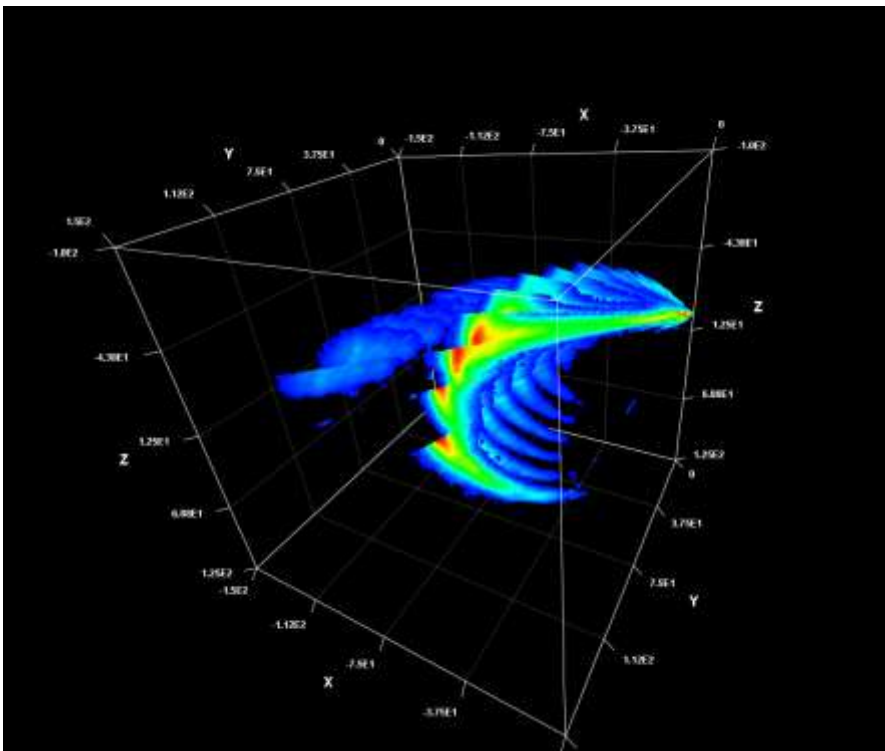
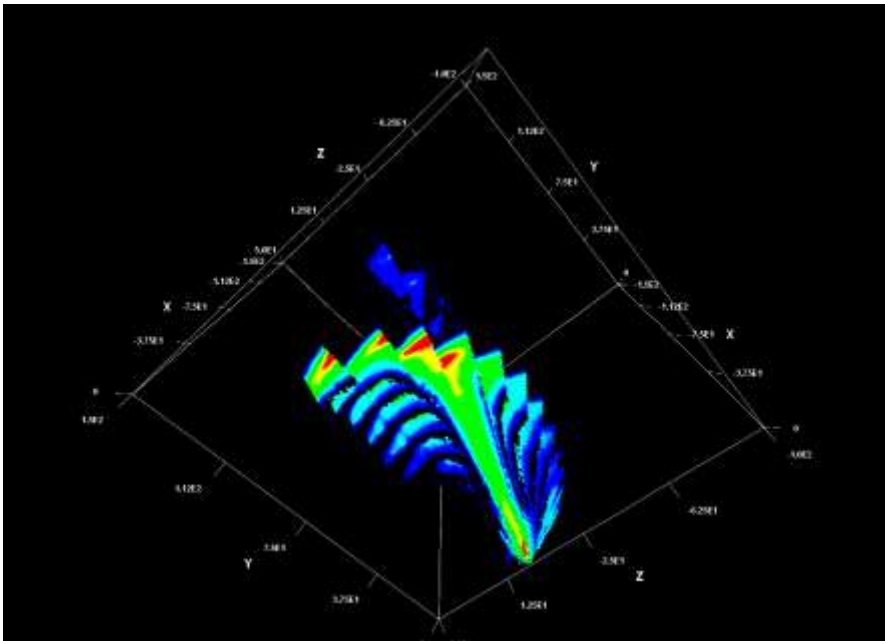


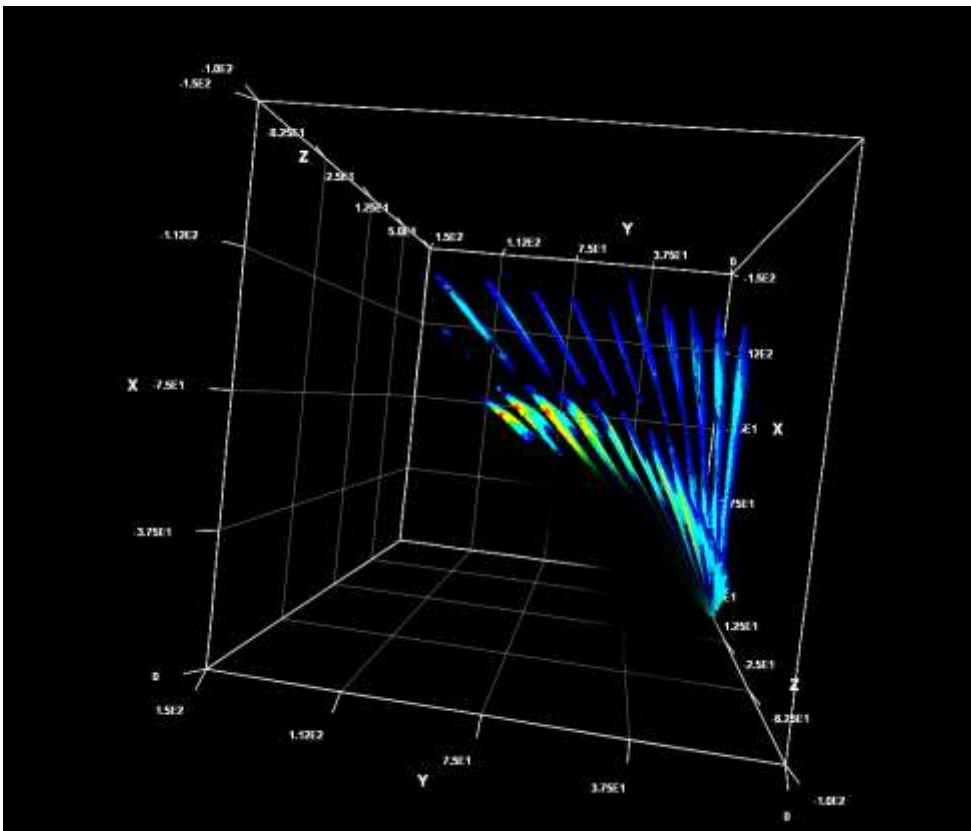
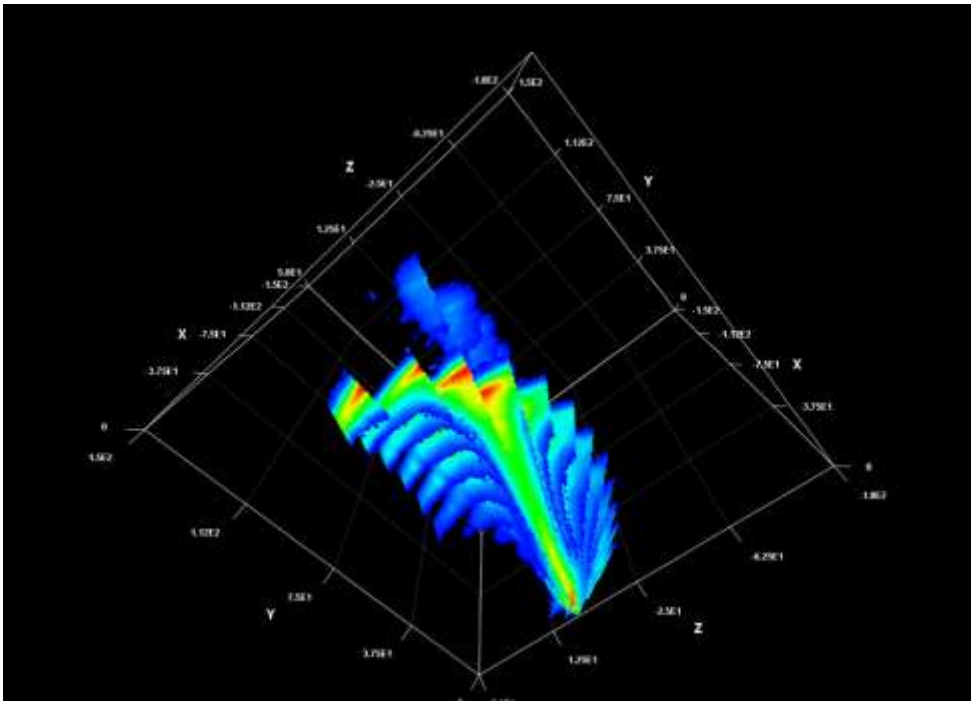
The following plots demonstrate two galactic arms (higher intensity closer to Milky Way centre, lower intensity further away from centre). Our solar system is located at one end of the inner arm (top left on next plot).

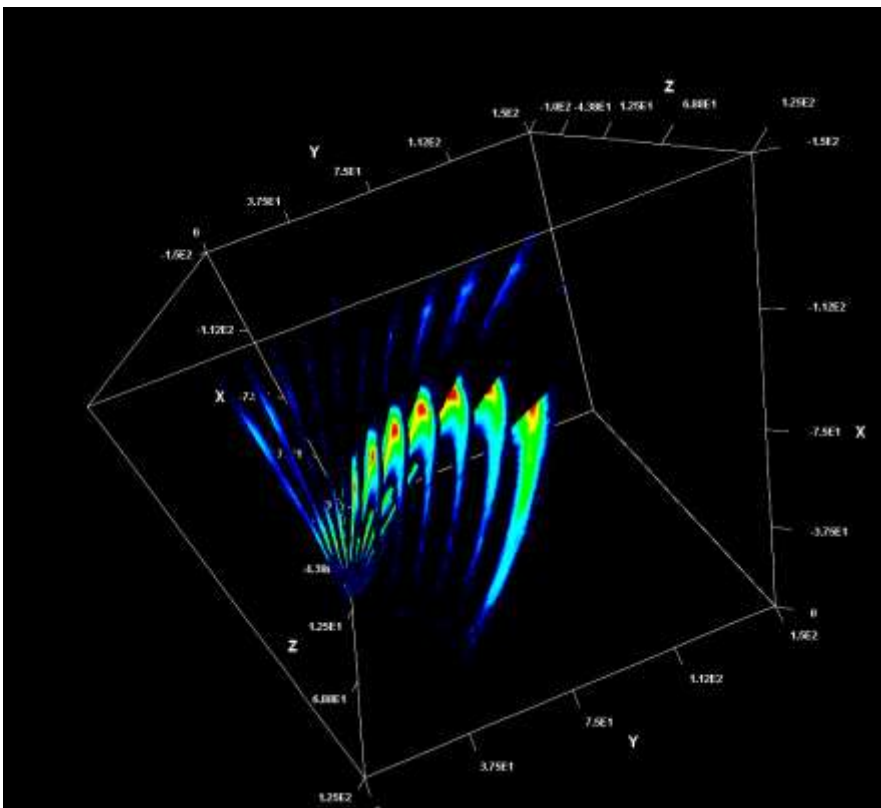
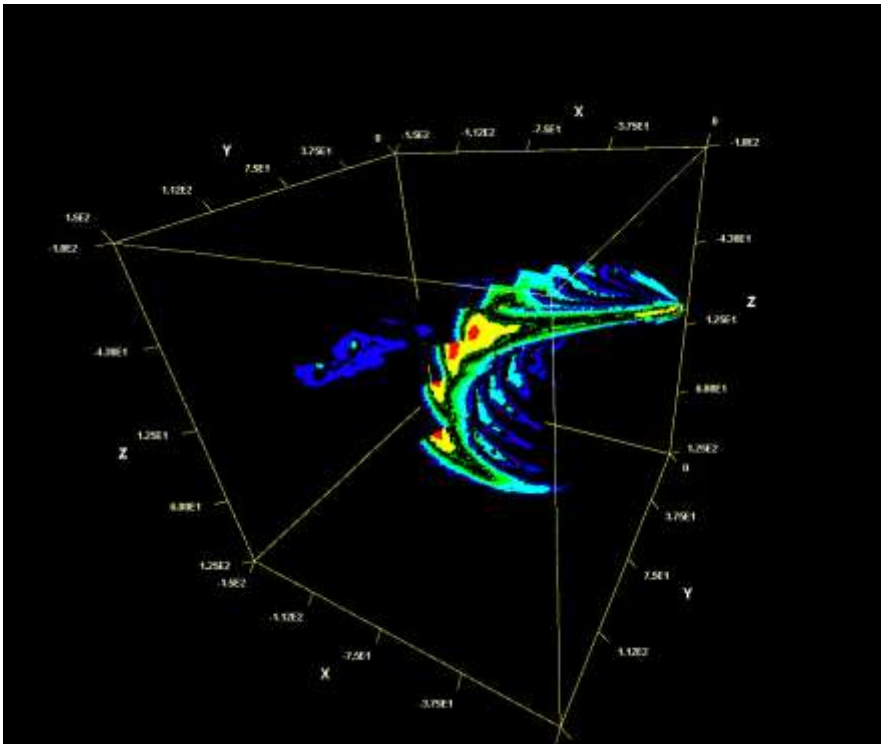
Plotting data in three spatial dimensions using Rinearn3D:

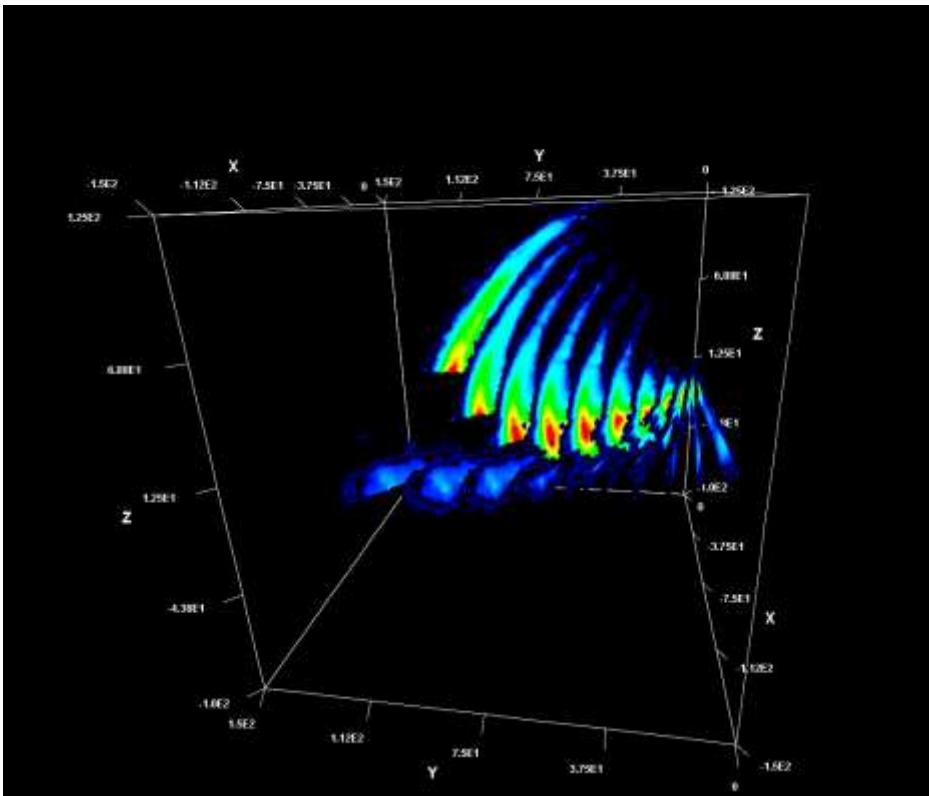
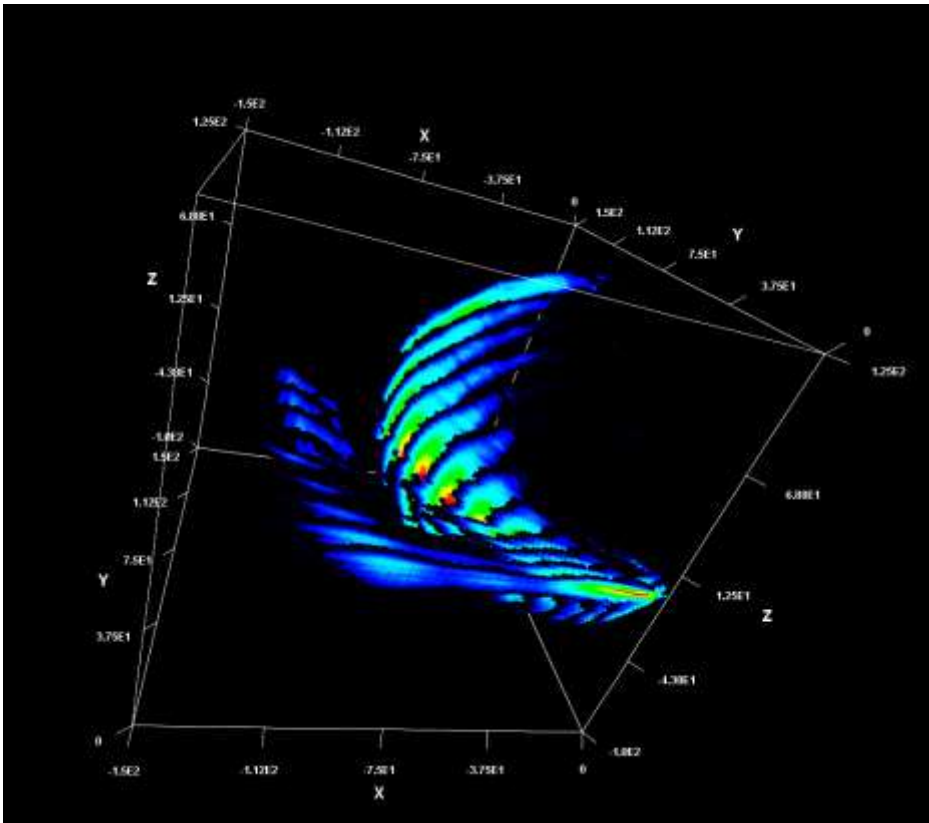


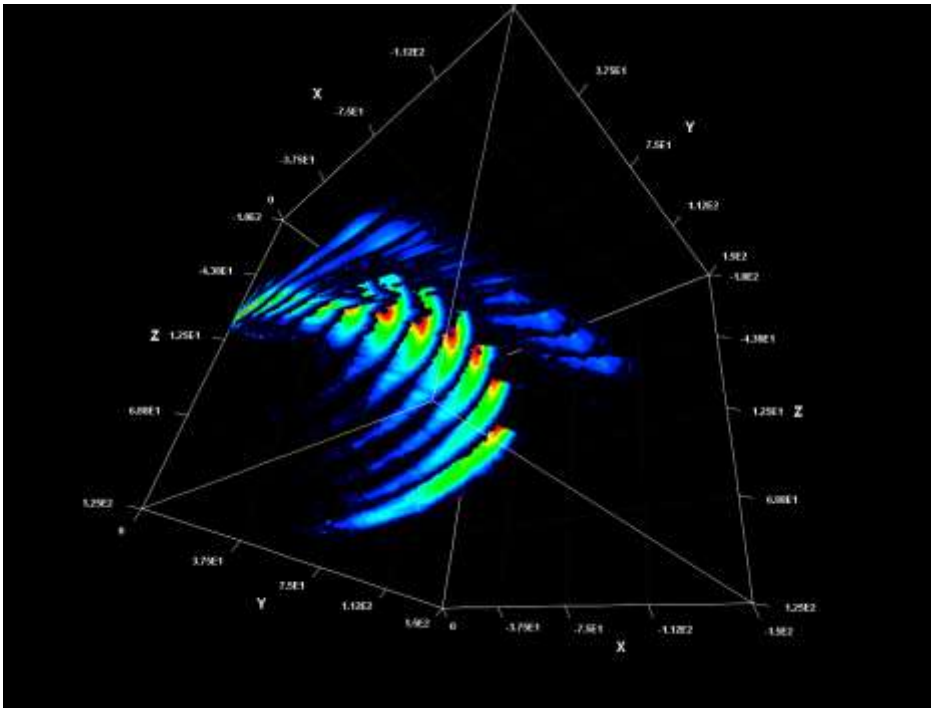












Animation of Milky Way arms in 3 spatial dimensions.

Animations of the Milky Way arms in 3 spatial dimensions can be viewed at <https://www.astronomy.me.uk/rinearn3d-4d-plots-and-animations-of-lro-ptarmigan-hydrogen-data-jan-2024-nov-2024-processed-10-11-12-2024>

Further information.

Further information about this project is available on the www.astronomy.me.uk website or by contacting me using the “contact us” page on that website.

A note on integration times in ezCol data collection programme in ezRA software suite.

Dr Andrew Thornett, M6THO, Lichfield Radio Observatory, Lichfield, UK www.astronomy.me.uk

Easy Radio Astronomy Suite (ezRA).

Ted Cline's free Easy Radio Astronomy Suite (ezRA, <https://github.com/tedcline/ezRA>) is widely used for the collection and processing of hydrogen line astronomy data by amateurs (1420.405MHz). Data collection is performed by the ezCol.py script within the suite. Its default setting is to integrate 31,000 samples in order to improve signal to noise ratio. This amount can be changed on the software's control panel.

Choosing an integration time.

The most common use of ezRA is to collect and process hydrogen line data from 24-hour drift scans of the Milky Way, where the radio telescope is pointed in the same direction in azimuth, and data is collected over full 24-hour periods. Elevation is changed between scans and the software calculates where the aerial was directed at each moment and presents this data on a number of plots.

For radio telescope aerials in the 1m range, an ideal integration time is around 4 to 5 minutes. The number of samples that need to be integrated in ezCol to achieve this time period will vary from computer to computer, depending upon the processing power and RAM of the host machine.

The "perfect" integration time in ezCol.

The number of samples required in ezCol to achieve 4 to 5 minutes per integrated sample was determined for both the LRO-H1 radio telescope, based on an ex-military 86cm x 86cm dipole array, and the LRO-H2 radio telescope, built around an 150cm parabolic solar cooker dish.

86cm dipole array: LRO-H1 – Integration number in ezCol 280,000 = 5.6 minutes single integrated sample.

150cm parabolic solar cooker dish: LRO-H2 = Integration number in ezCol 550,000 = 4.7 minutes single integrated sample.

Further information.

Further information about this project is available on the www.astronomy.me.uk website or by contacting me using the "contact us" page on that website.

Dear World Magnetic Model users,

This is a message from NOAA's National Centers for Environmental Information.

A regular update of the World Magnetic Model (WMM2025) is now available to you. The release includes model coefficients, downloadable software (available soon), online calculators, test values, and instructions to update your WMM software. For many users, updating the WMM software is as simple as replacing the old "WMM.COF" file with the new "WMM.COF" file, and testing the updated software with the latest test values. The new model is valid from 2024-11-13 through 2029-12-31.

What is new:

- ⚙ The World Magnetic Model - High Resolution (WMMHR) is an advanced magnetic field model that offers a more comprehensive depiction of geomagnetic fields than WMM.
- ⚙ The WMMHR has more spherical harmonic coefficients and more digits in each coefficient resulting in a more accurate representation of the magnetic field.
- ⚙ NGA recommends using the WMMHR in DoD systems instead of the WMM, if possible.
- ⚙ A new validity range for heights and depths of the WMM, based on geomagnetic activity levels, is provided.
- ⚙ The WMM error model has been updated, and an error model for the WMMHR is also provided. The new error models are now available via online calculators.
- ⚙ We updated the NOAA geomagnetic field calculators to use both WMM2025 and WMMHR2025. We expect the downloadable software to be updated soon. However, for many users, updating the WMM software is as simple as replacing the old "WMM.COF" file with the new "WMM.COF" file.
- ⚙ We updated the website with new maps of magnetic field components developed from WMM2025.
- ⚙ Blackout Zones around the north and south magnetic poles where compass accuracy is degraded are provided for both the WMM2025 and WMMHR2025 in all products (online calculators, maps, and shapefiles).

The WMM2025 Technical Report will be available in Spring 2025.

To download the model and maps, or use the online calculators, visit

<https://www.ncei.noaa.gov/products/world-magnetic-model>

While doing so, we request that you complete the survey page. Your feedback will strengthen the World Magnetic Model program. Questions and comments may be addressed to geomag.models@noaa.gov.

Observation report: M31 and M33 at 21 cm

Eduard Mol

Abstract

In this observation report I describe my observations of the galaxies M31 and M33 with a 3 metre dish. Observations on other galaxies (IC 342 and M101) are ongoing and will be reported on in a future SARA journal article on extragalactic hydrogen observation once the data are processed.

Methods

The 3 metre dish

For this project a homemade 3 metre f/0.5 dish was used. The dish has a plywood construction with an aluminium mesh reflector. It is not permanently set up in the backyard but consists of four segments which can be assembled around a central hub and stored in a shed when not in use.

The system temperature is about 110- 120 K, as estimated following the “SNR method” described in [1]



Figure 8: the modular 3 metre dish.

In summary, the electronics chain of the 3 metre dish setup consists of the following components:

- 1420 MHz W2IMU type feed
- G8FEK L-band LNA (noise figure 0.5 dB)
- 1420 MHz interdigital filter (built after the design of T. Saje and M. Vidmar)
- 16 dB amplifier (to overcome cable losses)
- Airspy mini SDR receiver

The SDR is cooled using an old PC fan to avoid gain drifting due to heating.

Data collection and processing

Because the 3 metre dish has no tracking capability, observations are done in driftscan mode. The methods for collecting and processing driftscan data used here are also described by Jason Burnfield in the March- April 2024 SARA journal [2]. The dish is placed on a table and pointed to the south at the elevation of the target. Every day, the target passes through the 5 degree wide beam for about 20 minutes. Spectra are integrated and saved every minutes using the SDR# IF average plugin running on a Windows 10 laptop. The collected spectra are later processed in Python using a custom script. A block of 20 spectra centered on the time of the transit is averaged and used as the “on-target” spectrum. In order to remove the SDR bandpass response, two 20 minute blocks of spectra centered 30 minutes before and after the transit are averaged and used as an off-target “dark” reference. The averaged “on-target” spectrum is then divided by the averaged “off-target” spectrum to get rid of the SDR bandpass response.

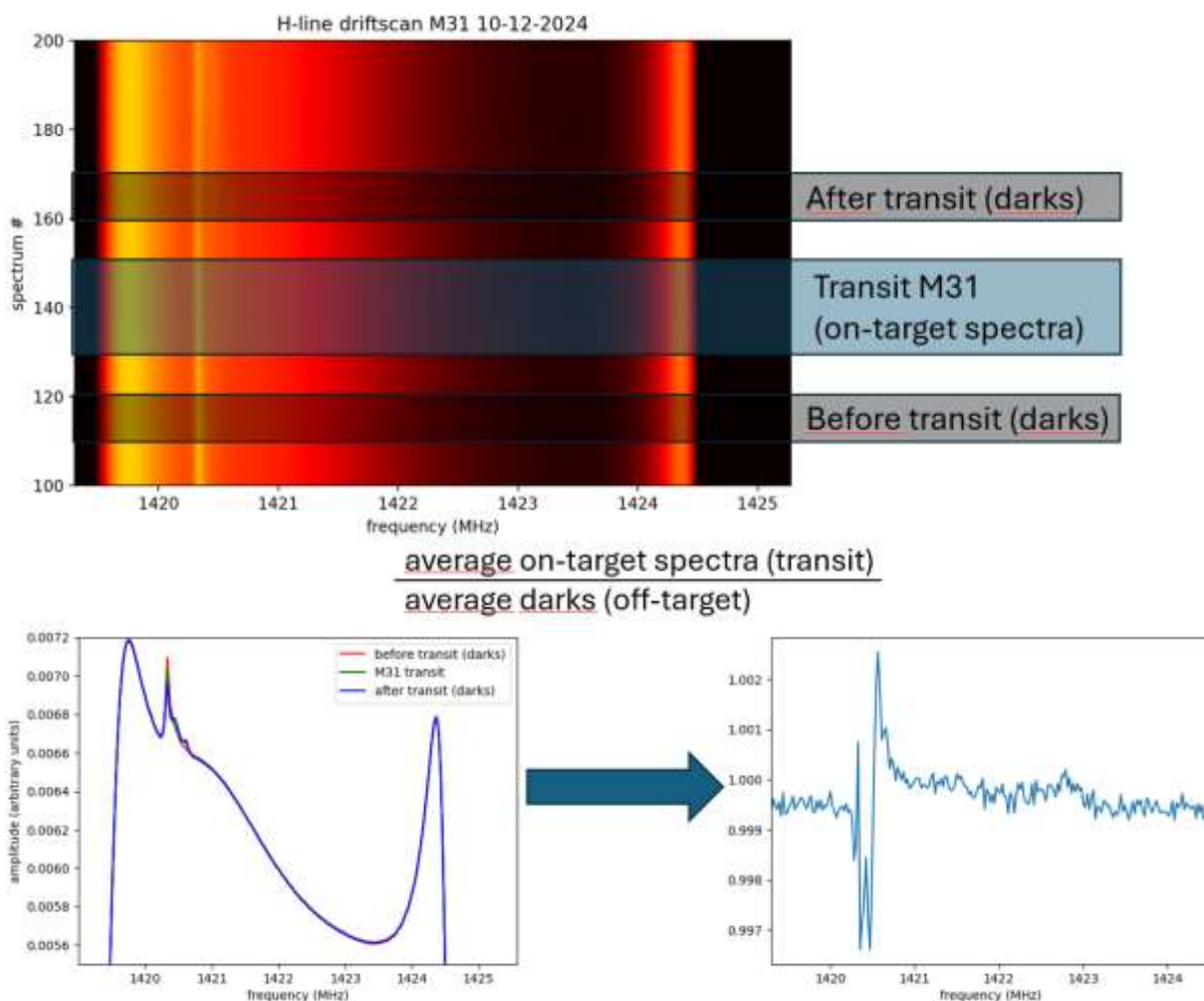


Figure 9: method for bandpass correction of driftscan data using spectra recorded before and after the transit as the “off-target” background reference.

The frequency axis is converted to velocity relative to the Local Standard of Rest (LSR). the LSR correction factor is derived using a Python Astropy script developed by T. J. Dijkema [3].

Results from multiple days are averaged together to reduce the RMS noise level and increase signal-to-noise ratio (SNR). In order to increase the SNR eve further the spectral resolution was reduced from 23.4 KHz (256 FFT bins) to 46.9 KHz (128 bins) by averaging together each two bins. I noticed that when the spectral

resolution is reduced beyond 46.9 KHz some details in the galaxies' spectral profiles are lost. A resolution of 46.9 KHz thus seemed to be a good middle ground between detail and noise level.

As a final step the vertical scale of the spectrum was converted to brightness temperature following the method described in [4]. Briefly, the output of IF average is in amplitude, thus when we divide on-target spectra by off-target spectra for bandpass correction we get a relative amplitude normalized to the system background. From this we can derive the brightness temperature using equation 1 if the system temperature is known.

$$Tb = \left(\frac{A_{on-target}}{A_{off-target}} \right)^2 - 1 * T_{sys} \text{ (equation 1).}$$

Results and discussion

Messier 31, the Andromeda galaxy

Messier 31 has an extremely wide spectral profile stretching nearly 600 km/s. The spectrum has a classical “double horned” profile typical for a spiral galaxy, with strong red- and blueshifted horns at -70 and -530 km/s and weaker emissions in between. The integrated flux density of M31 ranges from 100- 120 Jy at the red- and blueshifted peaks to 40- 60 Jy in between [5].

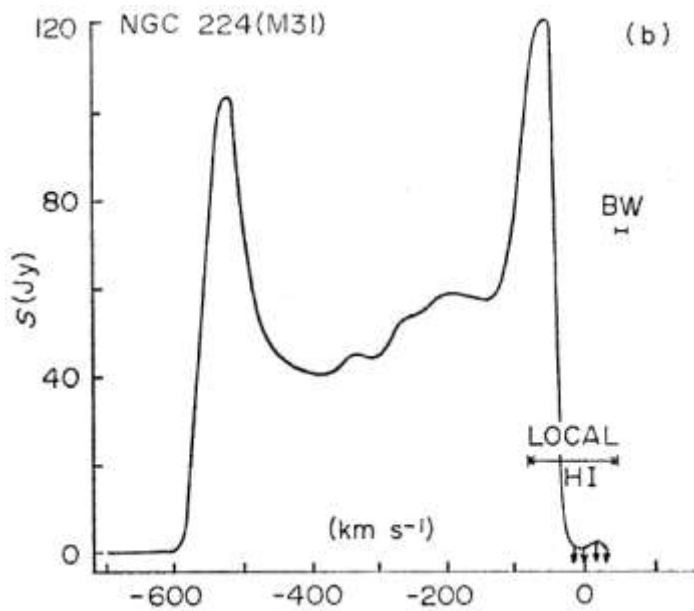


Figure 10: integrated neutral hydrogen spectrum of M31 (figure from Dean and Davies, 1974 [5])

Four transits of M31 were recorded from December 10 to December 13 2024. An additional transit was recently recorded on February 10 2025. The spectral profile of M31, and in particular the strongly blueshifted peak at -530 km/s, is already visible in the individual transit results (figure 4).

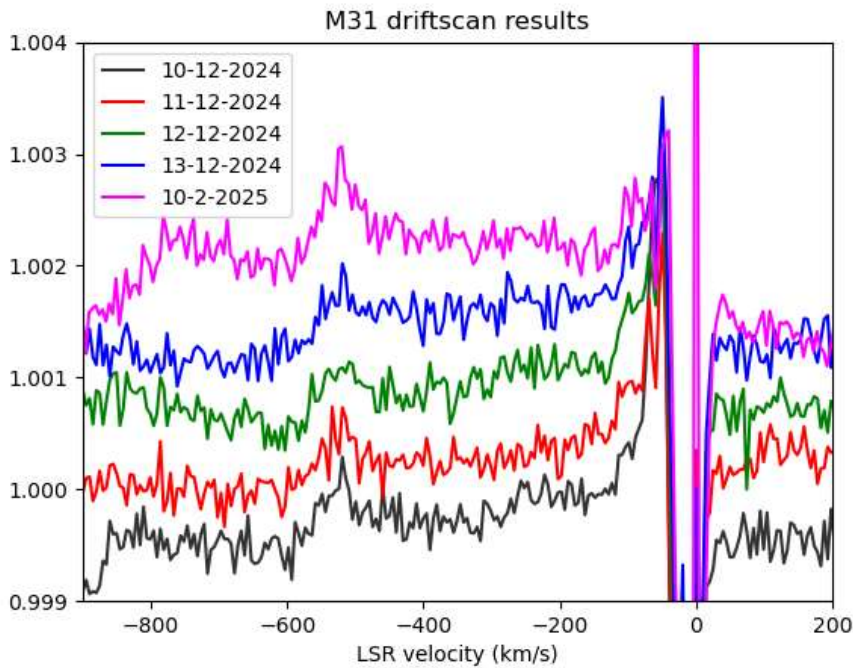


Figure 11: results of M31 driftscans.

Figure 5 shows the end result after averaging the results from these five driftscans and reducing the spectral resolution from 23.4 KHz to 46.9 KHz. The total integration time is 1 hour 40 minutes (5X 20 minutes). The spectral profile is generally in good agreement with the integrated spectrum from Dean and Davies (1974) shown in figure 3. The part of the spectrum between 0 km/s and 100 km/s overlaps with local HI emissions from the Milky Way.

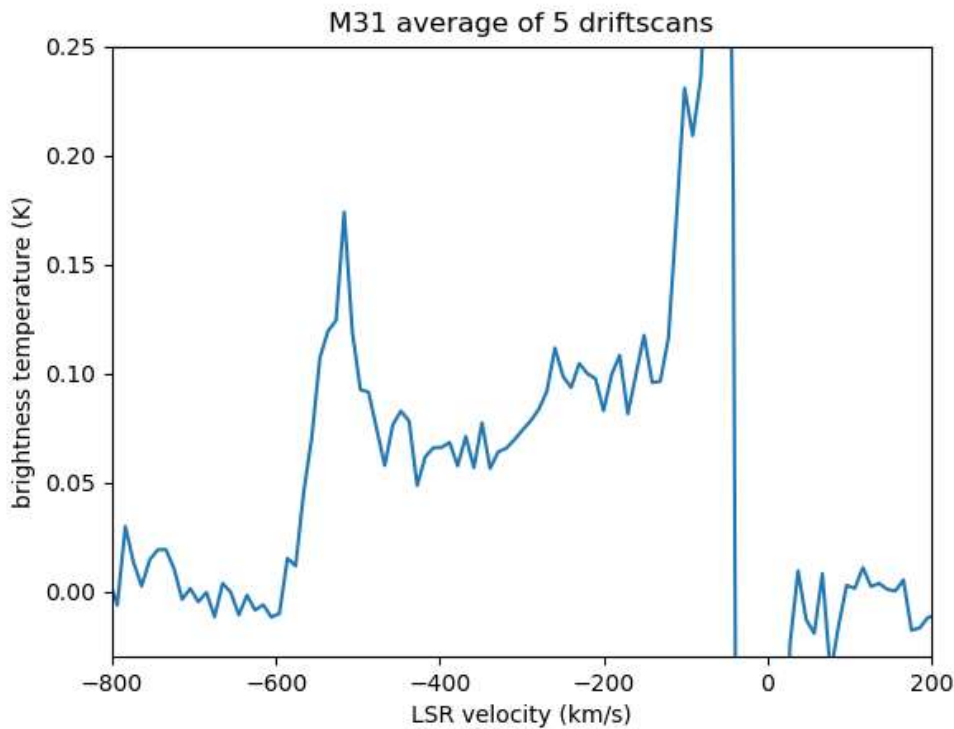


Figure 12: M31 final result.

As an additional test I compared my results to a simulated spectrum downloaded from the LAB survey dataset [6, 7]. To simulate the transit of M31 I downloaded a spectrum for the position of M31 with a 5 degree beamwidth, as well as for the before-transit and after-transit positions at 30 minutes right ascension ahead and behind M31. In order to simulate the transit method the before- and after-transit spectra were subtracted from the M31 spectrum. Unfortunately the LAB survey only covers between -400 and +400 km/s, we therefore miss the blueshifted horn in the simulated transit. Despite this limitation there is a good agreement between the LAB simulation and the actual result in the part of the spectrum covered by the LAB survey.

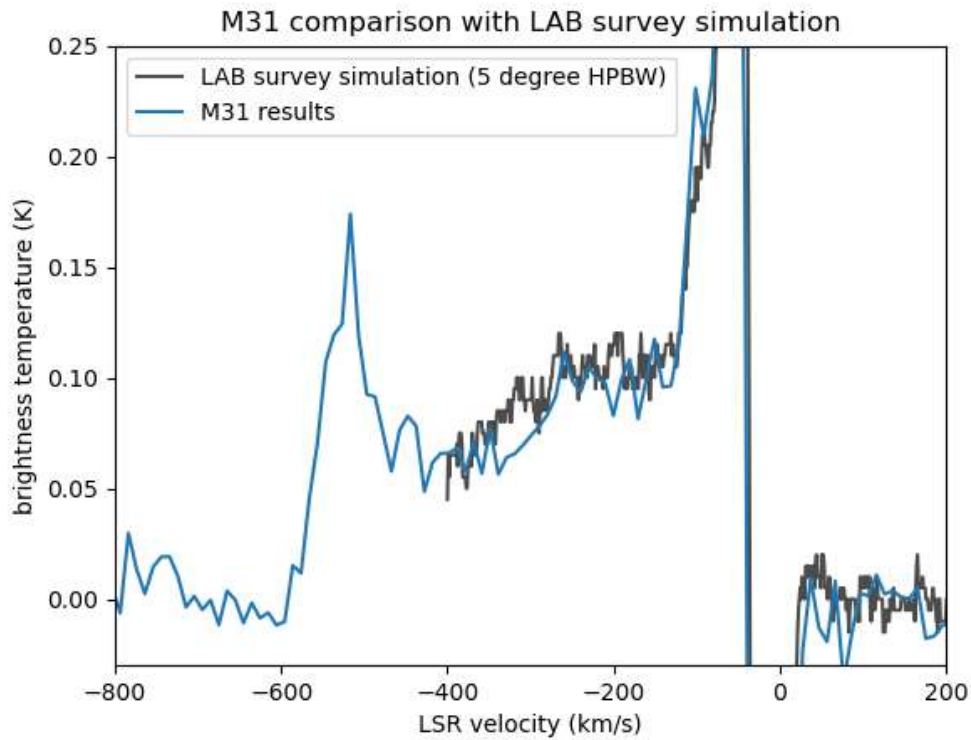


Figure 13: comparison between my M31 measurements and the LAB survey simulation

Messier 33

The integrated flux density of M33 is between 45 and 70 Jy, so it is about half to two-thirds of the brightness of M31. Its spectrum is not as wide, covering a velocity range between -50 km/s and -300 km/s. M33 also has the characteristic double-horned spiral galaxy profile, albeit not as pronounced as M31 [5].

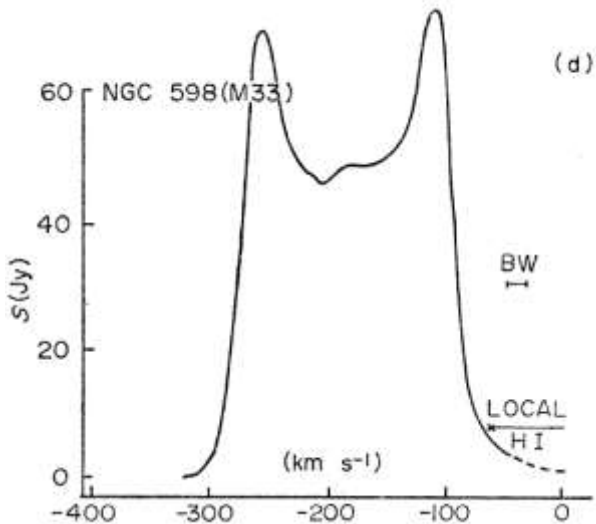


Figure 14: integrated neutral hydrogen spectrum of M31 (figure from Dean and Davies, 1974 [5])

A total of eight driftscans were collected during December 2024 and January 2025. As can be seen in figure 8 the spectrum from January 17 had a strongly curved background and was therefore excluded from the final average. An additional series of transits was done from February 1 to February 4 but unfortunately these transits were all contaminated with RFI, making the extraction of the faint extragalactic hydrogen signal unfeasible.

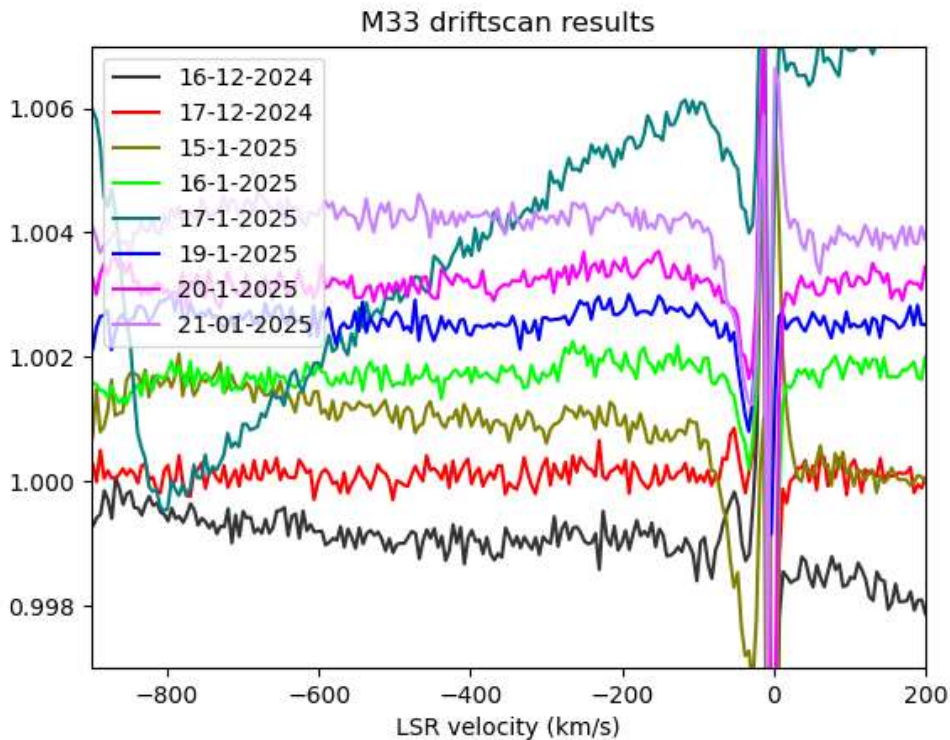


Figure 15: results of M33 driftscans.

After averaging the results from the transits together there was some residual slope in the spectrum. This was removed by fitting a trendline through the parts of the spectrum outside a window covering the local and M33 hydrogen emission, and subtracting that line.

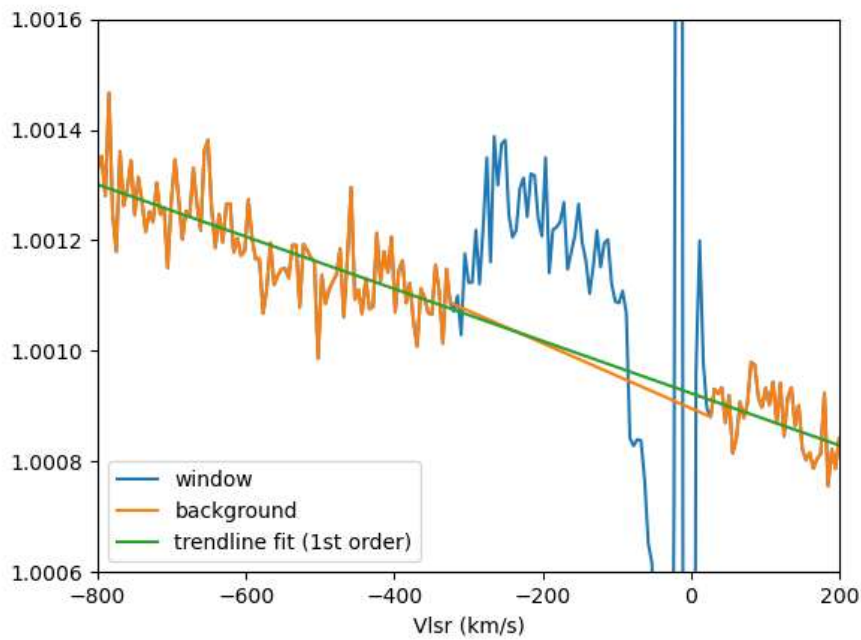


Figure 16: removal of residual slope with a 1st order trendline fit.

After averaging the results from the first few transits the M33 spectral profile was initially unexpectedly weak, barely rising above the noise floor. I noted that the transit of the Galactic plane (where the hydrogen line is at its strongest) was delayed by about 10 minutes, indicating that my dish was pointing slightly to the west of the south meridian. After reprocessing the data, keeping this 10 minute delay of the transit time into account, the spectral profile of M33 became much more obvious.

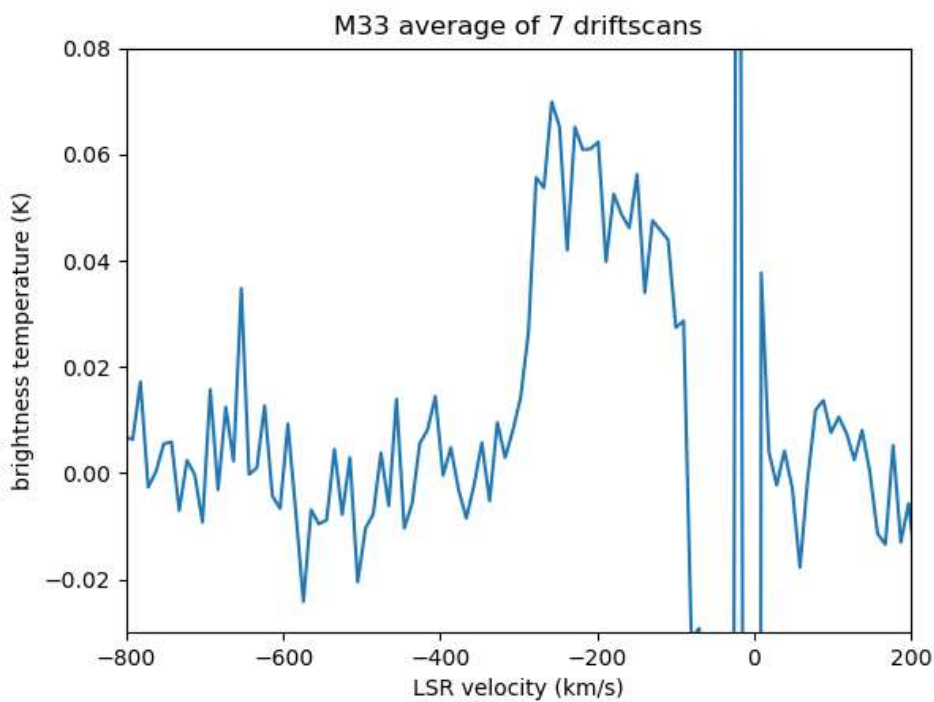


Figure 17: M33 final result

When comparing to the LAB survey simulation the observed brightness temperature is only about half of what would be expected as per the LAB survey. Furthermore the redshifted horn is missing.

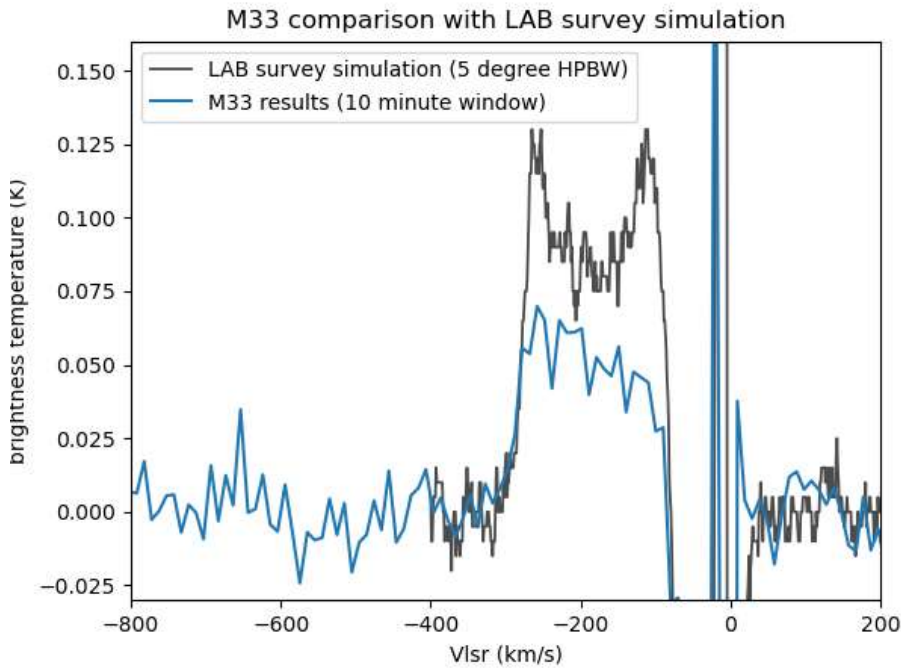


Figure 18: comparison between my M33 result and the LAB survey simulation.

Initially it was suspected that the pointing was a few degrees off, but then I realized that this result makes perfect sense. For the “on-target” spectra I average about 20 minutes of data centered on the M33 transit. However, M33 is at the center of the beam for only a short time. At 10 minutes before and after transit it will be just over 2 degrees away from the center of the beam where sensitivity is already almost half. Therefore, if we take the average over a 20 minute window the observed brightness temperature will be reduced. Using a shorter 10 minute window increases the noise level but this is compensated for by the higher signal level. Now the measured spectral profile is in good agreement with the LAB survey simulation, except for the still missing redshifted peak.

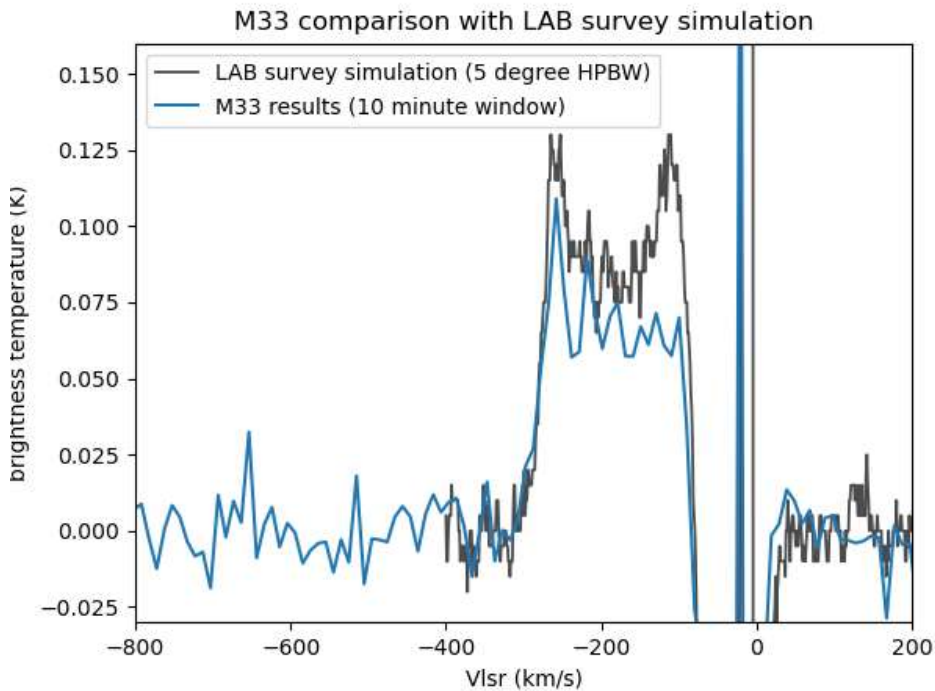


Figure 19: Same as figure 11, but with a 10 minute transit window.

References:

- 1) "The 3 metre dish at the "Astropeiler Stockert", part 2: characterization and observations", Wolfgang Herrmann. (https://astropeiler.de/wp-content/uploads/2017/12/Part2_The_3-Meter_Dish_Astropeiler_Stockert_Characterisation_and_Observations.pdf)
- 2) "Hydrogen line driftscan detection of M31 and M33 with a portable 2.64 meter dish", Jason Burnfield, SARA journal March- April 2024 p. 88- 96.
- 3) <https://gitlab.camras.nl/dijkema/HPIB/blob/185d241ad9bd7507ed90c9fa91fe0a63009d3eee/vlsr.py>
- 4) "Amateur radio astronomy: 21 cm hydrogen line survey of M31 and M33 galaxies" J. J. Maintoux F1EHN, 2018. (no longer online)
- 5) Dean, J. F., & Davies, R. D. (1975). The integrated neutral hydrogen properties of nearby galaxies. *Monthly Notices of the Royal Astronomical Society*, 170(3), 503-518.
- 6) Kalberla, P.M.W., Burton, W.B., Hartmann, Dap, Arnal, E.M., Bajaja, E., Morras, R., & Pöppel, W.G.L. (2005), A&A, 440, 775 ([Kalberla et al. \(2005\)](#))
- 7) <https://www.astro.uni-bonn.de/hisurvey/euhou/LABprofile/index.php>

**INTERNATIONAL EARTH ROTATION AND REFERENCE SYSTEMS SERVICE (IERS)
SERVICE INTERNATIONAL DE LA ROTATION TERRESTRE ET DES SYSTEMES DE REFERENCE**

SERVICE DE LA ROTATION TERRESTRE DE L'IERS OBSERVATOIRE DE PARIS

61, Av. de l'Observatoire 75014 PARIS (France)

Tel.: +33 1 40 51 23 35, e-mail : services.iers@obspm.fr

<http://hpiers.obspm.fr/eop-pc>

Paris, 06 January 2025

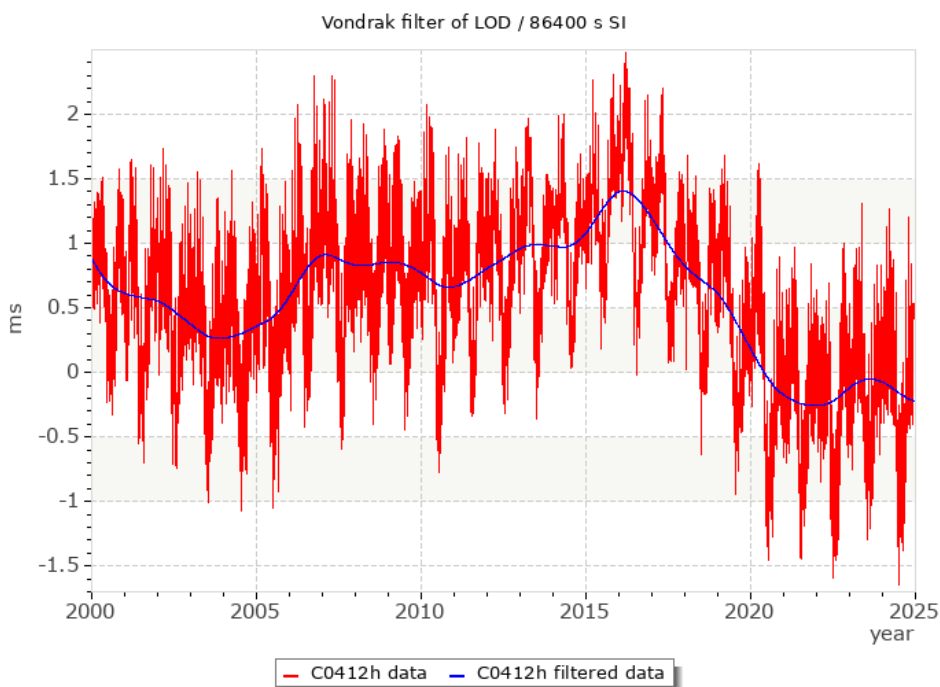
Bulletin C 69

To authorities responsible for the measurement and distribution of time
INFORMATION ON UTC - TAI

NO leap second will be introduced at the end of June 2025. The difference between Coordinated Universal Time UTC and the International Atomic Time TAI is : from 2017 January 1, 0h UTC, until further notice : UTC-TAI = -37 s

Leap seconds can be introduced in UTC at the end of the months of December or June, depending on the evolution of UT1-TAI. Bulletin C is mailed every six months, either to announce a time step in UTC, or to confirm that there will be no time step at the next possible date.

Christian BIZOUARD, Director
Earth Orientation Center of IERS Observatoire de Paris, France



Journal Archives and Other Promotions

The rich and diverse legacy of member contributed content is available in the SARA Journal Archives. Table of contents for journals is available online at: [SARA-Journal-Master-Index.xlsx \(live.com\)](#)

The entire set of The Journal of The Society of Amateur Radio Astronomers is available by online download. It goes from the beginning of 1981 to the present (over 6000 pages of SARA history!)

All SARA journals and conference proceedings are available through the previous calendar year.

SARA Store (radio-astronomy.org/store.)

SARA Online Discussion Group

SARA members participate in the online forum at <http://groups.google.com/group/sara-list>. This is an invaluable resource for any amateur radio astronomer.

SARA Conferences

SARA organizes multiple conferences each year. Participants give talks, share ideas, attend seminars, and get hands-on experience. For more information, visit <http://www.radio-astronomy.org/meetings>.

What is Radio Astronomy?

Radio Astronomy is just what the name implies.... Astronomy observed at radio wavelengths instead of optical. But why do radio astronomy? Radio astronomy has expanded the knowledge of the universe about as much since its discovery in 1932 as optical has since humans first looked up at the sky. (The sky in the different frequencies or colors of radio are as different and varied as all of the flowers on Earth. Each frequency has its own information about what is happening in the universe.) This knowledge has been gained by both professional astronomers as well as amateurs, with amateurs contributing to this day.

Do I need a big dish and expensive equipment?

No. Complete beginner projects are available at the [SARA store](#) at very reasonable prices. You can monitor the Sun's effects upon our planet with [SuperSID](#). This information is gathered for Stanford for research into our ionosphere and radio signal propagation. Another project is the detection the hydrogen line just like Dr. Ewen had done in 1951 for a fraction of the cost using the [Scope in a Box](#) kit.

That said, radio astronomy is like optical astronomy in that you can spend as much as you want to. Many amateurs push the lower boundaries of cost by using very low-cost receivers and low-noise low-cost amplifiers that were not available even a few years ago. (See the [Scope in a Box](#) kit in the store for examples of both.)

Is everything 'plug and play' and boring?

The kits mentioned above are a starting point which are mostly plug-and-play... that gets you started. After you have mastered the basics, where you go from there depends upon your interests. Monitoring pulsars is done by amateurs. (One even noticed a [pulsar glitch](#) before the professionals!) These amateurs are pushing the boundaries of what can be done. Papers are being published and discussions had about pulsar detection as well detection of a MASER with a 50-inch dish. Techniques on new detection methods are posted in the [SARA forum](#) and elsewhere. You are free to build your own equipment to receive the signals as well as software to collect and analyze the data.

What is SETI?

SETI is the Search for Extra-Terrestrial Intelligence. Some amateurs scan the sky and search for signals that might be from aliens. To date no one has received a definitive alien signal (professional or amateur), but the search continues. The search has resulted not just in better receiving equipment but also wide and lively discussions about how aliens might communicate and how they might be trying to contact us. Some of these techniques have interesting ideas for our own communication techniques here on Earth!

What should I do to get started?

You should start with reading our [Introduction to Radio Astronomy](#) and joining our online [SARA Forum](#). Look at the [SARA store](#) to get a project to get your feet wet without much expense and minimal risk. We will work with you so you can succeed.

Administrative

Officers, directors, and additional SARA contacts

The Society of Amateur Radio Astronomers is an all-volunteer organization. The best way to reach people on this page is by email with SARA in the subject line SARA Officers.

President: Dr. Rich Russel, AC0UB, <https://www.radio-astronomy.org/contact/President>

Vice President: Marcus Fisher, <https://www.radio-astronomy.org/contact/Vicepresident>

Secretary: Bruce Randall, NT4RT, <https://www.radio-astronomy.org/contact/Secretary>

Treasurer: Tom Jacobs, <https://www.radio-astronomy.org/contact/Treasurer>

Asst. Treasurer: Donna Hallin, <https://www.radio-astronomy.org/contact/Treasurer>

Past President: Dennis Farr

Founder Emeritus and Director: Jeffrey M. Lichtman, KI4GIY, jeff@radioastronomysupplies.com

Board of Directors

Name	Term expires	Email
Dennis Farr	2026	dennisfarr@verizon.net
Dr. Wolfgang Herrmann	2025	messbetrieb@astropeiler.de
Paul Butler	2025	paul.butler.melbourne@gmail.com
Charles Osborne	2025	k4cso@twc.com
Don Latham	2026	djl@montana.com
Steve Tzikas	2026	Tzikas@alum.rpi.edu
Ted Cline	2025	TedClineGit@gmail.com
Jay Wilson	2026	jwilson@radio-astronomy.org

Other SARA Contacts

All Officers	http://www.radio-astronomy.org/contact-sara	
All Directors and Officers	http://www.radio-astronomy.org/contact/All-Directors-and-Officers	
Eastern Conference Coordinator	http://www.radio-astronomy.org/contact/Annual-Meeting	
All Radio Astronomy Editors	http://www.radio-astronomy.org/contact/Newsletter-Editor	
Radio Astronomy Editor	Dr. Richard A. Russel	drrichrussel@radio-astronomy.org
Contributing Editor	Bogdan Vacaliuc	bvaculiuc@iee.org
Educational Co-Chairs	Ken Redcap, Tom Hagen: http://www.radio-astronomy.org/contact/Educational-Outreach	
Grant Committee	Tom Crowley	grants@radio-astronomy.org
Membership Chair	http://www.radio-astronomy.org/contact/Membership-Chair	
Technical Queries (David Westman)	http://www.radio-astronomy.org/contact/Technical-Queries	
Webmaster	Ciprian (Chip) Sufitchi, N2YO	webmaster@radio-astronomy.org

Resources

Great Projects to Get Started in Radio Astronomy

Radio Observing Program

The Astronomical League (AL) is starting a radio astronomy observing program. If you observe one category, you get a Bronze certificate. Silver pin is two categories with one being personally built. Gold pin level is at least four categories. (Silver and Gold level require AL membership which many clubs have membership. For the bronze level, you need not be a member of AL.)

Categories include.

- 1) SID
- 2) Sun (aka IBT)
- 3) Jupiter (aka Radio Jove)
- 4) Meteor back-scatter
- 5) Galactic radio sources

This program is a collaboration between NRAO and AL. Steve Boerner is the Lead Coordinator and a SARA member.

For more information:

Steve Boerner

2017 Lake Clay Drive

Chesterfield, MO 63017

Email: sboerner@charter.net

Phone: 636-537-2495

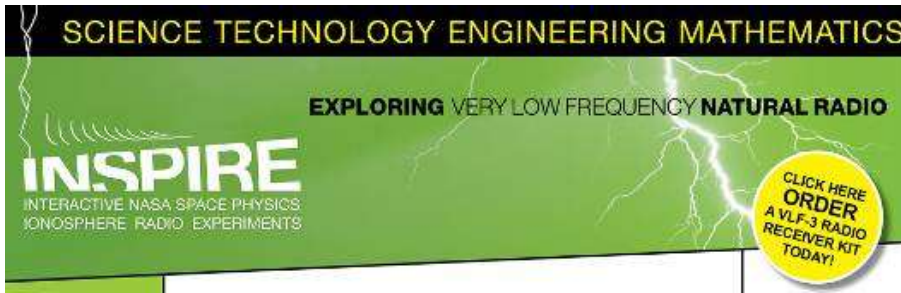
<http://www.astroleague.org/programs/radio-astronomy-observing-program>

Radio Jove



The Radio Jove Project monitors the storms of Jupiter, solar activity and the galactic background. The radio telescope can be purchased as a kit, or you can order it assembled. They have a terrific user group you can join. <http://radiojove.gsfc.nasa.gov/>

INSPIRE Program



The INSPIRE program uses build-it-yourself radio telescope kits to measure and record VLF emissions such as tweeks, whistlers, sferics, and chorus along with man-made emissions. This is a very portable unit that can be easily transported to remote sites for observations.

<http://theinspireproject.org/default.asp?contentID=27>

SARA/Stanford SuperSID



Stanford Solar Center and the Society of Amateur Radio Astronomers have teamed up to produce and distribute the SuperSID (Sudden Ionospheric Disturbance) monitor. The monitor utilizes a simple pre-amp to magnify the VLF radio signals which are then fed into a high-definition sound card. This design allows the user to monitor and record multiple frequencies simultaneously. The unit uses a compact 1-meter loop antenna that can be used indoors or outside. This is an ideal project for the radio astronomer that has limited space.

To request a unit, send an e-mail to supersid@radio-astronomy.org

Radio Astronomy Online Resources

SARA YouTube Videos: https://www.youtube.com/@radio-astronomy	Pisgah Astronomical Research Institute: www.pari.edu
AJ4CO Observatory – Radio Astronomy Website: http://www.aj4co.org/	A New Radio Telescope for Mexico - ORION 2021 01 20. Dr. Stan Kurtz https://www.youtube.com/watch?v=Q9aBWr1aBVc
Radio Astronomy calculators https://www.aj4co.org/Calculators/Calculators.html	National Radio Astronomy Observatory http://www.nrao.edu
Introduction to Amateur Radio Astronomy (presentation) http://www.aj4co.org/Publications/Intro%20to%20Amateur%20Radio%20Astronomy,%20Typinski%20(AAC,%202016)%20v2.pdf	NRAO Essential Radio Astronomy Course http://www.cv.nrao.edu/course/astr534/ERA.shtml
RF Associates Richard Flagg, rf@hawaii.rr.com 1721-1 Young Street, Honolulu, HI 96826	Exotic Ions and Molecules in Interstellar Space -- ORION 2020 10 21. Dr. Bob Compton https://www.youtube.com/watch?v=r6cKhp23SUo&t=5s
RFSpace, Inc. http://www.rfspace.com	The Radio JOVE Project & NASA Citizen Science – ORION 2020.6.17. Dr. Chuck Higgins https://www.youtube.com/watch?v=s6eWAXjywp8&t=5s
CALLISTO Receiver & e-CALLISTO http://www.reeve.com/Solar/e-CALLISTO/e-callisto.htm	UK Radio Astronomy Association http://www.ukraa.com/
Deep Space Exploration Society http://DSES.science	CALLISTO software and data archive: www.e-callisto.org
Deep Space Object Astrophotography Part 1 -- ORION 2021 02 17. George Sradnov https://www.youtube.com/watch?v=Pm_Rs17KlyQ	Radio Jove Spectrograph Users Group http://www.radiojove.net/SUG/
European Radio Astronomy Club http://www.era.net	Radio Sky Publishing http://radiosky.com
British Astronomical Association – Radio Astronomy Group http://www.britastro.org/baa/	The Arecibo Radio Telescope; It's History, Collapse, and Future - ORION 2020.12.16. Dr. Stan Kurtz, Dr. David Fields https://www.youtube.com/watch?v=rBZIPOLNX9E
Forum and Discussion Group http://groups.google.com/group/sara-list	Shirleys Bay Radio Astronomy Consortium marcus@propulsionpolymers.com
GNU Radio https://www.gnuradio.org/	SARA Twitter feed https://twitter.com/RadioAstronomy1
SETI League http://www.setileague.org	SARA Web Site http://radio-astronomy.org
NRAO Essential Radio Astronomy Course http://www.cv.nrao.edu/course/astr534/ERA.shtml	Simple Aurora Monitor: Magnetometer http://www.reeve.com/SAMDescription.htm
NASA Radio JOVE Project http://radiojove.gsfc.nasa.gov Archive: http://radiojove.net/archive.html https://groups.io/g/radio-jove	Stanford Solar Center http://solar-center.stanford.edu/SID/
Green Bank Observatory https://greenbankobservatory.org/	https://www.csiro.au/ There's a wealth of info on this site of the Australian National Science Agency. It's much more than just radio astronomy. Looking under "Research" opens a real family tree of interesting pages of things they are involved with.

Found an interesting Grote Reber link: <https://www.utas.edu.au/groterebmuseum> Their gallery is interesting, but sure wish they had some captions to indicate who and what some of it is about. I can guess, knowing some of Grote's stories, but others might need more info. Several pictures show the University of Tasmania 26m dish that

was once one of the NASA worldwide Satellite Tracking and Data Network (STDN) dishes like the ones at the Pisgah Astronomical Research Institute (www.pari.edu). PARI's dishes were the first qualification units for that network.

For Sale, Trade and Wanted

At the SARA online store: radio-astronomy.org/store.

New on-demand store for SARA SWAG! <https://saragifts.org/>

Scope in a Box

radio-astronomy.org/store.

Kit of parts and software to build a working Radio Telescope to detect Hydrogen Line emissions. Available to USA addresses only at this time.

SuperSID Complete Kit

radio-astronomy.org/store.



SARA Publication, Journals and Conference Proceedings (various prices)

radio-astronomy.org/store.

SARA Journal Online Download

radio-astronomy.org/store.

The Journal archive covers the society journal "Radio Astronomy" from the founding of the organization in 1981 through the present. Articles cover a wide range of topics including cosmic radiation, pulsars, quasars, meteor detection, solar observing, Jupiter, Radio Jove, gamma ray bursts, the Itty Bitty Telescope (IBT), dark matter, black holes, the Jansky antenna, methanol masers, mapping at 408 MHz and more.

New! SARA On-Demand Store: <https://saragifts.org>

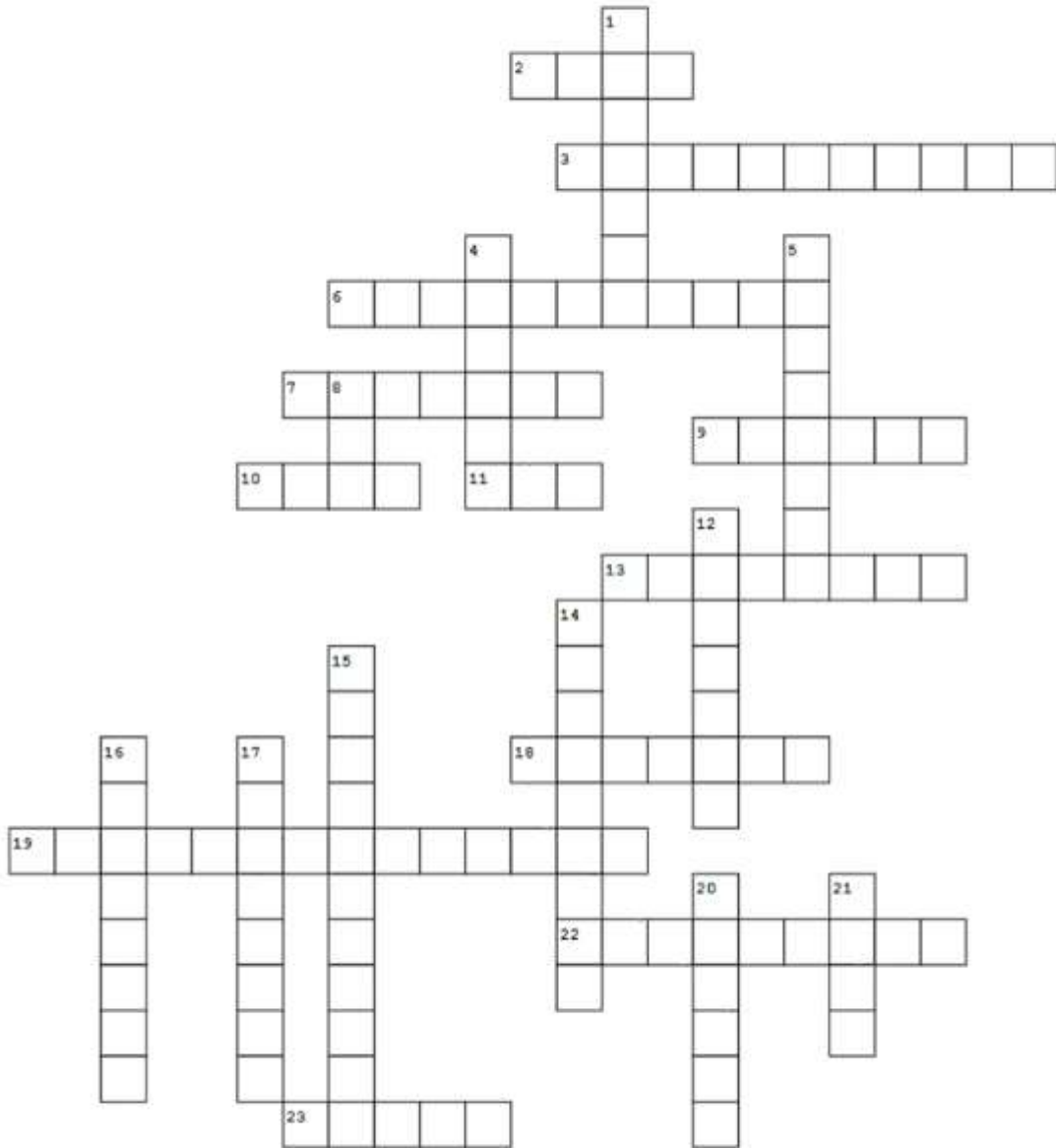
These are the current items – more to come in the future!

(Note: No returns or refunds possible because of the on-demand production approach)





Radio Meteor Observing



Across

- 2. radio meteor Observation Bulletin abv.
- 3. DL4YHF's Audio Spectrum Analyzer program
- 6. program used to display hourly counts

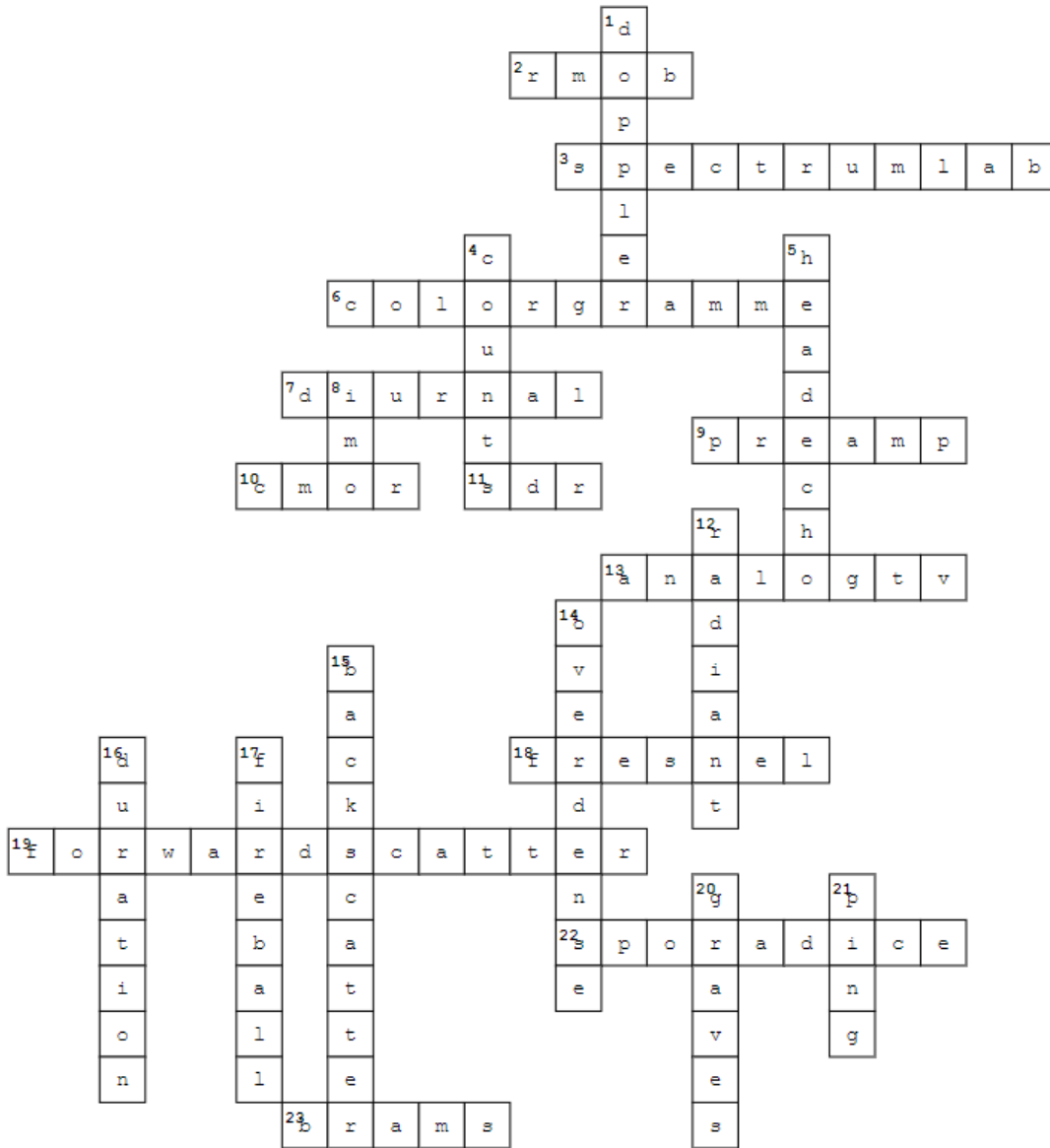
Down

- 1. shift of frequency caused by the physical relationship
- 4. number of reflections per hour

-
7. daily fluctuation of meteor rate from rotation of Earth
 9. amplifier between antenna and receiver
 10. Canadian Meteor Orbit Radar abv.
 11. receiver that plugs into a PC
 13. source transmitters in Canada
 18. oscillations of signal caused by reception from different parts of trail
 19. far off transmitter's reflected signal from meteor trail
 22. type of seasonal radio propagation off of electron clouds
 23. source transmitter in Belgium
 5. reflection off of the meteor instead of the trail
 8. international meteor organization abv.
 12. meteors seem to come from one spot in sky
 14. reflection that is strong and lasts longer
 15. transmitter at same site as receiver reflected signal
 16. length of echo
 17. big meteor brighter than the moon
 20. source transmitter in France
 21. meteor echo heard on receiver

Answers on next page

Radio Meteor Observing



Membership Information

Annual SARA dues Individual \$20, Classroom \$20, Student \$5 (US funds) anywhere in the world. Membership includes a subscription to Radio Astronomy, the bimonthly Journal of The Society of Amateur Radio Astronomers, delivered electronically (via a secure web link, emailed to you as each new issue is posted). We regret that printing and postage costs prevent SARA from providing hardcopy subscriptions to our Journal.

We would appreciate the following information included with your check or money order, made payable to SARA:

Name: _____
 Email Address: _____
(required for electronic Journal delivery)
 Ham call sign: _____ (if applicable)
 Address: _____
 City: _____
 State: _____
 Zip: _____
 Country: _____
 Phone: _____

Please include a note of your interests. Send your application for membership, along with your remittance, to our Treasurer.

For further information, see our website at:
<http://radio-astronomy.org/membership>

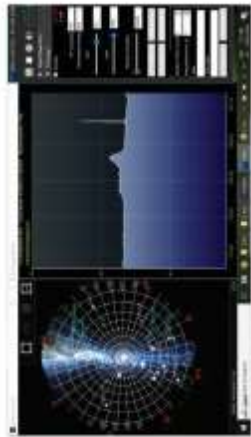


Society of Amateur Radio Astronomers, Inc.
 Founded 1981

Membership supported, nonprofit [501(c) (3)]
 Educational and Radio Astronomy Organization
**Knowledge through Common Research,
 Education and Mentoring**

How to get started?

SARA has a made a kit of software and parts to detect the Hydrogen line signal from space. This is an excellent method to get started in radio astronomy. It teaches the principles of antenna design, signal detection, and signal processing. Read more about this and other projects on our web site.



SARA members have been privileged to use this forty foot diameter drift-scan hydrogen line radio telescope every year at their annual meeting in Green Bank.

Why Radio Astronomy?

Because about sixty five percent of our current knowledge of the universe has stemmed from radio astronomy alone. The discovery of quasars, pulsars, black holes, the 3K background from the "Big Bang" and the discovery of biochemical hydrogen/carbon molecules are all the result of professional radio astronomy.



<http://radio-astronomy.org>

The Society of Amateur Radio Astronomers

SARA was founded in 1981, with the purpose of educating those interested in pursuing amateur radio astronomy.

The society is open to all, wishing to participate with others, worldwide.

SARA members have many interests, some are as follows:

SARA Areas of Study and Research:

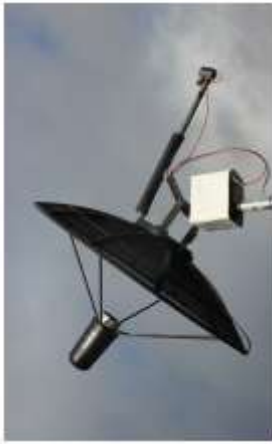
- Solar Radio Astronomy
- Galactic Radio Astronomy
- Meteor Detection
- Jupiter
- SETI
- Gamma Ray/High Energy Pulse
- Detection
- Antennas
- Design of Hardware / Software

The members of the society offer a friendly mentor atmosphere. All questions and inquiries are answered in a constructive manner. No question is silly!

SARA offers its members an electronic bi-monthly journal entitled Radio Astronomy. Within the journal, members report on their research and observations. In addition, members receive updates on the professional radio astronomy community and, society news.

Once a year SARA meets for a three-day conference at the Green Bank Observatory in Green Bank West Va.

There is also a spring conference held at various cities in the Western USA. Previous meetings have been at the VLA in Socorro, NM and at Stanford University.



How do amateurs do radio astronomy?

Radio astronomy by amateurs is conducted using antennas of various shapes and sizes, from smaller parabolic dishes to simple wire antennas. These antennas are connected to receivers and most of these receivers are software defined radios these days. Data from the receivers are collected by computers, and the received signals will be displayed as charts, graphs or maybe even sky maps. As diverse as the observed objects, so is the instruments and tools used. SARA members will always be supportive to find good solutions for what one wishes to observe.

Is amateur radio astronomy instrumentation expensive?

Technical information freely circulated in our monthly journal helps amateurs to obtain good low noise equipment from off the shelf assemblies, or to build their own units. The actual cash investment in radio astronomy equipment need not exceed that of any other hobby.

What are amateurs actually looking for in the received data?

The aim of the radio amateur is to find something new and unusual. Just as an amateur optical observer hopes to notice a supernova or a new comet, so does an amateur radio observer hope to notice a new radio source, or one whose radiation has changed appreciably.

How do I get started?

Just as a long journey begins with the first step, the project you elect must start with a clear idea of your objectives. Do you wish to study the sun? Jupiter? Make meteor counts? Do you wish to engage in imaging radio astronomy? What you decide will not only determine the type of equipment you will need, but also the local radio spectrum.



The Reber Telescope at NRAO. Constructed by Grote Reber in 1937 in his back yard in Wheaton, Illinois



SARA Members discussing the IBT (itty Blitty Telescope)

